



## ANNEX 12

*22<sup>nd</sup> Meeting of the  
International Scientific Committee for Tuna  
and Tuna-Like Species in the North Pacific Ocean  
Kona, Hawai'i, U.S.A.  
July 12-18, 2022*

# **STOCK ASSESSMENT AND FUTURE PROJECTIONS OF BLUE SHARKS IN THE NORTH PACIFIC OCEAN THROUGH 2020**

**July 2022**

Left Blank for Printing

## Table of Contents

Executive Summary .....	4
Stock Identification and Distribution .....	4
Catch History.....	4
Data and Assessment.....	5
Projections.....	6
Stock Status.....	6
Conservation Information .....	7
Special note .....	8
1. Introduction.....	13
2. Background.....	14
2.1. Biology.....	14
2.1.1. Stock structure .....	14
2.1.2. Reproduction.....	15
2.1.3. Growth .....	15
2.2. Fisheries .....	15
2.3. Previous stock assessments .....	16
3. Data.....	16
3.1. Spatial stratification.....	16
3.2. Temporal stratification .....	16
3.3. Definition of fisheries.....	16
3.4. Catch data.....	17
3.4.1. Japan .....	18
3.4.2. Chinese-Taipei (Taiwan).....	19
3.4.3. Republic of Korea.....	19
3.4.4. China.....	20
3.4.5. Canada.....	20
3.4.6. USA.....	21
3.4.7. Mexico .....	21
3.4.8. IATTC .....	21
3.4.9. SPC/Non-ISC.....	22
3.5. Indices of relative abundance.....	22
3.5.1. Main abundance indices.....	23
3.5.1.1. Japanese Kinkai shallow early and late CPUEs .....	23
3.5.1.2. Composite-late CPUE with Dynamic factor analysis.....	23
3.5.2. Alternative abundance indices .....	24
3.5.2.1. Hawaii longline.....	24
3.5.2.2. Taiwan longline .....	24
3.5.2.3. Japan RTV longline.....	24
3.5.2.4. Mexico longline.....	24
3.5.2.5. SPC longline .....	25
3.6. Catch-at-length.....	25
3.6.1. Japan .....	25

3.6.2.	Chinese-Taipei .....	26
3.6.3.	China .....	26
3.6.4.	USA.....	26
3.6.5.	Mexico .....	26
3.6.6.	Non-ISC .....	26
4.	Integrated model description.....	27
4.1.	Stock Synthesis software.....	27
4.2.	General characteristics .....	27
4.2.1.	Assessment strategy .....	27
4.2.2.	Parameter estimation.....	28
4.2.3.	Data weighting .....	28
4.2.4.	Uncertainty characterization .....	29
4.3.	Model structure .....	30
4.3.1.	Population dynamics.....	30
4.3.2.	Sex structure.....	30
4.3.3.	Recruitment.....	30
4.3.4.	Initial population state.....	31
4.3.5.	Growth .....	31
4.3.6.	Natural mortality.....	32
4.3.7.	Maturity and fecundity.....	32
4.3.8.	Length-weight relationship .....	32
4.3.9.	Plus group .....	33
4.4.	Fishery dynamics.....	33
4.4.1.	Input fishery data .....	33
4.4.2.	Initial fishing mortality .....	33
4.4.3.	Selectivity .....	33
4.5.	Likelihood components.....	34
4.6.	Stock assessment model diagnostics .....	34
4.6.1.	Residual analysis.....	35
4.6.2.	Age-structured production model (ASPM).....	35
4.6.3.	$R_0$ profile.....	35
4.6.4.	Retrospective analysis.....	36
4.6.5.	Hindcast cross-validation.....	36
4.6.6.	Jitter analysis.....	36
4.7.	Future projections.....	37
5.	Model runs .....	37
5.1.	Developments since the 2017 stock assessment .....	37
5.2.	Model ensemble .....	37
5.2.1.	S6_base model .....	38
5.2.2.	S11_base model .....	38
5.2.3.	S11_ess model.....	38
5.3.	Sensitivity analysis.....	38
5.3.1.	Alternative mortality schedule.....	38
5.3.2.	Alternative initial equilibrium catch .....	39
5.3.3.	Multiple abundance indices for late periods .....	39
5.3.4.	Alternative spawner recruit function .....	39

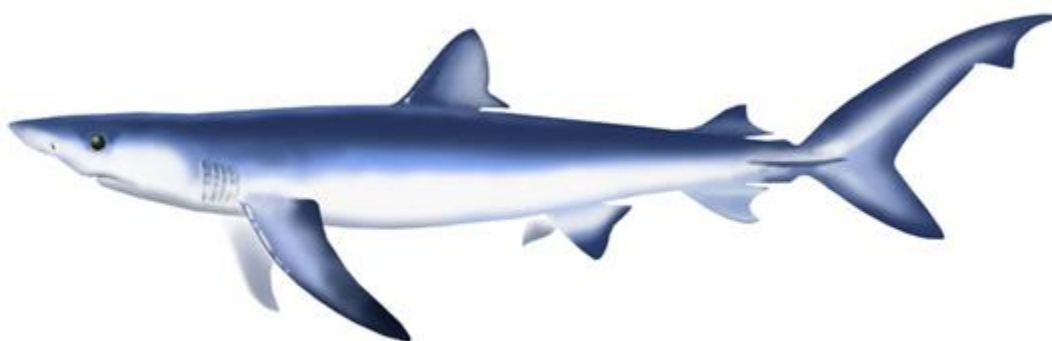
5.3.5.	Alternative Beverton-Holt steepness (h).....	39
5.3.6.	Alternative Sigma-R .....	39
5.3.7.	Alternative selectivity function for Taiwanese large scale longline fleet .....	39
5.3.8.	Alternative high seas small and large mesh driftnet catches .....	40
5.3.9.	Alternative high seas squid driftnet catch.....	40
5.3.10.	Alternative annual catch for Non-ISC member countries.....	40
5.3.11.	Alternative annual catch for Hawaii longline fleets .....	40
5.3.12.	Alternative SS model configuration (mimic 2017 BSH SS3 model) .....	40
6.	Model Results .....	41
6.1.	Model ensemble .....	41
6.1.1.	S6_base model .....	41
6.1.2.	S11_base model .....	42
6.1.3.	S11_ess model.....	43
6.2.	Sensitivity analysis.....	45
6.2.1.	Alternative mortality schedule.....	45
6.2.2.	Alternative initial equilibrium catch .....	45
6.2.3.	Multiple abundance indices for late periods .....	45
6.2.4.	Alternative spawner recruit function .....	46
6.2.5.	Alternative Beverton-Holt steepness (h).....	46
6.2.6.	Alternative Sigma-R .....	46
6.2.7.	Alternative selectivity function for Taiwanese large scale longline .....	46
6.2.8.	Alternative high seas small and large mesh driftnet catches .....	46
6.2.9.	Alternative high seas squid driftnet catch.....	46
6.2.10.	Alternative annual catch for Non-ISC member countries.....	46
6.2.11.	Alternative annual catch for Hawaii longline fleets .....	47
6.2.12.	Alternative SS model configuration (mimic 2017 BSH SS3 model) .....	47
6.3.	Model ensemble results.....	47
7.	Stock status and conservation conclusions .....	47
7.1.	Status of the stock .....	47
7.2.	Conservation information.....	48
8.	Discussions .....	49
8.1.	General remarks .....	49
8.2.	Improvements to the assessment.....	50
8.3.	Challenges .....	51
8.4.	Future stock assessment modeling considerations.....	52
8.5.	Research recommendations.....	52
9.	Acknowledgement .....	53
10.	References.....	54
11.	Tables .....	62
12.	Figures .....	81
13.	Appendix.....	138

*ANNEX 12***STOCK ASSESSMENT AND FUTURE PROJECTIONS OF BLUE SHARKS IN THE  
NORTH PACIFIC OCEAN THROUGH 2020**

*International Scientific Committee for Tuna and Tuna-Like Species  
in the North Pacific Ocean (ISC)*

12-18 July 2022

Hawaii, USA

**EXECUTIVE SUMMARY**

This document presents the results of the stock assessment for blue sharks in the North Pacific Ocean conducted by the ISC SHARKWG using a fully integrated, size-based, age-, and sex-structured model. The last stock assessment was conducted in 2017. Improvements and updates in the current assessment include: updated time series data through 2020 (catch, abundance indices, and sex-specific length composition from multiple fisheries), incorporation of new biological information, consideration of an alternative CPUE (catch-per-unit-effort) hypothesis for the late model period, and adoption of an ensemble modeling approach.

**Stock Identification and Distribution**

Blue sharks (BSH) are widely distributed throughout the temperate and tropical waters in the Pacific Ocean. The ISC SHARKWG recognizes two stocks in the North and South Pacific, respectively, based on biological and fishery evidence. Relatively few BSH are encountered in the tropical equatorial waters separating the two stocks. Tagging data demonstrate long distance movements and a high degree of mixing of BSH across the North Pacific Ocean. However, there is evidence of spatial and temporal structure by size and sex.

**Catch History**

Catch records for BSH in the North Pacific Ocean are limited and, where lacking, have been estimated using statistical models and information from a combination of historical landing data, fishery logbooks, observer records, and research surveys. In these analyses, estimated BSH catch data refer to total dead removals, including retained catch and dead discards. Estimated catch

data in the North Pacific Ocean date back to 1971, although longline and driftnet fisheries targeting tunas and billfish earlier in the 20<sup>th</sup> century likely caught BSH. The nations catching most BSH in the North Pacific Ocean include Japan, Chinese-Taipei, Mexico, and the USA, and account for more than 90 % of the estimated catch over the assessment period (**Figure E1**). Estimated catches of BSH were highest from 1976 to 1989, with an estimated peak catch of approximately 70,895 metric tons (mt) in 1981. Over the past decade, BSH estimated catches in the North Pacific Ocean have stabilized to an average of 29,613 mt annually from 2011-to 2020 (26,468-34,097 mt). While a variety of fishing gears catch BSH, most are caught in longline fisheries (89-97 % of total catch) after the ban on high-seas driftnet fisheries in 1993.

### **Data and Assessment**

Annual catch estimates were derived for a variety of fisheries by nation. Catch and size composition data were grouped into 20 fisheries from 1971 to 2020. Standardized CPUE data used to measure trends in relative abundance were provided by Chinese-Taipei, Japan, Mexico, the Pacific Community (SPC) Oceanic Fisheries Programme, and the USA.

The BSH in the North Pacific Ocean was assessed using a fully integrated, size-based, age-, and sex-structured model, Stock Synthesis (SS3; V3.30.19.01), fit to time series of standardized CPUE and sex-specific size composition data. Sex-specific growth curves and natural mortality rates were used to account for the sexual dimorphism of adult BSHs. A low-fecundity stock-recruitment relationship (SR) was used in the previous assessment to explain the lower survival ratio before recruitment after partition. ISC SHARKWG, however, recognized that more research is needed before the SR option is fully operationalized in this assessment because the parameters ( $\alpha$  and  $\beta$ ) of the low-fecundity SR were based on strong assumptions relating to the unfished stock-recruitment relationship. The ISC SHARKWG therefore determined to use a Beverton-Holt SR, which has been commonly used in the assessment of BSHs and other pelagic sharks in other oceans.

Input parameter values for models considered in the ensemble were chosen based on the best available information regarding the life history of BSH in the North Pacific Ocean and knowledge of the historical catch time series and existing fishery data. Standardized CPUE from the Japanese Kinkai shallow (Japanese offshore and distant-water longline shallow-set) fleets that operate out of Hokkaido and Tohoku ports for the early period (1976-1993) was used for all models in the ensemble (S5 index; **Figure E2**). For the late period (1994-2020), two indices were considered as measures of relative population abundance in the model ensemble: the Japanese Kinkai shallow index (S6; **Figure E2**) and a Dynamic Factor Analysis (DFA) composite index (S11; **Figure E2**). The composite-CPUE was derived using DFA applied to three candidate indices: Hawaii deep-set longline index; Taiwanese large-scale longline index; Japanese research and training vessel deep-set longline. The Japanese Kinkai shallow longline index comes from a fishery that seasonally targets BSH and covers a wide operational area in the main distribution area of BSH, encounters BSH across a large size range, and has a long operational period. The DFA-derived CPUE index combines three indices that show similar trends in CPUE and are derived from observer data or research and training vessel data. The combined index represents fisheries that primarily target tunas via deep-setting behavior across a broad range of the central Pacific Ocean and typically select larger individuals relative to the Japanese shallow-set index.

Models were fit to relative abundance indices and size composition data in a likelihood-based statistical framework. Maximum likelihood estimates of model parameters, derived outputs, and their variances were used to characterize stock status across the three models in the ensemble and to develop stock projections.

A model ensemble was used because a comparison of model fits to the Japanese Kinkai shallow longline index (S6) used in the previous assessment and model fits to the composite-CPUE index (S11), as well as other commonly used model diagnostics (fit comparisons, residual analysis,  $R_0$ -profile, Age-Structured-Production-Model, Retrospective analysis, and Jitter analysis), did not conclusively identify a better model. Both models showed retrospective bias in the estimation of absolute biomass and fishing mortality. This issue was improved in the composite-CPUE model by down weighting the large input sample sizes for the Taiwanese small scale longline length composition data in 2018 and 2020. Accordingly, the composite-CPUE model was separated into two hypotheses with and without the down-weighting of the Taiwanese size data from small scale longline fishery in 2018 and 2020. Based on the results of these analyses, uncertainty regarding the choice of BSH abundance indices led to a three-model ensemble approach for this assessment. The model ensemble assumed equal weighting (50%) for the two CPUE hypotheses, with the composite CPUE hypothesis further separated into two sub-hypotheses with equal weighting (each 25% of the total ensemble weight) for the models with and without down-weighting of the Taiwanese size data from small scale longline fishery.

Stock projections of biomass and catch for BSH in the North Pacific Ocean from 2021 to 2030 were conducted assuming four alternative fishing mortality (F) scenarios: 1) F of the average level for 2017-2019 ( $F_{2017-2019}$ ); 2) F at the maximum sustainable yield (MSY) ( $F_{MSY}$ ); 3) 20% higher F than average value ( $F_{20\%plus}$ ); 4) 20% lower F than average value ( $F_{20\%minus}$ ). Recruitment was assumed to follow the SR with the sigma-R and selectivity parameters fixed to the value from the terminal year in 2020.

## Projections

Uncertainty in stock status for the main assessment and projection periods was characterized across the ensemble using 100,000 samples from a multivariate lognormal (MVLN) parametric bootstrap. The median for each management quantity and associated uncertainty (e.g., 80th percentile) was derived from the combined distribution of bootstrapping for three models to more completely capture the structural and estimation uncertainty in stock status. Additionally, 27 one-off sensitivity analyses were conducted across the ensemble with alternative data/parameters to explore uncertainty in the input data and life history parameters that were not already captured in the three ensemble models.

## Stock Status

The current assessment provides the best available scientific information on North Pacific BSH stock status. The assessment used a fully integrated approach in SS3 with model inputs that have been updated since the previous assessment. The main difference between the present assessment and the 2017 assessment was 1) the use of an ensemble approach combining three models assuming alternative late period CPUE hypotheses and data weighting. Other differences were 2) catch, CPUE and size time series updated through 2019/2020; 3) improvements to the catch estimation and size data of the driftnet fishery and Non-ISC fishery ;4) improved life history

information, such as growth and reproductive biology, and their contribution to productivity assumptions; 5) reconsideration of SR using the Beverton-Holt model; and 6) application of an improved suite of model diagnostics.

Target and limit reference points have not yet been established for pelagic sharks in the Pacific Ocean by either the WCPFC or the IATTC. Stock status was reported in relation to MSY-based reference points. The following information on the status of North Pacific BSH was provided. The median of the annual spawning stock biomass (SSB) from the model ensemble had a steadily decreasing trend until 1992 and slightly increased until recent years (**Figure E3-A, B**). The median of the annual F from the model ensemble gradually increased in the late 1970s and 1980s and suddenly dropped around 1990, which slightly preceded the high-seas drift gillnet fishing ban, after which it has been slightly decreasing (**Figure E3-C, D**). The median of the annual age-0 recruitment estimates from the model ensemble appeared relatively stable with a slightly decreasing trend over the assessment period except for 1988, which shows a large pulse (**Figure E3-E**). The historical trajectories of stock status from the model ensemble revealed that North Pacific BSH had experienced some level of depletion and overfishing in previous years, showing that the trajectories moved through the overfishing zone, overfished and overfishing zone, and overfished zone in the Kobe plots relative to MSY reference points (**Figure E4**). However, in the last two decades, median estimates of the stock condition returned into the not overfished and not overfishing zone.

The following information on the status of the North Pacific BSH is provided:

1. **Median female SSB in 2020 was estimated to be 1.170 of  $SSB_{MSY}$  (80<sup>th</sup> percentile, 0.570 - 1.776) and is likely (63.5% probability) not in an overfished condition relative to MSY-based reference points.**
2. **Recent annual F ( $F_{2017-2019}$ ) is estimated to be below  $F_{MSY}$  and overfishing of the stock is very likely (91.9% probability) not occurring relative to MSY-based reference points.**
3. **The base case model results show that there is a 61.9% joint probability that NPO BSH stock is not in an overfished condition and that overfishing is not occurring relative to MSY based reference points.**

### Conservation Information

Stock projections of biomass and catch of NPO BSH from 2020 to 2030 were performed assuming four different harvest policies:  $F_{current}$  (2017-2019),  $F_{MSY}$ ,  $F_{current+20\%}$ , and  $F_{current-20\%}$  and evaluated relative to MSY-based reference points (**Figure E5**). Based on these findings, the following conservation information is provided:

1. **Future projections in three of the four harvest scenarios ( $F_{current}$  (2017-2019),  $F_{current+20\%}$ , and  $F_{current-20\%}$ ) showed that median SSB in the North Pacific Ocean will likely (>50 probability) increase; the  $F_{MSY}$  harvest scenario led to a decrease in median SSB.**
2. **Median estimated SSB of BSH in the North Pacific Ocean will likely (>50 probability) remain above  $SSB_{MSY}$  in the next ten years for all scenarios except  $F_{MSY}$ ; harvesting at  $F_{MSY}$  decreases SSB below  $SSB_{MSY}$  (Figure E5).**
3. **There remain some uncertainties in the time series based on the quality (observer vs.**

**logbook) and timespans of catch and relative abundance indices, limited size composition data for several fisheries, the potential for additional catch not accounted for in the assessment, and uncertainty regarding life history parameters. Continued improvements in the monitoring of BSH catches, including recording the size and sex of sharks retained and discarded for all fisheries, as well as continued research into the biology, ecology, and spatial structure of BSH in the North Pacific Ocean are recommended.**

### **Special note**

The decision to adopt an ensemble modelling approach from single base-case modelling approach was made late in the assessment model development process when it became apparent that there was no clear best base-case model. While a consensus on adopting a model ensemble approach was reached and the SHARKWG showed flexibility in adapting to the challenges imposed by the late change on its identification, understanding, development, and discussion of appropriateness of the candidate models. Although timelines can be adjusted to give more opportunity for discussion of key model developments, the SHARKWG should maintain the flexibility shown in the current assessment to adapt to unforeseen aspects of model development.

The SHARKWG notes that uncertainty in stock status in the current assessment is likely still underrepresented as the model ensemble did not consider key uncertainties such as natural mortality or stock-recruitment resilience which are not well-known for many shark species. In the future the SHARKWG will ensure that the model ensemble is informed by the sensitivity analyses.

**Table E1.** Estimates (median and 80<sup>th</sup> percentiles) of key management quantities for the North Pacific blue shark SS3 stock assessment model ensemble.

Management Quantity	Unit	Model Ensemble	80th percentile of bootstrapping
$B_0^*$	t	1,214,595	
$SSB_0^*$	t	222,736	
$\ln(R_0)^*$	numbers	9.559268	
$SSB_{1971}^*$	t	158,324	
$SSB_{1972}$	t	149,903	104,977 – 223,884
$SSB_{2020}$	t	92,954	38,695 – 179,870
$SSB_{MSY}^*$	t	83,545	
$F_{1971}^*$	per year	0.36	
$F_{1971}$	per year	0.26	0.16 - 0.42
$F_{2017-2019}$	per year	0.33	0.18 - 0.74
$F_{MSY}^*$	per year	0.76	
$SSB_{2020}/SSB_{MSY}$		1.17	0.570-1.776
$F_{2017-2019}/F_{MSY}$		0.445	0.236-1.011
$P(SSB_{2020} > SSB_{MSY})$		63.5%	
$P(F_{2017-2019} < F_{MSY})$		91.9%	
$P(SSB_{2020} > SSB_{MSY}$ and $F_{2017-2019} < F_{MSY})$		61.9%	

\*The weighted mean across the ensemble is given for these quantities since it is unavailable from the parametric bootstrap.

**Table E2.** Projected trajectory (median) of spawning stock biomass (in metric tons) for alternative harvest scenarios.

Year	Average F +20%	$F_{MSY}$	Average F -20%	Average $F_{2017-2019}$
2021	91,469	92,158	91,707	91,613
2022	90,826	85,954	92,096	91,489
2023	91,044	83,524	93,902	92,240
2024	93,878	82,681	98,034	94,718
2025	95,195	81,283	102,324	97,349
2026	99,385	81,482	106,332	99,853
2027	101,943	81,391	110,446	103,502
2028	104,333	81,296	114,099	105,987
2029	106,374	81,005	117,424	108,386
2030	108,041	80,770	120,542	110,949

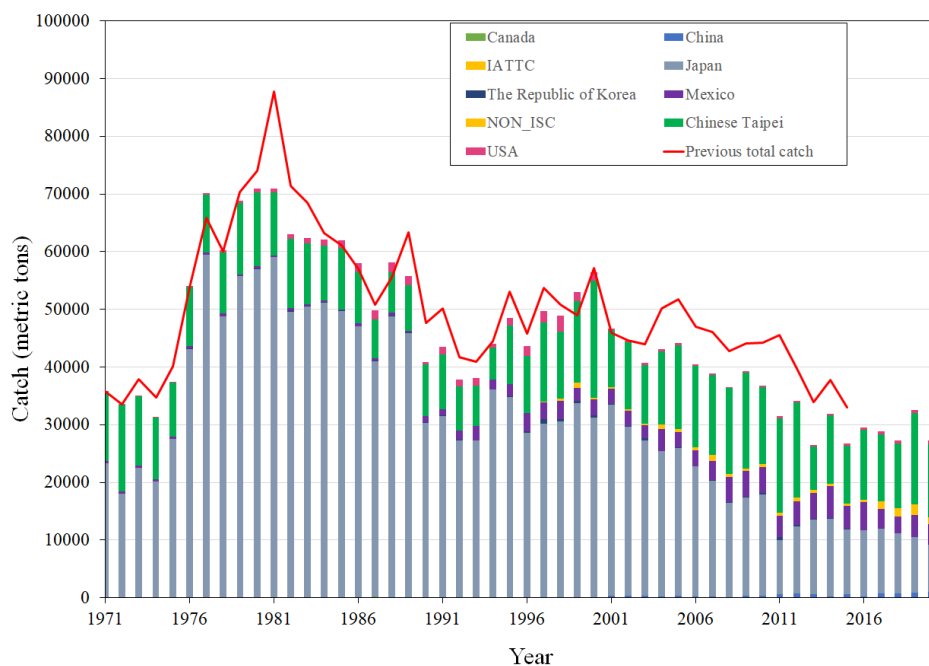


**Figure E1.** Total catch (total dead removals) of North Pacific blue shark by nation or region.

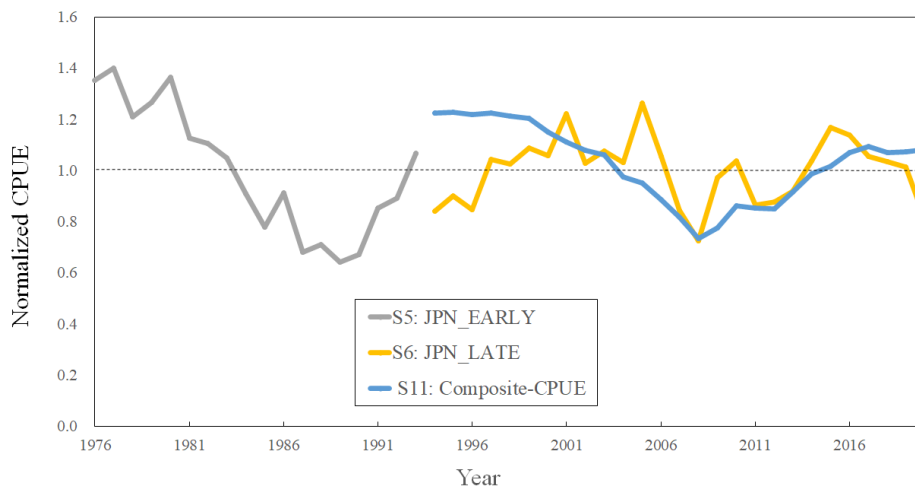


**Figure 2E.** Annual standardized CPUE of North Pacific blue shark during 1976 through 1993 (Japanese Kinkai shallow longline: JPN\_EARLY) and two standardized CPUE time series of blue shark between 1994 and 2020 (Japanese Kinkai shallow longline: JPN\_LATE, DFA\_LATE with Hawaii deep-set longline, Taiwanese large-scale longline and Japanese research and training vessel)

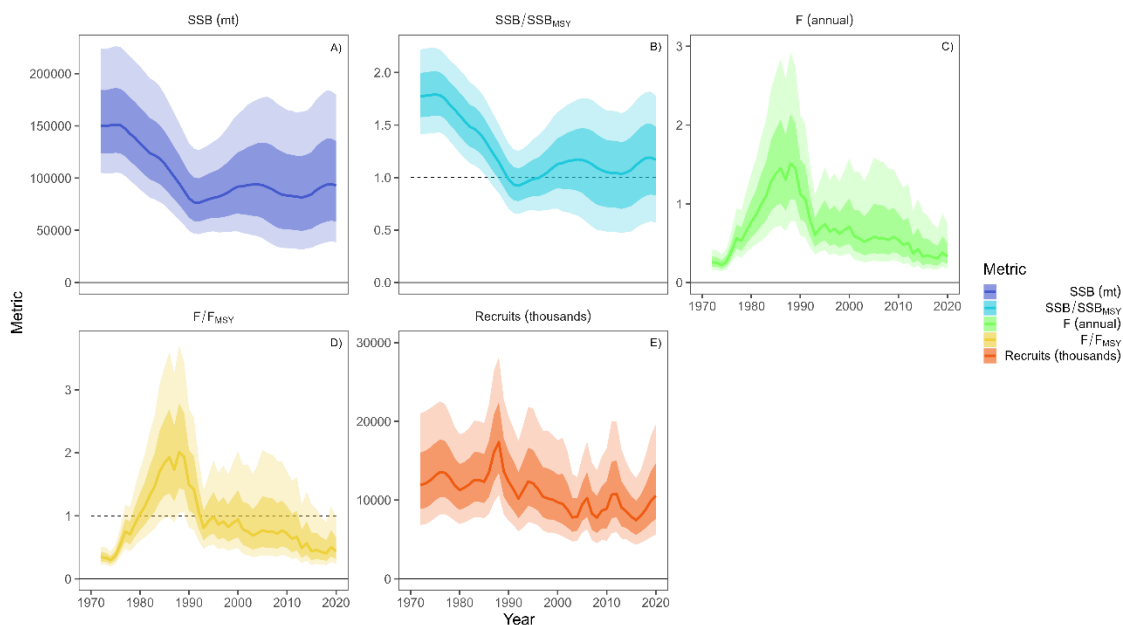


**Figure 3E.** Results of the SS3 stock assessment model ensemble: (upper left) estimated female spawning stock biomass (SSB; metric tons) relative to MSY level (horizontal broken line); (upper middle) estimated fishing mortality (sum of  $F$ 's across all fishing fleets) relative to MSY level (horizontal broken line); (upper right) estimated female SSB; (lower left) estimated fishing mortality (sum of  $F$ 's across all fishing fleets); (lower middle) estimated age-0 recruits. Light and dark shaded areas of all figures denote 80 and 50% percentiles around the median estimate, respectively.

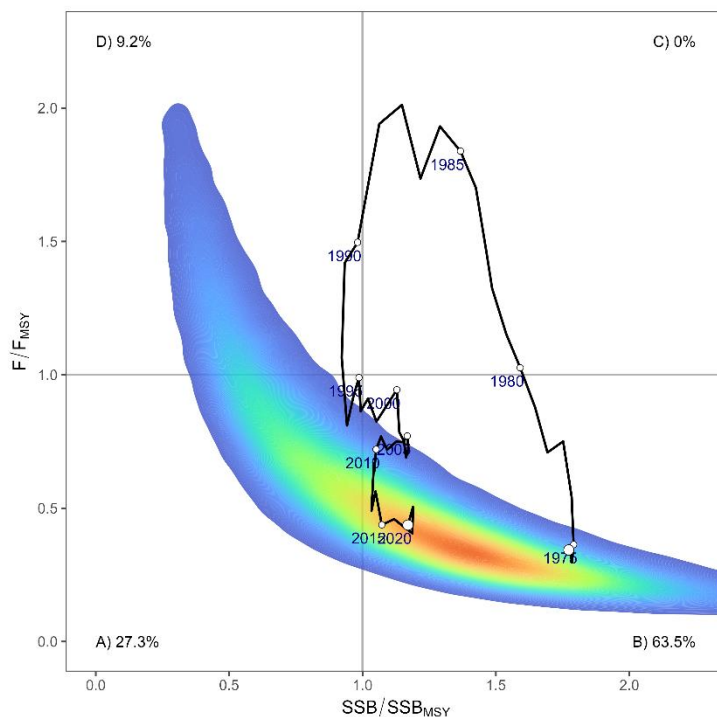


**Figure 4E.** Kobe plots of the historical trends in estimates of relative fishing mortality ( $F$ ) and spawning stock biomass (SSB) of North Pacific blue shark between 1971-2020 for the ensemble model and the density plot of the uncertainty (warmer color indicates higher probability of the stock status). Each zone denotes the stock status of a) overfished and not overfishing zone, b) not overfishing and not overfished zone, c) overfishing and not overfished zone, and d) overfishing and overfished zone relative to MSY reference points.

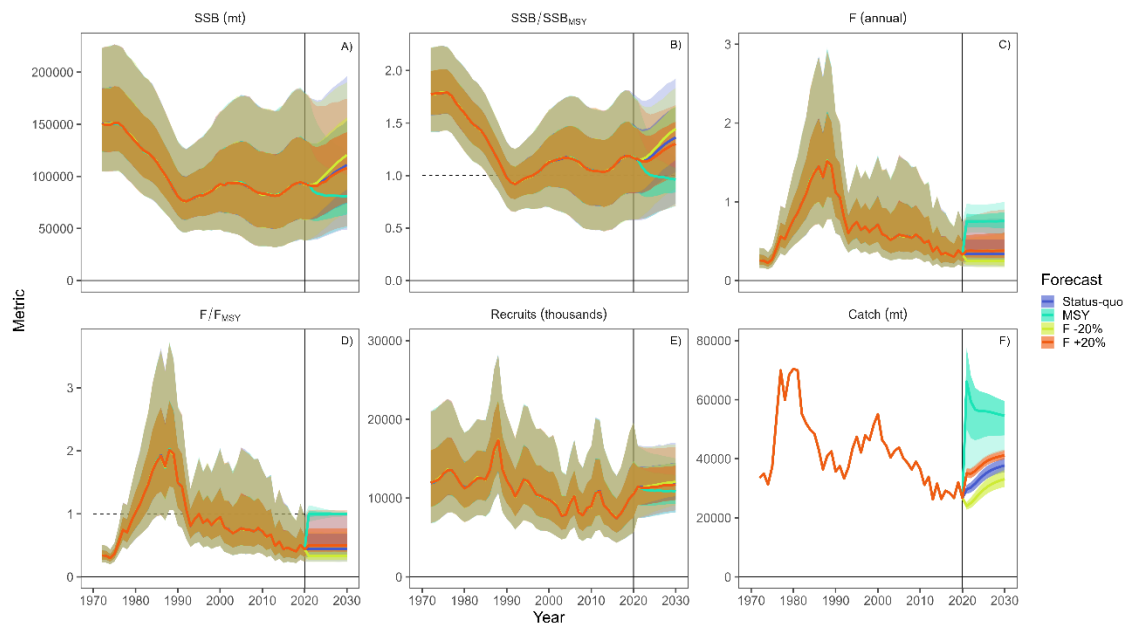


**Figure 5E.** Comparison of future projected north Pacific blue shark female spawning stock biomass (SSB) under different fishing mortality ( $F$ ) harvest policies (*status quo*, +20%, -20%, and  $F_{MSY}$ ) using the SS reference case model. *Status quo* fishing mortality was based on the average from 2017-2019.

## 1. INTRODUCTION

Blue shark (*Prionace glauca*) (BSH) is considered a highly migratory species (HMS) under the United Nations Convention on the Law of the Sea (ANNEX I)<sup>1</sup>. They are a commonly occurring species found primarily in the photic zone of temperate and tropical waters around the world. BSH populations are impacted by many fisheries as both a target and non-target component of catches, and their flesh is commonly consumed.

Historically, BSHs were caught as bycatch in fisheries targeting other species, primarily high seas tuna and swordfish fisheries (Ito et al., 1993; Nakano, 1994). However, as new processing techniques have developed, it has led to new markets, particularly in Asia (Clarke et al., 2007) and Mexico (Sosa-Nishizaki et al., 2002). As a result of new food products like surimi, fishing fleets have likely targeted BSH for at least two decades. Up through the 1980s shark catch was only loosely monitored and often aggregated as “shark” in vessel logbooks and landings receipts but starting in the 1990’s, conservation concerns about fisheries bycatch motivated the development and expansion of fishery observer programs and better record keeping.

To address uncertainty about the conservation status of high seas shark stocks in the North Pacific Ocean, the International Scientific Committee for Tuna and Tuna-like Species (ISC) created a Shark Working Group (SHARKWG or WG) in 2011 to begin compiling the necessary information to conduct stock assessments. The SHARKWG conducted its first assessment of BSH stock status in the North Pacific Ocean in 2013 and followed up with an update in 2014 to address requests from the Western and Central Pacific Fisheries Commission (WCPFC) about the former assessment (ISC, 2014; Rice et al., 2014; Takahashi et al., 2014). Upon adopting the 2014 assessment, the ISC and WCPFC concluded that the stock biomass ( $B$ ) was well above the maximum sustainable yield (MSY) level ( $B_{MSY}$ ) and fishing mortality ( $F$ ) below the MSY level ( $F_{MSY}$ ) as of 2011, and had been since the mid-1990s. The 2014 assessment was conducted using both a fully integrated age-structured assessment model (SS3: Stock Synthesis; Methot and Wetzel, 2013) and a surplus production model (BSPM: Bayesian Surplus Production Model; McAllister et al., 2006). The BSPM was the primary assessment model from which stock status conclusions were drawn due to uncertainty about the quality of size composition data available at the time and the need to conduct more biological research on the stock-recruitment relationship. The SHARKWG had not thoroughly examined the size data and explored fishery definitions and selectivities. In addition, due to a lack of understanding of the low-fecundity stock recruitment relationship (LFSR) (Taylor et al., 2013) and its application to BSHs, there was an incomplete specification of the model stock-recruitment relationship (SR). Thus, the primary objective moving forward from that assessment was to improve data and model fitting and conduct biological research to support the development of a more defensible age-structured assessment using a fully integrated model in 2017. The 2017 assessment was primarily conducted using SS3 (ISC, 2017). Time-series data updated through 2015 (catch, relative abundance, and sex-specific length composition from multiple fisheries), new biological information, and research into parameterization of the LFSR were available and enabled the development of an improved age-, and sex-structured model. The SHARKWG also conducted a series of models using a Bayesian State-Space Surplus Production Model (BSSPM; Carvalho et al., 2016) to facilitate comparison with the 2014 assessment (Kai et al., 2017). Based on the assessments in 2017, the ISC and

---

<sup>1</sup> United Nations Convention of the Law of the Sea as of 10 December 1982.  
[http://www.un.org/depts/los/convention\\_agreements/texts/unclos/UNCLOS-TOC.htm](http://www.un.org/depts/los/convention_agreements/texts/unclos/UNCLOS-TOC.htm)

WCPFC concluded that the spawning stock biomass (SSB) was well above  $SSB_{MSY}$  and fishing mortality below  $F_{MSY}$  in recent three years from 2013 to 2015, and had been since the mid-1990s (ISC, 2017; WCPFC, 2017).

This document presents the results of the benchmark stock assessment conducted in 2022 by ISC SHARKWG for BSH in the North Pacific Ocean using the latest version of SS3 (V3.30.19.01). Time-series data updated through 2020, new constructed catch and size data for several fleets, newly developed composite-CPUE (catch-per-unit-effort) from three standardized CPUEs for late period, new biological information, and first application of ensemble approach considering two alternative CPUE hypotheses enabled much improvement of this assessment.

## 2. BACKGROUND

BSH is one of the most abundant pelagic sharks, with a circum-global distribution in temperate to tropical waters (Compagno, 1984; Nakano and Stevens, 2008). The relative abundance in the North Pacific Ocean is highest in temperate pelagic zones and decreases in neritic and warmer tropical waters, as well as cooler waters at latitudes higher than approximately 50 degrees (Nakano, 1994). In the eastern North Pacific Ocean, they spend most of their time above 50 m in the upper mixed layer, with forays as deep as 400 m while occupying temperatures from 14-27 °C predominantly (Weng et al., 2005), and young of the year exhibited reverse diel vertical migration (Nosál, et al., 2019). They also showed spatial segregation between sex-size classes particularly in the summer months, with immature females found largely north of 33 °N, and males south of 35 °N. In fall, females traveled south, resulting in an overlap in distributions south of 37 °N (Maxwell et al., 2019). In the southwest Pacific Ocean, they have shown a similar preference for surface waters but with occasional dives in excess of 980 m while occupying comparable water temperatures to those in the eastern North Pacific Ocean (Stevens et al., 2010). In the northwestern Pacific Ocean, adult females showed a seasonal northeast-southwest migration between temperate and subtropical zones for reproduction (Fujinami, et al., 2021d), and adult males tended to stay in temperate waters but displayed seasonal longitudinal migrations (Kai et al., 2017; Fujinami et al., in prep.). Within the North Pacific Ocean, males and females smaller than 50 cm precaudal length (PCL) co-occur on the parturition grounds between approximately 35 and 40 °N. The habitat for subadults diverges between subadult females (35 and 50 °N) and males (30 and 40 °N) at around 100-150 cm PCL (Nakano, 1994). The subadult sharks in the lower latitudes, and adult habitats are believed to be more southerly, with mating thought to occur in pelagic waters between 20-40 °N (Fujinami et al., in prep.).

### 2.1. Biology

#### 2.1.1. *Stock structure*

Within the Pacific Ocean, BSHs are found in both hemispheres, with no genetic evidence of distinct hemispheric populations (King et al., 2015; Taguchi et al., 2015). However, their abundance is low in the tropics, and electronic-tagging and mark-recapture data have not documented movements across the equator (Fujinami et al, 2021d, in prep.; Kai and Fujinami, 2020; Maxwell et al., 2019; Sippel et al., 2011; Stevens et al., 2010; Weng et al., 2005). The SHARKWG concurs that current evidence justifies consideration of two distinct populations in the northern and southern hemispheres for stock assessment purposes.

### 2.1.2. *Reproduction*

Sex-specific length-frequency and satellite tracking data suggested that mating occurs in middle latitudes (20-40 °N) and pupping occurs between 35-40 °N in the northwestern Pacific Ocean and 25-50 °N in the northeastern Pacific Ocean (Fujinami et al, 2021d, in prep.; Maxwell et al., 2019; Sippel et al., 2016). Mating scars and fertilized eggs suggest mating occurs from June to August (Suda, 1953), and is corroborated by monthly changes in the observed gonadosomatic index (GSI) and maximum ova diameter (Fujinami et al., 2017; Nakano 1994). Litter size ranging from 15-112 (mean 35.5) has been observed in the northwestern Pacific Ocean (Fujinami et al., 2017) and was larger than that ranging from 1-62 (mean 25.6) reported previously in the North Pacific Ocean (Nakano, 1994). Fujinami et al. (2017) also estimated an annual cycle of female reproduction, with the potential for a small percentage of females to reproduce less frequently, although prior research indicated a biennial cycle (Joung et al., unpublished). Different gestation estimates range from 9-12 months (Cailliet and Bedford, 1983) and 11-12 months (Nakano, 1994; Fujinami et al., 2017). Overall, BSHs are considered highly productive relative to other pelagic sharks based on their younger maturation age, fecundity, and annual reproductive cycle (Cortés, 2002; Fujinami et al., 2017; Smith et al., 1998; Yokoi et al., 2017). Indeed, BSH exhibited the highest productivity among the viviparous elasmobranchs (Cortés et al. 2010), and the steepness of BSH ( $h = 0.588$ ) was higher than those for other pelagic sharks such as shortfin mako, *Isurus oxyrinchus*, ( $h < 0.36$ ) and spiny dogfish, *Squalus suckleyi*, ( $h < 0.3$ ) in the North Pacific Ocean (Kai and Fujinami, 2018; Kai, 2019; Taylor et al., 2013).

### 2.1.3. *Growth*

Pups are born at an estimated 40-50 cm fork length (FL; ~36 cm PCL) (Fujinami et al., 2017), and adults reach a maximum length of 380 cm total length (TL) (Hart, 1973). Fifty percent of females are considered mature at 156.6 cm PCL (Fujinami et al., 2017), at around 5-6 years old (Fujinami et al., 2019), and the size and age at 50% maturity for males is 161 cm PCL and about six years old, respectively (Cailliet and Bedford, 1983; Fujinami et al., 2017, 2019; Nakano, 1994). Growth models for BSH in the North Pacific Ocean have been previously estimated (Blanco-Parra et al., 2008; Cailliet and Bedford, 1983; Fujinami et al., 2019; Nakano, 1994; Tanaka et al., 1990). Factors including sample size and aging techniques varied across the earlier attempts, but recent efforts of the SHARKWG are focusing on corroborating age reading across studies, standardizing aging techniques, increasing sample sizes and collecting samples across a wider geographic range (Fujinami et al., 2018, 2019; ISC 2019).

## 2.2. Fisheries

The primary sources of known BSH fishing mortality are oceanic longline fisheries targeting swordfish and tuna, including mostly shallow-set longline fisheries in temperate waters (Hiraoka et al., 2016; Kai et al., 2017), and deep-set longline fisheries in more tropical areas (Kai, 2019). Sharks are targeted less often than tunas and swordfish, but new Asian shark markets have been developing for over a decade and are a common bycatch in these fisheries (Clarke et al., 2013). BSH bycatch is often discarded at sea, and the survivorship of those released depends on the condition of the released animals and environmental conditions (FAO, 2017). A study of the Canadian pelagic longline fishery in the Atlantic Ocean showed that more than 85% of BSHs survive after being hooked by a longline, and estimates of the post-release mortality rate based

on pop-off tagging was 9.8% (Campana et al., 2016). In addition, post-release mortality of BSHs released alive from longline fishing gear was reported to be 9-17% to 30 days after the release in the central Pacific Ocean (Hutchinson et al., 2021; Musyl and Gilman, 2018). Although these results indicated higher survival ratios for BSH, a recent study indicated that trailing gear at a shark's release appeared to be one of the interaction conditions that has a large impact on survival for BSH, and post release mortality with long trailing gear (17m) was reported to be 27% in 30 days (Hutchinson et al., 2021).

### **2.3. Previous stock assessments**

The SHARKWG conducted three benchmark stock assessments in the past. The first assessment was conducted using only a Bayesian Surplus Production (BSP) model, which was not adopted for management and was subsequently updated (ISC, 2013). Before these assessments, Kleiber et al. (2009) assessed the stock using data from the WCPFC (excluding the EPO) with a BSP model and a catch-at-length model. The second assessment was conducted using two different assessment models: a BSP model, and a catch-at-length analysis using SS3 (ISC, 2014). The most recent assessment was conducted in 2017 using an age-structured statistical catch-at-length model, Stock Synthesis (SS3; Methot and Wetzel, 2013), fit to time series of standardized CPUE and sex-specific size composition data (ISC, 2017). Sex-specific growth curves and natural mortality rates were used to account for the sexual dimorphism of adult BSHs. A low fecundity stock recruitment (LFSR) relationship was used to characterize the productivity of the stock based on plausible life history information available for North Pacific BSHs. Maximum likelihood estimates of model parameters, derived outputs, and their variances were used to characterize stock status based on a reference case and to develop stock projections. Results of the 2017 reference case model showed that female SSB in 2015 was 71% higher than  $SSB_{MSY}$  and the recent annual F (2012-2014) was estimated at approximately 37% of  $F_{MSY}$ . Therefore, according to the 2017 stock assessment, the stock was not overfished and overfishing was not occurring if MSY-based reference points were used.

## **3. DATA**

### **3.1. Spatial stratification**

This assessment assumes a single stock in the North Pacific Ocean, north of the equator (**Figure 1**).

### **3.2. Temporal stratification**

An annual (January 1– December 31) time-series of fishery data for 1971-2020 was used for the assessment.

### **3.3. Definition of fisheries**

The SHARKWG estimated catches of many fisheries from different nations and ISC member sources. Twenty different fisheries were defined (**Table 1, Figure 2**).

### 3.4. Catch data

Catches (metric tons) were provided by ISC member nations and cooperating partners (**Figure 2, Table 2**). The annual catch data includes catches from 20 fleets of 7 countries (Canada, China, Chinese-Taipei/Taiwan, Japan, Mexico, the Republic of Korea, and US) and two international organizations (IATTC; Inter American Tropical Tuna Commission and Pacific Community (SPC) Oceanic Fisheries Programme/Non-ISC countries). As in the 2017 assessments, the highest catches came from Japan, Taiwan, and Mexico. The primary sources of catch were from longline and drift gillnet fisheries, with smaller catches estimated from purse seine, trap, troll, trawl, and recreational fisheries. Catches were comprised of total dead removals, which included landings and discard mortalities. All the catch data were in whole weight (metric tons) except for three fleets with catch in 1000s of fish; small-mesh (high seas) squid driftnet fishery (F11: SM\_MESH), Hawaii deep-set longline fishery (F17: US\_HW\_DP), and Hawaii shallow-set longline fishery (F18: US\_HW\_SH). The fleet definitions were changed from the 2017 assessment by separating the Japanese large-mesh driftnet fishery into two fleets (F8: JPN\_LG\_MESH\_EARLY; F9: JPN\_LG\_MESH\_LATE) and the Hawaii longline fleet into two fleets (i.e., F17 and F18) compared to the previous stock assessment (ISC, 2017). Japan separated the large-mesh driftnet fishery into two fleets (F8 and F9) because the operation area of this fishery had changed from the high seas to coastal and offshore areas within the exclusive economic zone (EEZ) of Japan after the ban of the high-seas driftnet fishery in 1993 (Ito et al., 1993), and the catch for the early period for 1973-1993 (F8) was reconstructed (Fujinami et al., 2021a). The separation of the Hawaii longline fleet into shallow- and deep- sets was motivated by the different target species of both fleets, with different operation time/area and gear configurations that resulted in the catch of different sizes of BSHs. The US also reconstructed the catch of these longline fleets (F17 and F18) for 1992-2020 using a machine learning approach and rescaled the 1971-1991 catch based on the historical bigeye tuna catch using a catch-ratio calculated from the recent period (Ducharme-Barth et al., 2021, 2022a). For the annual catches of other fleets, Mexico reconstructed the catch for 1975-2006 (Sosa-Nishizaki and Castillo-Geniz, 2016). In addition to the update of the recent catch for 2016-2020 (F1: MEX), Japan reconstructed the catch of four longline fleets (F4: JPN\_KK\_SH, F5: JPN\_KK\_DP, F6: JPN\_ENY\_SH, and F7: JPN\_ENY\_DP) for 1994-2020 and one coastal and other fleet for 1994-2019 (F10: JPN\_CST\_OTH). The annual catch of high seas squid driftnet fisheries for 1979-1992 (F11) was reconstructed using the estimated catch of three countries; Japan (Fujinami et al., 2021b), the Republic of Korea and Chinese-Taipei (Kai et al., 2022a). The Republic of Korea reconstructed the catch of longline fishery from 1982 to 2020 (F13: KOREA). The catch of Non-ISC member countries (F14: NON-ISC) for 1997-2020 was reconstructed using the observed CPUE of longline fishery and reported total fishing effort in addition to the small catch of purse seine fishery (Kai et al., 2022b). The catches in 1995 and 1996 were replaced by the catch in 1997 to complement a lack of catch data for the periods. The catches of the other fleets were merely updated through 2020.

Annual catch by fleet indicated that most catches were made by F4, F7 and F20 throughout the assessment period (**Table 2, Figure 2**). The annual trends of catch increased in the 1970s, reached a peak in 1981 and then decreased until 1992. After that, the catch increased until 2000 and gradually decreased until recent years. In the 1980s and the early 1990s, the driftnet fisheries (F8 and F11) had large amounts of catch. The catch of the Mexican fleet has been increasing since 1990, and the proportion of the catch in recent years to total catch has increased

substantially. The annual catch from the 2017 assessment had a similar trend in total catch to this assessment.

### 3.4.1. Japan

Japan (JPN) provided estimated catch for four sectors of their longline fisheries categorized by vessel tonnage and gear configurations (F4\_JPN\_KK\_SH; F5\_JPN\_KK\_DP; F6\_JPN\_ENY\_SHL; F7\_JPN\_ENY\_DP). Offshore (Kinkai; KK) and distant-water (Enyo; ENY) longline was categorized as vessels with capacity between 20 and 120 GT (Gross tonnage) and larger than 120 GT, respectively, and these two-longline catches were further categorized as shallow-set (SH) and deep-set (DP), based on the gear configuration (number of hooks between floats; HBF, shallow-set - HBF < 6, and deep-set - HBF > 5). The landings of sharks were frequently underestimated due to the lower catches and the relatively higher proportion discarded compared to that of teleost species (e.g., tunas and billfish). Therefore, the total catches, including retained and discard/released catches, were estimated using a product of the yearly standardized CPUE and fishing effort. The estimates were separated into two time-series (1976–1993 and 1994–2020) because species disaggregated shark catch data were only available after 1993. The former early-period CPUE (1976–1993) was estimated by Hiraoka et al. (2013a) and the latter later-period CPUEs (1994–2020) for shallow- and deep- set were estimated by Kai (2021a, b). The catch in number for the former and latter periods were converted into biomass using the mean body weight by season and area (Hiraoka et al., 2013a). The detailed estimation method and the estimated catch amount can be found in Kai (2021c).

Japan also provided three catch time series for driftnet fisheries (F8\_JPN\_LG\_MESH\_EARLY; F9\_JPN\_LG\_MESH\_LATE; F11\_SM\_MESH) and a catch time series for a miscellaneous coastal fishery (F10\_JPN\_CST\_Oth). Before the United Nations moratorium on high seas large-scale pelagic driftnet fisheries implemented on 31 December 1992, Japanese driftnet fisheries in the North Pacific Ocean consisted of a large mesh driftnet fishery (F8\_JPN\_LG\_MESH\_EARLY) and a small mesh driftnet fishery (F11\_SM\_MESH) operating in the high seas (Ito et al., 1993). The large mesh driftnet fishery primarily targeted billfish (mainly striped marlin *Kajikia audax*) near coastal waters of Japan in the 1970's, and the main target species of this fishery changed to albacore (*Thunnus alalunga*) in 1980's, as the fishing ground expanded towards offshore and far-seas areas (Nakano et al. 1993; Kiyofuji et al. 2017). Meanwhile, the small mesh driftnet fishery commenced operations in 1978 and targeted flying squid (*Ommastrephes bartrami*) in the high seas (Yatsu et al., 1993). Due to the development of the fishery, a substantial number of sharks were caught by these driftnet fisheries as non-target species, especially BSH in the 1980s and the beginning of 1990s (McKinnell and Seki, 1998). For the estimation of annual catches for BSH caught by the large mesh driftnet fishery, the ratio of BSH to all sharks from the observer data and the catches in weight of all sharks reported by the Japanese statistical yearbook (“Norin-toukei”) were used (Fujinami et al., 2021a). For the estimation of annual catches for BSH caught by the small mesh driftnet fishery, the estimated coefficients from four statistical models (different model structures of generalized linear model and generalized additive model from simple to complex) of BSH catch based on scientific observer data, were used with explanatory variables from logbook data to predict the annual BSH catches (Fujinami et al., 2021b). Although the small mesh driftnet fishery was closed in the high seas after December 1992, the Japanese large mesh driftnet fishery (F9\_JPN\_LG\_MESH\_LATE) targeting mainly swordfish (*Xiphias gladius*) and striped marlin

continued to operate within Japan's exclusive economic zone, and the annual catch was updated through 2019 (Kai and Yano, 2021). The value in 2020 was tentatively assumed to be the same as in 2019. Since most of the official coastal landing data (coastal and other longline, set-net, bait fishing, and others; F10\_JPN\_CST\_Oth) for sharks were reported in an aggregated form as "sharks," annual catches of Japanese coastal fishery were estimated using the research data for the ratios of the catch of BSH to all sharks by fishing gear, and then the annual catch was updated through 2019 (Kimoto et al., 2012; Kai and Yano, 2021). Again, the 2020 value was tentatively assumed to be the same as in 2019.

### 3.4.2. *Chinese-Taipei (Taiwan)*

Chinese-Taipei (Taiwan) provided estimated catch for two sectors of their longline fisheries categorized by vessel tonnage (F19\_TAIW\_LG; F20\_TAIW\_SM). The large-scale longline vessels larger than 100 GT operated in the broad range of the North Pacific Ocean (145°E to 130°W, 0°N to 45°N) and mainly targeted bigeye tuna, *Thunnus obesus*, in the tropical and subtropical areas and albacore tuna in the temperate areas (Liu et al., 2021a,c). Meanwhile, small-scale longline vessels targeting tunas have two types; the vessels less than 50 GT operated in the coastal and offshore waters of Taiwan in the northwestern Pacific Ocean and vessels between 50 and 100 GTs often operated outside the exclusive economic zone of Taiwan in the North Pacific Ocean (Liu et al., 2021b).

The large-scale longline catch of BSH in Taiwan (1971-2020) was estimated in two areas (0–25°N of the equator and northwards of 25°) using the annual catch rates of BSH (i.e., nominal CPUE or area-specific standardized CPUE) multiplied by the total annual fishing effort in the two separate areas (Liu et al., 2021a,c). The catch and effort data of observer records for 2004-2020 were used to calculate the catch rates of BSH, and a delta-generalized linear model was used to standardize the CPUE. In addition, the average catch rates for 2004-2020 were used to estimate the historical catch of BSH from 1971 to 2003. The number of hooks in the logbook data provided by the Overseas Fisheries Development Council, Taiwan was used as the total fishing effort of Taiwanese large-scale longline fishery. Constant mean body weight derived from the mean fork length (FL) with the weight (W)-length (FL) relationships ( $W = 5.009 \times 10^{-6} FL^{3.054}$ ; Kohin and Wraith, 2010) was used to calculate the catch amount from catch number.

The small-scale longline catches of BSH in Taiwan (1971-2020) were calculated using the landings from three fishing markets (Nanfanao, Tongkong, and Chengkun) located in eastern and southwestern Taiwan (Liu et al., 2021b).

### 3.4.3. *Republic of Korea*

The Republic of Korea provided annual catches of BSH caught by the tuna longline fishery operated in the North Pacific Ocean from 1971 to 2020. The Korean distant water tuna longline fishery in the Pacific Ocean commenced in 1958, and has caught tuna and tuna-like species, particularly bigeye and yellowfin tunas as target species, and sharks as bycatch. For that reason, there was a problem in collecting the data of shark catch and estimating the catch by shark species. Therefore, the National Institute of Fisheries Science (NIFS) that is responsible for data collection and management separated the logbooks into two formats that consisted of one for target species such as tuna and tuna-like species and one for bycatch species such as Ecologically

Related Species (ERS; sharks, seabirds, sea turtles, etc.) to record the information on catch and bycatch by species, and have collected shark catch by species since 2009 (Lee et al., 2019).

In the 2014 stock assessment, the Korean BSH catch (1971-2011) was assumed to be equal to species-aggregated shark catch reported to the ISC because the catch of major shark species reported in logbooks included only blue and “other” sharks (reported as “porbeagle” sharks, but have since been corrected to “other” sharks, Y. Kwon pers. comm.) (ISC, 2013). In 2019, the Korean catch for 1982-2018 was updated using the catch from logbook and observer data (Lee et al., 2019). First, shark catch from logbooks were aggregated by year and raised based on the data coverage to represent the actual total catch, and then the BSH catch was estimated from the raised total catch. In the estimation of the BSH catch, the time period was divided into two parts where one is the period (from 1982-2012) when there was no available information or less information about the catch for identified sharks and the other is the period (2013-2018) when there was reasonable information about the catch for identified sharks by species. In the former case, the BSH catch was estimated using total shark catch and the ratio (0.52) of BSH catch to total shark catch, which came from observer data in recent years for 2013-2018. In the latter case, the BSH catch was directly calculated from the total catch without any processing. The Republic of Korea updated the last two years' (2019-2020) of annual catch data based on the reported catch.

#### 3.4.4. *China*

China provided annual catches of BSH caught by the tuna longline fishery operating in the North Pacific Ocean from 2001 to 2020. In the 2017 assessment, China's longline species-specific catch and effort data were available for 2007–2015, and effort data were available from 2001. The mean annual CPUE for 2007–2015 was applied to effort data for 2001–2006 to estimate catch for those years. It was assumed that the effort of Chinese longline fishery in the North Pacific Ocean was minimal prior to 2001. China provided the catch in number from 2016 to 2020 for this assessment. However, the catch data before 2015, which was used in the previous stock assessment in 2017, was in weight. Therefore, the catch in number was converted to the catch in weight using an average body weight (50 kg) estimated from the size frequency data for 2009-2014 and weight-length equations (Nakano, 1994).

#### 3.4.5. *Canada*

Canada provided annual catches of BSH caught by multiple Canadian fisheries operated in the North Pacific Ocean from 1979 to 2020. BSH have been encountered as incidental catch in a number of modern and historical Canadian fisheries, including groundfish trawl and longline fisheries; troll, gillnet and seine fisheries for salmon (*Oncorhynchus* spp.), Pacific Sardine (*Sardinops sagax*), Albacore Tuna, and Neon Flying Squid (*Ommastrephes bartrami*); as well as foreign and joint-venture fisheries for Pacific Hake (*Merluccius productus*). All commercial fisheries in Canada are covered by a dockside monitoring program that provides validated landings. There are very few landings of incidentally encountered BSH. BSH bycatch in Canadian fisheries was estimated from a combination of observer and logbook records from 1979–2018 for groundfish, salmon, sardine, albacore, hake, and squid fisheries (King and Surry, 2019). Catch statistics for 2019-2020 for BSH in Canadian waters were updated for this stock assessment using the same methodology in the previous estimates in 2019 (King, 2021).

### 3.4.6. USA

The USA provided annual catches of BSH caught by multiple fisheries operating in the North Pacific Ocean from 1971 to 2020. BSH catch through 2018 by US fisheries, including the Hawaii-based longline fleet, as well as the west coast drift gillnet, recreational, albacore troll fleets, and small longline fisheries were provided by Kohin et al. (2016) and Kinney (2019). Subsequently, catch statistics for the US domestic longline fisheries through 2020 were updated according to the protocols used in the 2017 stock assessment (Ducharme-Barth et al., 2021). The US Hawaii longline catch was the sum of 3 components: observer catch, logbook catch from reliable sets, and random forest predicted catch from unreliable logbook sets. Additionally, catch was adjusted to account for discard mortality and reported in numbers (Ducharme-Barth et al., 2022a). Finally, US Hawaii longline catch was separated into deep- and shallow- set fisheries (F17 and F18, respectively) for this assessment to account for the difference in selectivity due to differences in the spatial operating area, fishing operations, and target species. For the US domestic mainland fisheries, drift gillnet (F15) and recreational (F16), catch was also updated using the accepted protocols. For the US drift gillnet, catch was estimated as a multiple of annual nominal CPUE from observer records and total effort from logbook data. For the US recreational fisheries, catch estimates were derived from the RecFIN database and charter boats logbooks. In both cases, catch was converted to metric tons.

### 3.4.7. Mexico

Mexico provided annual catches of BSH caught by artisanal, commercial longline, and historical drift gillnet fisheries operated in the eastern North Pacific Ocean, including within Mexico's EEZ from 1971 to 2020. Since the species-specific catch statistics for sharks was not available until 2006, the annual catch of BSH from 1975 to 2006 was estimated assuming that BSH has been represented in total catches with different proportions through time. The values of the proportions were obtained from published papers in the scientific literature or by using more detailed local statistics. BSH are caught mainly by the artisanal and mid-sized longline fisheries, which target pelagic sharks or swordfish. Catches that were landed in the past by the former large size vessel long-line fisheries and the drift gill net fisheries were taken into consideration to construct the historical catch series (Sosa-Nishizaki, 2013). The annual catch of BSH from 2007 to 2020 were sourced from annual fishery statistics yearbooks of SAGARPA (since 2020 called SADER, the Mexican fishery authority provided by INAPESCA) from five Mexican states (Baja California, Baja California Sur, Sinaloa, Nayarit, and Colima), published articles, and reports (including grey literature) (Castillo-Geniz et al., 2017; Sosa-Nishizaki and Castillo-Geniz, 2016). The annual catch of BSH in 1975 was used to fill in catch in the early 1970s (1971-1994) due to a lack of information about the catch.

### 3.4.8. IATTC

The IATTC provided estimates of BSH bycatch in tuna purse seine fisheries in the north EPO from 1971 to 2020. The same methods were used for past stock assessments (IATTC, 2013). The number of BSH caught during 1971–2020 was estimated from observer bycatch data, and observer and logbook effort data. Some assumptions regarding the relative bycatch rates of BSHs were applied based on their temperate distribution and catch composition information. Estimates were calculated separately by set type, year, and area. Small purse seine vessels, for which there

are no observer data, were assumed to have the same BSH bycatch rates by set type, year, and area, as those of large vessels. Before 1993, when shark bycatch data were not available, BSH bycatch rates assumed to be equal to the average of 1993–1995 rates were applied to the available effort information by set type, area, and year. The number of sharks was converted to weight by applying an average annual weight estimate derived from BSHs measured through the IATTC observer program.

#### 3.4.9. *SPC/Non-ISC*

The ISC SHARKWG reconstructed annual catch of BSH caught by longline and purse seine fisheries of Non-ISC countries in the western and central North Pacific Ocean from 1997 to 2020 in collaboration with the data manager of SPC (Kai et al. 2021). The reported annual catch of BSHs caught by purse seine fleets was less than 0.1 metric tons and longline catch accounted for most of the catch. Since the public domain reported longline catch of BSHs is likely to be underreported, the longline catches of four major Non-ISC fleets, including Micronesia, Kiribati, Republic of Marshall Islands and Vanuatu were estimated using the observed CPUE and reported total fishing effort. The longline catches of the other four Non-ISC fleets including Belize, Papua New Guinea, Palau, and Solomon Islands were estimated using an average of the CPUE for four major Non-ISC fleets (Micronesia, Kiribati, Republic of Marshall Islands and Vanuatu) and their respective reported total fishing effort by Belize, Papua New Guinea, Palau, and Solomon Islands.

### 3.5. Indices of relative abundance

Indices of relative abundance (i.e., CPUEs) used in this assessment were developed with data from 10 fleets (**Figure 3, Table 3**) of 4 countries (Chinese-Taipei, Japan, Mexico, and US) and an international organization (SPC). In the previous stock assessment (ISC, 2017), 2 fleets (S5: JPN\_EARLY and S6: JPN\_LATE) were used as the base-case model and four alternative abundance indices (S1: HW\_DP, S3: TAIW\_LG, S9: SPC\_OBS\_TROPIC, and S10: MEX) for the late period were used in the sensitivity analysis. Since the issue of post-2000 reporting rate was resolved (Kai, 2019), the CPUE of Japanese research and training vessels (S7: JPN\_RTV) was newly added as an alternative abundance index (Kai, 2021b). The annual CPUEs for S1 and S3 were normalized by the mean CPUE. The coefficients of variation (CVs) for all CPUEs were updated using the annual CV estimated in the CPUE standardization. Since there was no information about the CV of S9 (Rice and Harley, 2014), the WG calculated the CV for this fleet using the standard error (SE) and the mean value of standardized CPUE. The SHARKWG considered all available abundance indices, and rated each for consideration in this assessment using the same criteria established in the 2014 assessment, including spatio-temporal coverage of the data, statistical soundness and other characteristics (see Table 3 of ISC 2017).

Annual CPUE of S5 was the only abundance index for the early period (**Figure 3, Table 4**). The CPUE indicated a declining trend until 1989 and then increased until 1993. The other six CPUEs were considered as abundance indices for the late period. However, only two CPUE indices (S6 and S7) were available for the entire late period from 1994 to 2020. The CPUE trend of S6 was relatively stable throughout the period, while the CPUE trend of S7 was mixed and went down from 1994 to 2008 before increasing until 2020. The CPUE of S1 indicated a similar trend to that of S7, though the length of CPUE for S1 was shorter than S7. The CPUE of S3 indicated an

increasing trend, whereas the CPUE of S10 indicated a slightly decreasing trend. The CPUE of S9 indicated a sharp increase until 1998 and then decreased until 2009.

### **3.5.1. Main abundance indices**

#### **3.5.1.1. Japanese Kinkai shallow early and late CPUEs**

Abundance indices based on the Japan Kinkai shallow fishery were partitioned into “early” and “late” time periods, 1975-1993 and 1994-2020, respectively. In the estimation of the CPUE for the early period, the season-area-specific ratio of BSH catch to the total shark catch was assumed to be the same for the period before 1994 as that after 1993 because there was no species-specific catch data for sharks before 1994. The early abundance index (S5) was unchanged from what was used in the 2017 BSH assessment (Hiraoka et al., 2013b).

The late abundance index (S6) was developed using a more sophisticated approach than the conventional approaches such as generalized linear model (GLM) and generalized additive model (GAM) (Kai, 2021a). Since the catch data of sharks caught by commercial tuna longline fishery are usually underreported due to the discard of sharks, the logbook data were filtered using the similar filtering methods applied in the 2017 assessment. The nominal CPUE of filtered shallow-set data was then standardized using the spatio-temporal generalized linear mixed model (GLMM) to provide the annual changes in the abundance of BSHs in the northwestern Pacific Ocean focusing on seasonal and interannual variations of the density in the model to account for spatially and seasonally changes in the fishing location due to the target changes between BSH and swordfish. The estimated annual changes in the CPUE of BSH revealed an upward trend from 1994 to 2005, and then a downward trend until 2008. Thereafter the CPUE gradually increased until 2015 and then slightly decreased in recent years. The SHARKWG considered these indices to be good indicators of stock abundance based on their broad spatio-temporal coverage, statistical soundness of the standardization process, size and sex composition, and larger catch relative to other fisheries.

#### **3.5.1.2. Composite-late CPUE with Dynamic factor analysis**

An alternative late abundance index for the base-case model was based on the composite CPUE. In the previous 2017 stock assessment, individually fitting to multiple late period indices resulted in different population trajectories in the recent period compared to the Japanese shallow-set index (S6). Three of the indices; the Hawaii longline (S1), Taiwanese largescale longline (S3), and Japanese research and training vessel (S7); come from fisheries that predominantly target tunas, typically via deep setting operations (Ducharme-Barth and Vincent, 2020). Though the Hawaii longline index is based on observer data which may more accurately reflect the rate of BSH encounter relative to logbook records (Ducharme-Barth et al., 2022a), the use of this index was discounted in the previous assessment due to its limited spatial extent. However, the Hawaii longline index appears to show similar trends in BSH to the Taiwanese longline and Japanese research and training vessel indices, which have much broader spatial extents (Kai, 2019; Liu et al., 2021c). The apparent consistency in trend across three fisheries could present an alternative CPUE hypothesis to the Japanese shallow-set longline which seasonally targets BSH. Dynamic Factor Analysis (Zuur et al., 2003; Peterson et al. 2021) was used to create a composite index from the Hawaii longline index, Taiwanese longline index, and Japanese research and training

vessel index records (Ducharme-Barth et al., 2022b). This resulted in a smooth index which reduced the noise seen in the three input indices but did a good job capturing the overall trend. This composite-CPUE (S11) declined through the mid-2000s before gradually increasing through the mid-2010s where the index has remained fairly stable across the last several years of the model period.

### **3.5.2. *Alternative abundance indices***

Multiple alternative indices for the late period were considered in sensitivity analyses for this assessment.

#### **3.5.2.1. Hawaii longline**

Abundance indices for the Hawaii deep-set and shallow-set longline fisheries were developed with delta lognormal models using observer data. Indices from the 2017 assessment (Carvalho, 2016) were updated through 2020 (Ducharme-Barth et al., 2022a). The updated standardized CPUE for each index was similar to the previous CPUE for the overlapping years. The shallow-set fishery was impacted by closures from 2001-2004 due to bycatch concerns, but the deep-set fishery was not similarly affected. The index for the deep-set fishery was regarded as a better option for an alternative abundance index.

#### **3.5.2.2. Taiwan longline**

Abundance index for the Taiwanese large-scale longline fishing vessels operating in the North Pacific Ocean during the period of 2004-2020 were updated using a delta lognormal approach with observer data. The standardized CPUE of BSH showed a stable increasing trend (Liu et al., 2021c).

#### **3.5.2.3. Japan RTV longline**

The abundance index for the Japanese research and training vessels (S7: JPN\_RTVs) longline fishery from 1994 to 2020 was a newly developed BSH abundance index in the North Pacific Ocean (Kai, 2021b). A statistical filtering method was used to remove unreliable set-by-set data after 2000s collected by JPN\_RTVs (Kai, 2019). The nominal CPUE of the JPN\_RTVs was then standardized using a spatio-temporal GLMM. The predicted abundance indices of BSH revealed a downward trend until 2008 and an upward trend after that, with a stable trend in recent years (Kai, 2021b).

#### **3.5.2.4. Mexico longline**

An abundance index for 2006-2020 was developed using a GLM model with data obtained through a pelagic longline observer program (Fernández-Méndez et al., 2021). This analysis focused on the effect of environmental factors such as sea surface temperature, distance to the nearest point on the coast and time-area factors. Sea surface temperature (SST), mean SST anomalies, distance to the coast, year, area fished, quarter and fraction of night hours in the fishing set were all significant factors included in the model. The results of this analysis showed a relatively stable trend with a sharp descent in the last year of the time series in the standardized abundance index in the period considered.

### 3.5.2.5. SPC longline

The same relative abundance index developed with longline observer data during 1993-2009 for the 2017 assessment was included (Rice and Harley, 2014).

### 3.6. Catch-at-length

Annual length composition data included data from 13 fleets (**Table 5**) of 5 countries (China, Chinese-Taipei, Japan, Mexico and US) and an international organization (SPC). Sex-specific data (including unknown sex) were reported in the observed measurement units (FL – fork length, TL – total length, AL – alternate length, which is the length from the leading edge of the first dorsal fin to the leading edge of the second dorsal fin), and were subsequently converted to precaudal length (PCL) in cm using fishery specific conversion equations if available, or the following agreed-upon conversion equations.

$$\text{PCL} = (\text{FL} \times 0.894) + 2.547 \quad (1)$$

$$\text{PCL} = (\text{TL} \times 0.748) + 1.063 \quad (2)$$

$$\text{PCL} = (\text{AL} \times 2.462702) + 12.7976 \quad (3)$$

The coordinates where the samples were taken were reported when possible to investigate spatially explicit size and sex structure. Some data were provided with exact coordinates, whereas some were summarized into spatial blocks ( $1^\circ \times 1^\circ$ ,  $5^\circ \times 5^\circ$ , or  $20^\circ \times 10^\circ$ ) (Sippel et al., 2016). For the assessment, sex-specific size data were grouped by fishery.

#### 3.6.1. Japan

In total, size data from 894,060 individual BSHs were collected between 1967 and 2020 (Semba, 2021). 67% of them were from the commercial Kinkai-shallow longline (port sampling), followed by research data from the deep-set longline (23%) and the ratio of other type of fishery was less than 5%. Generally, BSH caught by deep-set longline (median and mode: larger than 160 cm precaudal length: PCL) tended to be larger than that of other type of fishery (median and mode: smaller than 150 cm PCL). Annual change of PCL (sex-combined) by data sources indicated no major or continuous trend for commercial longline (Kinkai-shallow, deep-set, and coastal) and the driftnet fishery between 2008 and 2020, and the research shallow-set (2000-2020) and deep-set (1967-2020) longline. Japan updated the size data of three longline fleets (F4, F5 and F7) until 2020 and large-mesh driftnet fleets (F8 and F9) until 2019 (Semba, 2021). To align the fleet definition with catch data, Japan removed the size data of F5 for 2009-2015 from the previous data file and added those size data to F7. Japan also added newly available size data of F8 for 1979-1983, and F9 for 1994, 1996, and 1998 using observer and research survey data (Semba, 2021, 2022).

Kai et al. (2022b) digitally extracted the length composition data in total length of BSHs sampled by Canadian observers in the Japanese flying squid driftnet fishery in 1991 from a figure in McKinnell and Seki (1998). The size data was used as a newly available length composition data for F11, and the sex-combined length composition data indicated that the catch consisted of small-sized BSH.

### **3.6.2. Chinese-Taipei**

Chinese-Taipei provided newly available size data from large- and small-scale longline fleets for 2004-2020 (F19: TAIW\_LG) (Liu et al., 2021a) and 2012-2020 (F20: TAIW\_SM) (Liu et al., 2021b), respectively. The size data of 5,897 specimens were collected by scientific observers on-board the Taiwanese large-scale tuna longline vessels. The size data indicated size segregation of BSHs by area, with the mean size of BSHs in area B (0-25°N) being significantly smaller than that in area A (north of 25°N). No significant sex segregation was found. Males predominated in the size range of 170-280 cm and 170-200 cm TL in area A and B, respectively. The average size of BSHs caught by the Taiwanese small-scale tuna longline was estimated to be 183 cm and 185 cm FL for females and males, respectively. Juvenile females were found in the tropical and subtropical areas, but adults were more often found in the temperate area. The smallest mean sizes for both sexes were found in season 2.

### **3.6.3. China**

Size data for 2146 BSHs measured by observers on Chinese longline vessels during 2009-2015 were provided in the previous assessment in 2017. China updated the size data until 2020 and also provided newly available size data from 1993 to 2008 (F3: CHINA).

### **3.6.4. USA**

Size and sex composition data collected by observers in the Hawaii-based longline fisheries (deep- and shallow-set), and the US West Coast (California, Oregon, and Washington) drift gillnet fishery were included in the 2017 assessment (Kohin et al., 2016). The US updated these size and sex composition data through 2020 (Ducharme-Barth et al., 2021) and separated the size data of the Hawaii longline fleet into two fleets (F17 and F18) in association with the division of the catch and removed the size data for 1994-2002 from the previous size data, which was prior to the sectorization of the two longline fleets (Ducharme-Barth et al., 2022a).

### **3.6.5. Mexico**

Size and sex composition data during 2006-2014 collected by observers opportunistically deployed in Mexico's Ensenada and San Carlos based longline fleets were used in the 2017 assessment (Castillo-Geniz et al., 2017). These size and sex composition data were updated until 2020.

### **3.6.6. Non-ISC**

SPC provided newly available size data of longline fleets that mainly operated in the sub-tropical and tropical areas in the North Pacific Ocean for 1994-2020 (F14). The size data from Guam and Indonesia were removed from the size data of Non-ISC member countries.

## 4. INTEGRATED MODEL DESCRIPTION

### 4.1. Stock Synthesis software

As in the previous stock assessment, the present assessment was conducted using the SS3 model (version 3.30.19.01). Descriptions of SS3 algorithms and options are available in the SS3 User's Manual (Methot et al., 2021), the NOAA Fisheries Toolbox website (<https://nmfs-fish-tools.github.io/>), and Methot and Wetzel (2013). SS3 is a widely used integrated statistical catch-at-age (SCAA) model platform that has been widely used for stock assessments in the US, and also throughout the world (see Dichmont et al., 2016 for review). SCAA models consist of three closely linked modules: the population dynamics module, an observation module, and a likelihood function. Input biological parameters are used to propagate abundance and biomass forward from initial conditions (population dynamics model) and SS3 develops expected data sets based on estimates of F, selectivity, and catchability (the observation model). The observed and expected data are compared (the likelihood module) to determine best fit parameter estimates using a statistical maximum likelihood framework.

### 4.2. General characteristics

#### 4.2.1. *Assessment strategy*

The development of a stock assessment model is comprised of the model processes, data, and statistical methods for comparing data to predictions. Systematic misfit to data or conflict between data within an assessment model should be considered as a diagnostic of model misspecification.

Unacceptable model fit (i.e., model predictions do not match the data) can be detected by either the magnitude of the residuals being larger than implied by the observation error, or trends in residuals indicating systematic misfit. Data conflicts occur when different data series, given the model structure, provide different information about important aspects of the dynamics. Unacceptable model misfit or conflict between data can be dealt with by either data weighting or model process changes/flexible model parametrization.

Because it is difficult to determine the underlying cause of the model misfit and conflict, it is often assumed that some data are more reliable than other data for determining particular aspects of the population dynamics (Francis, 2011). The goal was to create a dynamic model of all the available data that fit the data well and was internally consistent. Internal consistency implies all data are fit as well as their observational errors and trends in residuals are minimized. Important aspects of the dynamics (scale, trend, and relative scale) should be derived from the most trusted data sources.

The modeling approach is summarized as follows:

1. Selection of the data and estimation of the true sampling error;
2. Development of the initial model with original sampling error;
3. Determine if CPUE indices have information on scale and prioritize data;

4. Run stock assessment model;
5. Apply model diagnostics;
6. Modify or add additional processes based on diagnostics and complete steps 4 to 6 again until an internally consistent model is achieved; and
7. Re-weight the data and/or fixed the parameters as needed.

The models retained for the ensemble used the CPUE series recommended by the SHARKWG (JPN-early and JPN-late; JPN-early and Composite-CPUE-late); the best practice approach for weighting size frequency data to ensure that the data did not overwhelm the abundance indices; sigma-R of 0.4; initial catch fixed at 40,000 mt, and the steepness of 0.613.

#### 4.2.2. *Parameter estimation*

SS3 estimates population and fishing parameters by minimizing the negative log-likelihood of an objective function from the provided input datasets or assumptions. In this stock assessment, 329 parameters were estimated, of which 160 were active parameters. These parameters include: year specific F for each fleet, parameters informing selectivity, stock-recruit relationship parameters (the log of virgin recruitment ( $\ln(R_0)$ )), the stock-recruit deviations, and initial F.

#### 4.2.3. *Data weighting*

It is well known that the results of fishery stock assessments based on integrated models can be sensitive to the values used to weight each of the data types included in the objective function. The weight given to each data point in a stock assessment model is determined by a measure of the assumed size of the error associated with that point: typically a coefficient of variation (CV) for abundance indices, and a sample size for composition data. If the data weighting is changed, the balance between the different data sets is changed, and thus the parameter estimates change. Punt (2017) provided a comprehensive review and a comparison of various iterative re-weighting methods for length composition data. The iterative re-weighting approach attempts to reduce the potential for particular data sources to have a disproportionate effect on total model fit, while creating estimates of uncertainty that are commensurate with the uncertainty inherent in the input data. In this assessment, data weighting for CPUE and length composition data were conducted using a two-step data weighting approach; calculated the variance adjustment factors for fleet-specific relative abundance indices (CPUE) and fleet-specific length composition data (Francis 2011; Courteney et al. 2016).

The CPUE was weighted using the CV (Courteney et al. 2016). The procedure is as follows:

- 1) The mean annual CV ( $CV_{\text{mean}}$ ) is calculated for each CPUE series;
- 2) The root mean square error (RMSE) on the natural log scale of CPUE is calculated using the following equation:

$$RMSE = \sqrt{\frac{1}{N} \sum_{i=1}^N \{\log(\text{CPUE}_i) - \log(\widehat{\text{CPUE}}_i)\}^2} \quad (4)$$

where  $N$  is total number at year  $i$  of input CPUE time series ( $\text{CPUE}_i$ ) for each fleet,  $\widehat{\text{CPUE}}_i$  is an

average estimated CPUE from a LOESS smoother. Since it is commonly known that the CVs on the arithmetic scale are approximately equal to the standard errors (SEs) on the natural log scale, the RMSE can be regarded as a minimum average CV ( $CV_{\min}$ ) for each CPUE series (i.e.,  $CV_{\min} \approx RMSE$ );

3) If the  $CV_{\text{mean}} < CV_{\min}$ , the variance adjustment for each CPUE series in SS3 was conducted by adding the value to the average CV ( $CV_{\text{mean}} + \text{variance adjustment}$ ) and scaled up to 20% CV in order to maintain a certain level of variance for each CPUE. If the  $CV_{\text{mean}} > CV_{\min}$ , the variance of the CPUE series was not adjusted in the SS3.

The calculated CVs and recommended variance adjustment is summarized in **Table 6**. Annual changes in the residuals between fitted and observed CPUEs and fitting of LOESS to observed CPUE were also shown in **Figure 4**. The values of  $CV_{\text{mean}}$  for S1, S6, and S7 were larger than those of  $CV_{\min}$ , so that the variance adjustment was fixed to 0. The other fleets were opposite results, so the variance adjustment was added up to 0.2 for each fleet.

The length composition data was weighted based on down weighting, which was implemented by reducing the variance adjustment factors in the control file of SS3, to reduce the effect of the large sample size of fleet-specific length composition data. The values of variance adjustment factors of all fleets were set to 0.002161 (50/23142), where 50 is a criterion, and 23,412 is the average sample size of fleet4 (F4: JPN\_KK\_SH). The representative fleet (F4) was designated based on the wide operational area in the main distributed area of BSH, large amount of the catch from small to large fish, and the prolonged operational period relative to the other fisheries (Kai, 2021a). In addition, the Method “TA1.8” (Francis, 2011) was applied to down weight the length composition data. The method is based on variability in the observed mean length by year, where the sample sizes are adjusted such that the fit of the expected mean length should fit within the uncertainty intervals at a rate that is consistent with variability expected based on the adjusted sample sizes (Method et al., 2021). Outcomes of the Method “TA1.8” are summarized in **Table 7**. Since all the suggested multiplier was larger than one except for F4, the second down-weighting was only applied to the size composition data for F4 after finishing the parameterization for all the selectivity curves.

#### 4.2.4. Uncertainty characterization

Three alternative model configurations<sup>2</sup>, making different assumptions on the late period CPUE, were considered in developing the 2022 stock assessment. The diagnostics from each model were carefully scrutinized and the WG agreed that a single best model could not be distinguished based on diagnostics alone. As a result, uncertainty in the current stock assessment was characterized using a model ensemble that combines the structural model uncertainty from the three different model configurations with the estimated statistical uncertainty from each individual model. This is a similar approach that was applied by the ISC billfish WG (BILLWG) in characterizing the uncertainty for the 2021 Pacific blue marlin stock assessment (ISC, 2021).

The statistical uncertainty in key management quantities (SSB, F, recruitment,  $SSB/SSB_{\text{MSY}}$  and  $F/F_{\text{MSY}}$ ) for an individual model in the ensemble was characterized using 100,000 samples from

---

<sup>2</sup> Described in Section 5.2

a multivariate lognormal (MVLN), parametric bootstrap. The MVLN approach as implemented in the R package *ss3diags* (Carvalho et al., 2021), preserves the correlation structure between estimated management quantities. Samples from the parametric bootstrap of each of the three models in the ensemble were combined into a single distribution according to their assumed weight (described in Section 5.2.4). The median for each management quantity and associated uncertainty (e.g., 80<sup>th</sup> percentile) was derived from the combined distribution in order to more completely capture the structural and estimation uncertainty in stock status.

### 4.3. Model structure

A list of biological and spawner-recruit parameters between previous and current assessments are shown in **Table 8**. Some parameters of the growth curve, spawner-recruit steepness, and the time period of main recruitment deviation were updated slightly, but the same values as assumed in the previous assessment were used for most of these parameters.

#### 4.3.1. Population dynamics

The model partitions the population into 25 yearly (0-24) age-classes in one region, defined as the North Pacific Ocean. The last age-class comprises a “plus group” in which mortality and other characteristics are assumed constant. The population is “monitored” in the model at yearly time steps, extending through a time window of 1971-2020. The main population dynamics processes are indicated below.

#### 4.3.2. Sex structure

Past knowledge indicated that BSH in the North Pacific Ocean exhibited substantial size and sex-structure patterns through space and time (e.g., Nakano, 1994; Fujinami et al., 2021d). The use of sex-specific fishery and biological data is therefore needed in this assessment. The sex-ratio at birth is assumed to be 1:1 in the model because the ratio of male to female embryos was not significantly different from 1:1 (Fujinami et al., 2017).

#### 4.3.3. Recruitment

In this model “recruitment” is the appearance of age-0 fish. The results were derived using one recruitment episode per year, which is assumed to occur at the start of each year. Annual recruitment deviates from the recruitment relationship were estimated but constrained reflecting the limited scope for compensation given estimates of fecundity.

A major change to the model configuration is the assumed shape of the stock-recruitment (SR) relationship. A low-fecundity SR (LFSR; Taylor et al., 2013) was used in the previous stock assessment to explain the lower survival ratio prior to the recruitment after partition (**Figure 5**). Although the application of low-fecundity SR is theoretically reasonable for elasmobranchs, the WG decided that more research is needed before this SR option is fully operationalized in ISC stock assessments for sharks. In particular, the parameters ( $\alpha$  and  $\beta$ ) of low-fecundity SR were based on strong assumptions relating to the unfished SR relationship in the 2017 stock assessment. The WG, therefore, determined to use the Beverton-Holt-SR in the 2022 assessment. Kai and Fujinami (2018) developed the simulation method based on Mangel et al. (2010) to estimate probable values of SR steepness ( $h$ ) for a Beverton-Holt SR curve for BSH. The mean

steepness ( $h = 0.613$ ) was updated in this assessment using newly available biological parameters such as growth and natural mortality for females (Fujinami et al., 2021c). In order to examine the effects of assuming an alternative SR, sensitivity analysis was conducted using the LFSR assumption (see section 5.3).

Annual recruitment deviations were estimated from the information available in the data. The central tendency that penalizes the log (recruitment) deviations for deviating from zero was assumed to sum to zero over the estimated period. The log of  $R_0$  and annual recruitment deviates were estimated by the model. The offset for the initial recruitment relative to  $R_0$  was estimated in the model. The deviations from the SR were estimated in two parts: (1) early period recruitment deviates for the ten years before the main model period; and (2) the main recruitment deviates that covered the period 1971-2020. The period of main recruitment deviation was changed from 1990-2013 in the 2017 assessment because there were a few years of size data before 1990. Recruitment variability (Sigma-R) - the standard deviation of log recruitment - was tuned by repeatedly changing the value using the following equation:

$$\text{Sigma-R} = \sqrt{\text{Var}(devs.) + \text{Mean}(devs.se^2)} \quad (5)$$

where *devs.* and *devs.se* indicates recruitment deviations and standard error of the recruitment deviations, respectively. The values of Sigma-R were calculated by using the r4ss package (Taylor et al., 2021) and the value was finally fixed to 0.4 after tuning 6 times.

A log-bias adjustment factor was used to assure that the estimated mean log-normally distributed recruitments were mean-unbiased. SS3 allows for a user-defined fraction of the log bias adjustment implied by the specified Sigma-R to be consistent with the estimated variability of the recruitment deviates. Bias adjustment parameters for SR relationships (Method and Taylor, 2011) were adjusted using the estimated alternative inputs to the SS3 control file. Max bias adjustment in Maximum Posterior Density (MPD) was fixed to 0.5 based on the output of SS3 at the final stage of the conditioning.

#### 4.3.4. *Initial population state*

It is not assumed that the BSH population was at an un-fished state of equilibrium at the start of the model (1971) as significant longline fishing occurred in the region from the 1950s and in Japanese coastal waters prior to that (Okamoto, 2004). Instead, the initial BSH population was assumed to be in a state of equilibrium with 40,000 mt of catch by the F4 fleet (see Section 4.4.2).

The population age structure and overall size in the first year is determined as a function of the estimate of the first year's recruitment ( $R_1$ ) offset from virgin recruitment ( $R_0$ ) - the initial 'equilibrium'  $F$  (described in Section 4.4.2) - and the initial recruitment deviations (described in Section 4.3.3). The size data were found to be uninformative about initial depletion and recruitment variation, and ten years of initial recruitment deviations were estimated.

#### 4.3.5. *Growth*

Sex-specific estimates of growth from Fujinami et al. (2019) were assumed in this assessment.

The length at age relationships were based on reading vertebrae samples from 620 females and 659 males, ranging from about 33 to 258 cm PCL (Fujinami et al., 2019). The standard assumptions made concerning age and growth in the model are; (i) the lengths-at-age are assumed to be normally distributed for each age-class; (ii) the mean lengths-at-age are assumed to follow a von Bertalanffy growth equation used in SS3:

$$L_2 = L_\infty + (L_1 - L_\infty)e^{-K(A_2 - A_1)} \quad (6)$$

where  $L_1$  and  $L_2$  are the sizes associated with ages near a first age ( $A_1$ ) and second age ( $A_2$ ),  $L_\infty$  is the theoretical maximum length, and  $K$  is the growth coefficient.  $K$  and  $L_\infty$  can be solved based on the length-at-age;  $L_\infty$  was thus re-parameterized as:

$$L_\infty = L_1 + \frac{L_2 - L_1}{1 - e^{-K(A_2 - A_1)}} \quad (7)$$

The growth parameters  $K$ ,  $L_1$  and  $L_2$  were fixed in the SS3 model, with  $K$  at 0.147 (0.117)  $y^{-1}$  for female (male) and  $L_1$  and  $L_2$  at 64.4 (68.2) cm and 244.6 (261.3) cm for  $A_1$  (age 1) and  $A_2$  (age 20), respectively (Fujinami et al., 2021c). A CV of 0.25 was used to model variation in length-at-age. The value of CV was fixed to a common value used in other tuna and tuna-like species stock assessments. No attempt was made to estimate growth due to the uninformative nature of the size data to track cohorts through time. All lengths listed are precaudal length (PCL) unless otherwise specified. The parameters of the sex-specific Richard growth curves (**Figure 6**), derived from sex-specific von-Bertalanffy growth curves, were almost the same as those used in the previous assessment in 2017.

#### 4.3.6. *Natural mortality*

Age and sex-specific natural mortality ogives were considered in this assessment. They were calculated under the assumption that mortality is inversely proportional to body length (Lorenzen, 2005), and a constant natural mortality rate derived from the meta-analysis (Campana et al., 2005) was allocated to each age class. The estimation procedures are described in Kai and Fujinami (2018). The sex- and age-specific natural mortality rates were updated using the newly available growth curve parameters, resulting in natural mortality schedules almost the same as those in the previous assessment (**Table 9, Figure 7**).

#### 4.3.7. *Maturity and fecundity*

For a shark stock assessment, it is critically important to estimate the correct units of spawning potential. This assessment considered a single maturity ogive and did not consider age/length specific changes in fecundity in the final set of model runs. For the purpose of computing the SSB, the WG assumed a logistic maturity schedule based on length with the size-at-50% maturity for females ( $n = 431$ ) equal to 156.6 cm (Fujinami et al., 2017) (**Figure 8**).

#### 4.3.8. *Length-weight relationship*

Sex-specific weight-at-length relationships were used to convert body length (PCL) in cm to whole body weight (W) in kg (Nakano, 1994). The sex-specific weight-length relationships are:

$$W = 5.388 \times 10^{-6} L^{3.102}, \text{ for female.} \quad (8)$$

$$W = 3.291 \times 10^{-6} L^{3.225}, \text{ for male.} \quad (9)$$

These weight-at-length relationships were applied as fixed parameters in the model (**Figure 9**).

#### **4.3.9. Plus group**

For any age-specific model, it is necessary to assume the number of significant age-classes in the exploited population, with the last age-class being defined as a “plus group”, i.e., all fish of the designated age and older. For the results presented here, 25 yearly age-classes have been assumed, as age 24 approximates to the age at the theoretical maximum length of an average fish for male (Taylor, 1958).

### **4.4. Fishery dynamics**

#### **4.4.1. Input fishery data**

The input fisheries and survey data consist of catch, catch/effort (CPUE) and sex-specific length-composition data (**Figure 10**). An annual (Jan 1-Dec 31) time-series of fishery data for 1971-2020 was used in this assessment.

#### **4.4.2. Initial fishing mortality**

SS3 has several approaches to start from a fished state and two of these were considered for the previous assessments (ISC, 2014; ISC, 2017). The first approach involves assuming an initial equilibrium  $F$ , while the second approach, that was used in this assessment, involved assuming an initial equilibrium catch. Whichever approach is used, it is necessary to specify a selectivity curve to apply either to the  $F$  or the equilibrium catch. The SHARKWG decided that catch was easier to fix in a pragmatic way, i.e., if  $F$  was fixed, then catch can differ depending upon estimated abundance resulting in an unintended discontinuity (Carvalho et al., 2017). In this assessment, a single value for equilibrium catch was assumed - 40,000 mt based on the 2017 assessment. The value represents approximately 100% of the first four years’ estimated catch.

The selectivity estimated for one of the Japanese fleets (F4: JPN\_KK\_SH) was used for the equilibrium catches as it dominated catches in the early years and its selectivity was not extreme towards small or large fish (Semba, 2021).

#### **4.4.3. Selectivity**

All the selectivity curves were assumed to be double normal with defined initial and final selectivity levels (No 24) except that high-seas drift-net fishery (F11: SM\_MESH) and US Hawaii shallow set fishery (F18: US\_HW\_SH). Since F11 has only one year of sex-combined length composition data with different sizes of length bins, the generalized size composition data option in SS3 was used. A more flexible cubic spline selectivity function with sex-specific offset was used for the F18 in order to achieve a better fit to the bimodal distribution seen in the length composition data for this fishery. A time block of selectivity was set for F8 (JPN\_LG\_MESH\_EARLY) to explain a distinct historical shift of body size due to the change in

the operational area and/or target fish. Similar to the 2017 assessment, time varying selectivity was applied to F19 (TAIW\_LG) to improve the fits to the size data. At the final stage of SS3 conditioning, the selectivity parameter of “top\_logit” for all fleets, except for F8 and F18, was fixed at -6.0 because the parameters were uninformed by data and had no impact on the model outcomes.

The sex-specific selectivity parameters for 13 fleets (F1: MEX, F3: CHINA, F4: JPN\_KK\_SH, F5: JPN\_KK\_DP, F7: JPN\_ENY\_DP, F8: JPN\_LG\_MESH\_EARLY, F9: JPN\_LG\_MESH\_LATE, F11: SM\_MESH, F14: NON\_ISC, F15: US\_GILL, F17: US\_HW\_DP, F18: US\_HW\_SH, F19: TAIW\_LG and F20: TAIW\_SM) were estimated in the model. The selectivity patterns of other fleets were mirrored in to the selectivity of a corresponding fleet with similar operations (**Table 10**).

#### 4.5. Likelihood components

The assessment model fit three data components: 1) total catch; 2) relative abundance indices; and 3) composition data. The observed total catches were assumed to be unbiased and relatively precise, and were fitted assuming a lognormal error distribution with a standard error (SE) of 0.05. The relative abundance indices were assumed to have log-normally distributed errors with SE in log-space ( $\log(\text{SE})$ ) which was  $\log(\text{SE}) = \sqrt{\log(1 + \text{CV}^2)}$ , where CV is the standard error of the observation divided by the mean value of the observation and sqrt is the square root function.

The composition data were assumed to have multinomial error distributions with the error variances determined by the effective sample sizes. Measurements of fish are usually not random samples from the entire population. Instead, they tend to be highly correlated within a set or trip (Pennington et al., 2002). The effective sample size is usually substantially lower than the actual number of fish measured because the variance within each set or trip is substantially lower than the variance within a population. For this assessment, the input sample sizes for each fishery were rescaled by a constant so that the average input sample size for the fishery with the most fish sampled (F4) was approximately 50. Therefore, the input sample sizes varied between fishery and over time, depending on the sampling that occurred for that fishery and period.

The recruitment information was also included as a likelihood component. This component allows the estimation procedure to account for the deviations between recruitment estimates for individual years and predicted values from the estimated SR curve.

#### 4.6. Stock assessment model diagnostics

Diagnostic tests are important in determining the robustness of estimates for management advice in integrated stock assessment models. There is little guidance and few objective criteria to determine how to best summarize the results of integrated assessment models, determine if the model fits the data adequately and if the model is well specified (Carvalho et al., 2017). Moreover, it is very difficult to easily evaluate convergence or identify problematic areas given the large number of estimable parameters in these assessments. However, selection of diagnostics, in other words, a diagnostic toolbox, is recommended to increase the ability to detect model misspecification while acknowledging that the use of multiple diagnostics may increase

the probability that a diagnostic test results in a false positive. In this context, Carvalho et al. (2021) proposed a series of interconnected diagnostic tests that should be carried out to establish a base model or an ensemble of candidate models.

#### **4.6.1. Residual analysis**

The main approach used to address model fit and performance was residual analysis of model fit to each of the data sets (e.g., catch, indices, length/age compositions, discards). Any temporal trends in model residuals (or trends with age or length for compositional data) can be indicative of model misspecification and poor performance. It is not expected that any model will perfectly fit any of the observed data sets, but ideally, residuals will be randomly distributed and conform to the assumed error structure for that data source. Any extreme patterns of positive or negative residuals are indicative of poor model performance and potential unaccounted for processes or observation errors.

The runs test was used to evaluate the residuals of the CPUE indices and size composition mean length trends. This is a nonparametric test for randomness in the sequence of residuals (Carvalho et al., 2021; Wald and Wolfowitz, 1940). In other words, this test uses a 2-sided p-value to estimate the number of positive or negative residuals in a row (a “run”). CPUE or size composition data that fail the runs test indicate that there may be a pattern in the residuals and the model is unable to fit the data well or is mis-specified.

#### **4.6.2. Age-structured production model (ASPM)**

An age-structured production model (ASPM; Maunder and Piner, 2015; Carvalho et al., 2017) diagnostic was implemented for this assessment by fixing selectivity to its estimated values in the fully integrated stock assessment model, fixing recruitment equal to the SR curve obtained from the fully integrated stock assessment model, and then estimating the remaining parameters of the stock assessment model. Trends in relative spawning stock size from the fully integrated stock assessment model were compared to the ASPM. Additionally, an ASPM-dev model was fit, where recruitment deviates were estimated.

Carvalho et al. (2017) suggest that if the ASPM is able to fit well to the indices of abundance that have good contrast (i.e., those that have declining and/or increasing trends), then this is evidence of the existence of a production function, and the indices will likely provide information about absolute abundance. On the other hand, Carvalho et al. (2017) suggest that if there is not a good fit to the indices, then the catch data alone cannot explain the trajectories depicted in the indices of relative abundance. This can have several causes: (i) the stock is recruitment-driven; (ii) the stock has not yet declined to the point at which catch is a major factor influencing abundance; (iii) the model is mis-specified; or (iv) the indices of relative abundance are not proportional to abundance.

#### **4.6.3. $R_0$ profile**

Profile likelihoods are used to examine the change in log-likelihood for each data source in order to address the stability of a given parameter estimate, and to see how each individual data source influences the estimate. The analysis is performed by holding the given parameter at a constant value and rerunning the model. This is repeated for a range of reasonable parameter values.

Ideally, the graph of likelihood values against parameter values will give a well-defined minimum, indicating that data sources are in agreement. When a given parameter is not well estimated, the profile plot may show conflicting signals across the data sources. The resulting total likelihood surface will often be flat, indicating that multiple parameter values are equally likely given the data. In such instances, the model assumptions need to be reconsidered. For this assessment, this diagnostic was implemented by sequentially fixing the equilibrium recruitment parameter,  $R_0$ , on the natural log scale,  $\log(R_0)$ , to a range of values.

#### **4.6.4. Retrospective analysis**

A retrospective analysis is a useful approach for addressing the consistency of terminal year model estimates. The analysis sequentially removes a year of data at a time and reruns the model. If the resulting estimates of derived quantities such as SSB or F differ significantly, particularly if there is serial over- or underestimation of any important quantities, it can indicate that the model has some unidentified process error, and requires reassessing model assumptions. It is expected that removing data will lead to slight differences between the new terminal year estimates and the updated estimates for that year in the model with the full data. Oftentimes additional data, especially compositional data, will improve estimates in years prior to the new terminal year, because the information on cohort strength becomes more reliable. Therefore, slight differences are expected between model runs as more years of data are peeled away. Ideally, the difference in estimates will be slight and more or less randomly distributed above and below the estimates from the model with the complete data sets. For this assessment, a three-year retrospective window was selected as the Japanese Kinkai Deep fishery (F5) only has length composition data for the last five years of the model.

#### **4.6.5. Hindcast cross-validation**

The recent cookbook by Carvalho et al. (2021) recommended that model validation should be conducted using prediction skill based on observations. For this stock assessment, we use hindcasting to estimate prediction skill, a measure of the accuracy of a predicted value unknown by the model relative to its observed value, to explore model misspecification and data conflicts. To measure the predictive skill, the mean absolute scaled error (MASE) was used to determine if the predicted value improves the model forecast compared to the baseline. A MASE score of  $>1$  indicates that the average model forecasts are worse than one-step ahead naïve predictor, and a value of  $<1$  indicates the model has prediction skill. Although MASE, is a robust statistic to measure a predictor's accuracy compared to its observed value unknown by the model, it tends to produce large numbers ( $\gg 1$ ) when the observed time series is relatively flat. To address this issue, an adjusted MASE value was produced. The adjustment is basically a mathematical inner work to reduce the penalty on the MASE due to a few years with little contrast in the observation. For this stock assessment, the hindcasting cross-validation and MASE scores were calculated for the CPUE indices in the last three years of the assessment.

#### **4.6.6. Jitter analysis**

Jitter analysis is a relatively simple method that can be used to assess model stability and to determine whether a global as opposed to local minima has been found by the search algorithm. The premise is that all of the starting values are randomly altered (or 'jittered') by an input

constant value and the model is rerun from the new starting values. If the resulting population trajectories across a number of runs converge to the same final solution, it can be reasonably assumed that a global minimum has been obtained. This process is not fault-proof and no guarantee can ever be made that the ‘true’ solution has been found or that the model does not contain misspecification. However, if the jitter analysis results are consistent, it provides additional support that the model is performing well and has come to a stable solution. For this assessment, a jitter value of 0.1 (10%) was applied to the starting values and two rounds of 100 jittering runs were completed. The best model from the first round of jittering was used as the starting point for the second round of jittering.

#### 4.7. Future projections

A 10 year future projection from 2021 to 2030 was conducted in SS3 using the same method used in the 2017 stock assessment. Four harvest scenarios were implemented: 1) *status-quo* which defines  $F$  in the projection period as the average level for 2017-2019 ( $F_{2017-2019}$ ); 2)  $F_{MSY}$  which defines  $F$  in the projection period as the  $F$  which produces MSY ( $F_{MSY}$ ); 3)  $F + 20\%$  which defines  $F$  in the projection period as 20% higher  $F$  than the average level for 2017-2019; 4)  $F - 20\%$  which defines  $F$  in the projection period as 20% lower  $F$  than the average level for 2017-2019. Deterministic recruitment was assumed based on the SR relationship. The selectivity parameters were fixed to the value from the terminal model year (2020).

### 5. MODEL RUNS

#### 5.1. Developments since the 2017 stock assessment

The assessment used a fully integrated approach in SS3 with model inputs that have been updated since the previous assessment. The latest version of SS3 (V3.30.19.01) was used after checking the effect of the version update (Kai, et al., 2022c). The main difference between the present assessment and the 2017 assessment was 1) the use of an ensemble approach combining one model with the representative late period CPUE in the North Pacific Ocean (i.e., Japan Kaikai shallow index) and two models assuming alternative late period Composite-CPUE hypotheses (Ducharme-Barth et al., 2022b). Other differences were 2) catch, CPUE and size time series updated through 2019/2020 (Kai et al., 2022g); 3) improvements to the catch estimation and size data of the driftnet fishery and Non-ISC fishery (Kai et al., 2022a,b, and d); 4) improved life history information, such as growth and reproductive biology, and their contribution to productivity assumptions (Fujinami et al., 2021c; Kai et al., 2022e); 5) reconsideration of SR using the Beverton-Holt model (Kai et al., 2022e); 6) application of a suite of model diagnostics (Ducharme-Barth et al., 2022b; Kai et al., 2022f) based on the cookbook published in 2021 (Carvalho et al., 2021).

#### 5.2. Model ensemble

The model ensemble used as the basis for management of North Pacific BSH emerged from the model development process and was constructed using a *hypothesis tree* approach (Maunder et al., 2020). During model development, two candidate models were proposed, each fitting to a different late period index, the Japanese Kaikai shallow-set longline ( $S6\_base$  model) or the composite-CPUE ( $S11\_model$ ). This formed the basis of the hypothesis tree and each alternative

late period CPUE hypothesis was assumed to have equal weight in the ensemble. The composite-CPUE branch of the hypothesis tree was further divided into two models. A retrospective pattern was identified for the model fitting to the S11 index, the cause of which was identified to be two anomalously large length composition samples for the Taiwanese small-scale longline fishery (F20). Down-weighting these anomalous length composition samples ameliorated the retrospective bias for the *S11\_model* and this formed the basis of the second split in the hypothesis tree. Two models fitting to the S11 index were considered with equal weight in the ensemble, one without (*S11\_base* model) and one with down-weighting the anomalous length composition data (*S11\_ess* model). This hypothesis tree approach resulted in a three-model ensemble with the *S6\_base* model receiving 50% of the weighting, and the *S11\_base* and *S11\_ess* models receiving 25% of the weighting each. Additional details on the two S11 models, including sensitivities to assumptions made in developing the DFA composite index, can be found in Ducharme-Barth et al. 2022b.

### 5.2.1. *S6\_base model*

The *S6\_base* model follows the default model configuration as described in Sections 3 and 4. It fits to the S6 Japanese Kinkai shallow longline index in the late period (1994 – 2020).

### 5.2.2. *S11\_base model*

The *S11\_base* model is identical to *S6\_base* model with the only difference being that the model fits to the S11 DFA composite-CPUE in the late period (1994 – 2020). Selectivity for this survey was assumed to be length-based, sex-specific and mirrored with the F7 Japanese Enyo deep longline.

### 5.2.3. *S11\_ess model*

The *S11\_ess* model is identical to *S11\_base* model with the only difference being that the input sample size for F20 Taiwanese small scale longline was down-weighted in 2018 and 2020 (20,416 and 21,571 sample size, respectively). The new input sample size (1,513) for these years was taken as the average of years 2012-2017 and 2019.

## 5.3. Sensitivity analysis

A large number of alternative model configurations of different levels of complexity were explored. A selected number of the most relevant alternate model configurations are summarized in **Table 11**. A total of 27 runs of sensitivity analysis for 12 items were performed. These configurations include alternative assumptions regarding historical commercial removals of BSHs, fishery selectivity, alternate values for natural mortality (M), SS3 parameterizations used in previous stock assessments, and a different SR relationship (LFSR). Outcomes of the sensitivity analysis for each base model were summarized using the Kobe plot of the latest stock status on SSB in 2020 and F during 2017 and 2019 relative to MSY level.

### 5.3.1. *Alternative mortality schedule*

The sensitivity of the base models to alternative assumptions about the estimation of age and sex-specific natural mortality was examined using an empirical equation (Peterson and

Wroblewski, 1984):

$$M = 1.28 \times W^{0.25}, \quad (7)$$

where  $M$  is age-specific natural mortality rate per year and  $W$  is age-specific dry body weight (g). This equation was used to estimate alternative mortality schedules in the previous assessment in 2017 (ISC, 2017). However, the mortality schedules used in this analysis (**Table 12**) were slightly varied due to the changes in the growth curves (Fujinami et al., 2021c).

### 5.3.2. *Alternative initial equilibrium catch*

The sensitivity of the base models to alternative assumptions about the initial equilibrium catch was examined by setting the lower catch (20,000 mt) and higher catch (60,000 mt) compared to the initial catch (40,000 mt) of the base model.

### 5.3.3. *Multiple abundance indices for late periods*

The sensitivity of the  $S6\_base$  model to multiple assumptions about the abundance indices for late periods was examined using seven scenarios. Five scenarios were the use of single time series for each CPUE (S1: HW\_DP; S3: TAIW\_LG; S7: JPN\_RTV; S9: SPC\_OBS\_TROPIC; S10: MEX). One scenario was the simultaneous use of CPUE indices for S1, S3 and S7 because these CPUEs had a similar trend in the late period since 1994. One scenario was the use of all CPUEs simultaneously. The remaining scenarios removed the S3 index from the simultaneous CPUE scenario and all CPUEs scenario, respectively.

### 5.3.4. *Alternative spawner recruit function*

The sensitivity of the base models to alternative assumptions about the SR function was examined using a LFSR function (Taylor et al., 2013). The same relationship used in the base model for the previous stock assessment in 2017 was applied with  $S_{Frac} = 0.391$  and  $\beta = 2$ .

### 5.3.5. *Alternative Beverton-Holt steepness (h)*

The sensitivity of the base models to alternative assumptions about the Beverton-Holt SR relationships was examined by assuming the lower steepness (0.513) and higher steepness (0.713) based on the steepness (0.613) of base models.

### 5.3.6. *Alternative Sigma-R*

The sensitivity of the base models to alternative assumptions about the Sigma-R was examined by assuming the lower Sigma-R (0.2) and higher Sigma-R (0.6), while the Sigma-R of the base models was fixed to 0.4 after tuning the parameter in the conditioning of SS3.

### 5.3.7. *Alternative selectivity function for Taiwanese large scale longline fleet*

The sensitivity of the base models to alternative assumptions about the selectivity function was examined using asymptotic selectivity (Pattern: 1; Simple logistic) on Taiwanese large scale longline fleet (F19) as used in the sensitivity analysis in the previous assessment in 2017.

### **5.3.8. *Alternative high seas small and large mesh driftnet catches***

The sensitivity of the base models to alternative assumptions about high seas small and large mesh driftnet catch was examined using the annual catch from 1971 to 1993 used in the previous assessment in 2017 (**Table 13**).

### **5.3.9. *Alternative high seas squid driftnet catch***

The sensitivity of the base models to alternative assumptions about high seas squid driftnet catch from 1980 to 1992 was examined by setting the lower and upper values of 95% confidence intervals based on the standard deviation ( $CV = 0.21$ ) of BSH's catch by Japanese fleet (**Table 14**) (Yatsu et al., 1993).

### **5.3.10. *Alternative annual catch for Non-ISC member countries***

The sensitivity of the base models to alternative assumptions about annual catch for Non-ISC member countries was examined using three scenarios (**Table 15**). The first scenario is the annual catch used in the previous stock assessment in 2017. The annual catch for 1995 to 2010 and for 2011-2015 were estimated by SPC and ISC, respectively. Due to the lack of observer data for 2009-2013, the catch rate of BSH for the Federated State of Micronesia (FSM) was fixed to a constant value for the time period using an average value of the other years in the base case model. However, the catch rate sharply dropped after 2013 coinciding with the implementation of a new shark-related WCPFC conservation and management measure (Kai et al., 2022d). Therefore, two alternative scenarios were considered. The second scenario is a gradual decrease of catch rate for FSM starting in 2009. The third scenario is a gradual decrease of catch rate for Federated State of Micronesia (FSM) starting in 2011.

### **5.3.11. *Alternative annual catch for Hawaii longline fleets***

The sensitivity of the base models to alternative assumptions about annual catch for Hawaii shallow- and deep- set longline fleets was examined using upper and lower ranges of reconstructed catch from random forest with all unobserved logbook records (**Table 16**) (Ducharme-Barth et al., 2022b).

### **5.3.12. *Alternative SS model configuration (mimic 2017 BSH SS3 model)***

The sensitivity of the base models to alternative assumptions about SS3 model configuration was examined using the 2017 stock assessment SS3 control file settings. All the data were updated until 2019/2020 without including the new structure such as length composition data of high seas driftnet fishery and splitting of the fleets for Japanese large mesh driftnet fishery and Hawaii longline fishery. This can be considered as a bridging analysis to bridge the previous and current assessment.

## 6. MODEL RESULTS

### 6.1. Model ensemble

#### 6.1.1. *S6\_base model*

The *S6\_base* model in SS3 ran without warning, all parameters were estimated to be within the bounds, the model converged to a low gradient (9.66354e-05), and the Hessian matrix was positive definite. The first round of jittering identified a best model, and this model remained the best model following a second round of jittering. The  $R_0$  likelihood profile (**Figure 11**) did not identify a better solution. The total  $R_0$  profile indicated that the maximum likelihood estimate (MLE) was strongly informed by the recruitment assumptions. The two main data components, index and length composition data, showed reasonable agreement and favored a marginally lower  $R_0$  estimate. Within the index component (**Figure 12**), there was a conflict between the early and late indices, where the early *S5* index preferred an  $R_0$  closer to the MLE and the *S6* late index preferred a lower  $R_0$ . The  $R_0$  profile for the length composition data (**Figure 12**) was strongly informed by the F4: JPN\_KK\_SH and F7: JPN\_ENY\_DP data which showed reasonable agreement and preferred a lower  $R_0$  than the MLE estimate.

Overall model fits to the two main data components, length composition and CPUE indices, were satisfactory. Fit to the aggregate length composition data appears reasonable for most fisheries (**Figure 13**), and overall fit to the mean length composition data over time showed low residual error (RMSE = 0.101; **Figure 14**). Analysis of the residual pattern in the fit to the temporal mean length trend did identify non-random residual patterns for F1: MEX, F3: CHINA, F4: JPN\_KK\_SH, F15: US\_GILL, and F18: US\_HW\_SH Shallow (**Figure 15**). Fits to the relative abundance indices were good for both the early (*S5*; **Figure 16**) and late (*S6*; **Figure 17**) indices with low overall residual error (RMSE = 0.082; **Figure 18**). Analysis of the fit to the CPUE did not identify non-random structure to the residual pattern for either the early or the late index (**Figure 19**).

Parametrizing the *S6\_base* model as an age-structured production model (ASPM) indicated the presence of a production function as the removals alone were able to provide adequate fits to the early (*S5*; **Figure 20**) and late (*S6*; **Figure 21**) indices. Though the estimated trend was similar between the ASPM and full model, estimates of scale were not consistent unless recruitment deviates were also estimated (**Figure 22**). Estimating recruitment deviates (ASPM-dev) also substantially improved the fits to the indices.

A three-year retrospective analysis indicated the presence of positive retrospective bias in SSB estimates (Mohn's  $\rho = -0.2$ ; **Figure 23**) and negative retrospective bias for estimates of  $F$  relative to  $F_{MSY}$  ( $F/F_{MSY}$ ; hereafter this value is referred to  $F$ ) (Mohn's  $\rho = 0.27$ ; **Figure 24**) which is outside of the desirable range (Hurtado-Ferro et al. 2015). One-step ahead forecasting from hindcast cross-validation of the late period index using the three-year retrospective analysis did not indicate that the model was able to outperform the naïve predictor (MASE = 1.29; **Figure 25**) though overall predictive accuracy showed that mean average predictive error was still close to 0.1 (adj. MASE = 1.15; **Figure 25**).

Selectivity was estimated to be strongly dome-shaped across most fisheries, though the US Hawaii based longline fisheries (F17 and F18) indicated the highest levels of selectivity for the largest sizes (**Figure 26**). Across all fisheries, female selectivity was estimated to be much lower than male selectivity and only approached full selectivity for F18: US\_HW\_SH. The F11: SM\_MESH assumed sex-invariant selectivity so both males and females were fully selected. For fishery F19: TAIW\_LG, time-varying selectivity was estimated which indicated a somewhat persistent shift to smaller sizes relative to the earliest years (**Figure 27**).

Estimates of SSB steadily declined from the mid-1970s to a low point in the early-1990s before climbing again through the mid-2000s (**Figure 28**). SSB appears to have stabilized in the last decade at around 150,000 mt though the last two years indicated a marginally declining trend. The trend in SSB is largely mirrored in temporal estimates of F which increase rapidly to a peak in the late-1980s before dropping quickly through the early-1990s (**Figure 29**). Estimates of F have declined more gradually over the last two-and-a-half decades though they had increased slightly in recent years. Estimated recruitment fluctuated around levels indicated by the SR relationship through the mid-1980s before surging to a peak in the late-1980s which coincides with the largest estimates of F (**Figure 30**). Recruitments appear correlated in the last three decades of the model period and have generally been smaller than those expected by the SR relationship over the last two decades.

### 6.1.2. *S11\_base model*

The *S11\_base* model in SS3 ran without warning, all parameters were estimated to be within the bounds, the model converged to a low gradient (8.66462e-05), and the Hessian matrix was positive definite. The first round of jittering identified a best model, and this model remained the best model following a second round of jittering. The  $R_0$  likelihood profile (**Figure 31**) did not identify a better solution. The total  $R_0$  profile indicated that the MLE was strongly informed by the recruitment assumptions. The two main data components, index and length composition data, showed good agreement with each other, and an  $R_0$  estimate consistent with the MLE. Within the index component (**Figure 32**) there was minor conflict between the early and late indices, where the early S5: JPN\_EARLY index preferred an  $R_0$  very close to the MLE and the S11: Composite-CPUE index preferring a slightly lower  $R_0$ . The  $R_0$  profile for the length composition data (**Figure 32**) was strongly informed by the F4: JPN\_KK\_SH and to a lesser extent by the F7: JPN\_ENY\_DP data. These data showed reasonable agreement consistent with the MLE estimate.

Overall model fits to the two main data components, length composition and CPUE indices, were satisfactory. Fit to the aggregate length composition data appears reasonable for most fisheries (**Figure 13**), and overall fit to the mean length composition data over time showed low residual error (RMSE = 0.103; **Figure 33**). Analysis of the residual pattern in the fit to the temporal mean length trend did identify non-random residual patterns for F1: MEX, F3 CHINA, F4: JPN\_KK\_SH, F15: US\_GILL, and F18: US\_HW\_SH (**Figure 34**). Fits to the relative abundance indices were good for both the early (S5; **Figure 16**) and late (S11; **Figure 35**) indices with low overall residual error (RMSE = 0.06; **Figure 36**). Analysis of the fit to the CPUE identified non-random structure to the residual pattern in the late index (**Figure 37**). However, given the smooth trend and lack of noise in the composite-CPUE it is unsurprising to have significant auto-correlation in the residuals.

Parametrizing the *S11\_base* model as an ASPM indicated the presence of a production function as the removals alone were able to provide adequate fits to the early (S5; **Figure 38**) and late (S11; **Figure 39**) indices. Estimated trend and scale were similar between the ASPM and the full model (**Figure 40**). Estimating recruitment deviates (ASPM-dev) substantially improved the fits to the indices.

A three-year retrospective analysis indicated the presence of positive retrospective bias in SSB estimates (Mohn's  $\rho = -0.29$ ; **Figure 41**) and negative retrospective bias for estimates of F (Mohn's  $\rho = 0.44$ ; **Figure 42**) both of which are substantially outside of the desirable range (Hurtado-Ferro et al., 2015). One-step ahead forecasting from hindcast cross-validation of the late period index using the three-year retrospective analysis did not indicate that the model was able to outperform the naïve predictor (MASE = 4.2; **Figure 43**). However, given the flatness of the index over the last three years of the model period, the naïve predictor had excellent predictive ability. Overall predictive accuracy was quite good and showed mean average predictive error was less than 0.1 (adj. MASE = 0.5; **Figure 43**).

Patterns in estimated selectivity were similar to the *S6\_base* model albeit shifted slightly to larger sizes. Selectivity was estimated to be strongly dome-shaped across most fisheries with the US Hawaii based longline fisheries (F17 & F18) indicating the highest levels of selectivity for the largest sizes (**Figure 26**). As before, female selectivity was estimated to be much lower than male selectivity and only approached full selectivity for F18: US\_HW\_SH. The F11: SM\_MESH fishery assumed sex-invariant selectivity so both males and females were fully selected. Similarly, for fishery F19: TAIW\_LG, time-varying selectivity indicated a somewhat persistent shift to smaller sizes relative to the earliest years (**Figure 27**).

Estimates of SSB steadily declined from the mid-1970s to a low point in the early-1990s before oscillating around this low point (~80,000 mt) for the remainder of the model period (**Figure 28**). Temporal estimates of F which increased rapidly to a peak in the late-1980s before dropping quickly through the early-1990s (**Figure 29**). Estimates of F were stable through the 1990s and 2000s before declining over the last decade. However, terminal estimates of F indicate an increase relative to the last five years. Estimated recruitment fluctuated around levels indicated by the stock recruit relationship through the mid-1980s before surging to a peak in the late-1980s which coincides with the largest estimates of F (**Figure 30**). Recruitments appear correlated in the last three decades of the model period and have generally been smaller than those expected by the SR relationship over the last two decades.

### 6.1.3. *S11\_ess* model

The *S11\_ess* model in SS3 ran without warning, all parameters were estimated to be within the bounds, the model converged to a low gradient (5.01008e-05), and the Hessian matrix was positive definite. The first round of jittering identified a best model, and this model remained the best model following a second round of jittering. The  $R_0$  likelihood profile (**Figure 44**) did not identify a better solution. The total  $R_0$  profile indicated that the MLE was strongly informed by the recruitment assumptions. Similar to the *S11\_base* model the two main data components, index and length composition data, were consistent with each other and the  $R_0$  estimate from the MLE. Within the index component (**Figure 45**) there was very minor conflict between the early and late indices, where the early S5: JPN\_EARLY index preferred an  $R_0$  slightly larger than the

MLE and the S11: Composite-CPUE late index preferring a slightly lower  $R_0$ . The  $R_0$  profile for the length composition data (**Figure 45**) was strongly informed by the F4:JPN\_KK\_SH and to a lesser extent by the F7: JPN\_ENY\_DP data. These data showed reasonable agreement consistent with the MLE estimate.

Overall model fits to the two main data components, length composition and CPUE indices, were satisfactory. Fit to the aggregate length composition data appears reasonable for most fisheries (**Figure 13**), and overall fit to the mean length composition data over time showed low residual error (RMSE = 0.104; **Figure 46**). Analysis of the residual pattern in the fit to the temporal mean length trend did identify non-random residual patterns for F1: MEX, F3: CHINA, F4: JPN\_KK\_SH, F15: US\_GILL, and F18: US\_HW\_SH (**Figure 47**). Fits to the relative abundance indices were good for both the early (S5; **Figure 16**) and late (S11; **Figure 35**) indices with low overall residual error (RMSE = 0.063; **Figure 48**). Analysis of the fit to the CPUE identified non-random structure to the residual pattern in the late index (**Figure 49**). Again as in the *S11\_base* model, given the smooth trend and lack of noise in the composite-CPUE it is unsurprising to have significant auto-correlation in the residuals.

Parametrizing the *S11\_ess* model as an ASPM showed weak evidence for a production function. The removals alone were able to explain the early index (S5; **Figure 50**) and however fit to the late index (S11; **Figure 51**) was comparably poor. Overall the estimated trend was similar between the ASPM and full model (**Figure 52**), though estimates of population scale were not. Estimating recruitment deviates (ASPM-dev) substantially improved the fits to the indices.

A three-year retrospective analysis indicated the presence of slight positive retrospective bias in SSB estimates (Mohn's  $\rho = -0.1$ ; **Figure 53**) and negative retrospective bias for estimates of F (Mohn's  $\rho = 0.13$ ; **Figure 54**) both of which are within the acceptable range (Hurtado-Ferro et al., 2015). One-step ahead forecasting from hindcast cross-validation of the late period index using the three-year retrospective analysis did not indicate that the model was able to outperform the naïve predictor (MASE = 2.87; **Figure 55**). Again similar to *S11\_base*, given the flatness of the index over the last three years of the model period, the naïve predictor had excellent predictive ability. Overall predictive accuracy was very good and showed mean average predictive error was less than 0.1 (adj. MASE = 0.34; **Figure 55**).

Patterns in estimated selectivity were similar to the previous models though selectivity estimates were shifted to select the largest individuals. Selectivity was estimated to be dome-shaped across most fisheries with the US Hawaii based longline fisheries (F17 & F18) indicating the highest levels of selectivity for the largest sizes (**Figure 26**). As before, female selectivity was estimated to be much lower than male selectivity and only approached full selectivity for F18 US Hawaii shallow set longline. The F11: SM\_MESH assumed sex-invariant selectivity so both males and females were fully selected. Similarly, for fishery F19: TAIW\_LG, time-varying selectivity indicated a somewhat persistent shift to smaller sizes relative to the earliest years (**Figure 27**).

Estimates of SSB followed a similar pattern to the *S11\_base* model though at a lower population scale. Spawning stock biomass steadily declined from the mid-1970s to an inflection point around 65,000 mt in the early-1990s before generally trending lower for the remainder of the model period (**Figure 28**). Temporal estimates of F were the highest across the three models considered. Fishing mortality increased rapidly to a peak in the late-1980s before dropping

quickly through the early-1990s (**Figure 29**). Estimates of  $F$  were increased gradually through the 1990s and 2000s before declining over the last 15 years. However, terminal estimates of  $F$  indicate a sharp increase in  $F$ . Estimated recruitment followed the same general pattern as the *S11\_base* model though estimated a series of smaller recruitments prior to the beginning of the model period. Again, recruitment peaked in the late-1980s which coincided with the largest estimates of  $F$  (**Figure 30**). Recruitments also appear correlated in the last three decades of the model period and have generally been smaller than those expected by the stock-recruit relationship over the last two decades.

## 6.2. Sensitivity analysis

Sensitivities to structural assumptions were conducted for each of the three component models of the model ensemble. The exception to this is that sensitivities to the choice of late CPUE index, which were not applied to the *S11\_base* model as this is effectively already a sensitivity of the *S6\_base* model. In addition, a scenario of “same model specification (Mimic 2017 assessment)” was only applied to the *S6\_base* model.

The results of sensitivity analyses are summarized in **Table 17**. Most of the models were converged with a small value of maximum gradient components. Sensitivity results across the three models in the ensemble indicated that  $SSB_{2020}$  of all scenarios were higher than  $SSB_{MSY}$  except for all the scenarios of alternative-late-CPUEs and low steepness scenario, while the  $F_{2017-2019}$  of all the scenarios were lower than  $F_{MSY}$  except for LFSR and low-steepness scenarios. The Kobe plot of sensitivity analysis for three base models clearly showed different stock statuses (**Figure 56**). *S6\_base* model indicated that  $SSB_{2020}$  of most scenarios were higher than  $SSB_{MSY}$ , while the  $F_{2017-2019}$  of all the scenarios were lower than  $F_{MSY}$ . *S11\_base* model indicated that  $SSB_{2020}$  of most scenarios were higher than  $SSB_{MSY}$ , however,  $SSB_{2020}$  of many scenarios were close to the  $SSB_{MSY}$  unlike *S6\_base* model, while the  $F_{2017-2019}$  of all the scenarios were lower than  $F_{MSY}$  except for the scenarios of LFSR and low-steepness value. *S11\_ess* model indicated that  $SSB_{2020}$  of most scenarios were lower than  $SSB_{MSY}$ , and the  $F_{2017-2019}$  of all the scenarios were higher than  $F_{MSY}$  except for five scenarios.

### 6.2.1. *Alternative mortality schedule*

The sensitivity result showed that the model was sensitive to this assumption, with noticeably higher estimates of SSBs (i.e.,  $SSB_{1971}$ ,  $SSB_{2020}$ , and  $SSB_{MSY}$ ) when using the alternative natural mortality schedules (**Table 17**).

### 6.2.2. *Alternative initial equilibrium catch*

The sensitivity result showed that the model was slightly sensitive to this assumption, with higher and lower estimates of  $SSB_{1971}$  for lower catch (20,000 mt) and higher catch (60,000 mt) scenario, respectively (**Table 17**).

### 6.2.3. *Multiple abundance indices for late periods*

The sensitivity result showed that the model was highly sensitive to this assumption of alternative late CPUE series. All models fitting to either the S7 Japanese research and training vessel index or the S9 SPC observer index resulted in  $SSB_{2020}$  to be lower than  $SSB_{MSY}$  (**Table**

17).

#### **6.2.4. *Alternative spawner recruit function***

The sensitivity result of model ensemble showed that  $SB_{2020}$  was very close to  $SB_{1971}$  due to the change in the spawner recruit function with higher  $SB_{MSY}$  compared to the other scenarios. The LFSR increased the  $F_s$  in 1971 and 2020 and decreased the  $F_{MSY}$  compared to the those for base model. The *SII\_ess* model had a convergence issue with a large maximum gradient (**Table 17**).

#### **6.2.5. *Alternative Beverton-Holt steepness (h)***

The sensitivity result showed that the model was slightly sensitive to this assumption, with higher and lower estimates of  $SSB_{MSY}$  and  $F_{MSY}$  for lower and higher steepness scenario, respectively. The  $SSB_{2020}$  was increased and  $F_{2017-2019}$  was decreased from the 1971 level as the steepness become lower and higher. The *S6\_base* model for this sensitivity scenario had a convergence issue with a large maximum gradient (**Table 17**).

#### **6.2.6. *Alternative Sigma-R***

The sensitivity result showed that the model was highly sensitive to lower Sigma-R and less sensitive to higher Sigma-R, with higher and lower estimates of SSBs (i.e.,  $SSB_{1971}$ ,  $SSB_{2020}$ , and  $SSB_{MSY}$ ) and lower and higher estimates of  $F_s$  (i.e.,  $F_{1971}$ ,  $F_{2020}$ , and  $F_{MSY}$ ) for lower and higher Sigma-R, respectively (**Table 17**).

#### **6.2.7. *Alternative selectivity function for Taiwanese large scale longline***

The sensitivity result showed that the model was slightly sensitive to assuming an asymptotic selectivity for one fishery, though the scenario had an impact on the estimates in 1971. The estimates of the MSY-related quantities (i.e.,  $SSB_{MSY}$ , and  $F_{MSY}$ ) were very similar to those obtained in the base model. Model fit to the size composition data of *S6\_base* model was not bad compared to that in the base model. The *SII\_ess* model had a convergence issue with a large maximum gradient (**Table 17**).

#### **6.2.8. *Alternative high seas small and large mesh driftnet catches***

The sensitivity result showed that the model was highly sensitive to the assumption of previous catches for high seas drift net fisheries, with noticeably higher estimates of SSBs and lower estimates of  $F_s$  (**Table 17**).

#### **6.2.9. *Alternative high seas squid driftnet catch***

The sensitivity result showed that the model was slightly sensitive to this assumption, with lower and higher estimates of SSBs and higher and lower estimates of  $F_s$  for lower and upper 95% confidence intervals, respectively (**Table 17**).

#### **6.2.10. *Alternative annual catch for Non-ISC member countries***

The sensitivity result showed that the model was insensitive to this assumption (**Table 17**).

### 6.2.11. *Alternative annual catch for Hawaii longline fleets*

The sensitivity result showed that the model was insensitive to this assumption. The *SII\_ess* model had a convergence issue with a large maximum gradient (**Table 17**).

### 6.2.12. *Alternative SS model configuration (mimic 2017 BSH SS3 model)*

The sensitivity analysis using the SS3 model parameterization from the previous ISC BSH stock assessment in 2017, showed substantially different values in the SSBs and Fs due to the change of the assumption of spawner recruit function from Beverton-Holt model to LFSR with lower sigma-R (=0.3).

## 6.3. Model ensemble results

Median annual SSB from the model ensemble followed the same general pattern as the three component models of the ensemble (**Figure 57**). Median annual SSB showed a steadily decreased trend through 1992 before generally increasing through 2004. Estimates of median annual SSB then declined through 2013 before increasing through to 2019 (2020 estimates of SSB are marginally lower than the 2019 estimates). Median annual F from the model ensemble gradually increased in the late 1970s and 1980s before suddenly dropping around 1990. This drop in F appears to slightly precede the high-seas drift gillnet fishing ban, and F was estimated to decrease gradually following this inflection point in 1993 (**Figure 57**). The median of the annual age-0 recruitment estimates from the model ensemble appeared relatively stable in the early part of the model period with a slight decreasing trend over the assessment period other than the large recruitment pulse in 1988 (**Figure 46**).

## 7. STOCK STATUS AND CONSERVATION CONCLUSIONS

### 7.1. Status of the stock

The current assessment provides the best available scientific information on North Pacific BSH stock status. The assessment used a fully integrated approach in SS3 with model inputs that have been updated since the previous assessment. The main difference between the present assessment and the 2017 assessment was 1) the use of an ensemble approach combining three models assuming alternative late period CPUE hypotheses and data weighting. Other differences were 2) catch, CPUE and size time series updated through 2019/2020; 3) improvements to the catch estimation and size data of the driftnet fishery and Non-ISC fishery; 4) improved life history information, such as growth and reproductive biology, and their contribution to productivity assumptions; 5) reconsideration of SR using the Beverton-Holt model; and 6) application of an improved suite of model diagnostics (Carvalho et al., 2021).

Target and limit reference points have not yet been established for pelagic sharks in the Pacific Ocean by either the WCPFC or the IATTC. Stock status was reported in relation to MSY-based reference points. The following information on the status of North Pacific BSH was provided.

The median of the annual SSB of model ensemble had a steadily decreasing trend until 1992 and slightly increased until recent years (**Figure 57A, B**). The median of the annual F of model ensemble gradually increased in the late 1970s and 1980s and suddenly dropped around 1990

which slightly preceded the high-seas drift gillnet fishing ban, after which it has been slightly decreasing (**Figure 57C, D**). The median of the annual age-0 recruitment estimates from the model ensemble appeared relatively stable with a slightly decreasing trend over the assessment period except for 1988 which shows a large pulse (**Figure 57E**). The historical trajectories of stock status from the model ensemble revealed that North Pacific BSH had experienced some level of depletion and overfishing in previous years showing that the trajectories moved through the overfishing zone, overfished and overfishing zone, and overfished zone in the Kobe plots relative to MSY reference points (**Figure 58**). However, in the last two decades, median estimates of the stock condition returned into the not overfished and not overfishing zone.

Based on these findings, the following information on the status of the North Pacific BSH was provided (**Table 18**):

1. Median female SSB in 2020 was estimated to be 1.170 of  $SSB_{MSY}$  (80<sup>th</sup> percentile, 0.570 - 1.776) and is likely (63.5% probability) not in an overfished condition relative to MSY-based reference points;
2. Recent annual  $F$  ( $F_{2017-2019}$ ) is estimated to be below  $F_{MSY}$  and overfishing of the stock is very likely (91.9% probability) not occurring relative to MSY-based reference points; and
3. The base case model results show that there is a 61.9% joint probability that NPO BSH stock is not in an overfished condition and that overfishing is not occurring relative to MSY based reference points.

## 7.2. Conservation information

Stock projections of biomass and catch of NPO BSH from 2020 to 2030 were performed

assuming four different harvest policies:  $F_{current}$  (2017-2019),  $F_{MSY}$ ,  $F_{current+20\%}$ , and  $F_{current-20\%}$  and evaluated relative to MSY-based reference points. Based on these findings (**Table 19**), the following conservation information is provided:

1. Future projections in three of the four harvest scenarios ( $F_{current}$  (2017-2019),  $F_{current+20\%}$ , and  $F_{current-20\%}$ ) showed that median SSB in the North Pacific Ocean will likely (>50 probability) increase; the  $F_{MSY}$  harvest scenario led to a decrease in median SSB.
2. Median estimated SSB of BSH in the North Pacific Ocean will likely (>50 probability) remain above  $SSB_{MSY}$  in the next ten years for all scenarios except  $F_{MSY}$ ; harvesting at  $F_{MSY}$  decreases SSB below  $SSB_{MSY}$  (Figure 59).
3. There remain some uncertainties in the time series based on the quality (observer vs. logbook) and timespans of catch and relative abundance indices, limited size composition data for several fisheries, the potential for additional catch not accounted for in the assessment, and uncertainty regarding life history parameters. Continued improvements in the monitoring of BSH catches, including recording the size and sex of sharks retained and discarded for all fisheries, as well as continued research into the biology, ecology,

and spatial structure of BSH in the North Pacific Ocean are recommended.

## 8. DISCUSSIONS

### 8.1. General remarks

The current stock assessment of North Pacific BSH estimates that the stock is unlikely to be overfished and that overfishing is unlikely to be occurring, based on MSY based reference points derived from the current ensemble modeling approach (**Figure 58**). Stock status appears to be trending in an increasingly positive direction based on estimates from the last five years of the model period (**Figures 57A, B**). However, yield based reference points such as MSY are particularly sensitive to modeling assumptions that impact the estimated production function, such as natural mortality and steepness. Both of these critical parameters are not estimated in the current stock assessment approach and uncertainty in the assumed values for these parameters is not considered in the current ensemble modeling framework. Sensitivity analyses to these assumptions did indicate that stock status was impacted by alternative assumptions for steepness (lower assumed steepness expectedly resulting in more pessimistic estimates of stock status, and vice-versa), though the *S11\_base* model had a convergence issue with higher maximum gradient (**Table 17**). Population scale was estimated to be substantially higher when assuming the alternative, lower natural mortality schedule. However, even at the new higher population scale, stock status estimates for the *S6\_base* and *S11\_base* models were reasonably insensitive to the change in natural mortality. However, the *S11\_ess* model indicated a noticeably more optimistic stock status with the assumed change in natural mortality (**Table 17, Figure 56**).

Though the current stock status is estimated to be qualitatively similar to the previous 2017 benchmark stock assessment, current population scale estimates are approximately 50% lower than what was estimated using the 2017 base case model. Current estimates of population scale are more consistent with the scale estimated in 2017 from models which did not fit to the Japanese Enyo Shallow late period CPUE index (S7: JPN\_RTV). Additionally, when the statistical and structural uncertainty across the model ensemble is taken into account, current estimates of stock status are considerably more pessimistic than the 2017 base case model. This again is consistent with sensitivity models from the 2017 stock assessment which did not fit to the Japanese Enyo Shallow late period CPUE.

The overall historical pattern of the stock indicates that when the model commenced in 1971 the population was already in a depleted state relative to virgin biomass (~70%). This is not unrealistic, considering the expansion of industrialized longline fishing activity into the North Pacific Ocean following World War II (Okamoto et al., 2004). While uncertainty to the level of initial equilibrium catch is explored as a part of the sensitivity analyses, it is not currently accounted for in the model ensemble. Notably, the trajectory of the stock shows a sharp period of decline from the mid-1970s through to the early-1990s (**Figure 57A**). Results from the ASPM (**Figures 22, 40, and 52**) show that this decline is supported by the concomitant increase in catches, predominantly from high seas drift gillnet fisheries (F8: JPN\_LG\_MESH\_EARLY; F11: SM\_MESH) (**Figure 2 upper panel**), and decline over the same period by the Japanese Kinkai shallow longline early period CPUE index (S5: JPN\_EARLY) (**Figure 3**). However, the ASPM

analysis also indicates that a reduction in catches alone is unable to explain the rapid increase in the S5: JPN\_EARLY (**Figures 20, 38, and 50**), and recruitment deviates are needed to be estimated in order to match this increase (**Figure 30**). Additional investigations are likely needed but it is possible that this apparent inconsistency between observed catches and the S5: JPN\_EARLY from 1990 – 1993 is responsible for the large pulse in recruitment seen in 1986 – 1988 since the Japanese Kinkai shallow longline fishery fully selects male BSHs of ~150 cm or ~5 years old. Regardless, further investigations are needed to identify the cause for (and potentially resolve) this anomalous recruitment pulse.

Both F and SSB appear to have stabilized over the last 20 years of the model period. As mentioned previously, stock status appears to be trending in an increasingly positive direction based on estimates from the last five years of the model period with estimated declines in F and increases in SSB (**Figures 57B, D**). However, over that same period recruitment has been estimated to be below average levels (**Figure 57E**) and below levels indicated by the assumed Beverton-Holt stock recruit relationship (**Figure 5**). These persistent low recruitments could be an indication of model mis-specification or un-modelled process. However, this has implications for the projection period, which assumes that recruitment is projected forward deterministically using the stock recruit relationship. The projection results could be overly optimistic if low recruitments continue into the future (**Figure 59**).

Lastly, the  $R_0$  profiles from all three models in the ensemble show that while the MLE estimate is reasonably consistent with the two main data components (survey and length composition), it is strongly informed by recruitment (**Figures 11, 31, and 44**). This is of some concern given that two critical components of the stock recruit relationship, steepness and sigma-R, are assumed to be fixed in this assessment, though it is not easy to internally estimate these parameters in the model due to a lack of data about the recruitment at the depleted spawner level. Sensitivity analyses showed that stock status was sensitive to alternative assumptions for both steepness and sigma-R however uncertainty in these parameters is not accounted for within the current model ensemble framework.

## 8.2. Improvements to the assessment

This stock assessment mainly improved the input data of SS3, SS3-model configuration, and model diagnostics. The updates/revisions of annual catch for driftnet fisheries (i.e., F8, F9 and F11) and longline fisheries (i.e., F1, F4-F7, F14, F17, F18, F19, and F20) improved the estimation of annual F. The updates/revisions of annual CPUEs for the late time period (i.e., S1, S3, S6, S7, and S10), especially for Japanese Kinkai shallow longline (S6) and Japanese research and training vessel (S7) indices (Kai et al., 2021a,b), contributed to improved estimations of trends in the annual abundance. In addition, the newly available CPUE (S7) played a critical role to make Composite-CPUE (S11). The updates/revisions of annual length composition data also contributed to improved estimations of age/length compositions of catch and abundance.

The accuracy of this stock assessment also improved by updating to new version of SS3, by revising biological parameters such as growth curve and steepness, by revamping stock-recruitment relationships, by using more objective twostep data-weighting method, by tuning the value of Sigma-R, by extending the estimation period of recruitment deviations, by changing the model structure through adding new fleet definition, and by conducting the comprehensive

model diagnostics. Finally, the introduction of a model ensemble approach also substantially improved the assessment.

### 8.3. Challenges

This stock assessment is the first time that the SHARKWG used an ensemble modelling approach and represents a notable change from the previous “single best base-case” approach used to characterize stock status. Moving to an ensemble modelling approach allows for a more complete characterization of the structural and statistical uncertainty in a stock assessment, and is a significant development for the SHARKWG. However, in taking this step forward it has highlighted challenges, some of general to ensemble modelling and some specific to the SHARKWG, and there remains opportunity for future improvement.

In developing the 2022 North Pacific BSH stock assessment, the SHARKWG applied current best practices for model diagnostics to try and objectively identify a single base model from a suite of proposed candidate models. This was a challenging task as none of the three candidate models consistently outperformed the others across the range of model diagnostics considered. The *S11\_ess* model showed the least retrospective bias (**Figures 23, 24, 41, 42, 53, and 54**), the *S11\_base* model appeared to have the best results from the ASPM (**Figures 22, 40, and 52**), and both *S11* models had the least conflict between data components as indicated by the  $R_0$  profile (**Figures 11, 31, and 44**). While the *S6\_base* model had the lowest MASE from hindcast cross-validation of the late period index, the adjusted MASE score for the *S6\_base* model was substantially worse than for the *S11* models (**Figures 25, 43, and 55**). Additionally, model fit to data common across all three models (early CPUE index and length composition data excluding the Taiwanese small scale longline) did not meaningfully differ (**Figures 14, 18, 23, 26, 46, and 48**). Accordingly, the SHARKWG elected to use a model ensemble approach for the current stock assessment.

Though a model ensemble approach was applied in the current assessment, construction of the model ensemble from candidate models was largely disconnected from the sensitivity analyses that were conducted. As a result, the structural uncertainty represented in the model ensemble is less than the structural uncertainty considered in the sensitivity analyses. Subsequent SHARKWG assessments should consider the possibility of a model ensemble from the onset of the assessment process (e.g., Data preparatory workshop) so that key uncertainties are investigated early on, and that the sensitivity analysis feeds into the construction of the model ensemble.

Stock assessment model development is an iterative process. The decision to adopt an ensemble modelling approach from a single base-case modelling approach was made late in the assessment model development process when it became apparent that there was no clear best base-case model. While a consensus on adopting a model ensemble approach was reached and the SHARKWG showed flexibility in adapting to challenges identified in the model development, the change in approach was difficult to process so close to the end of the assessment cycle. In the future, any new approaches (including an ensemble framework) should be agreed upon at the beginning of the assessment process to allow sufficient time for the identification, understanding, development, and discussion of appropriateness of the candidate models. Though timelines can be adjusted to give more opportunity for discussion of key model developments, the SHARKWG

should maintain the flexibility shown in the current assessment to adapt to unforeseen aspects of model development.

#### 8.4. Future stock assessment modeling considerations

The current stock assessment model assumes deterministic projections where future recruitments are assumed to follow the stock recruit relationship. Stochastic recruitments should be reconsidered in future assessments via resampling of the estimated recruitment deviates from the main model period. Additionally, this could allow for additional forecast scenarios to be explored. Projections could be conducted by only resampling the recent recruitments to investigate how stock status may change if low recruitments continue into the future.

Time-varying selectivity was assumed for the Taiwanese large-scale longline fishery (F19) in order to better fit the observed change in lengths over time (**Figure 27**). This modelling decision could be revisited in future assessments to see if improvements to the fit to the length composition data justifies the increased number of model parameters. Furthermore, the time-varying selectivity indicates a shift to smaller sizes. This phenomenon should be explored further to see if it is representative of a change in population structure or a change in the availability of BSH to the fishery due to a change in either fishing operations or fishing area. Though not a perfect comparison, a sensitivity to changing the selectivity shape of the F19 fishery to an asymptotic time invariant selectivity curve did not greatly change estimates for either the *S6\_base* or *S11\_base* models (**Table 17, Figure 56**).

The choice of likelihood for the length composition data was discussed at the SHARKWG pre-assessment meeting, and the Dirichlet multinomial was proposed as a candidate likelihood. Unfortunately, this likelihood structure was not thoroughly explored within the time constraints of the current stock assessment cycle, and should be re-considered in subsequent assessments.

Selectivity of female BSHs was estimated to be substantially lower than male BSHs of the same length for nearly all fisheries except the US Hawaii shallow-set longline (F18) and the high sea small mesh driftnet fishery (F11) (**Figure 26**). Though the current assessment model does not assume an explicit spatial structure and as such selectivity accounts for spatial/behavioral availability to the gear, it is worthwhile to further investigate the comparative invulnerability to fishing pressure for females across many of the model's fisheries and the implications that this might have on stock assessment results. Improved collection of sex-specific size composition data and an analysis of spatiotemporal patterns in the sex-specific composition data is needed.

#### 8.5. Research recommendations

Considerable effort was spent in the early stages of this assessment to refine the catch estimates and associated uncertainty for several fisheries: Non-ISC longline (F14), the high sea small mesh driftnet fisheries (F11), and the US Hawaii longline fisheries (F17 & F18). However, other than the F11 fishery, these fisheries do not account for a significant amount of the total North Pacific BSH catch. Further work remains for reconstructing the catches from the fisheries catching large amounts of BSH. Specifically, additional work is needed in developing uncertainty in reconstructed catch estimates for those fisheries. Though Ducharme-Barth et al. (2022a) used a machine learning approach applied to observer data to reconstruct catches for F17 & F18, this

approach is data intensive and may not be applicable to all fisheries. Additionally, catch should be provided in terms of numbers so that the conversion to weight can be done internally to the assessment model in a way that is consistent with the size composition, length-weight relationship, and fishery selectivity.

Quality of abundance indices for the current stock assessment generally improved relative to the 2017 stock assessment. Spatiotemporal approaches were used for the Japanese Kinkai shallow longline (S6) and Japanese research and training vessel (S7) indices in the recent period (Kai et al., 2021a,b). Application of these modelling techniques should be applied to the other key indices for future assessments. In future assessments, the SHARKWG should work with the WCPFC scientific services provider to update the SPC longline observer abundance index since it could provide additional information on BSH population trends in more tropical latitudes. Lastly, the use of a DFA composite index (S11; Ducharme-Barth et al. 2022b) was a first for the SHARKWG though it is an established analytical approach in other stock assessments (Peterson et al., 2021). Future research could be directed at investigating the effects of expanding the DFA analysis to include other input indices and using the model ensemble framework to account for the uncertainties in assumptions made during the DFA modeling process

Relative to the ensemble modelling approach, the current assessment did not consider uncertainty in key biological processes: growth, maturity, weight-at-length, maximum age, natural mortality, and steepness. Additionally, though the previous stock assessment made the recommendation to improve understanding and estimates in all of these processes, only the growth curve has been updated in the current assessment. It remains critical that additional biological research is conducted to improve the quality of the stock assessment. Regardless of future biological research, uncertainty in these biological processes could be developed (e.g., following the approach from Ducharme-Barth et al. 2021) in order to incorporate uncertainty in these quantities into estimates of stock status via a model ensemble framework.

Relatedly, research needs to continue to refine the stock recruitment relationship assumed in this assessment. While the LFSR is theoretically appealing, more work is needed to derive an appropriate parametrization and to understand how sensitivity to assumptions made in parametrizing this stock-recruitment relationship impact assessment outcomes.

## 9. ACKNOWLEDGEMENT

Completion of the BSH benchmark stock assessment was a collaborative effort by the ISC Shark Working Group. Those who greatly contributed include Mikihiro Kai (SHARKWG Chair, Editor/Author of assessment report and lead modeler), Nicholas Ducharme-Barth (Author of assessment report and lead modeler), Steven Teo (Author of assessment report and modeler), Felipe Carvalho (Author of assessment report and modeler), Michael Kinney (SHARKWG Vice-Chair, Data provision of US), Yasuko Semba (SHARKWG data manager, Data provision of Japan), Jacquelynne King (Data provision of Canada), Leonardo Castillo-Geniz (Data provision of Mexico), Sung-II Lee (Data provision of The Republic of Korea), Kwang-Ming Liu (Data provision of Chinese-Taipei), Xiaojie Dai (Data provision of China), Cleridy Lennert-Cody (Data provision of IATTC), Peter Williams (Data provision of WCPFC/SPC), Minoru Kanaiwa, Yuki Fujinami, Chien-Pang Chin, Wen-Pei Tsai, José Ignacio Fernández-Méndez, Luis González-Ania, Georgina Ramirez Soberon, and Atsuya Yamamoto.

## 10. REFERENCES

- Blanco-Parra, M.D.P., Galvan-Magana F., Marquez-Farias F. 2008. Age and growth of the blue shark, *Prionace glauca* Linnaeus, 1758, on the northwest coast of Mexico. *Revista de Biología Marina y Oceanografía*. 43, 513–520.
- Cailliet, G.M., Bedford, D. 1983. The biology of three pelagic sharks from California waters, and their emerging fisheries: a review. *CalCOFI. Rep.* 24, 57–69.
- Campana, S.E., Marks, L., Joyce, W., Kohler, N. 2005. Catch, bycatch and indices of population status of blue shark (*Prionace glauca*) in the Canadian Atlantic. *ICCAT Coll. Vol. Sci. Pap.* 58, 891–934.
- Carvalho, F., 2016. Standardized CPUE for blue shark (*Prionace glauca*) caught by the longline fisheries based in Hawaii (1994 – 2015). *ISC/16/SHARKWG-1/16*.
- Carvalho, F., Punt, A.E., Chang, Y.J., Maunder, M.N., Piner., K.R., 2017. Can diagnostic tests help identify model misspecification in integrated stock assessments?, *Fish. Res.* 192, 28–40. <https://doi.org/10.1016/j.fishres.2016.09.018>.
- Carvalho, F., Winker, H., Brodziak, J. 2016. Stock assessment and future projections for the North Pacific blue shark (*Prionace glauca*): An alternative Bayesian State-Space Surplus Production Model. *ISC/16/ SHARKWG -1/17*.
- Carvalho, F., Winker, H., Courtney, D., Kapur, M., Kell, L., Cardinale, M., Schirripa, M. et al. 2021. A cookbook for using model diagnostics in integrated stock assessments. *Fish. Res.* 240.105959. <https://doi.org/10.1016/j.fishres.2021.105959>.
- Castillo-Geniz, J.L., Godinez-Padilla, C.J., González-Ania, L.V., Haro-Avalos, H., Mondragón-Sánchez, L.F., Tovar-Ávila, J. 2017. Size and sex of the blue sharks caught by the Mexican longline industrial fleets recorded by on board observers in the Pacific 2006-2015. *ISC/17/SHARKWG-1/1*.
- Clarke, S.C., Milner-Gulland, E.J., Bjørndal, T., 2007. Social, economic, and regulatory drivers of shark fin trade. *Mar. Resour. Econ.* 22, 305–327.
- Clarke, S.C., Harley, S.J., Hoyle, S.D., Rice, J.S. 2013. Population Trends in Pacific Oceanic Sharks and the Utility of Regulations on Shark Finning. *Conserv. Biol.* 27, 197–209.
- Compagno, L.J.V. 1984. *FAO species catalog, Vol.4: Sharks of the world; Fisheries Synopsis No. 125.* Food and Agricultural Organization of the United Nations, Rome, Italy. 655 pp.
- Cortés, E. 2002. Incorporating Uncertainty into Demographic Modeling: Application to Shark Populations and Their Conservation. *Conserv. Biol.* 16, 1048–1062.
- Cortés, E., Arocha, F., Beerkircher, L., Carvalho, F., Domingo, A., Heupel, M., Holtzhausen, H., Santos, M.N., Ribera, M., Simpfendorfer, C. 2010. Ecological risk assessment of pelagic sharks caught in Atlantic pelagic longline fisheries. *Aquat. Living Recour.* 23, 25–34.
- Courtney, D., Cortes, E., Zhang, X., Carvalho, F. 2016. Stock synthesis model sensitivity to data weighting: An example from preliminary model runs conducted for North Atlantic blue shark. *SCRS/2016/066*.
- Dichmont, C.M., Deng, R.A., Punt, A.E., Brodziak, J., Chang, Y.J., Cope, J.M., Ianelli, J.M. et al. 2016. A review of stock assessment packages in the United States. *Fish. Res.* 183, 447–

60. <https://doi.org/10.1016/j.fishres.2016.07.001>.
- Ducharme-Barth, N., Kinney, M., Carvalho, F. 2021. 2021 ISC North Pacific blue shark stock assessment: US domestic fishery data updates: Catch, CPUE and length frequency. ISC/21/SHARKWG-2/P-01.
- Ducharme-Barth, N., Siders, Z., Ahrens, R. 2022a. Blue shark catch and CPUE for the US Hawaii longline fleet. ISC/22/SHARKWG-1/2.
- Ducharme-Barth, N., Teo, S., Kai, M., Carvalho, F. 2022b. Alternative Late-Period CPUE Hypothesis & Implications for the Stock Assessment of Blue Sharks in the North Pacific. ISC/22/SHARKWG-2/07.
- Ducharme-Barth, N., Matthew, V. 2020. Analysis of Pacific-Wide Operational Longline Dataset for Bigeye and Yellowfin Tuna Catch-per-Unit-Effort (CPUE). SC16-SA-IP-07. <https://meetings.wcpfc.int/node/11703>.
- Ducharme-Barth, N.D., Matthew, T.V. 2021. Focusing on the front end: a framework for incorporating uncertainty in biological parameters in model ensembles of integrated stock assessments. WCPFC-SC17-2021/SA-WP-05.
- FAO. 2017. Report of the Expert Workshop on Shark Post-Release Mortality Tagging Studies ([http://www.fao.org/fileadmin/user\\_upload/common\\_oceans/docs/Tuna/Report.pdf](http://www.fao.org/fileadmin/user_upload/common_oceans/docs/Tuna/Report.pdf)).
- Fernández-Méndez, J.I., Castillo-Géniz, J.L., Ramírez-Soberón, G., Haro-Ávalos, H., González-Ania, L.V. 2021. Update on standardized catch rates for blue shark (*Prionace glauca*) in the 2006-2020 Mexican Pacific longline fishery based upon a shark scientific observer program. ISC/21/SHARKWG-2/15.
- Francis, R.I.C.C. 2011. Data weighting in statistical fisheries stock assessment models. Can. J. Fish. Aquat. Sci. 68, 1124–1138.
- Fujinami, Y., Kanaiwa, M., Kai, M. 2021a. Blue shark catches in the Japanese large-mesh driftnet fishery in the North Pacific Ocean from 1974 to 1993. ISC/21/SHARKWG-2/8.
- Fujinami, Y., Kanaiwa, M., Kai, M. 2021b. Estimation of annual catch for blue shark caught by Japanese high seas squid driftnet fishery in the North Pacific Ocean from 1981 to 1992. ISC/21/SHARKWG-2/7.
- Fujinami, Y., Kurashima, A., Shiozaki, K., Hiraoka, Y., Semba, Y., Ohshimo, S., Nakano, H., Kai, M. (In prep.) New insights into spatial segregation by sex and life-history stage in blue sharks *Prionace glauca* in the northwestern Pacific.
- Fujinami, Y., Semba, Y., Kai, M. 2021c. Review and proposal of key life history parameters for North Pacific blue shark stock assessment. ISC/21/SHARKWG-2/9.
- Fujinami, Y., Semba, Y., Ohshimo, S., Tanaka, S. 2018. Development of an alternative ageing technique for blue shark (*Prionace glauca*) using the vertebra. J. Appl. Ichthyol. 34, 590–600.
- Fujinami, Y., Semba, Y., Okamoto, H., Ohshimo, S., Tanaka, S., 2017. Reproductive biology of the blue shark (*Prionace glauca*) in the western North Pacific Ocean. Mar. Freshw. Res. 68, 2018–2027.
- Fujinami, Y., Semba, Y., Tanaka, S. 2019. Age determination and growth of the blue shark

- (*Prionace glauca*) in the western North Pacific Ocean. Fish. Bull. 117, 107–120.
- Fujinami, Y., Shiozaki, K., Hiraoka, Y., Semba, Y., Ohshimo, S., Kai, M. 2021d. Seasonal migrations of pregnant blue shark *Prionace glauca* in the northwestern Pacific. Mar. Ecol. Prog. Ser. 658, 163–179.
- Hart, J.L. 1973. Pacific fishes of Canada. Fisheries Research Board of Canada Bulletin 180. 740pp.
- Hatchinson, M., Siders, Z., Stahl, J., Bigelow, K. 2021. Quantitative estimates of post-release survival rates of sharks captured in Pacific tuna longline fisheries reveal handling and discard practices that improve survivorship. PIFSC. Data Report DR-21-001.
- Hiraoka, Y., Kanaiwa, M., Ohshimo, S., Takahashi, N., Kai, M., Yokawa, K. 2016. Relative abundance trend of the blue shark *Prionace glauca* based on Japanese distant-water and offshore longliner activity in the North Pacific. Fish. Sci. 82, 687–699.
- Hiraoka, Y., Kanaiwa, M., Yokawa, K., 2013a. Re-estimation of abundance indices and catch amount for blue shark in the North Pacific ISC/13/SHARKWG-1/3.
- Hiraoka, Y., Kanaiwa, M., Yokawa, K., 2013b. Summary of estimation process of abundance indices for blue shark in the North Pacific. ISC/13/SHARKWG-2/2.
- Hurtado-Ferro, F., Szuwalski, C.S., Valero, J.L., Anderson, S.C., Cunningham, C.J., Johnson, K.F., Licandeo, R., McGilliard, C.R., Monnahan, C.C., Muradian, M.L., Ono, K., Vert-Pre, K.A., Whitten, A.R., Punt, A.E., 2015. Looking in the rear-view mirror: bias and retrospective patterns in integrated, age-structured stock assessment models. ICES J. Mar. Sci. 72, 99–110.
- IATTC. 2013. Preliminary estimates of total purse-seine bycatch of blue sharks (in number of animals), 197-2010, for the northern Eastern Pacific Ocean. ISC/13/SHARKWG-1/INFO-01.
- ISC, 2013. Stock assessment and future projections of blue sharks in the North Pacific Ocean. (Report of the Shark Working Group Stock Assessment Workshop No. Annex 11). International Scientific Committee for Tuna and Tuna-like Species in the North Pacific Ocean, Busan, South Korea.
- ISC, 2014. Stock assessment and future projections of blue sharks in the North Pacific Ocean (Report of the Shark Working Group Stock Assessment Workshop No. Annex 13). International Scientific Committee for Tuna and Tuna-like Species in the North Pacific Ocean, Taipei, Taiwan.
- ISC, 2017. Stock assessment and future projections of blue shark in the North Pacific Ocean through 2015. (Report of the Shark Working Group Stock Assessment Workshop No. Annex 13). International Scientific Committee for Tuna and Tuna-like Species in the North Pacific Ocean, Vancouver, Canada.
- ISC. 2019. ISC19 Plenary Report. (Report of the Shark Working Group Workshop No. Annex 4). International Scientific Committee for Tuna and Tuna-like Species in the North Pacific Ocean, Taipei, Chinese-Taipei.
- ISC. 2021. Stock Assessment Report for Pacific Blue Marlin (*Makaira nigricans*) through 2019. (Report of the Shark Working Group Stock Assessment Workshop No. Annex 10).

- International Scientific Committee for Tuna and Tuna-like Species in the North Pacific Ocean, Web-meeting.
- Ito, J., Shaw, W., Burger, R.L. 1993. Symposium on biology, distribution and stock assessment of species caught in the High Seas driftnet fisheries in the North Pacific Ocean held by the standing committee on biology and research at Tokyo, Japan in 1991. Vancouver, Canada.
- Kai M, Thorson JT, Piner KR, Maunder MN (2017) Predicting the spatio-temporal distributions of pelagic sharks in the western and central North Pacific. *Fish. Oceanogr.* 26, 569–582.
- Kai, M. 2019. Spatio-temporal changes in catch rates of pelagic sharks caught by Japanese research and training vessels in the western and central North Pacific. *Fish. Res.* 216, 177-195.
- Kai, M. 2020. Numerical approach for evaluating impacts of biological uncertainties on estimates of stock-recruitment relationships in elasmobranchs: example of the North Pacific shortfin mako, *ICES J. Mar. Sci.* 77, 200–215.
- Kai, M. 2021a. Spatio-temporal model for CPUE standardization: Application to blue shark caught by Japanese offshore and distant water shallow-set longliner in the western North Pacific. *ISC/21/SHARKWG-2/1*.
- Kai, M. 2021b. Spatio-temporal model for CPUE standardization: Application to blue shark caught by longline of Japanese research and training vessels in the western and central North Pacific. *ISC/21/SHARKWG-2/3*.
- Kai, M. 2021c. Update of Japanese annual catches for blue shark caught by Japanese offshore and distant water longliner in the North Pacific Ocean from 1994 to 2020. *ISC/21/SHARKWG-2/4*.
- Kai, M., Carvalho, F., Yokoi, H., Kanaiwa, M., Takahashi, N., Brodziak, J., Sippel., T., Kohin, S. 2017. Stock assessment for the North Pacific blue shark (*Prionace glauca*) using Bayesian State-space Surplus Production Model. *ISC/17/SHARKWG-1/4*.
- Kai, M., Ducharme-Barth, N., Fujinami, Y., Teo, S. 2022a. Reconstruction of catch for blue sharks caught by high seas squid driftnet fishery of Republic of Korea and Chinese Taipei in the North Pacific from 1980 to 1992. *ISC/22/SHARKWG-2/1*.
- Kai, M., Ducharme-Barth, N., Semba, Y., Teo, S. 2022b. Length frequency of blue sharks sampled by Canadian observers in the Japanese flying squid driftnet fishery in 1991. *ISC/22/SHARKWG-2/2*.
- Kai, M., Fujinami, Y. 2018. Stock-recruitment relationships in elasmobranchs: Application to the North Pacific blue shark. *Fish. Res.* 200, 104–115.
- Kai, M., Fujinami, Y. 2020. Estimation of mean movement rates for blue sharks in the northwestern Pacific Ocean. *Anim. Biotelemetry* 8:article, 35.
- Kai, M., Oshima, M., Carvalho, F. 2022c. Effects of version update of Stock Synthesis on the stock assessment results for blue shark in the North Pacific. *ISC/22/SHARKWG-2/3*.
- Kai, M., Semba, Y., Ducharme-Barth, N., Rice, J., Williams, P. 2022d. Reconstruction of catch for blue sharks caught by non-ISC countries in the western and central North Pacific from 1997 to 2020. *ISC/22/SHARKWG-1/1*.

- Kai, M., Teo, S, Ducharme-Barth, N., Carvalho, F. 2022e. Stock Synthesis settings of control file for the stock assessment of blue shark in the North Pacific. ISC/22/SHARKWG-2/5.
- Kai, M., Teo, S, Ducharme-Barth, N., Carvalho, F. 2022f. Main outcomes and model diagnostics of the Stock Synthesis base-case model candidate in the stock assessment for blue sharks in the North Pacific. ISC/22/SHARKWG-2/6.
- Kai, M., Teo, S, Ducharme-Barth, N., Semba, Y., Carvalho, F. 2022g. Stock Synthesis settings of data file for the stock assessment of blue shark in the North Pacific. ISC/22/SHARKWG-2/4.
- Kai, M., Yano, T. 2021. Updated annual catches of blue shark caught by Japanese coastal fisheries in the North Pacific Ocean from 1994 to 2019. ISC/21/SHARKWG-2/5.
- Kim, D.N., Kwon, Y., Lee, S., Cho, H., Ku, J., Lee, M. 2016. Catch and size data of blue shark by Korean tuna longline fishery in the North Pacific Ocean. ISC/16/SHARKWG-1/23.
- Kimoto, A., Yano, T., Yokawa, K. 2012. Historical catch amount of blue shark caught by the Japanese coastal fisheries. ISC/12/SHARKWG-1/11.
- King, J.R. 2021. Updated (2020) blue Shark (*Prionace glauca*) bycatch statistics in Canadian fisheries. ISC/21/SHARKWG-2/06.
- King, J.R., A.M. Surry. 2019. Blue shark (*Prionace glauca*) bycatch statistics in Canadian fisheries. ISC/19/SHARKWG-1/6.
- King, J.R., Wetklo, M., Supernault, J., Taguchi, M., Yokawa, K., Sosa-Nishizaki, O., Withler, R.E. 2015. Genetic analysis of stock structure of blue shark (*Prionace glauca*) in the north Pacific Ocean. Fish. Res. 172, 181–189.
- Kinney, M.J. 2019. Updated catch of blue shark in US West coast fisheries. ISC/19/SHARKWG-1/P4.
- Kiyofuji, H., Ijima, H., Ochi, D. 2017. A brief description of the Japanese data (size and drift net) for the NPALB stock assessment in 2017. ISC/17/ALBWG-1/3
- Kleiber, P., Clarke, S., Bigelow, K., Nakano, H., McAllister, M., Takeuchi, Y. 2009. North Pacific Blue Shark Stock Assessment. NOAA Tech. Memo. NMFS-PIFSC-17, 1–83.
- Kohin, S. and Wraith, J. 2010. NMFS SWFSC Juvenile Shark Abundance Survey Results. NOAA/NMFS/SWFC Admin. Rep.
- Kohin, S., Sippel, T., Carvalho, F. 2016. Catch and size of blue sharks caught in U.S. fisheries in the North Pacific. ISC/16/SHARKWG-2/15.
- Lee, S.I., Kim, D.N., Lee, M.K., Kwon, Y. 2019. Estimation of blue shark catch by Korean tuna longline fishery in the North Pacific Ocean. ISC/19/SHARKWG-1/8.
- Liu, K.M., Su, K.Y., Tsai, W.P., Chin, C.P. 2021a. Size and spatial distribution of the blue shark, *Prionace glauca*, caught by the Taiwanese large-scale longline fishery in the North Pacific Ocean. ISC/21/SHARKWG-2/13.
- Liu, K.M., Su, K.Y., Tsai, W.P., Chin, C.P. 2021b. Catch, size and distribution pattern of the blue shark caught by the Taiwanese small-scale longline fishery in the North Pacific. ISC/21/SHARKWG-2/12.

- Liu, K.M., Su, K.Y., Tsai, W.P., Chin, C.P. 2021c. Updated standardized CPUE and catch estimation of the blue shark from the Taiwanese large scale tuna longline fishery in the North Pacific Ocean. ISC/21/SHARKWG-2/14.
- Lorenzen, K., 2005. Population dynamics and potential of fisheries stock enhancement: practical theory for assessment and policy analysis: *Philos. Trans. R. Soc. Lond. B Biol. Sci.* 360, 171–189.
- Mangel, M., Brodziak, J., DiNardo, G. 2010. Reproductive ecology and scientific inference of steepness: a fundamental metric of population dynamics and strategic fisheries management. *Fish Fish.* 11, 89–104.
- Maunder, M.N., Piner, K.R. 2015. Contemporary fisheries stock assessment: many issues still remain. *ICES J. Mar. Sci.* 72, 7–18. <https://doi.org/10.1093/icesjms/fsu015>.
- Maunder, M.N., Xu, H., Lennert-Cody, C., Valero, J., Aires-da-Silva, A., Carolina Minte-Vera, C. 2020. Implementing reference point-based fishery harvest control rules within a probabilistic framework that considers multiple hypotheses.” SAC-1 INF-F REV 3. Inter-American Tropical Tuna Commission: Scientific Advisory Committee. [https://www.iattc.org/Meetings/Meetings2020/SAC-11/Docs/\\_English/SAC-11-INF-F\\_Implementing%20risk%20analysis.pdf](https://www.iattc.org/Meetings/Meetings2020/SAC-11/Docs/_English/SAC-11-INF-F_Implementing%20risk%20analysis.pdf).
- Maxwell, S.M., Scales, K.L., Bograd, S.J., Briscoe, D.K., Dewar, H., Hazen, E.L., Lewison, R.L., Welch, H., Crowder, L.B. 2019. Seasonal spatial segregation in blue sharks (*Prionace glauca*) by sex and size class in the northeast Pacific Ocean. *Divers. Distrib.* 25, 1304–1317.
- McAllister, M.K., Babcock, E.A. 2006. Bayesian surplus production model with the Sampling Importance Resampling algorithm (BSP): a user’s guide.
- McKinnel, S., Seki, M.P. 1998. Shark bycatch in the Japanese High Seas squid driftnet fishery in the North Pacific Ocean. *Fish. Res.* 39, 127–138.
- Method, R.D., Taylor, I.G. 2011. Adjusting for bias due to variability of estimated recruitments in fishery assessment models. *Can. J. Fish. Aquat. Sci.* 68, 1744–1760.
- Method, R.D., Wetzel, C.R., Taylor, I.G., Doering, K., Johnson, K.F. 2021. Stock Synthesis User Manual Version 3.30.18. NOAA Fisheries, Seattle, WA.
- Methot, R.D., Wetzel, C.R., 2013. Stock synthesis: a biological and statistical framework for fish stock assessment and fishery management. *Fish. Res.* 142, 86–99.
- Musyl, M.K., Gilman, E.L. 2018. Post-release fishing mortality of blue (*Prionace Glauca*) and silky shark (*Carcharhinus Falciformes*) from a palauan-based commercial longline fishery.” *Rev. Fish. Biol. Fish.* 28, 567–86.
- Nakano, H., 1994. Age, reproduction and migration of blue shark (*Prionace glauca*) in the North Pacific Ocean. *Bull. Nat. Res. Inst. Far, Seas Fish.* 31:141-256
- Nakano, H., Okada, K., Watanabe, Y., Uosaki, K. 1993. Outline of the large-mesh driftnet fishery of Japan. *Int. N. Pac. Fish. Comm. Bull.* 53, 25-37.
- Nakano, H., Stevens, J.D. 2008. The biology and ecology of the blue shark, *Prionace glauca*. In: Camhi, M.D., Pikitch, E.K., Babcock, E.A. (eds) *Sharks of the open ocean: biology,*

- fisheries and conservation. Blackwell Scientific, Oxford, p 140–151.
- Nosal, A.P., Cartamil, D.P., Wegner, N.C., Lam, C.H., Hastings, P.A. 2019. Movement ecology of young-of-the-year blue sharks *Prionace glauca* and shortfin mako *Isurus oxyrinchus* within a putative binational nursery area. *Mar. Ecol. Prog. Ser.* 623, 99–115.
- Okamoto, H. 2004. Search for the Japanese tuna fishing data before and just after World War II. *Pacific Ocean. Bull. Nat. Res. Inst. Far, Seas Fish.* 31:141-256.
- Pennington, M., Burmeister, L.M., Hjellvik, V. 2002. Assessing the precision of frequency distributions estimated from trawl-survey samples. *Fish. Bull.* 100, 74–80.
- Peterson, C.D., Michael, J.W., Enric, C., and Robert, J.L. 2021. Dynamic Factor Analysis to Reconcile Conflicting Survey Indices of Abundance. Edited by Emory Anderson. *ICES J. Mar. Sci.* 78, 1711–29. <https://doi.org/10.1093/icesjms/fsab051>.
- Peterson, I., Wroblewski, J.S. 1984. Mortality rate of fishes in the pelagic ecosystem. *Can. J. Fish. Aqua. Sci.* 41, 1117–1120.
- Punt, A.E. 2017. Some insights into data weighting in integrated stock assessments. *Fish. Res.* 192, 52–65.
- Rice, J., Harley, S. 2014. Standardization of blue shark catch per unit effort in the North Pacific Ocean based on SPC held longline observer data for use as an index of abundance. *ISC/14/SHARKWG-2/04*.
- Rice, J., Harley, S., Kai, M. 2014. Stock assessment of blue shark in the North Pacific Ocean using stock Synthesis. *WCPFC-SC-10-2014/SA-WP-08*.
- Semba, Y. 2021. Size distribution of blue shark (*Prionace glauca*) collected by Japanese fleet and research program in the North Pacific. *ISC/21/SHARKWG-2/11*.
- Semba, Y. 2022. Revision of fleet definition of size data of blue shark (*Prionace glauca*) collected by Japanese commercial longline fishery and longline research program in the North Pacific. *ISC/22/SHARKWG-1/3*.
- Sippel, T., Semba, Y., Shiozaki, K., Carvalho, F., Castillo-Geniz, L., Tsai, W., Liu, K.M., Kwon, Y., Chen, Y., Kohin, S., 2016. Size and sex structure of blue sharks in the North Pacific Ocean. *ISC/16/SHARKWG-1/14*.
- Sippel, T., Wraith, J., Kohin, S., Taylor, V., Holdsworth, J., Taguchi, M., Matsunaga, H., Yokawa, K. 2011. A summary of blue shark (*Prionace glauca*) and shortfin mako shark (*Isurus oxyrinchus*) tagging data available from the North and Southwest Pacific Ocean. *ISC/11/SHARKWG-2/4*.
- Smith, S.E., Au, D.W., Show, C. 1998. Intrinsic rebound potentials of 26 species of Pacific sharks. *Mar. Freshw. Res.* 49, 663–678.
- Sosa-Nishizaki, O. 2013. Unofficial blue shark catches estimations for the Mexican Pacific (1976-2011). *ISC/13/SHARKWG-2/INFO-01*.
- Sosa-Nishizaki, O., Castillo-Geniz, L., 2016. Blue shark catches estimations for the Mexican Pacific (1976-2014) (No. *ISC/16/SHARKWG-1/24*). Centro de Investigación Científica y de Educación Superior de Ensenada (CICESE), Busan, South Korea.
- Stevens, J.D., Bradford, R.W., West, G.J. 2010. Satellite tagging of blue sharks (*Prionace*

- glauca*) and other pelagic sharks off eastern Australia: depth behaviour, temperature experience and movements. *Mar. Biol.* 157, 575–591.
- Suda, A. 1953. Ecological study of blue shark (*Prionace glauca* Linne). In: Bulletin of the Nankai Fisheries Research Laboratory, No 26. Nankai Regional Fisheries Research Laboratory, Kochi, Japan, p 1–11. [In Japanese]
- Taguchi, M., King, J.R., Wetklo, M., Withler, R.E., Yokawa, K. 2015. Population genetic structure and demographic history of Pacific blue shark (*Prionace glauca*) inferred from mitochondrial DNA analysis. *Mar. Freshw. Res.* 66, 267–275.
- Takahashi, N., Kanaiwa, M., Ohshimo, S., Sippel, T., Yokawa, K. 2014. Stock assessment and future projections of blue shark in the North Pacific Ocean by Bayesian surplus production model using revised data. *ISC/14/SHARKWG-2/1*.
- Tanaka, S., Cailliet, G.M., Yudin, K.G. 1990. Differences in growth of the blue shark, *Prionace glauca*: technique or population? In: Pratt H.L., Gruber, S.H., Taniuchi, T. (eds). *Elasmobranchs as living resources: advances in the biology, ecology, systematics, and status of the fisheries*. NOAA Tech. Rep. 90, 177–187.
- Taylor, C.C., 1958. Cod growth and temperature. *Journal du Conseil International pour L’exploration de la Mer* 23, 366–370.
- Taylor, I.G., Doering, K.L., Johnson, K.F., Wetzel, C.R, Stewart, I.J. 2021. Beyond visualizing catch-at-age models: Lessons learned from the r4ss package about software to support stock assessments, *Fish. Res.* 239, 105924. <https://doi.org/10.1016/j.fishres.2021.105924>
- Taylor, I.G., Gertseva, V., Methot, R.D., Maunder, M.N. 2013. A stock- recruitment relationship based on pre-recruit survival, illustrated with application to spiny dogfish shark. *Fish. Res.* 142, 15–21.
- WCPFC. 2017. Stock assessment and future projections of blue shark in the North Pacific Ocean through 2015. *WCPFC-SC13-2017/SA-WP-10*.
- Wald, A., Wolfowitz, J. 1940. On a test whether two samples are from the same population. *Ann. Math. Statist.* 11, 147–62.
- Weng, K.C., Castilho, P.C., Morissette, J.M., Landeira-Fernandez, A.M., Holts, D.B., Schallert, R.J., Goldman, K.J., Block, B.A. 2005. Satellite tagging and cardiac physiology reveal niche expansion in salmon sharks. *Science* 310, 104.
- Yatsu, A., Hiramatsu, K., Hayase, S. 1993. Outline of Japanese squid driftnet fishery with notes on the by-catch. *Int. N. Pac. Fish. Comm. Bull.* 53, 5-24.
- Yokoi, H., Ijima, H., Ohshimo, S., Yokawa, K. 2018. Impact of biology knowledge on the conservation and management of large pelagic sharks. *Sci. Rep.* 7, 10619.
- Zuur, A.F., R.J. Fryer, I.T. Jolliffe, R. Dekker, J.J. Beukema. 2003. Estimating Common Trends in Multivariate Time Series Using Dynamic Factor Analysis. *Environmetrics.* 14, 665–85. <https://doi.org/10.1002/env.611>.

## 11. TABLES

**Table 1.** Summary of fleet-specific catch data used in the stock assessment for North Pacific blue shark.

Fishery number	Reference Code	Fishing Countries	Gear Types	Units	Time series	Source
F1	MEX	Mexico	Mexican Pacific longline	Biomass	1971-2020	Sosa-Nishizak and Castillo-Geniz (2016), Castillo-Geniz, pers. Comm., Oct 1, 2021
F2	CAN	Canada	Troll, gillnet, seine fishery, foreign and joint-venture fisheries	Biomass	1979-2020	King (2021)
F3	CHINA	China	Longline	Biomass	2001-2020	Meng Xia, pers. comm., Nov 3, 2021
F4	JPN_KK_SH	Japan	Offshore shallow-set longline	Biomass	1971-2020	Hiraoka et al.(2013a); Kai (2021c)
F5	JPN_KK_DP	Japan	Offshore deep-set longline	Biomass	1975-2020	Hiraoka et al.(2013a); Kai (2021c)
F6	JPN_ENY_SH	Japan	Distant water shallow-set longline	Biomass	1971-2020	Hiraoka et al.(2013a); Kai (2021c)
F7	JPN_ENY_DP	Japan	Distant water deep-set longline	Biomass	1975-2020	Hiraoka et al.(2013a); Kai (2021c)
F8	JPN_LG_MESH_EARLY	Japan	High-sea large-mesh driftnet	Biomass	1973-1992	Fujinami et al. (2021a)
F9	JPN_LG_MESH_LATE	Japan	Coastal large-mesh driftnet	Biomass	1993-2019	Fujinami et al. (2021a); Kai and Yano (2021)
F10	JPN_CST_OTH	Japan	Coastal longline, other longline, trap net, bait fishing, other fisheries	Biomass	1971-2019	Kai and Yano (2021)
F11	SM_MESH	Japan, The Republic of Korea, Chinese Taipei	High-sea small-mesh driftnet	Number	1981-1993	Fujinami et al. (2021b); Kai et al. (2022a)
F12	IATTC	RFMO	Offshore longline, coastal longline, gillnet, harpoon, and others	Biomass	1971-2020	Lennert, pers. comm., Oct 14, 2021
F13	KOREA	The Republic of Korea	Tuna longline, observer data	Biomass	1975-2020	Lee et al. (2019) and Lee, pers. Comm. Nov 11, 2021
F14	NON_ISC	Non-ISC member countries	Longline	Biomass	1997-2020	Kai et al. (2022b)
F15	US_GIILL	USA (American Samoa)	Gill net	Biomass	1978-2020	Kohin et al. (2016) and Kinney, pers. Comm. Oct 23, 2021
F16	US_SPORT	USA (American Samoa)	Recreational fishing	Biomass	1971-2020	Kohin et al. (2016) and Kinney, pers. Comm. Oct 23, 2021
F17	US_HW_DP	USA (Hawaii)	Deep-set longline	Number	1971-2020	Duchrme-Barth (2022)
F18	US_HW_SH	USA (Hawaii)	Shallow-set longline	Number	1981-2020	Duchrme-Barth (2022)
F19	TAIW_LG	Chinese Taipei	Large-scale longline	Biomass	1971-2020	Liu et al. (2021a)
F20	TAIW_SM	Chinese Taipei	Small-scull longline	Biomass	1971-2020	Liu et al. (2021b)

**Table 2.** Time series of catch (total dead removals; metric tons) for different countries/data sources. “Previous total catch” is total catch used in the previous assessment in 2017. The catch number for some fleets were converted to catch weight by each member country.

Year	Canada	China	IATTC	Japan	The Republic of Korea	Mexico	Non_ISC	Chinese Taipei	USA	Total	Previous total catch
1971	0	0	7	23,252	0	440	0	12,070	30	35,799	35,799
1972	0	0	5	17,977	0	440	0	15,056	30	33,508	33,508
1973	0	0	5	22,491	0	440	0	12,025	30	34,991	37,828
1974	0	0	5	20,075	0	440	0	10,742	30	31,292	34,763
1975	0	0	7	27,468	5	440	0	9,392	33	37,345	40,153
1976	0	0	7	43,154	32	374	0	10,286	129	53,982	53,854
1977	0	0	6	59,427	55	386	0	10,045	225	70,145	65,861
1978	0	0	8	48,717	17	561	0	10,603	329	60,235	60,069
1979	1	0	10	55,684	0	338	0	12,360	466	68,859	70,368
1980	11	0	10	56,952	114	336	0	12,840	630	70,894	74,002
1981	0	0	9	59,000	0	256	0	10,961	669	70,895	87,805
1982	0	0	6	49,538	317	306	0	12,003	784	62,954	71,405
1983	25	0	6	50,406	128	293	0	10,586	954	62,397	68,554
1984	0	0	6	51,117	117	263	0	9,509	1,112	62,123	63,265
1985	60	0	3	49,600	95	227	0	10,712	1,291	61,989	61,054
1986	90	0	2	46,924	91	407	0	9,048	1,496	58,059	57,025
1987	159	0	2	40,837	174	351	0	6,729	1,508	49,760	50,758
1988	0	0	6	48,754	147	509	0	6,966	1,783	58,166	55,553
1989	0	0	5	45,883	83	280	0	7,897	1,607	55,756	63,407
1990	4	0	3	30,323	80	1,130	0	8,885	460	40,885	47,603
1991	0	0	2	31,490	103	1,016	0	9,619	1,276	43,507	50,098
1992	0	0	3	27,270	105	1,636	0	7,615	1,209	37,838	41,735
1993	0	0	3	27,242	52	2,540	0	6,919	1,312	38,068	40,881
1994	0	0	2	36,055	58	1,758	0	5,470	736	44,080	44,505
1995	0	0	10	34,759	165	2,100	52	10,100	1,353	48,539	53,117
1996	1	0	2	28,564	294	3,117	52	9,917	1,721	43,667	45,862
1997	1	0	4	30,212	732	2,948	52	13,773	1,945	49,666	53,716
1998	2	0	2	30,499	427	3,134	402	11,640	2,735	48,841	50,760
1999	1	0	1	33,671	397	2,261	947	14,118	1,608	53,003	48,973
2000	1	0	2	31,257	406	2,719	228	20,391	1,392	56,395	57,202
2001	5	340	0	33,140	115	2,587	318	9,831	362	46,698	45,989
2002	5	334	3	29,258	223	2,524	347	11,582	286	44,562	44,626
2003	17	305	1	27,006	285	2,307	225	10,244	380	40,772	43,923
2004	4	282	1	25,135	37	3,781	770	12,668	370	43,047	50,118
2005	0	343	0	25,643	34	2,721	564	14,478	327	44,112	51,742
2006	20	201	3	22,576	15	2,765	472	14,175	263	40,489	46,965
2007	9	234	2	20,004	139	3,324	986	13,848	376	38,923	46,090
2008	6	134	3	16,333	52	4,355	625	14,824	208	36,539	42,801
2009	8	298	2	17,102	98	4,423	479	16,559	246	39,215	44,024
2010	7	357	1	17,481	293	4,469	532	13,349	286	36,774	44,281
2011	13	613	1	9,353	556	3,719	424	16,451	302	31,432	45,520
2012	9	758	2	11,555	345	4,108	597	16,451	273	34,097	39,777
2013	26	598	2	12,976	75	4,494	474	7,534	290	26,468	33,863
2014	9	251	0	13,426	100	5,502	409	11,856	374	31,927	37,707
2015	23	627	0	11,220	74	3,985	361	10,042	408	26,741	32,956
2016	12	258	2	11,367	0	4,973	388	12,130	440	29,570	
2017	25	764	0	11,166	4	3,384	1,333	11,676	526	28,879	
2018	46	727	0	10,388	2	2,852	1,488	11,189	511	27,204	
2019	78	856	0	9,634	4	3,772	1,864	15,743	569	32,521	
2020	150	865	0	8,231	0	3,533	1,158	12,734	627	27,297	

**Table 3.** Summary of abundance indices data used in the stock assessment for North Pacific blue shark.

<b>Fishery number</b>	<b>Reference Code</b>	<b>Fishery Description</b>	<b>Used</b>	<b><i>n</i></b>	<b>Time series</b>	<b>Source</b>
S1	US_HW_DP	Hawaiian deep-set longline	Yes	19	2002-2020	Duchrme-Barth et al. (2021)
S2	US_HW_SH	Hawaiian shallow-set longline	No			
S3	TAIW_LG	Taiwanese large-scale longline	Yes	17	2004-2020	Liu et al. (2021c)
S4	TAIW_SM	Taiwanese small-scale longline	No			
S5	JPN_EARLY	Japanese offshore and distant-water shallow-set longline (early period)	Yes	18	1976-1993	Hiraoka et al. (2013b)
S6	JPN_LATE	Japanese offshore and distant-water shallow-set longline (late period)	Yes	27	1994-2020	Kai (2021a)
S7	JPN_RTV	Japanese research and training vessels	Yes	27	1994-2020	Kai (2021b)
S8	SPC_OBS	SPC observer data	No			
S9	SPC_OBS_TROPIC	SPC hold longline observer data in the tropical area	Yes	17	1993-2009	Rice and Harley (2014)
S10	MEX	Mexican Pacific longline	Yes	15	2006-2020	Fernández et al. (2021)
S11	Composite-CPUE	A composite index from S1, S3, and S7	Yes	27	1994-2020	Duchrme-Barth et al. (2022b)

**Table 4.** CPUE time series (relative to its mean) for different fleets and the coefficient of variations (CV).

Year	S1		S3		S5		S6		S7		S9		S10		S11	
	US_HW_DP		TAIW_LG		JPN_EARLY		JPN_LATE		JPN_RTV		SPC_OBS_TR OPIC		MEX		Composite- CPUE	
	CPUE	CV	CPUE	CV	CPUE	CV	CPUE	CV	CPUE	CV	CPUE	CV	CPUE	CV	CPUE	CV
1976					1.35	0.02										
1977					1.40	0.01										
1978					1.21	0.02										
1979					1.27	0.01										
1980					1.36	0.02										
1981					1.13	0.01										
1982					1.11	0.01										
1983					1.05	0.01										
1984					0.91	0.01										
1985					0.78	0.01										
1986					0.91	0.01										
1987					0.68	0.01										
1988					0.71	0.01										
1989					0.64	0.01										
1990					0.67	0.01										
1991					0.85	0.01										
1992					0.89	0.01										
1993					1.07	0.01					0.87	0.15				
1994							0.84	0.15	1.48	0.10	0.96	0.14			1.22	0.04
1995							0.90	0.15	1.44	0.12	0.46	0.14			1.23	0.03
1996							0.85	0.14	1.39	0.10	0.87	0.14			1.22	0.03
1997							1.04	0.13	1.44	0.10	1.18	0.14			1.22	0.03
1998							1.03	0.13	1.39	0.12	1.80	0.14			1.21	0.03
1999							1.09	0.12	1.44	0.19	1.50	0.14			1.20	0.03
2000							1.06	0.12	1.24	0.12	1.35	0.14			1.15	0.04
2001							1.22	0.10	1.17	0.10	1.37	0.15			1.11	0.04
2002	1.04	0.63					1.03	0.11	1.09	0.10	1.06	0.15			1.08	0.04
2003	1.43	0.45					1.08	0.09	1.05	0.11	0.85	0.17			1.06	0.04
2004	1.34	0.43	0.24	0.12			1.03	0.10	0.96	0.10	1.05	0.14			0.98	0.04
2005	1.05	0.35	1.40	0.04			1.26	0.10	0.78	0.12	0.79	0.14			0.95	0.04
2006	0.90	0.42	0.80	0.05			1.06	0.10	0.72	0.12	0.85	0.14	1.32	0.07	0.89	0.04
2007	0.97	0.37	0.51	0.06			0.84	0.10	0.64	0.14	0.80	0.14	1.07	0.04	0.82	0.05
2008	0.57	0.30	0.69	0.06			0.73	0.12	0.41	0.13	0.69	0.14	1.26	0.05	0.74	0.05
2009	0.70	0.46	0.41	0.06			0.97	0.11	0.58	0.13	0.57	0.14	0.99	0.06	0.78	0.05
2010	0.81	0.32	0.97	0.07			1.04	0.13	0.79	0.15			0.83	0.05	0.86	0.04
2011	0.84	0.32	0.74	0.06			0.86	0.13	0.66	0.15			0.76	0.06	0.85	0.04
2012	0.71	0.39	1.03	0.05			0.88	0.14	0.59	0.15			1.23	0.11	0.85	0.04
2013	0.75	0.40	1.09	0.06			0.92	0.15	0.79	0.15			1.28	0.06	0.92	0.04
2014	0.97	0.37	0.70	0.07			1.04	0.15	1.04	0.16			1.10	0.06	0.99	0.04
2015	1.05	0.37	1.59	0.08			1.17	0.15	0.83	0.15			0.78	0.07	1.02	0.04
2016	1.05	0.30	1.21	0.07			1.14	0.15	1.09	0.13			1.05	0.07	1.07	0.04
2017	1.24	0.42	1.55	0.05			1.06	0.15	1.06	0.12			0.74	0.06	1.09	0.03
2018	1.12	0.39	1.22	0.07			1.04	0.15	0.98	0.13			0.91	0.07	1.07	0.04
2019	1.14	0.41	1.46	0.05			1.01	0.15	0.98	0.15			1.10	0.07	1.07	0.04
2020	1.35	0.47	1.39	0.06			0.81	0.17	0.97	0.17			0.57	0.09	1.08	0.04

**Table 5.** Summary of size data used in the stock assessment for North Pacific blue shark.

<b>Fishery number</b>	<b>Reference Code</b>	<b>Used</b>	<b>Time series</b>	<b>Units</b>	<b>Bin</b>	<b>n</b>	<b>Source</b>
F1	MEX	Yes	2006-2020	cm	5	15	Castillo-Geniz, pers. Comm., Oct 27, 2021
F2	CAN	No					
F3	CHINA	Yes	1993-2020 except for 2002	cm	5	26	Meng Xia, pers. comm., Nov 3, 2021
F4	JPN_KK_SH	Yes	2008-2020	cm	5	13	Semba (2021)
F5	JPN_KK_DP	Yes	2016-2020	cm	5	5	Semba (2021)
F6	JPN_ENY_SH	No					
F7	JPN_ENY_DP	Yes	1992-2020	cm	5	30	Semba (2021)
F8	JPN_LG_MESH_EARLY	Yes	1979-1983	cm	5	5	Semba (2021)
F9	JPN_LG_MESH_LATE	Yes	1994,1996,1998, 2011-2019	cm	5	12	Semba (2021)
F10	JPN_CST_Oth	No					
F11	SM_MESH	No	1991	cm	5, 8.6	1	Kai et al (2022b)
F12	IATTC	No					
F13	KOREA	No					
F14	NON_ISC	Yes	1994,1996-2008,2012,2016, 2018-2020	cm	5	19	Williams, pers. comm., Nov 19, 2021
F15	US_GIILL	Yes	1990-2020	cm	5	31	Kohin et al. (2016) and Kinney, pers. Comm. Nov 27, 2021
F16	US_SPORT	No					
F17	US_HW_DP	Yes	2003-2020	cm	5	18	Duchrme-Barth, pers. Comm., Jan 26, 2022
F18	US_HW_SH	Yes	2004-2020	cm	5	16	Duchrme-Barth, pers. Comm., Jan 26, 2022
F19	TAIW_LG	Yes	2004-2020	cm	5	17	Liu et al. (2021b)
F20	TAIW_SM	Yes	2012-2020	cm	5	9	Liu et al. (2021a)

**Table 6.** Summary of CVs for each fleet and recommended variance adjustment.  $CV_{\min}$  and  $CV_{\text{mean}}$  denotes a minimum average CV and a mean CV for each CPUE series respectively.

<b>Fleet</b>	<b><math>CV_{\min}</math></b>	<b><math>CV_{\text{mean}}</math></b>	<b>Adjusted variance</b>
S1_HW_DP	0.132	0.398	0.000
S3_TAIW_LG	0.360	0.064	0.136
S5_JPN_EARLY	0.065	0.012	0.188
S6_JPN_LATE	0.100	0.129	0.000
S7_JPN_RTV	0.128	0.130	0.000
S9_SPC_OBS_TROPIC	0.201	0.144	0.056
S10_MEX	0.170	0.066	0.134

**Table 7.** Multiplier and its 95% confidence intervals for fleets suggested by Francis data weighting method of length composition data.

<b>Fleet name</b>	<b>Suggested multiplier</b>	<b>Lower 95% interval</b>	<b>Upper 95% interval</b>
F1_MEX	1.19	0.76	3.25
F3_CHINA	70.37	43.42	158.07
F4_JPN_KK_SH	0.32	0.20	1.08
F5_JPN_KK_DP	23.19	15.38	219.13
F7_JPN_ENY_DP	2.87	1.17	20.07
F8_JPN_LG_MESH_EARLY	4.49	2.27	681.74
F9_JPN_LG_MESH_LATE	10.43	6.04	32.21
F14_NON_ISC	77.24	53.63	192.95
F15_USA_GILL	19.38	13.55	34.35
F17_USA_Lonline_DP	118.39	66.87	530.31
F18_USA_Lonline_SH	21.83	12.84	69.87
F19_TAIW_LG	4.49	2.69	11.53
F20_TAIW_SM	7.84	5.69	21.94

**Table 8.** Biological and spawner-recruitment parameters used in the previous and current stock assessment for North Pacific blue shark. Red denotes different values compared to those used in the previous assessment in 2017.

No	Parameter	Previous	Update	Source
1	Gender	2	2	ISC (2017)
2	Natural mortality	Age- and sex- specific (See Table 5)		Fujinami et al. (2021)
3	Reference age (a1)	1	1	
4	Maximum age (a2)	20	20	
5	Theoretical maximum age	24 for both sexes	24 for both sexes	Taylor (1958)
6	Female at first age	4	4	Fujinami et al. (2017)
7	Length at a1 (L1)	64.4 (Female)	64.3 (Female)	Fujinami et al. (2019)
8		68.2 (Male)	68.2 (Male)	
9	Length at a2 (L2)	244.6 (Female)	245.2 (Female)	Fujinami et al. (2019)
10		261.3 (Male)	261.5 (Male)	
11	Growth rate (K)	0.147 (Female)	0.146 (Female)	Fujinami et al. (2019)
12		0.117 (Male)	0.117 (Male)	
13	CV of L1 (CV=f(LAA))	0.25 (Female)	0.25 (Female)	ISC (2017)
14		0.25 (Male)	0.25 (Male)	
15	CV of L2	0.1 (Female)	0.1 (Female)	ISC (2017)
16		0.1 (Male)	0.1 (Male)	
17	Weight-at-length	$W=5.388 \times 10^{-6}L^{3.102}$ (Female);	$W=5.388 \times 10^{-6}L^{3.102}$ (Female);	Nakano (1994)
18		$W=3.293 \times 10^{-6}L^{3.225}$ (male)	$W=3.293 \times 10^{-6}L^{3.225}$ (male)	
19				
20	Length-at-50% Maturity	156.6 (Female)	156.6 (Female)	Fujinami et al. (2017)
21	Slope of maturity ogive	- 0.16 (Female)	- 0.16 (Female)	
22	Fecundity (Litter size; (4)eggs=a+b*L)	Proportional to body length	Proportional to body length	Fujinami et al. (2017)
23				
24	Slope of fecundity (b)	0.46	0.46	
25	Intercept of fecundity (a)	-45.54	-45.54	
26	Spawning season	1	1	ISC (2017)
27	Spawner-recruit steepness ( <i>h</i> )	0.670 (shape: BH)	0.613 (shape: BH)	Fujinami et al. (2021)
28	Recruitment variability ( $\sigma_R$ )	0.3	0.3	ISC (2017)
29	Main recruitment deviations	1990-2013	1971-2020	

**Table 9.** Estimates of age- and sex- specific natural mortality used in the previous and current stock assessment for North Pacific blue shark. The schedules are based on the allocation method with life history parameters.

Age	Previous		Update	
	Female	Male	Female	Male
0	0.785	0.728	0.787	0.726
1	0.488	0.492	0.489	0.491
2	0.370	0.383	0.371	0.382
3	0.306	0.320	0.307	0.320
4	0.267	0.279	0.267	0.279
5	0.240	0.251	0.240	0.251
6	0.221	0.230	0.221	0.230
7	0.207	0.214	0.207	0.214
8	0.196	0.202	0.196	0.202
9	0.187	0.192	0.187	0.192
10	0.180	0.184	0.180	0.184
11	0.175	0.177	0.175	0.178
12	0.171	0.172	0.170	0.172
13	0.167	0.167	0.167	0.168
14	0.164	0.163	0.164	0.164
15	0.161	0.160	0.161	0.160
16	0.159	0.157	0.159	0.158
17	0.157	0.155	0.157	0.155
18	0.156	0.153	0.156	0.153
19	0.155	0.151	0.154	0.151
20	0.154	0.149	0.153	0.150
21	0.153	0.148	0.152	0.148
22	0.152	0.147	0.151	0.147
23	0.151	0.146	0.151	0.146
24	0.151	0.145	0.150	0.145

**Table 10.** Fleet-specific selectivity assumptions used in the stock assessment for North Pacific blue shark. The selectivity curves for fisheries lacking length composition data were assumed to be the same (i.e., mirror gear) as a related fishery operating in the manner or area.

Fishery number	Reference Code	Selectivity assumption	Time block or time varying selectivity	Mirror gear
F1	MEX	Double-normal-24		Estimate
F2	CAN	Double-normal-24		F1
F3	CHINA	Double-normal-24		Estimate
F4	JPN_KK_SH	Double-normal-24		Estimate
F5	JPN_KK_DP	Double-normal-24		Estimate
F6	JPN_ENY_SH	Double-normal-24		F4
F7	JPN_ENY_DP	Double-normal-24		Estimate
F8	JPN_LG_MESH_EARLY	Double-normal-24	1973-1981, 1982-1993	Estimate
F9	JPN_LG_MESH_LATE	Double-normal-24		Estimate
F10	JPN_CST_OTH	Double-normal-24		F9
F11	SM_MESH	Double-normal-24(Sex combined)		Estimate
F12	IATTC	Double-normal-24		F1
F13	KOREA	Double-normal-24		F3
F14	NON_ISC	Double-normal-24		Estimate
F15	US_GIILL	Double-normal-24		Estimate
F16	US_SPORT	Double-normal-24		F15
F17	US_HW_DP	Double-normal-24		Estimate
F18	US_HW_SH	Cubic spline in length-27		Estimate
F19	TAIW_LG	Double-normal-24	2004-2020	Estimate
F20	TAIW_SM	Double-normal-24		Estimate
S1	US_HW_DP	Double-normal-24		F17
S2	US_HW_SH	Double-normal-24		F18
S3	TAIW_LG	Double-normal-24		F19
S4	TAIW_SM	Double-normal-24		F20
S5	JPN_EARLY	Double-normal-24		F4
S6	JPN_LATE	Double-normal-24		F4
S7	JPN_RTV	Double-normal-24		F7
S8	SPC_OBS	Double-normal-24		F14
S9	SPC_OBS_TROPIC	Double-normal-24		F14
S10	MEX	Double-normal-24		F1
S11	Composite-CPUE	Double-normal-24		F7

**Table 11.** Summary of the sensitivity analysis used in the stock assessment for North Pacific blue shark. Scenarios of late CPUE series were not used in the *SII\_base* or *SII\_ess* models. Composite CPUE denotes the use of each index simultaneously, not DFA composite-CPUE.

No	Items	Details	Values
1	Natural mortality schedules	Petersen and Wroblewski	
2	Initial equilibrium catch (MT)	2-1. Low	20000
		2-2. High	60000
3	Late CPUE series	3-1. S1:HW_DP	
		3-2. S3:TAIW_LG	
		3-3. S7: JPN_RTV	
		3-4. S9: SPC_OBS_TROPIC	
		3-5. S10: MEX	
		3-6. Composite CPUE (S1, S3 and S7)	
		3-7. All CPUEs	
		3-8. Composite CPUE (S1 and S7)	
		3-9. All CPUEs excluding S3	
4	Spawner-recruit function	LFSR used in the previous assessment	Alfa=0.391
			Beta=2
5	Beverton-Holt steepness (h)	5-1. Low	0.513
		5-2. High	0.713
6	Sigma-R	6-1. Low	0.2
		6-2 High	0.6
7	Selectivity function	Asymptotic selectivity on F19 (TAIW_LG)	
8	High seas small and large mesh driftnet catch (1971-1993)	Base-case	
		Previous catch used in 2017	
9	High seas driftnet catch	9-1. Lower value of 95% CI based on the SD of JP fishery (Yatsu et al., 1993)	CV=0.21
		9-2. Higher value of 95% CI based on the SD of JP fishery (Yatsu et al., 1993)	CV=0.21
10	Non-ISC catch	10-1. Previous catch estimates from SPC and ISC	
		10-2. Gradual decrease of catch rate for FSM starting in 2009	
		10-3. Gradual decrease of catch rate for FSM starting in 2011	
11	US-HW LL catch for shallow-set and deep-set	11-1. Upper range of reconstructed catch from RF with all unobserved logbook records	
		11-2. Lower range of reconstructed catch from RF with all unobserved logbook records	
12	Model specification	Mimic 2017 blue shark assessment	

**Table 12.** Alternative assumptions about natural mortality (year<sup>-1</sup>) schedule estimated from Petersen and Wroblewski (1984).

Age	Alternative		Base-case	
	Female	Male	Female	Male
0	0.311	0.262	0.787	0.726
1	0.186	0.178	0.489	0.491
2	0.141	0.141	0.371	0.382
3	0.118	0.120	0.307	0.320
4	0.104	0.107	0.267	0.279
5	0.094	0.097	0.240	0.251
6	0.087	0.090	0.221	0.230
7	0.082	0.085	0.207	0.214
8	0.078	0.081	0.196	0.202
9	0.075	0.078	0.187	0.192
10	0.073	0.075	0.180	0.184
11	0.071	0.073	0.175	0.178
12	0.069	0.071	0.170	0.172
13	0.068	0.069	0.167	0.168
14	0.067	0.068	0.164	0.164
15	0.066	0.067	0.161	0.160
16	0.065	0.066	0.159	0.158
17	0.065	0.065	0.157	0.155
18	0.064	0.064	0.156	0.153
19	0.064	0.064	0.154	0.151
20	0.063	0.063	0.153	0.150
21	0.063	0.063	0.152	0.148
22	0.063	0.062	0.151	0.147
23	0.062	0.062	0.151	0.146
24	0.062	0.061	0.150	0.145

**Table 13.** Alternative assumptions about high seas small and large mesh driftnet catch (metric tons) used in the previous assessment in 2017.

<b>Year</b>	<b>Large_mesh</b>	<b>Small_mesh</b>
1971	0	0
1972	0	0
1973	6296.9	0
1974	6296.9	0
1975	6296.9	0
1976	6296.9	0
1977	6296.9	0
1978	6296.9	0
1979	6296.9	0
1980	6296.9	0
1981	6296.9	13331.3
1982	6296.9	13331.3
1983	5926.8	13331.3
1984	4727.5	13331.3
1985	3763.6	13331.3
1986	4081.1	13331.3
1987	3990.5	13331.3
1988	3707.7	13331.3
1989	3707.7	20022
1990	3707.7	8758.4
1991	3707.7	8758.4
1992	3387.7	4379.2
1993	660.5	0

**Table 14.** Alternative assumptions about high seas squid driftnet catch number (1000s). The lower and upper values were estimated using the coefficient of variation of the Japanese driftnet catch.

<b>Year</b>	<b>Lower 95%</b>	<b>Upper 95%</b>
1980	108	166
1981	232	356
1982	1211	1855
1983	1649	2525
1984	2224	3406
1985	2436	3732
1986	2649	4057
1987	2629	4027
1988	3407	5219
1989	2923	4477
1990	1683	2579
1991	1307	2003
1992	798	1222

**Table 15.** Alternative assumptions about annual catch (MT) for non-ISC member countries.

<b>Year</b>	<b>Previous catch in 2017</b>	<b>Gradual decrease in catch from 2009</b>	<b>Gradual decrease in catch from 2011</b>
1995	161	51.7	51.7
1996	165	51.7	51.7
1997	261	51.7	51.7
1998	634	402.3	402.3
1999	782	946.5	946.5
2000	1350	227.9	227.9
2001	944	317.5	317.5
2002	2126	346.5	346.5
2003	1708	224.9	224.9
2004	5846	769.5	769.5
2005	3081	564.3	564.3
2006	3111	472.1	472.1
2007	3153	986.2	986.2
2008	2066	625.2	625.2
2009	1778	479.4	479.4
2010	1808	432.8	531.5
2011	2624	245.6	424.3
2012	2778	307.6	414.8
2013	2131	215.1	252.6
2014	2059	408.6	408.6
2015	2059	360.9	360.9
2016		387.8	387.8
2017		1332.6	1332.6
2018		1487.9	1487.9
2019		1863.7	1863.7
2020		1157.5	1157.5

**Table 16.** Alternative assumptions about the lower and upper annual catch number (1000s) for Hawaii deep-set and shallow-set longline fleets.

Year	Deep_ high	Deep_ low	Shallow_ high	Shallow_ low	Year	Deep_ high	Deep_ low	Shallow_ high	Shallow_ low
1971	0.0	0.0	0.0	0.0	1996	33.4	29.4	42.5	18.2
1972	2.2	0.1	0.0	0.0	1997	37.5	35.2	43.0	26.9
1973	2.3	0.2	0.0	0.0	1998	41.0	38.8	40.7	32.6
1974	1.9	0.1	0.0	0.0	1999	44.8	43.2	32.4	20.1
1975	1.9	0.1	0.0	0.0	2000	39.5	37.7	33.4	22.0
1976	1.6	0.1	0.0	0.0	2001	35.8	19.3	22.9	9.7
1977	2.0	0.1	0.0	0.0	2002	27.6	7.7	1.5	0.5
1978	2.4	0.1	0.0	0.0	2003	29.7	7.1	0.5	0.1
1979	2.0	0.1	0.0	0.0	2004	32.7	8.4	0.5	0.4
1980	0.8	0.1	0.0	0.0	2005	39.9	9.2	5.1	4.9
1981	0.0	0.0	0.0	0.0	2006	32.2	8.3	3.4	3.2
1982	0.1	0.0	0.0	0.0	2007	38.4	6.5	5.4	5.2
1983	0.3	0.0	0.0	0.0	2008	39.1	7.5	4.5	4.3
1984	0.9	0.1	0.1	0.0	2009	36.2	5.6	3.0	2.8
1985	0.4	0.0	0.1	0.1	2010	39.3	6.3	6.2	6.0
1986	0.7	0.0	0.3	0.2	2011	45.7	7.5	2.6	2.4
1987	1.2	0.1	0.7	0.4	2012	51.9	8.1	2.3	2.1
1988	0.9	0.1	1.5	0.9	2013	56.4	7.8	1.9	1.8
1989	1.2	0.1	3.6	2.0	2014	55.8	8.1	4.0	3.9
1990	5.9	0.4	8.4	4.5	2015	55.3	9.5	5.3	5.0
1991	14.3	0.9	19.7	10.3	2016	58.4	9.9	4.1	4.0
1992	13.9	0.9	46.1	23.2	2017	59.5	10.4	3.7	3.5
1993	16.9	14.9	69.9	35.7	2018	61.4	11.4	1.3	1.2
1994	19.1	16.6	81.9	39.5	2019	62.6	11.9	1.7	1.6
1995	22.1	18.5	41.5	9.1	2020	75.5	13.8	2.8	2.7

**Table 17.** Estimates of key management quantities for the North Pacific blue shark stock assessment base model and the outcomes of the sensitivity analysis. The values of management quantity were derived from model ensemble formed by the weighted average of results from the three component models.

No	Scenarios	Manegment Quantity							Maximum gradient				
		SB <sub>1971</sub>	SB <sub>2020</sub>	SB <sub>MSY</sub>	MSY	F <sub>1971</sub>	F <sub>2017-2019</sub>	F <sub>MSY</sub>	SB <sub>2020</sub> / SB <sub>MSY</sub>	F <sub>2017-2019</sub> / F <sub>MSY</sub>	S6_base	S11_base	S11_ess
0	Base model	158,324	102,913	83,545	50,897	0.36	0.51	0.76	1.20	0.67	0.0001	0.0001	0.0001
1	Alternative Natural mortality schedules	796,669	604,465	379,930	66,849	0.26	0.27	0.47	1.58	0.57	0.0000	0.0000	0.0001
2	Alternative Initial catch-Low	196,106	108,543	82,390	50,097	0.26	0.46	0.75	1.30	0.61	0.0001	0.0005	0.0000
3	Alternative Initial catch-High	115,837	117,663	101,090	62,198	0.65	0.63	0.75	1.19	0.79	0.0001	0.0001	0.0006
4	Alternative late CPUE-S1: HW_DP	157,086	117,926	84,072	51,475	0.36	0.36	0.75	1.40	0.48	0.0000		
5	Alternative late CPUE-S3: TAIW_LG	159,286	132,297	86,981	52,728	0.36	0.33	0.74	1.52	0.44	0.0001		
6	Alternative late CPUE-S7: JPN_RTV	127,973	45,136	76,465	46,904	0.32	0.94	1.23	0.59	0.76	0.0001		
7	Alternative late CPUE-S9: SPC_OBS_TROPIC	122,637	69,494	78,138	47,655	0.39	0.62	1.09	0.89	0.57	0.0001		
8	Alternative late CPUE-S10: MEX	186,729	158,385	94,316	56,400	0.32	0.30	0.71	1.68	0.42	0.0001		
9	Alternative late CPUE-Composite CPUE (S1, S3, and S7)	126,660	44,229	76,575	46,909	0.28	1.02	1.49	0.58	0.6879	0.0001		
10	Alternative late All CPUEs	113,998	38,915	76,204	46,282	0.31	1.19	1.74	0.51	0.69	0.0001		
11	Alternative late Composite CPUE (S1 and S7)	127,951	45,112	76,433	46,987	0.32	0.95	1.23	0.59	0.77	0.0003		
12	Alternative late All CPUEs excluding S3	114,422	39,231	76,515	46,393	0.31	1.12	1.69	0.51	0.67	0.0001		
13	Alternative SR function (LFSR)	141,009	109,367	102,698	59,135	0.74	0.93	0.63	1.09	1.35	0.0001	0.0001	0.1842
14	Alternative Beverton-Holt steepness -Low	169,382	98,897	101,343	47,680	0.43	0.65	0.59	0.96	1.11	0.0000	1.4176	0.0005
15	Alternative Beverton-Holt steepness -High	155,825	114,579	69,832	55,128	0.29	0.33	0.95	1.62	0.35	0.0001	0.0001	0.0006
16	Alternative Sigma-R-Low	220,650	173,123	102,308	62,398	0.28	0.45	0.67	1.58	0.71	0.0000	0.0001	0.0000
17	Alternative Sigma-R-High	144,123	82,989	80,492	48,972	0.39	0.56	0.80	1.03	0.70	0.0001	0.0001	0.0001
18	Asymptotic selectivity for F19: TAIW_LG	136,158	101,366	83,982	51,285	0.57	0.52	0.74	1.18	0.71	0.0001	0.0000	1099.95
19	Previous catch for high seas driftnet fisheries	740,884	633,260	274,994	163,985	0.08	0.08	0.62	2.30	0.13	0.0000	0.0000	0.0005
20	High seas squid drinet catch-Lower 95%	139,430	84,940	78,564	47,894	0.40	0.60	0.81	1.06	0.74	0.0001	0.0000	0.0003
21	High seas squid drinet catch-Upper 95%	179,408	123,026	89,788	54,580	0.33	0.44	0.72	1.33	0.60	0.0001	0.0001	0.0000
22	Alternative Non-ISC catch- previous catch in 2017	156,962	98,345	82,376	50,484	0.37	0.52	0.74	1.17	0.71	0.0000	0.0000	0.0006
23	Alternative Non-ISC catch- catch rate starting in 2009	158,358	103,045	83,621	50,925	0.36	0.51	0.76	1.20	0.66	0.0000	0.0001	0.0001
24	Alternative Non-ISC catch- catch rate starting in 2011	158,598	104,324	83,696	50,957	0.36	0.49	0.76	1.22	0.64	0.0001	0.0001	0.0001
25	Alternative US-HW-LL catch- Lower range	158,598	105,823	83,579	50,745	0.36	0.48	0.77	1.24	0.63	0.0000	0.0000	14.668
26	Alternative US-HW-LL catch- Upper range	157,410	97,791	83,302	51,208	0.37	0.56	0.74	1.15	0.75	0.0000	0.0000	0.0001
27	Same model specification (Mimic 2017 assessment)	159,945	262,076	117,601	62,542	0.54	0.22	0.48	2.23	0.46	0.0023		

**Table 18.** Estimates (median and 80<sup>th</sup> percentiles) of key management quantities for the North Pacific blue shark SS3 stock assessment model ensemble.

Management Quantity	Unit	Model Ensemble	80th percentile of bootstrapping
$B_0^*$	t	1,214,595	
$SSB_0^*$	t	222,736	
$\ln(R_0)^*$	numbers	9.559268	
$SSB_{1971}^*$	t	158,324	
$SSB_{1972}$	t	149,903	104,977 – 223,884
$SSB_{2020}$	t	92,954	38,695 – 179,870
$SSB_{MSY}^*$	t	83,545	
$F_{1971}^*$	per year	0.36	
$F_{1971}$	per year	0.26	0.16 - 0.42
$F_{2017-2019}$	per year	0.33	0.18 - 0.74
$F_{MSY}^*$	per year	0.76	
$SSB_{2020}/SSB_{MSY}$		1.17	0.570-1.776
$F_{2017-2019}/F_{MSY}$		0.445	0.236-1.011
$P(SSB_{2020} > SSB_{MSY})$		63.5%	
$P(F_{2017-2019} < F_{MSY})$		91.9%	
$P(SSB_{2020} > SSB_{MSY}$ and $F_{2017-2019} < F_{MSY})$		61.9%	

*\*The weighted mean across the ensemble is given for these quantities since it is unavailable from the parametric bootstrap.*

**Table 19.** Projected trajectory of spawning biomass (in metric tons) for alternative harvest scenarios.

<b>Year</b>	<b>Average F +20%</b>	<b>F<sub>MSY</sub></b>	<b>Average F -20%</b>	<b>Average F<sub>2017-2019</sub></b>
2021	91,469	92,158	91,707	91,613
2022	90,826	85,954	92,096	91,489
2023	91,044	83,524	93,902	92,240
2024	93,878	82,681	98,034	94,718
2025	95,195	81,283	102,324	97,349
2026	99,385	81,482	106,332	99,853
2027	101,943	81,391	110,446	103,502
2028	104,333	81,296	114,099	105,987
2029	106,374	81,005	117,424	108,386
2030	108,041	80,770	120,542	110,949

## 12. FIGURES

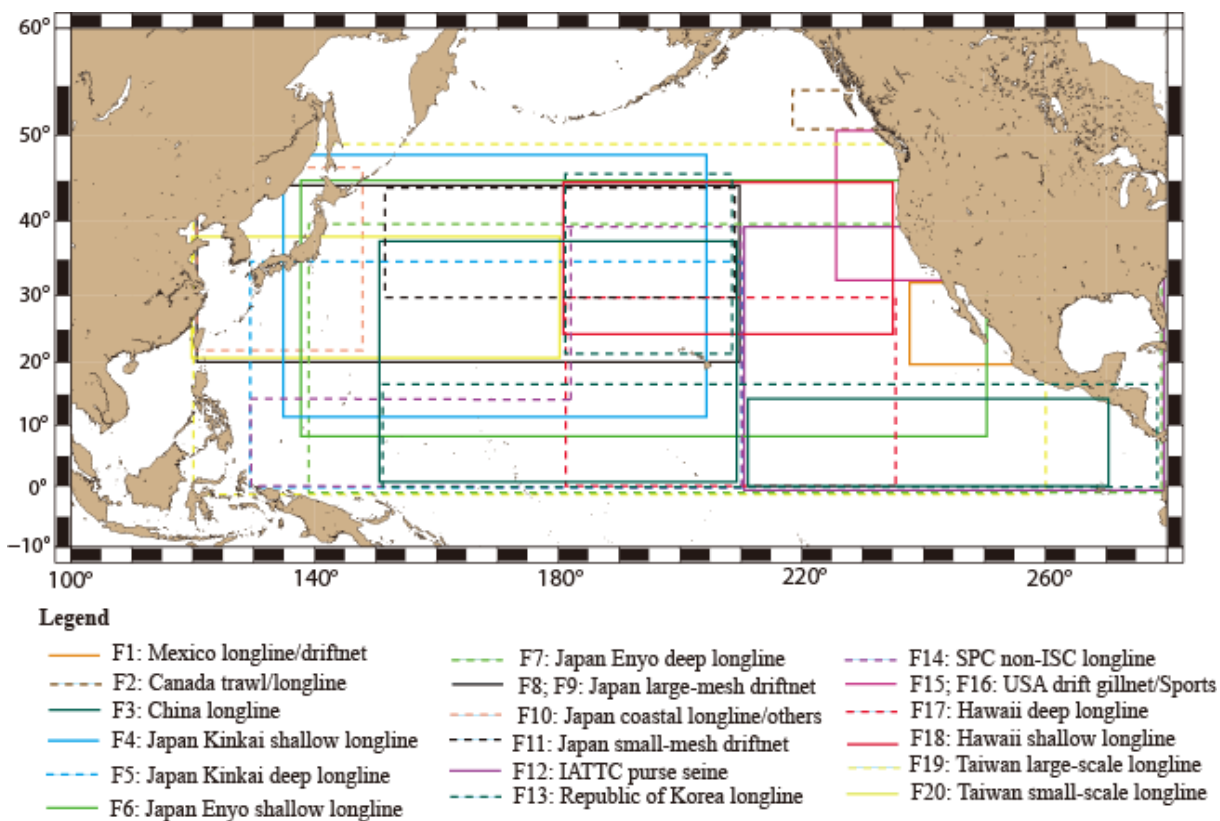


**Figure 1.** Blue shark (*Prionace glauca*) stock boundaries and approximate spatial extent of all fleets used in this stock assessment.

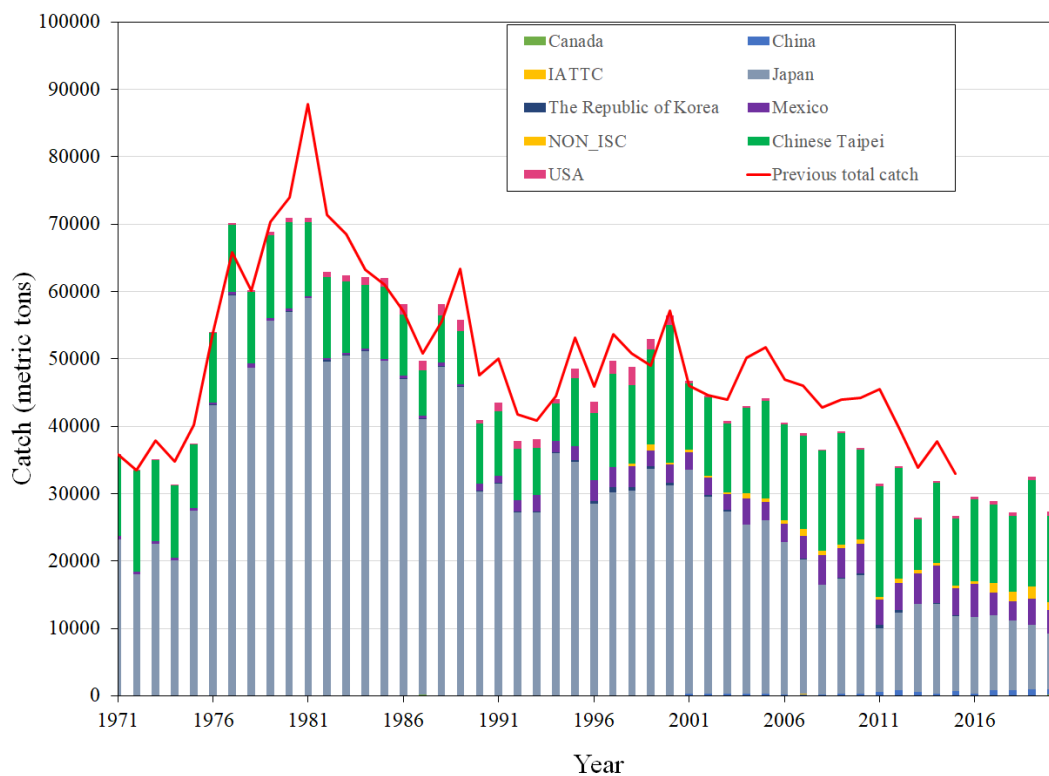
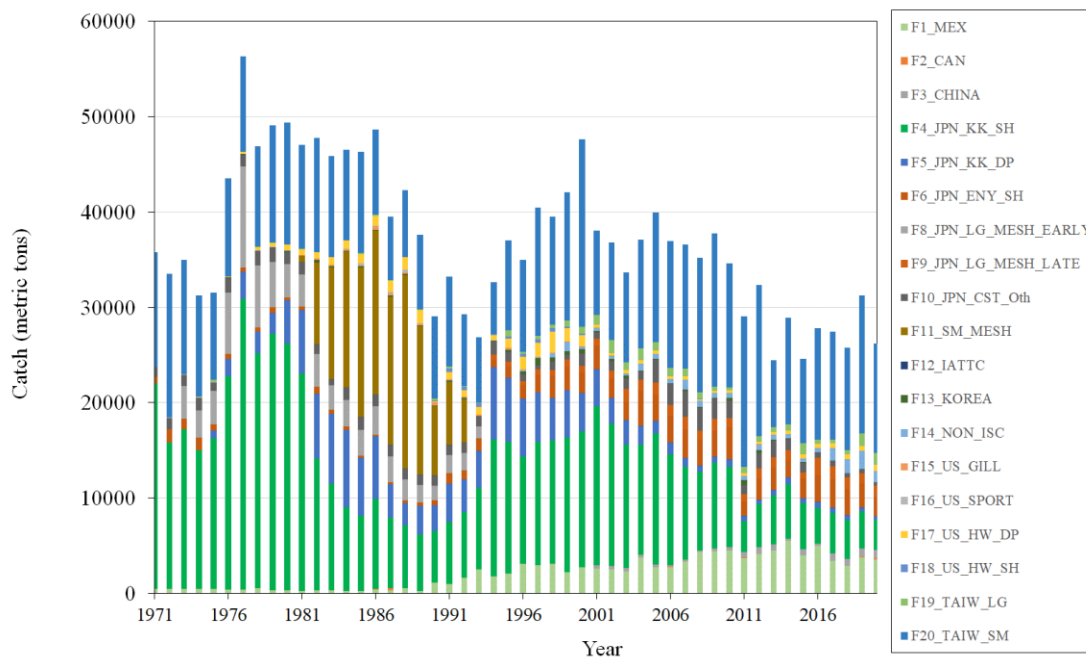


**Figure 2.** Annual catch (metric tons) of blue shark by fleet (upper panel) and by country (lower panel) for 1971-2020 used in this stock assessment. The red line of lower panel denotes total catch for 1971-2020 used in the previous assessment in 2017.

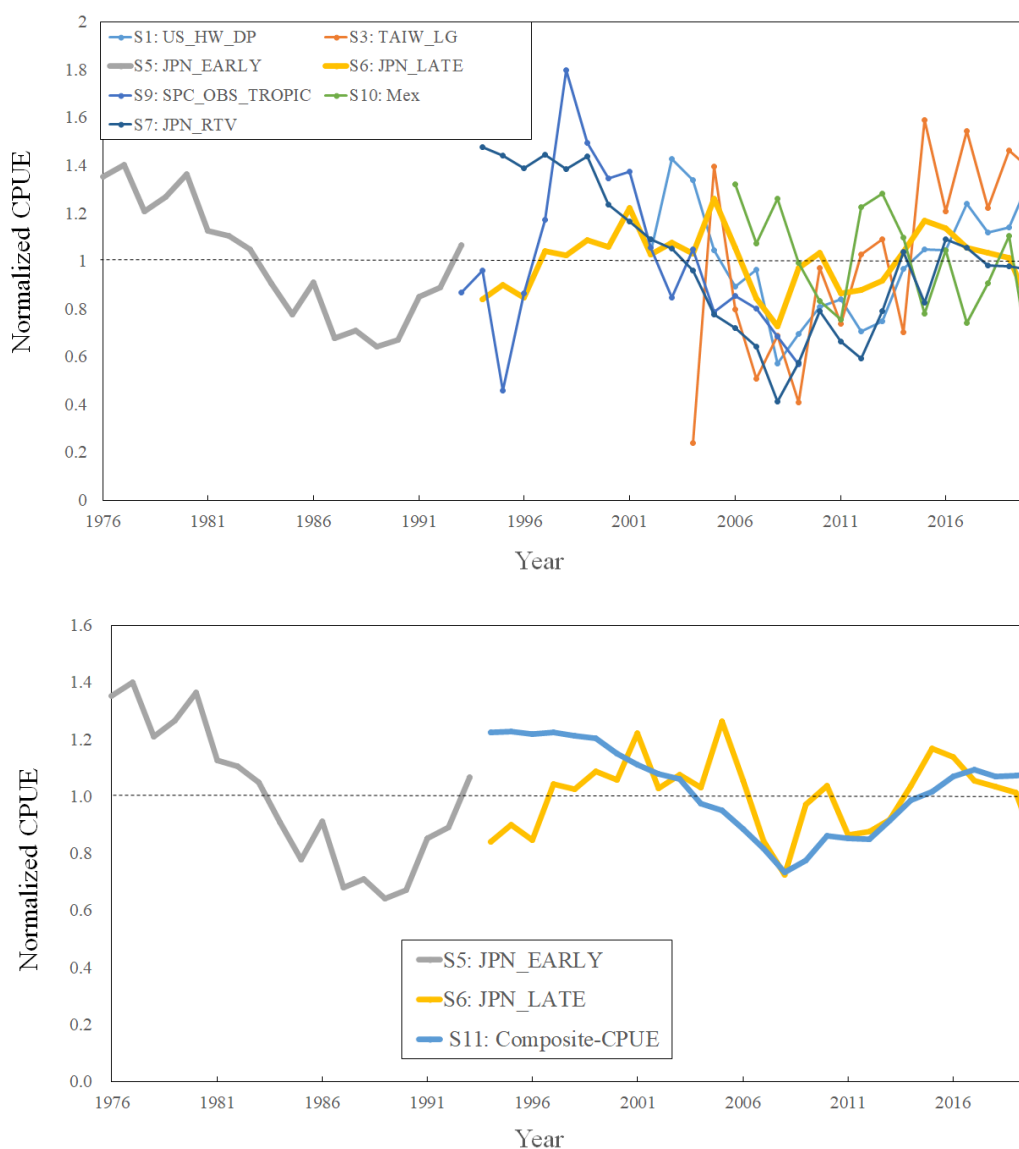


**Figure 3.** Annual standardized CPUE of North Pacific BSH during 1976 through 1993 (Japanese offshore and distant water shallow-set longline: **S5: JPN\_EARLY**), and (upper panel) six standardized CPUEs of BSH between 1993 and 2020 (Hawaii deep-set longline: **S1: US\_HW\_DP**, Taiwanese large-scale longline: **S3: TAIW\_LG**, Japanese offshore and distant water shallow-set longline: **S6: JPN\_LATE**, Japanese research and training vessel: **S7: JPN\_RTV**, SPC observed longline: **S9: SPC\_OBS\_TROPIC**, Mexico longline: **S10: Mex**), and (lower panel) two standardized CPUE of BSH between 1993 and 2020 (**S6: JPN\_LATE** and **S11: Composite-CPUE** with S1, S3, and S7). The horizontal broken line denotes the mean value (1.0) of each CPUE. The time series were normalized by mean value of each CPUE and the horizontal broken line denotes the mean value (1.0) of each CPUE.

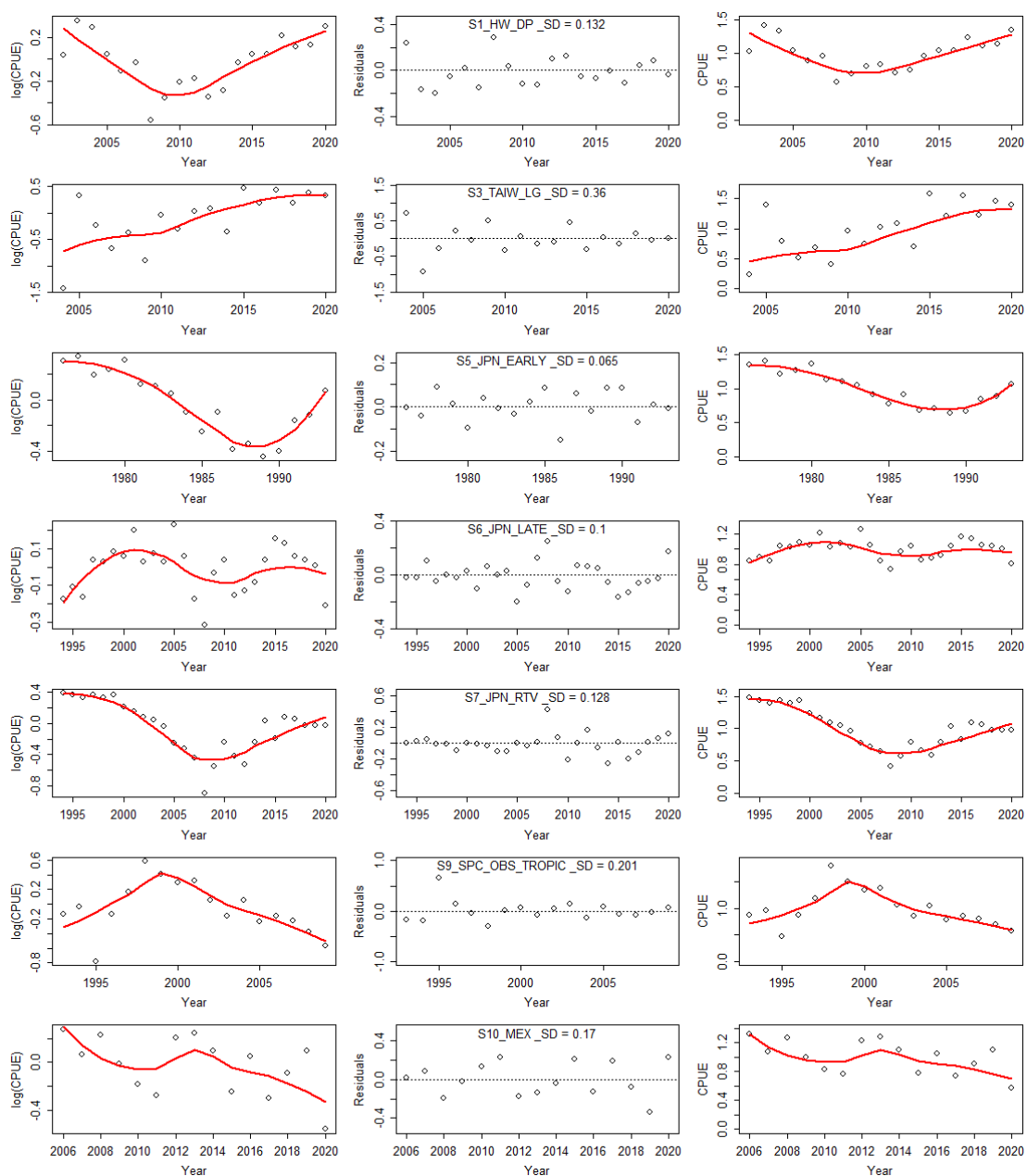


**Figure 4.** Annual changes in logarithmic CPUE, residuals between fitted and observed CPUE on the log-scale and observed CPUE for each fleet. The red curves denote the fit of CPUE using a LOESS smoother.

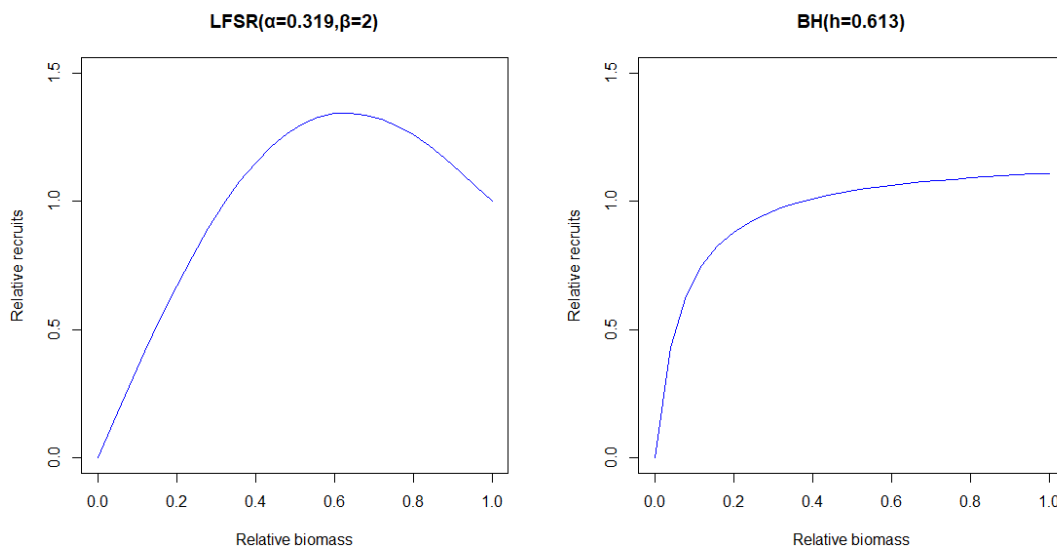


**Figure 5.** The low-fecundity stock-recruitment (SR) relationships used in the stock assessment in 2017 and the Beverton-Holt SR-relationships used in the base-case model of this assessment in 2022.

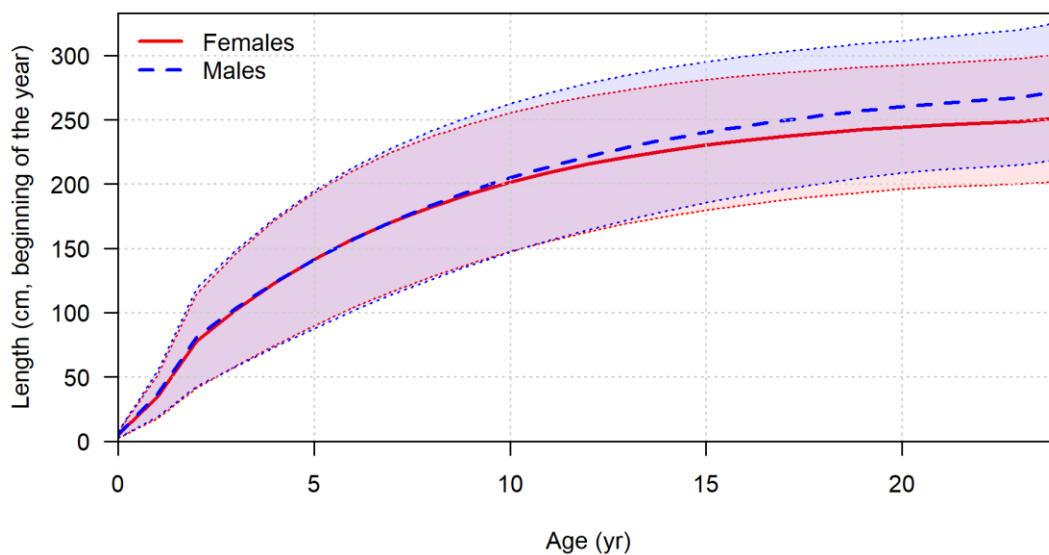


**Figure 6.** The sex-specific length-at-age for female and male blue shark used in the stock assessment.

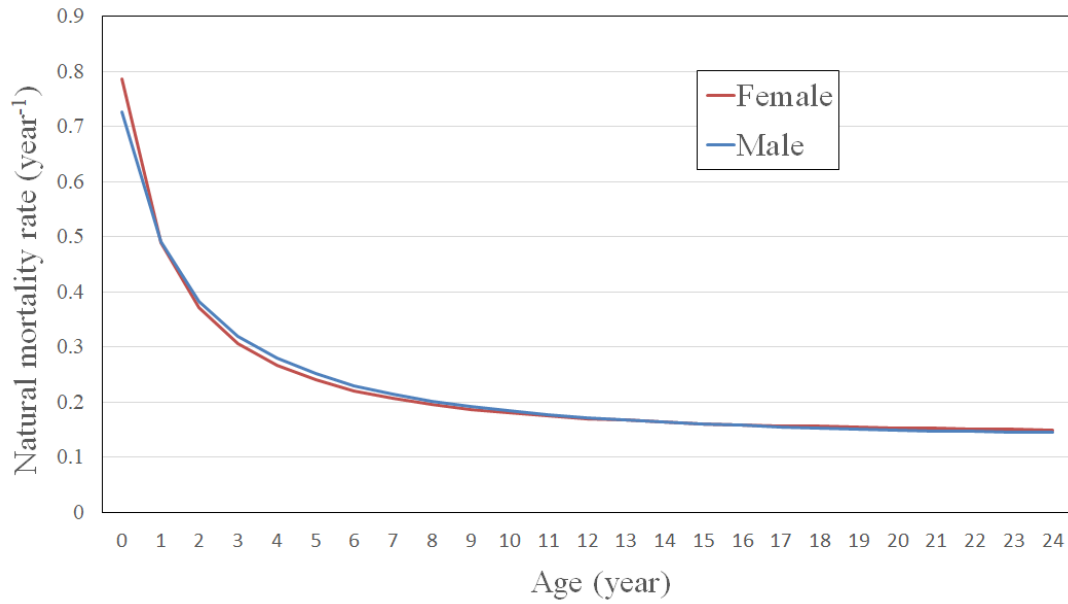


**Figure 7.** The sex-specific natural mortality schedule for blue shark used in the stock assessment.

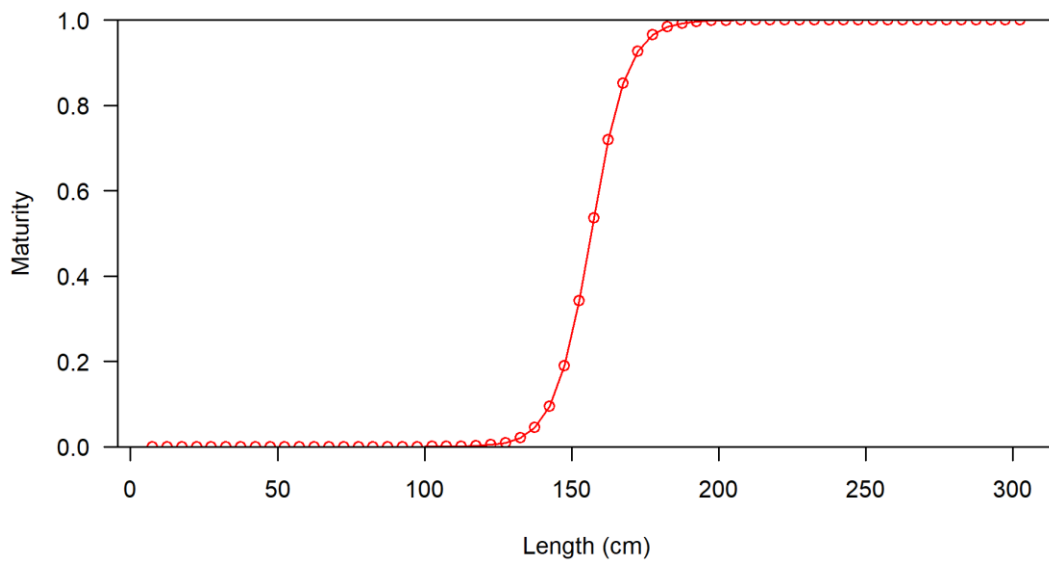


**Figure 8.** The maturity-at-length for female blue shark used in the stock assessment.

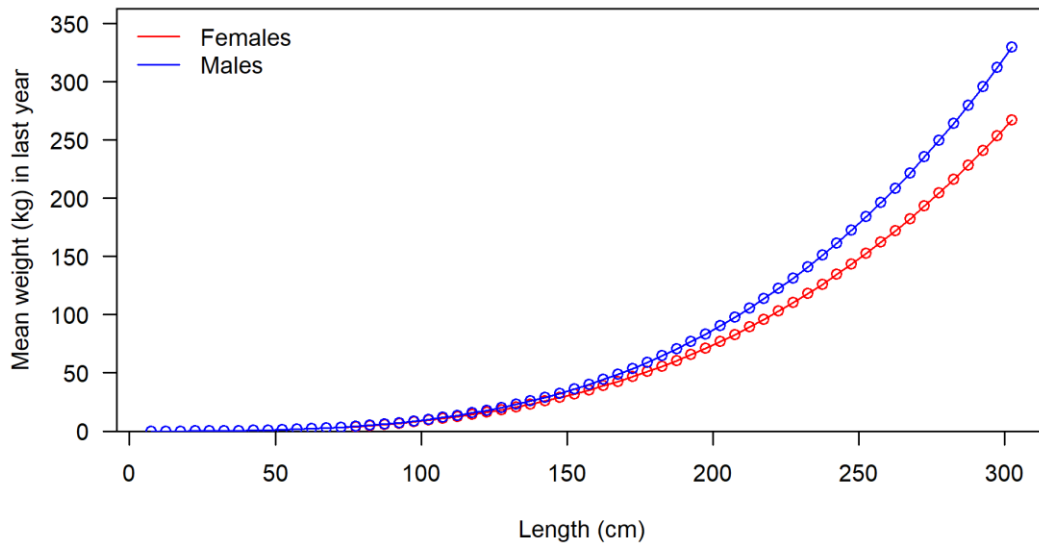


**Figure 9.** The sex-specific weight-at-length for female and male blue shark used in the stock assessment.

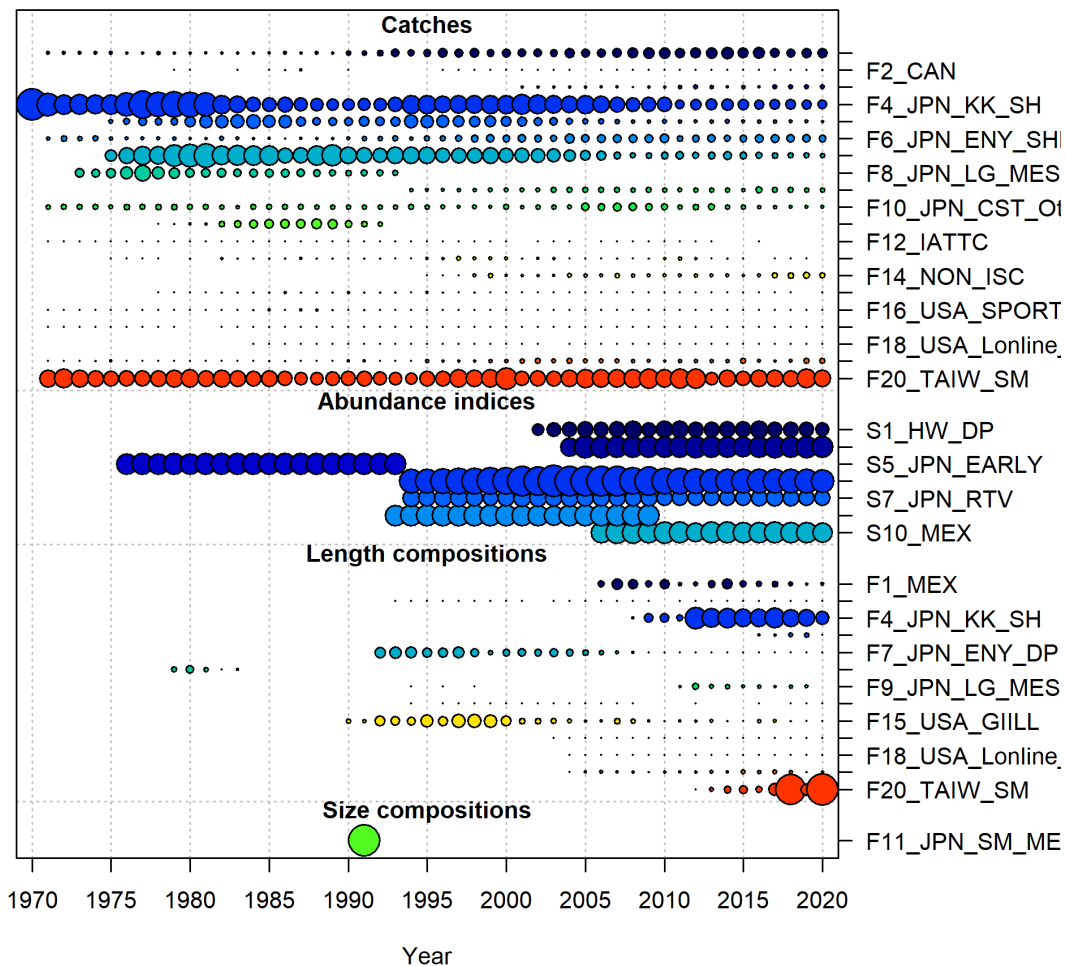


**Figure 10.** Coverage of catch, abundance indices, and length composition data by year for each fleet used in this stock assessment. Circle area is relative within a data type. Circles are proportional to total catch for catches; to precision for indices, and to total sample size for length compositions. Note that since the circle are scaled relative to maximum within each type, the scaling within separate plots should not be compared.

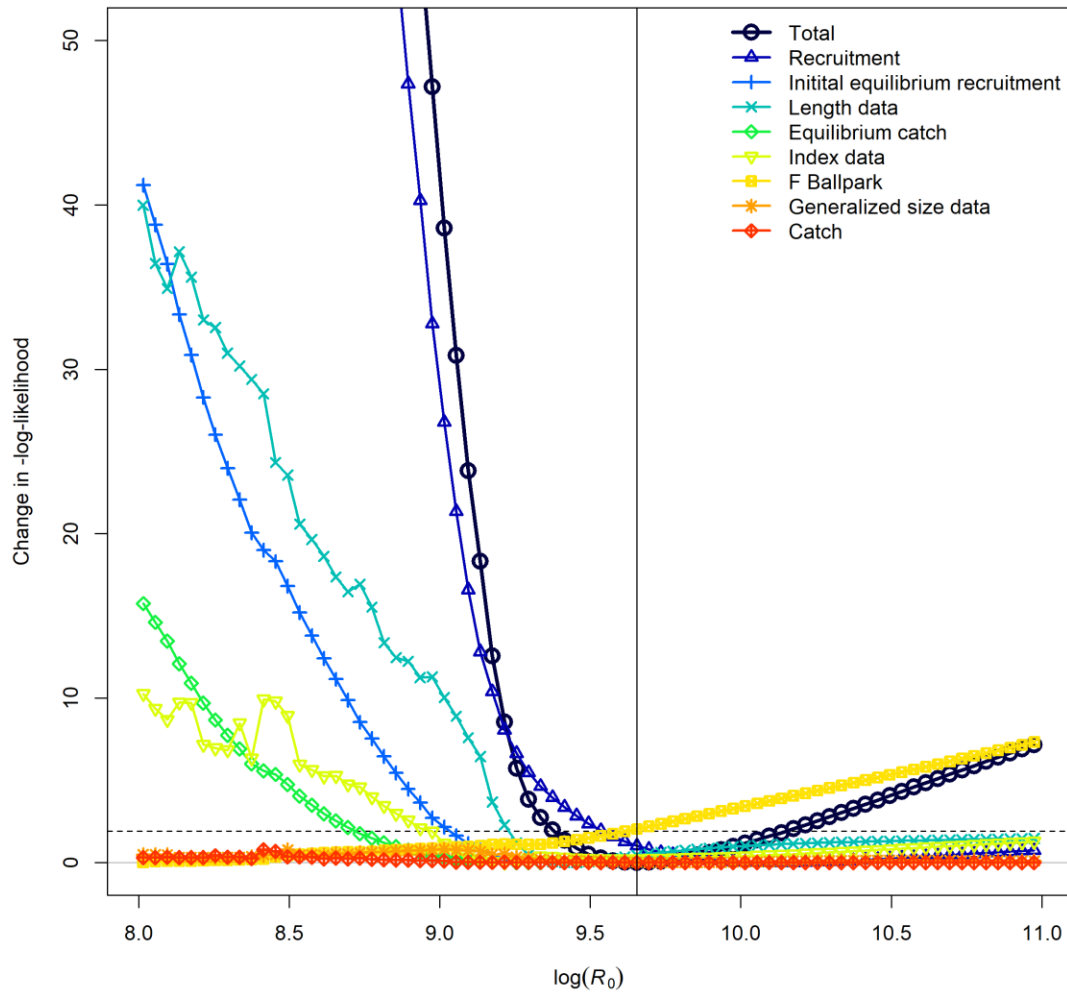


**Figure 11.** Profiles of the relative-negative log likelihoods by different data components for the virgin recruitment in log-scale ( $\log(R_0)$ ) for the *S6\_base* model. The vertical line denotes the maximum likelihood estimate (MLE).

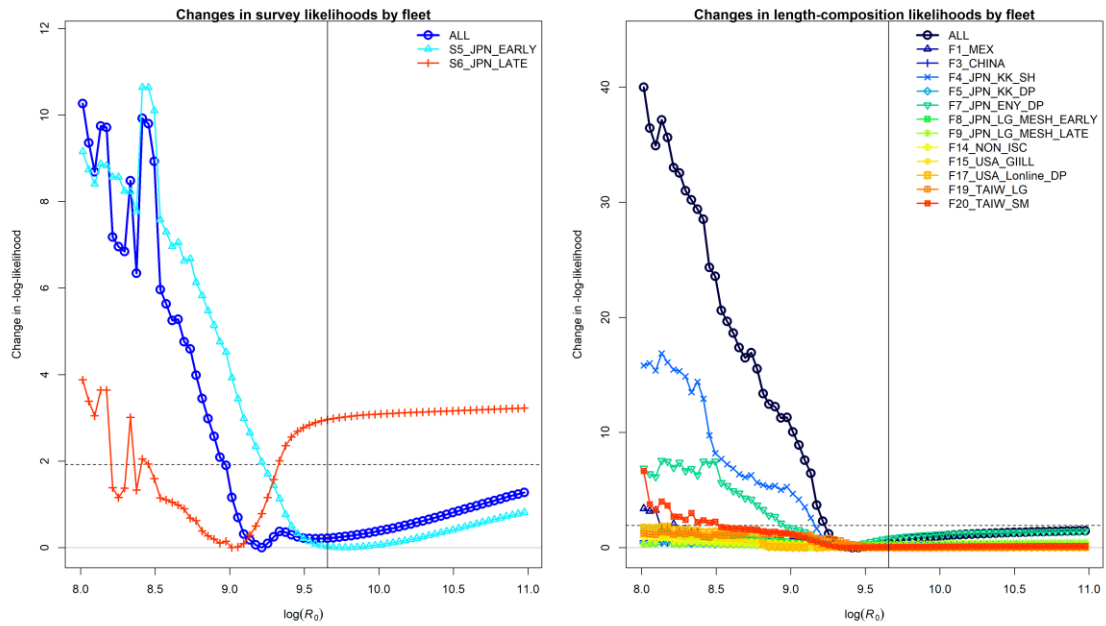


**Figure 12.** Profiles of the relative-negative log likelihoods by survey index (left panel) and fishery length composition (right panel) for the virgin recruitment in log-scale ( $\log(R_0)$ ) for the *S6\_base* model. The vertical line denotes the maximum likelihood estimate (MLE).

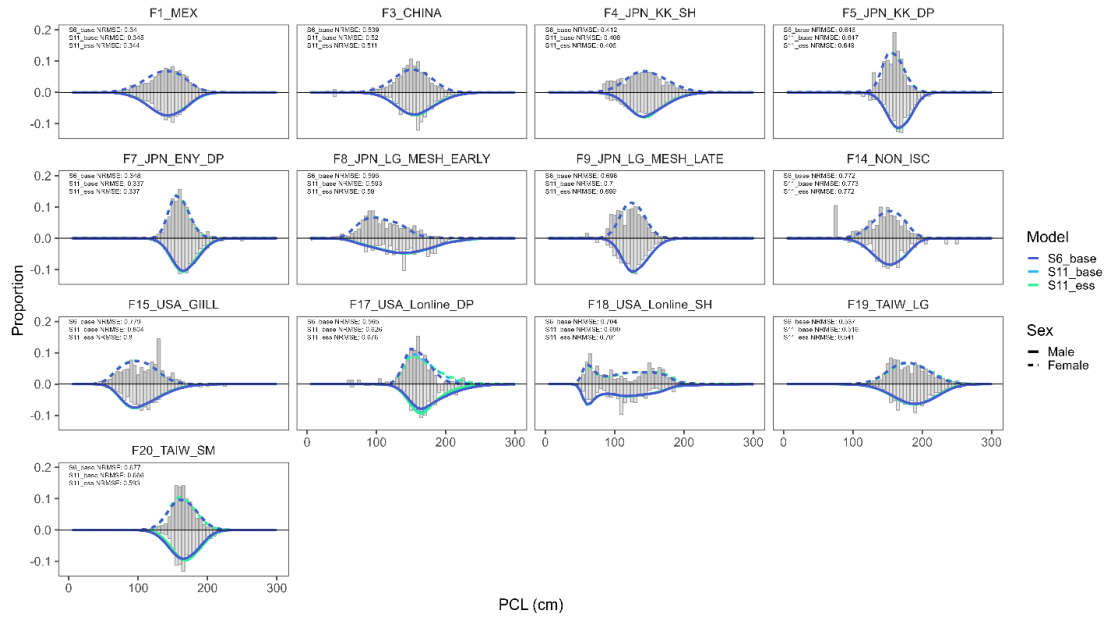


**Figure 13.** Sex specific comparison of observed (gray bars) and model predicted (lines) length compositions for different fisheries across all three models in the ensemble. Fit to female data (dotted lines) is above the x-axis and fit to the male data (solid lines) is below the x-axis. Line color indicates the different models in the ensemble.

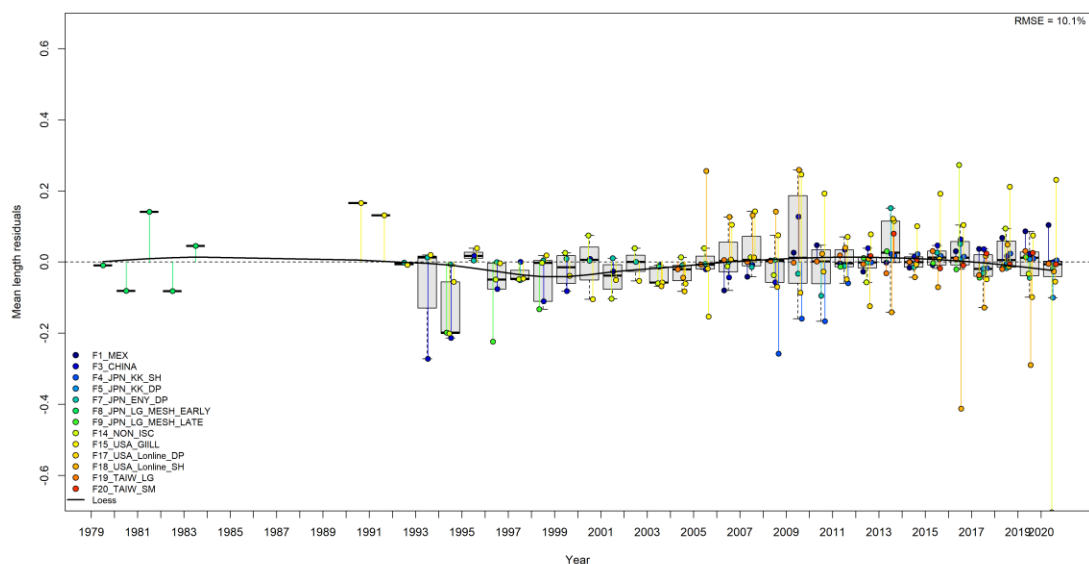


**Figure 14.** Joint residual plot for annual mean length estimates for multiple fishing fleets from the *S6\_base* model. Vertical lines with points show the residuals (in colors by fishery), and solid black lines show loess smoother through all residuals. Boxplots indicate the median and quantiles in cases where residuals from the multiple indices are available for any given year. The overall root-mean squared error (RMSE) is included in the upper right-hand corner.

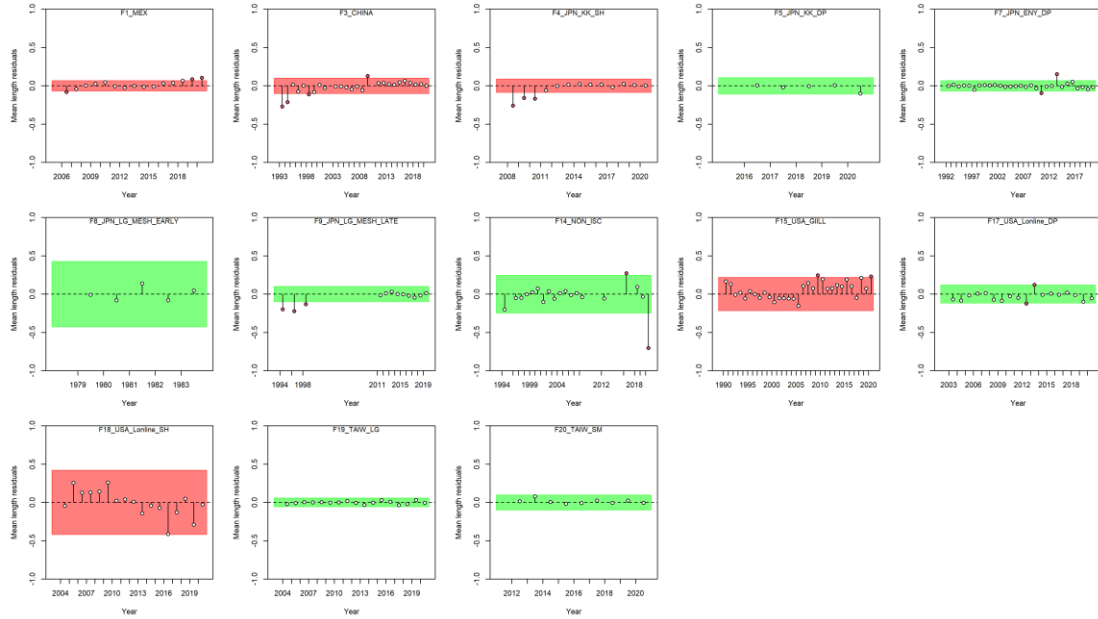


**Figure 15.** Runs tests results from the mean length residuals illustrated for all fisheries in the *S6\_base* model. Green shading indicates no evidence ( $p \geq 0.05$ ) and red shading evidence ( $p < 0.05$ ) to reject the hypothesis of a randomly distributed time-series of residuals, respectively. The shaded (green/red) area spans three residual standard deviations to either side from zero, and the red points outside of the shading violate the ‘three-sigma limit’ for that series.

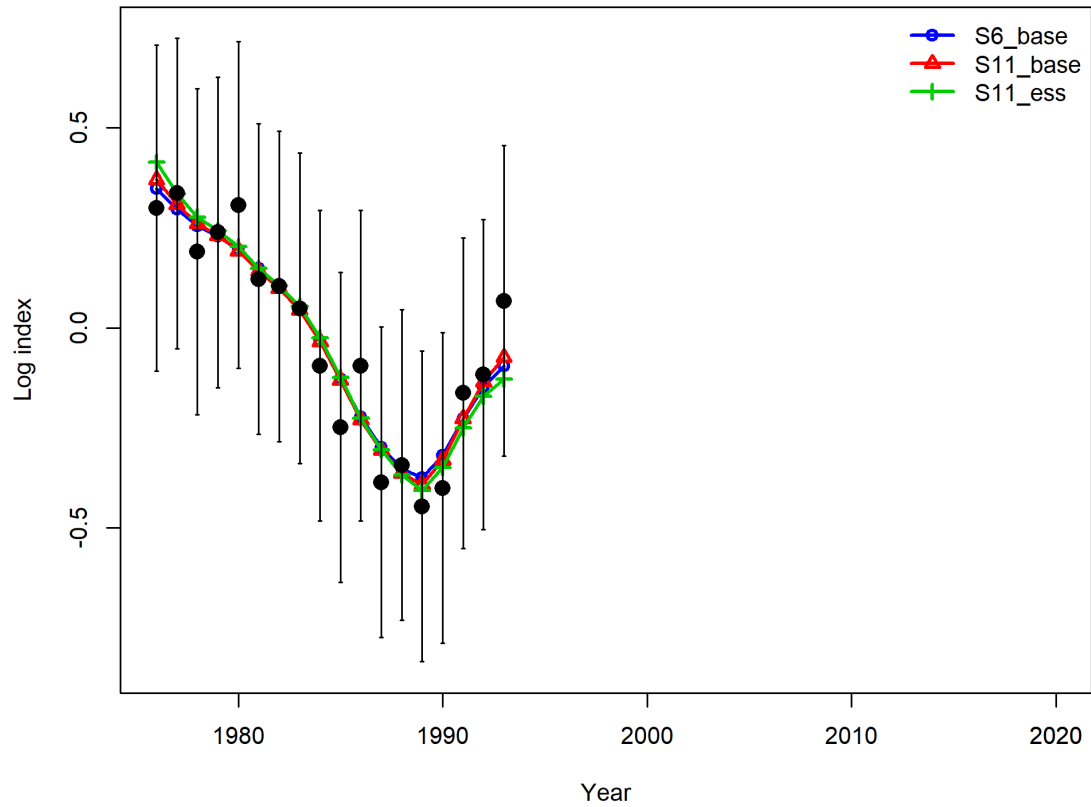


**Figure 16.** Model fits to the S5: JPN\_EARLY standardized catch-per-unit-effort (CPUE) (in log scale) data sets for each of the three models in the ensemble. The solid colored line is the model predicted value and the solid black circles are observed data values. Vertical black lines represent the estimated confidence intervals ( $\pm 1.96$  standard deviations) around the CPUE values.

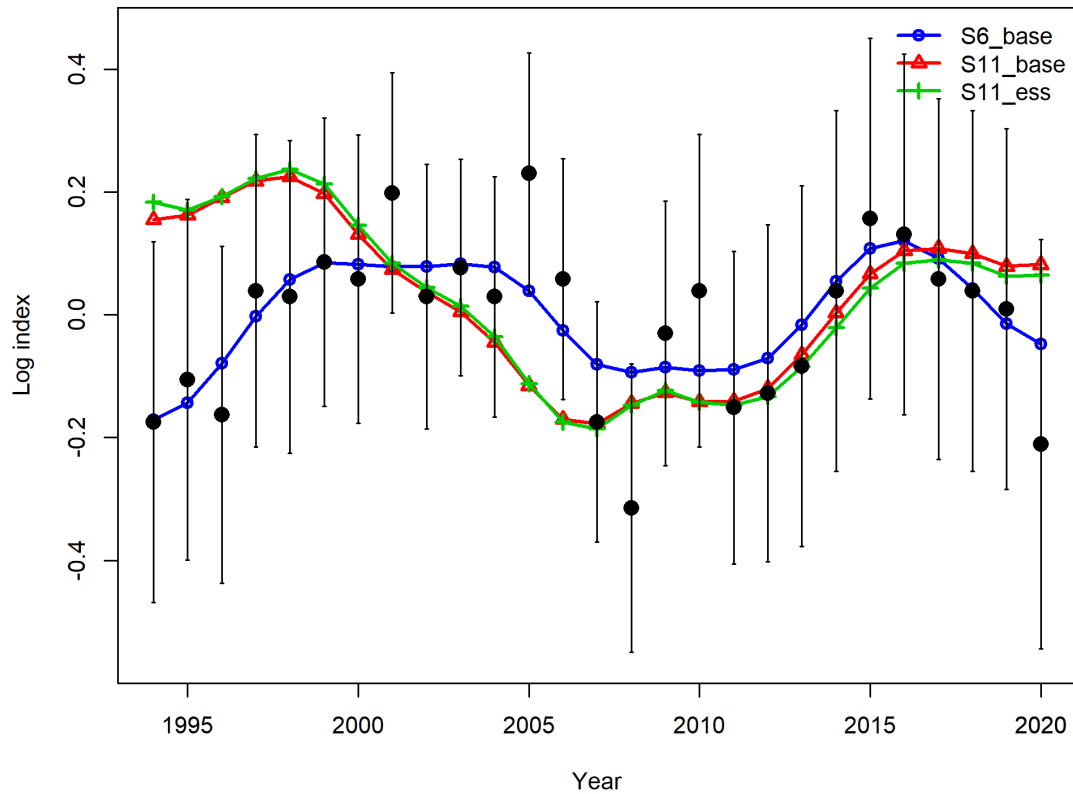


**Figure 17.** Model fits to the S6: JPN\_LATE standardized catch-per-unit-effort (CPUE) (in log scale) data sets for each of the three models in the ensemble. The solid colored line is the model predicted value and the solid black circles are observed data values. Vertical black lines represent the estimated confidence intervals ( $\pm 1.96$  standard deviations) around the CPUE values. Note that the two S11 models do not fit to this index.

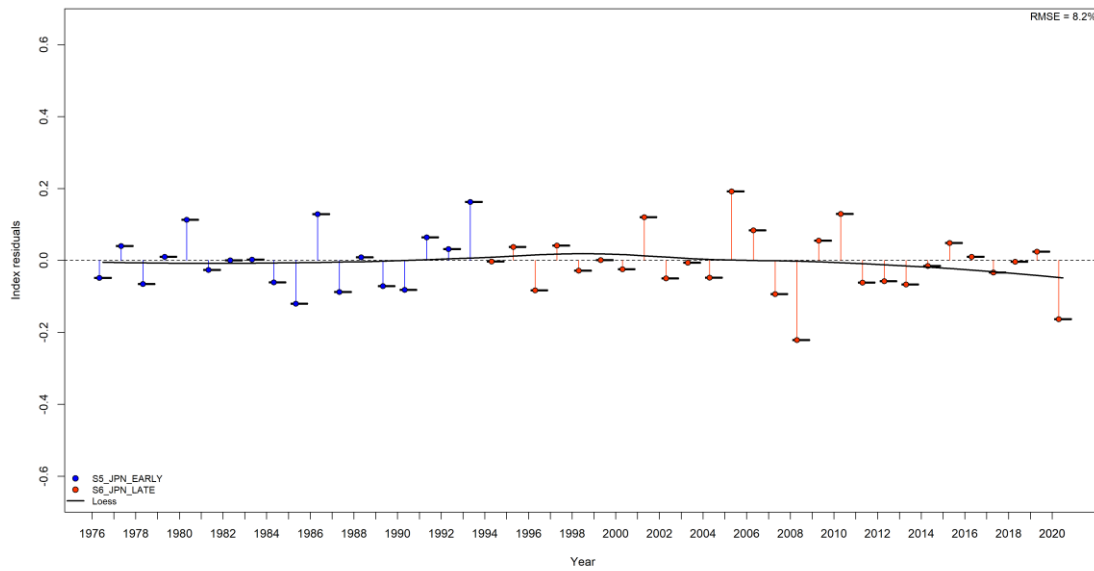


**Figure 18.** Joint residual plot for the two survey indices in the *S6-base* model. Vertical lines with points show the residuals (in colors by survey), and solid black lines show loess smoother through all residuals. Boxplots indicate the median and quantiles in cases where residuals from the multiple indices are available for any given year. The overall root-mean squared error (RMSE) is included in the upper right-hand corner.

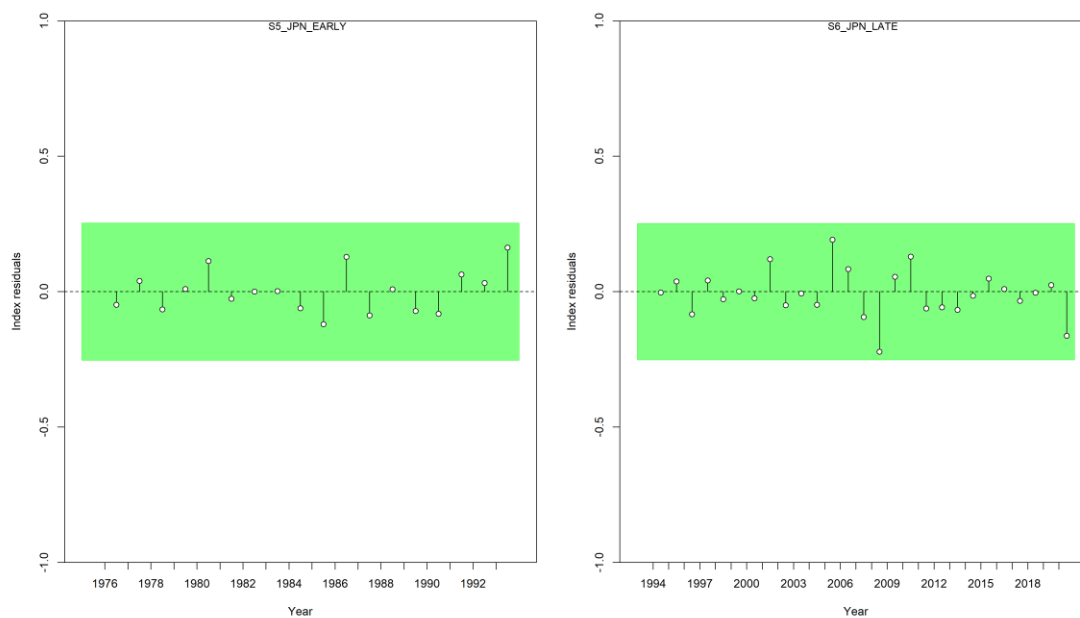


**Figure 19.** Runs tests results for the two survey indices in the *S6\_base* model. Green shading indicates no evidence ( $p \geq 0.05$ ) and red shading evidence ( $p < 0.05$ ) to reject the hypothesis of a randomly distributed time-series of residuals, respectively. The shaded (green/red) area spans three residual standard deviations to either side from zero, and the red points outside of the shading violate the ‘three-sigma limit’ for that series.

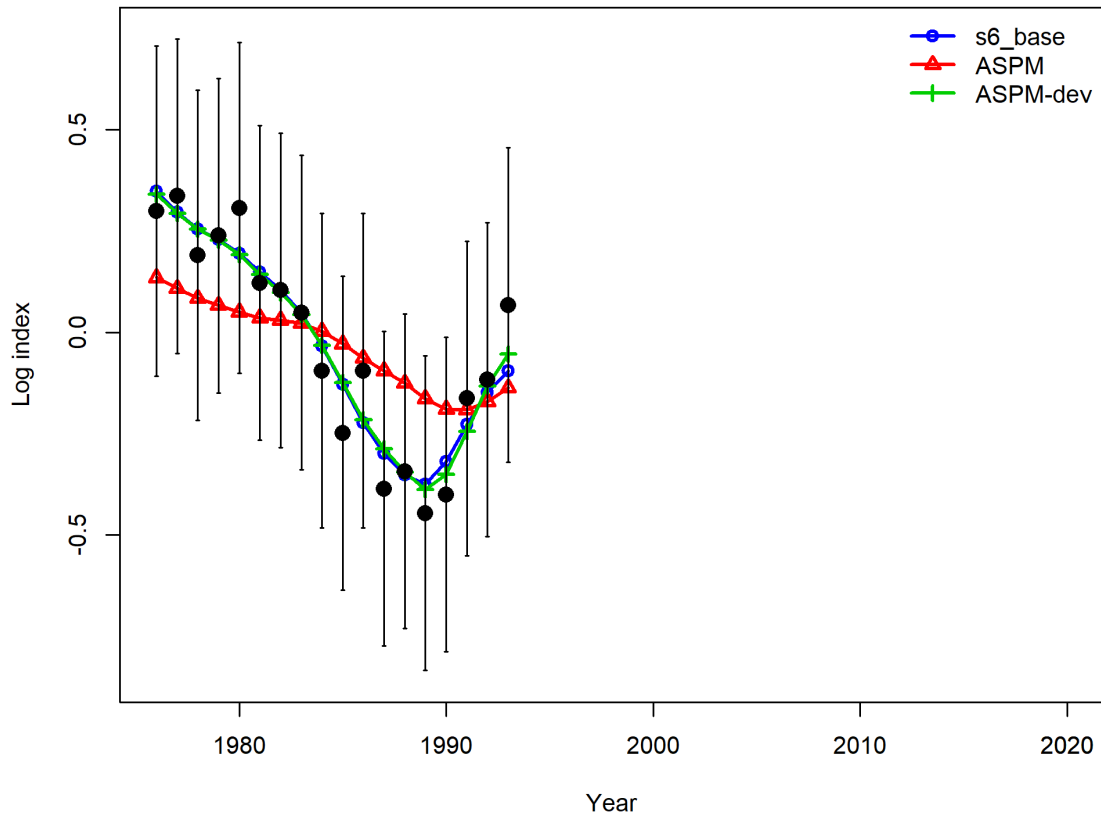


**Figure 10.** Model fits to the S5: JPN\_EARLY standardized catch-per-unit-effort (CPUE) (in log scale) data set for each of the *S6\_base* model and two age-structured production models (ASPM and ASPM-rev). The solid colored line is the model predicted value and the solid black circles are observed data values. Vertical black lines represent the estimated confidence intervals ( $\pm 1.96$  standard deviations) around the CPUE values.

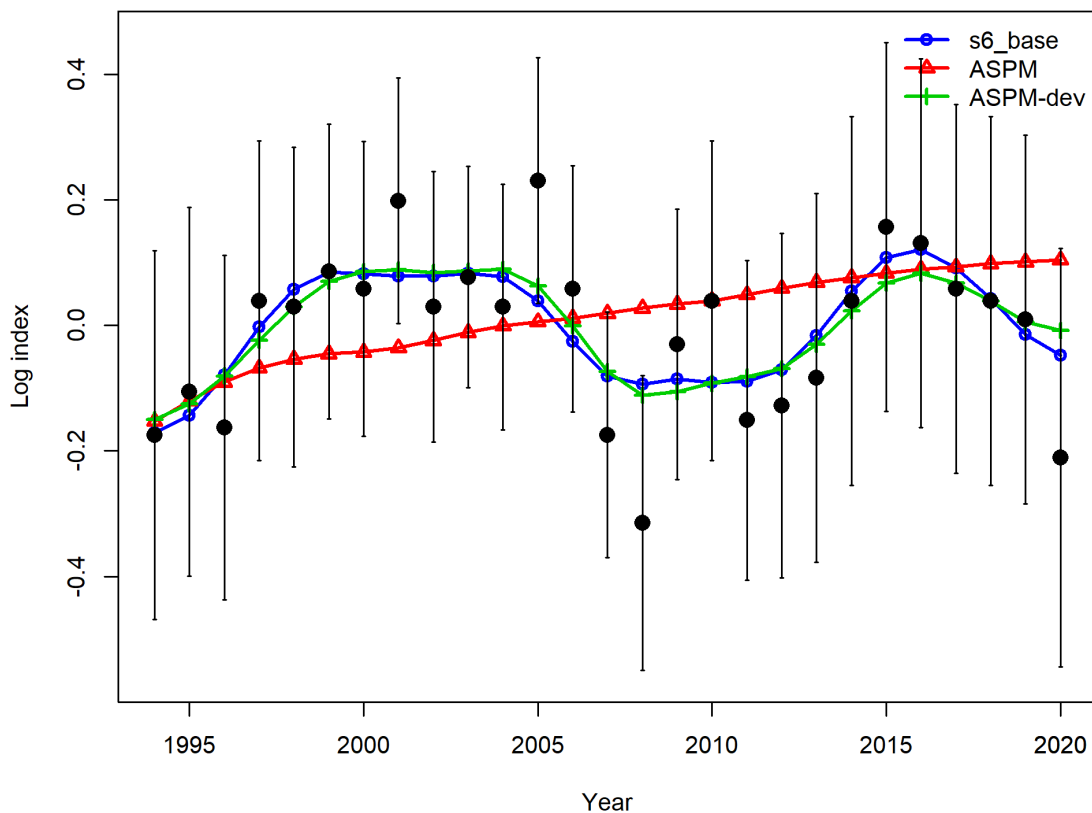


**Figure 11.** Model fits to the S6: JPN\_LATE standardized catch-per-unit-effort (CPUE) (in log scale) data set for each of the *S6\_base* model and two age-structured production models (ASPM and ASPM-dev). The solid colored line is the model predicted value and the solid black circles are observed data values. Vertical black lines represent the estimated confidence intervals ( $\pm 1.96$  standard deviations) around the CPUE values.

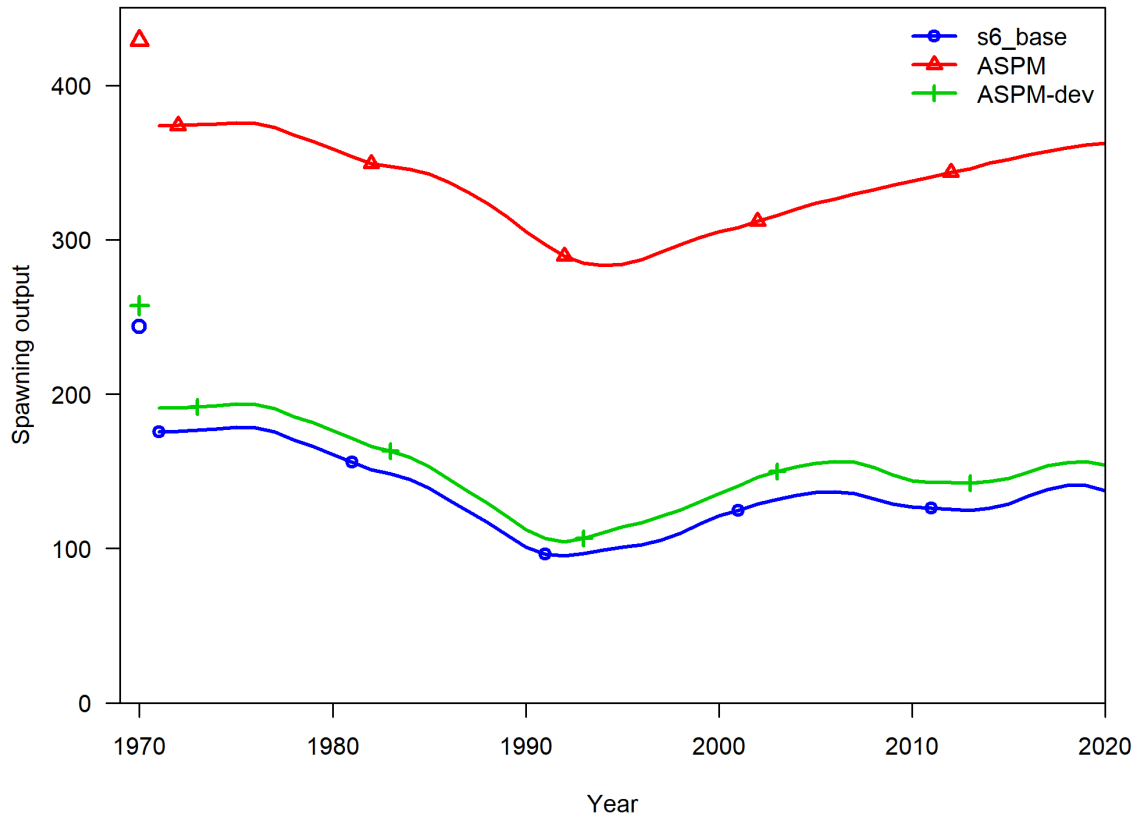


**Figure 12.** Annual spawning stock biomass estimates for the *S6\_base* model and two versions of the age-structured production models (ASPM and ASPM-rev).

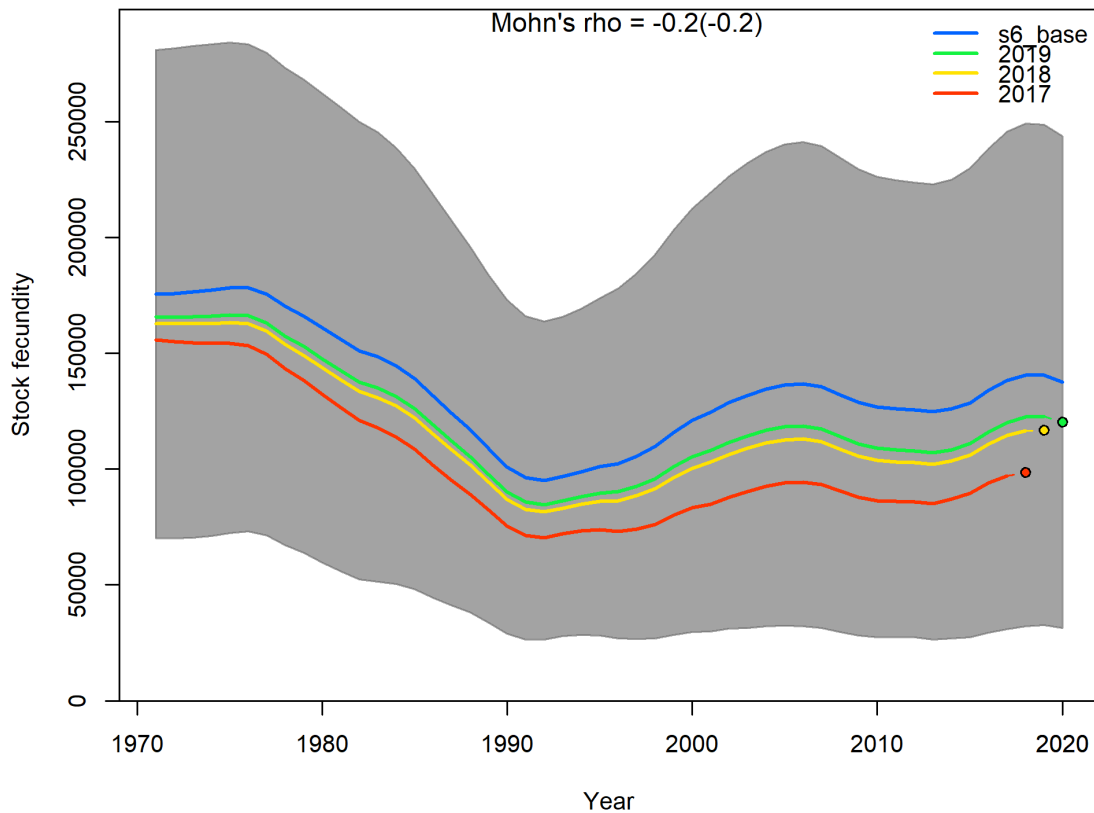


**Figure 13.** Retrospective analysis of spawning stock biomass for the *S6\_base* model conducted by sequentially removing the last three years of data from the model. Mohn's rho statistic and the corresponding 'hindcast rho' values (in brackets) are printed at the top of the figure. Grey shaded areas are the 95 % confidence intervals from the reference model.

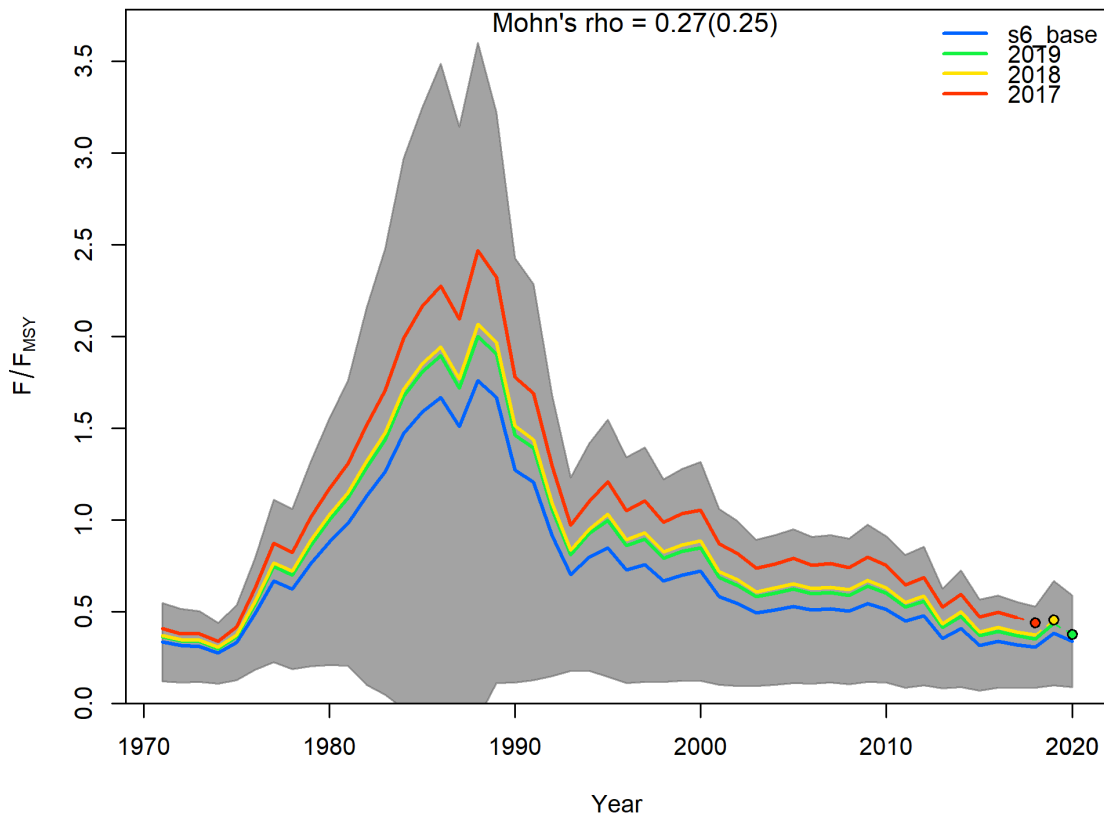


**Figure 14.** Retrospective analysis of fishing mortality rate relative to maximum sustainable (MSY) level for the *S6\_base* model conducted by sequentially removing the last three years of data from the model. Mohn's rho statistic and the corresponding 'hindcast rho' values (in brackets) are printed at the top of the figure. Grey shaded areas are the 95 % confidence intervals from the reference model.

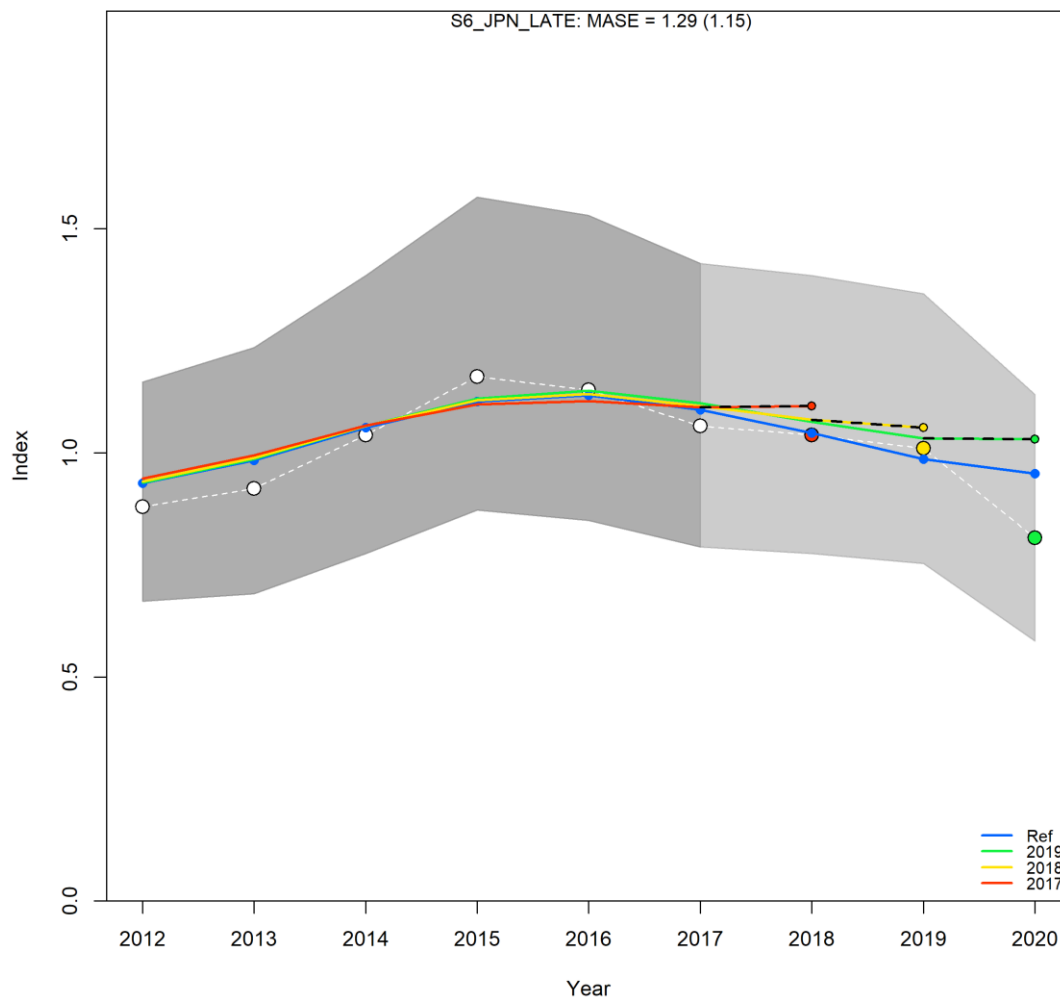


**Figure 15.** Hindcasting cross-validation (HCxval) results for the fit to the S6 Japanese Kinkai shallow late standardized catch-per-unit-effort (CPUE) data set for each of the *S6\_base* model, showing observed (large points connected with dashed line), fitted (solid lines) and one-year-ahead forecast values (small terminal points). HCxval was performed using one reference model (*S6\_base*) and three hindcast model runs (solid lines) relative to the expected CPUE. The observations used for cross-validation are highlighted as color-coded solid circles with associated 95 % confidence intervals (light-gray shading). The model reference year refers to the endpoints of each one-year-ahead forecast and the corresponding observation (i.e., year of peel + 1). The mean absolute scaled error (MASE) score and adjusted MASE (in parentheses) is shown at the top of the figure.

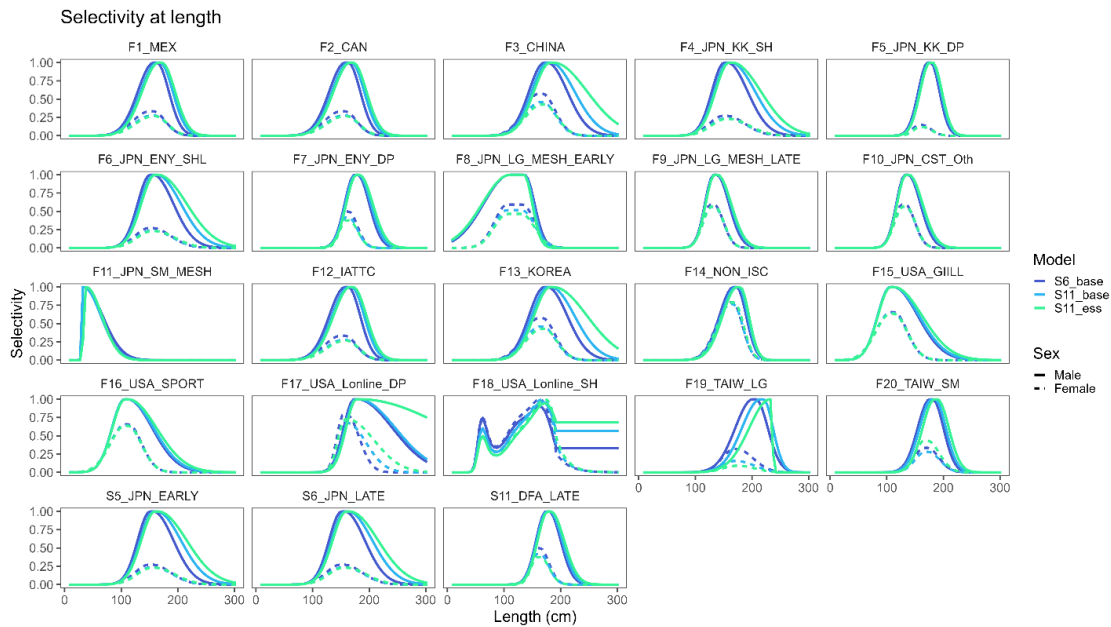


**Figure 16.** Selectivity at length by fishery and sex (males solid line, females dotted line) for each of the three models in the ensemble (line color).

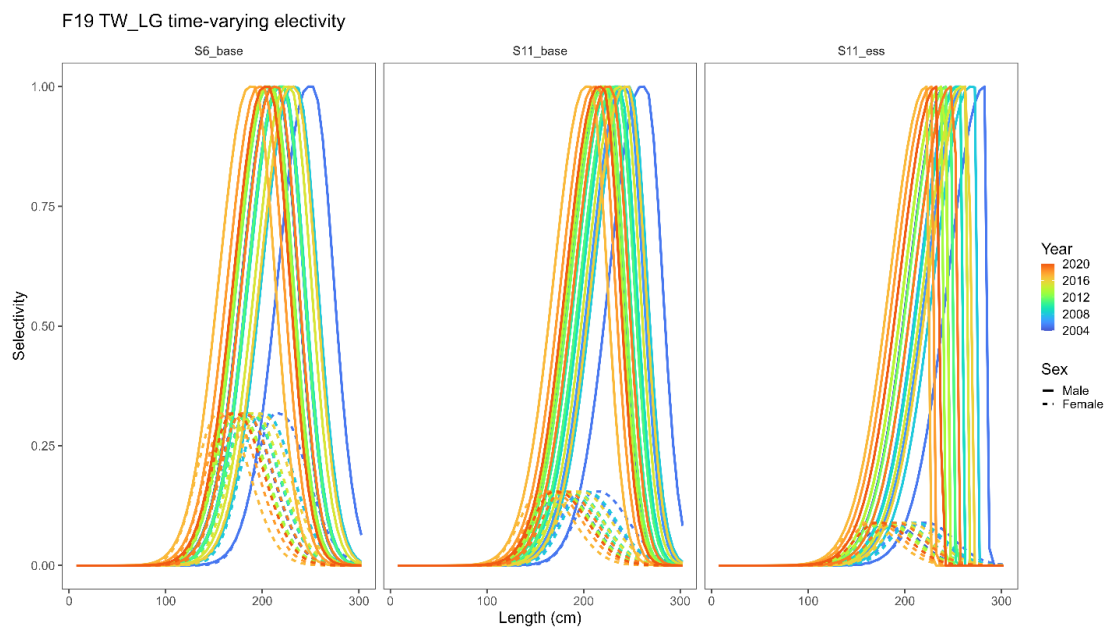


**Figure 17.** Time-varying selectivity by sex (males solid line, females dotted line) for the Taiwanese large scale longline fishery (F19) for each of the three models (*S6\_base* left panel, *S11\_base* central panel, *S11\_ess* right panel). Line color indicates the year of the estimated selectivity.

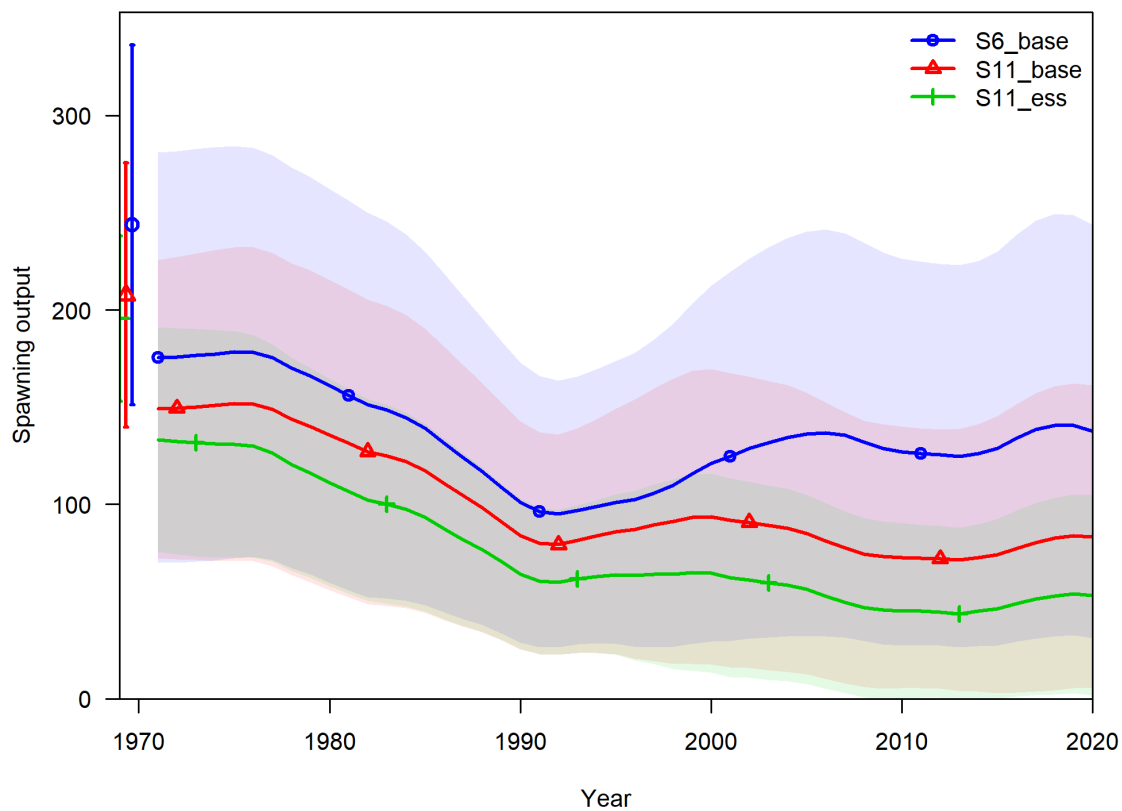


**Figure 18.** Annual spawning stock biomass estimates (1000 metric tons) for the three models in the ensemble (line color). Solid lines indicate mean estimates while the shaded region indicates the associated 95% confidence interval.

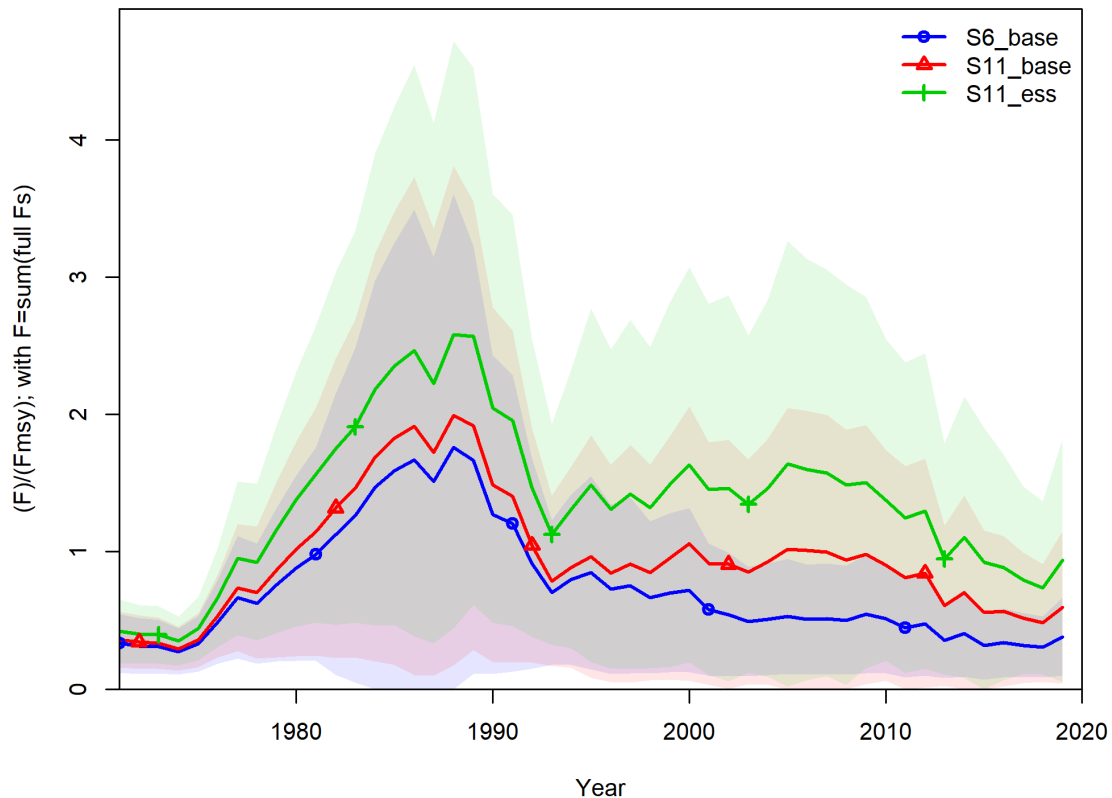


**Figure 19.** Average annual fishing mortality estimates relative to maximum sustainable yield (MSY) level for the three models in the ensemble (line color). Solid lines indicate mean estimates while the shaded region indicates the associated 95% confidence interval.

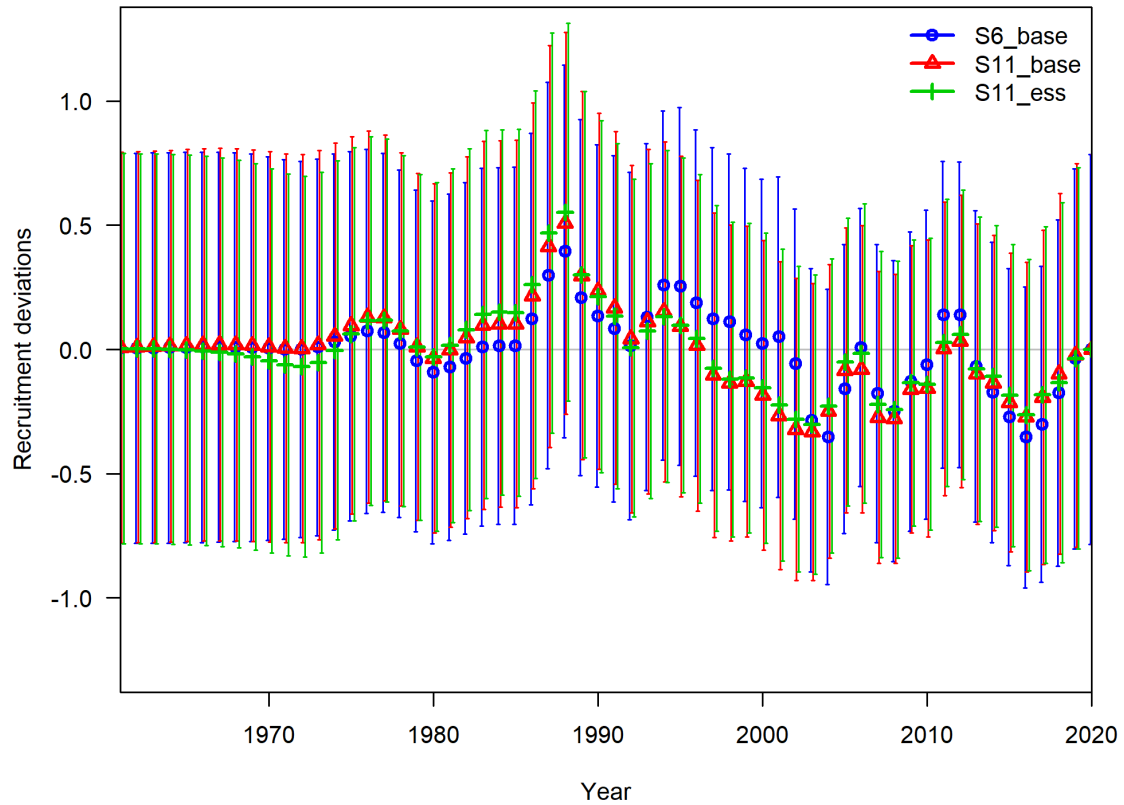


**Figure 20.** Annual recruitment deviates for the three models in the ensemble (color). The colored symbols indicate the mean estimate and the vertical bars indicate the associated 95% confidence interval.

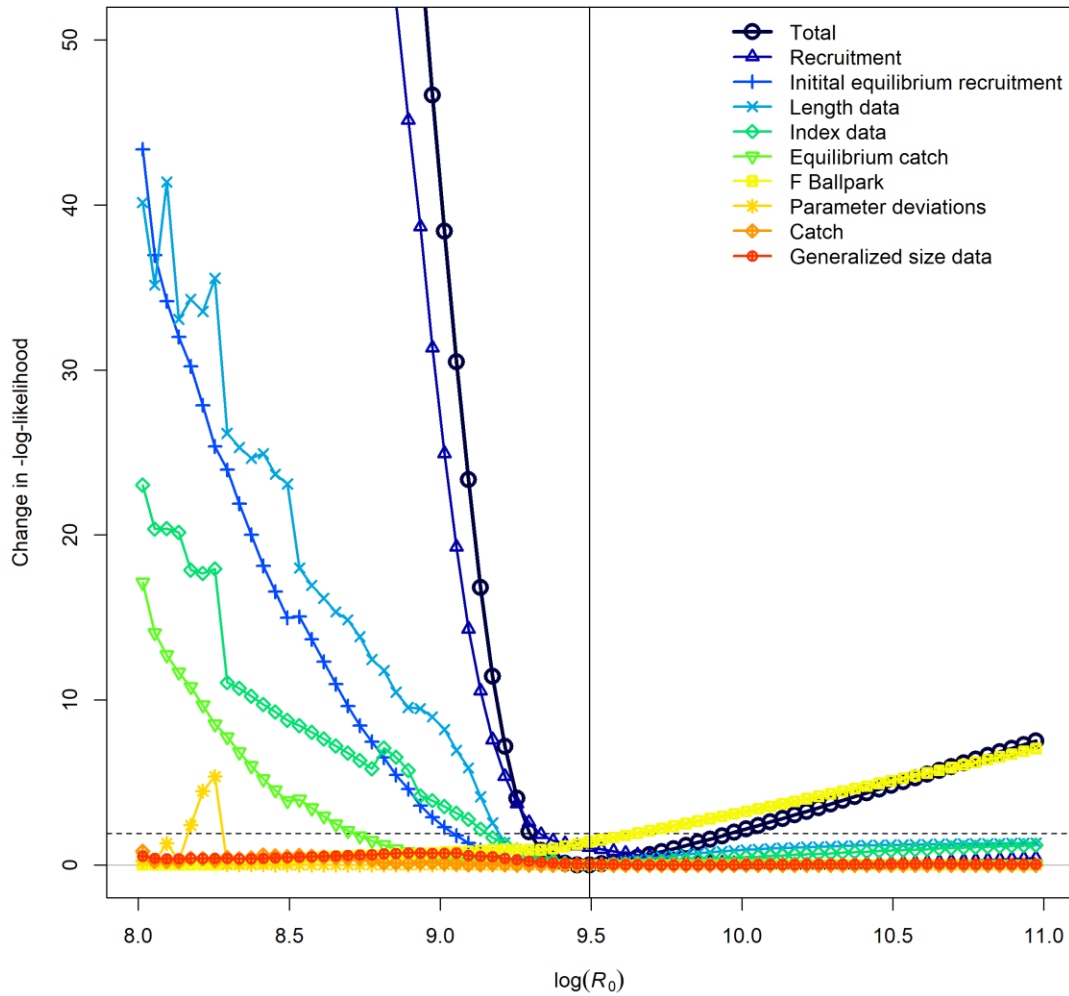


**Figure 21.** Profiles of the relative-negative log likelihoods by different data components for the virgin recruitment in log-scale ( $\log(R_0)$ ) for the *S11\_base* model. The vertical line denotes the maximum likelihood estimate (MLE).

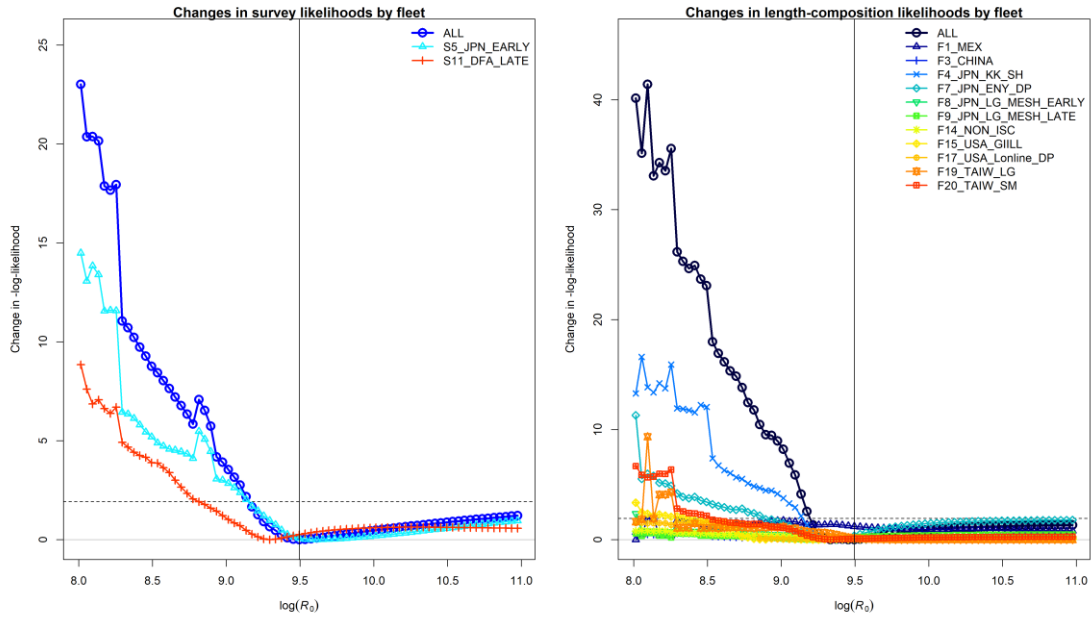


**Figure 22.** Profiles of the relative-negative log likelihoods by survey index (left panel) and fishery length composition (right panel) for the virgin recruitment in log-scale ( $\log(R_0)$ ) for the *S11\_base* model. The vertical line denotes the maximum likelihood estimate (MLE).

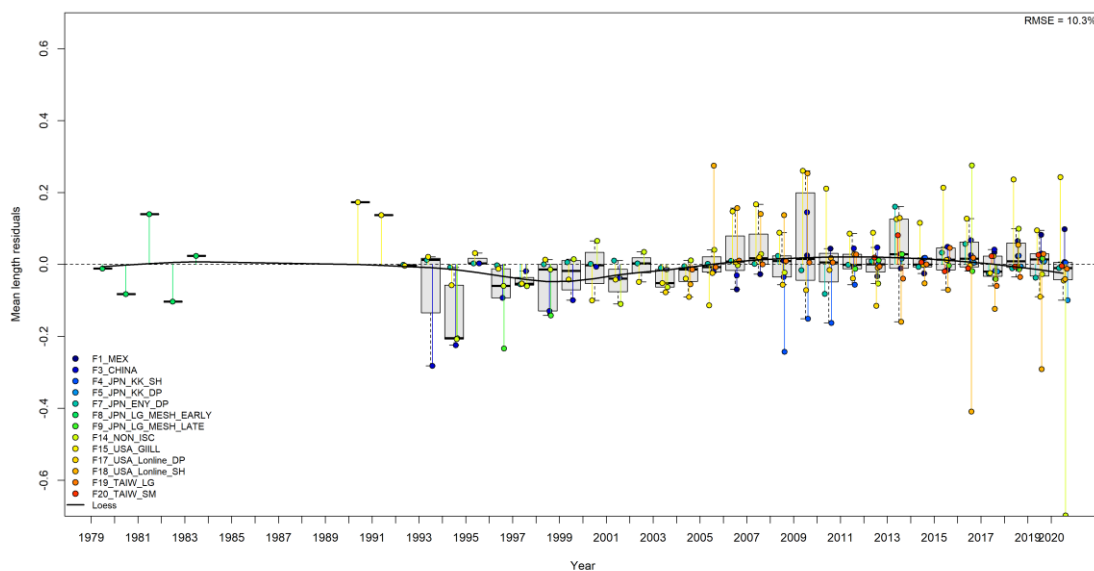


**Figure 23.** Joint residual plot for annual mean length estimates for multiple fishing fleets from the *S11\_base* model. Vertical lines with points show the residuals (in colors by fishery), and solid black lines show loess smoother through all residuals. Boxplots indicate the median and quantiles in cases where residuals from the multiple indices are available for any given year. The overall root-mean squared error (RMSE) is included in the upper right-hand corner.

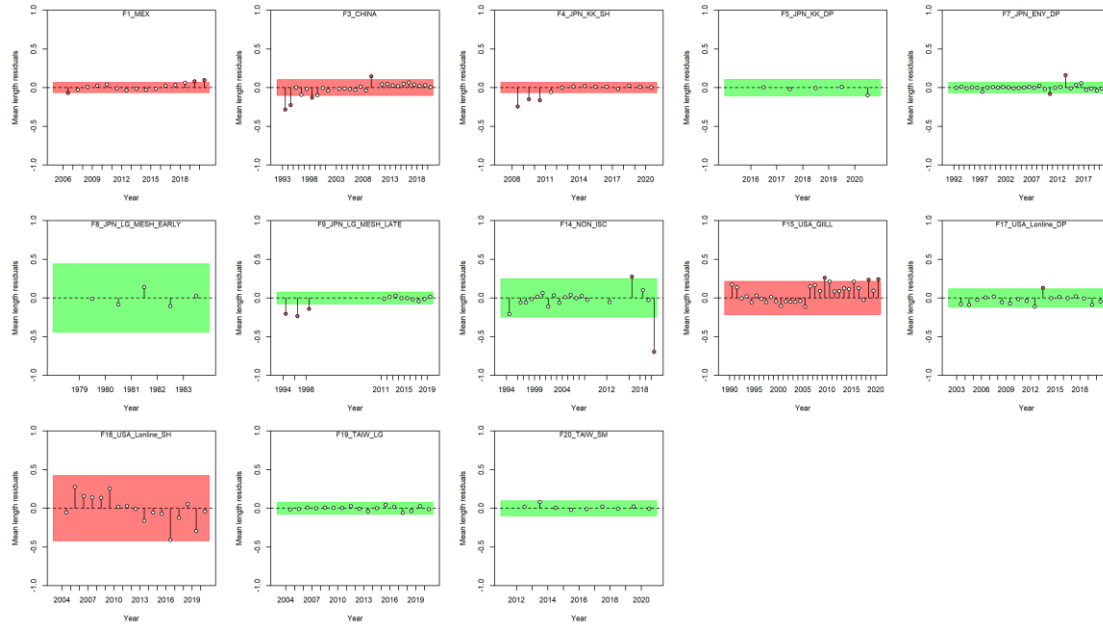


**Figure 24.** Runs tests results from the mean length residuals illustrated for all fisheries in the *S11\_base* model. Green shading indicates no evidence ( $p \geq 0.05$ ) and red shading evidence ( $p < 0.05$ ) to reject the hypothesis of a randomly distributed time-series of residuals, respectively. The shaded (green/red) area spans three residual standard deviations to either side from zero, and the red points outside of the shading violate the ‘three-sigma limit’ for that series.

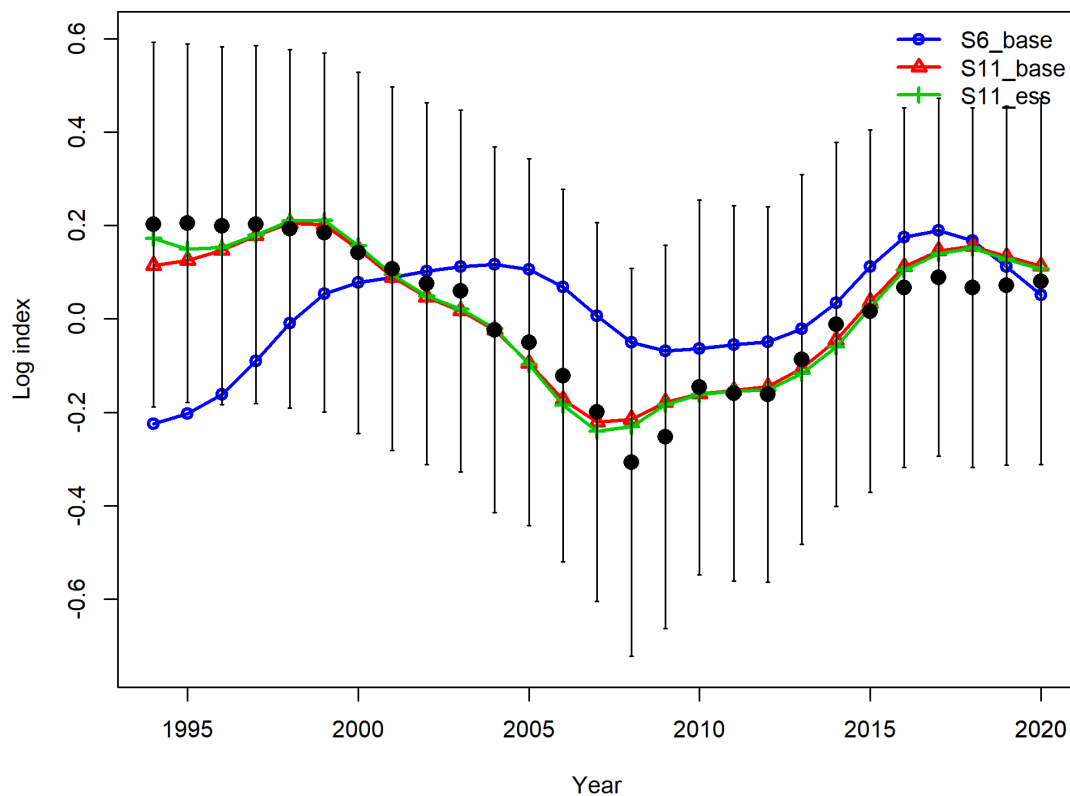


**Figure 25.** Model fits to the S11 DFA composite late standardized catch-per-unit-effort (CPUE) (in log scale) data sets for each of the three models in the ensemble. The solid colored line is the model predicted value and the solid black circles are observed data values. Vertical black lines represent the estimated confidence intervals ( $\pm 1.96$  standard deviations) around the CPUE values. Note that the S6 model does not fit to this index.

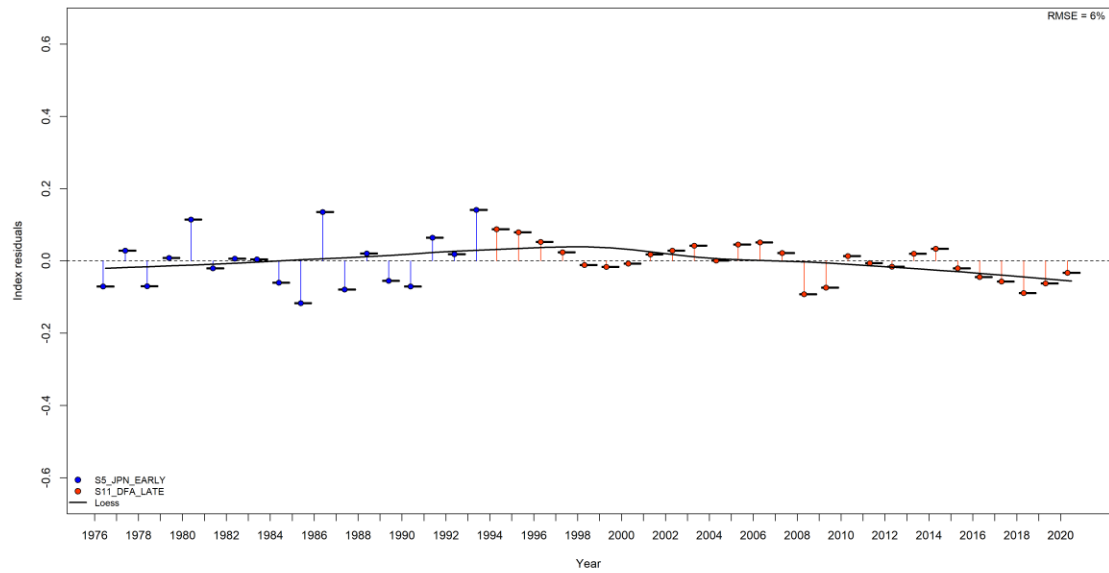


**Figure 26.** Joint residual plot for the two survey indices in the *S11\_base* model. Vertical lines with points show the residuals (in colors by fishery), and solid black lines show loess smoother through all residuals. Boxplots indicate the median and quantiles in cases where residuals from the multiple indices are available for any given year. The overall root-mean squared error (RMSE) is included in the upper right-hand corner.

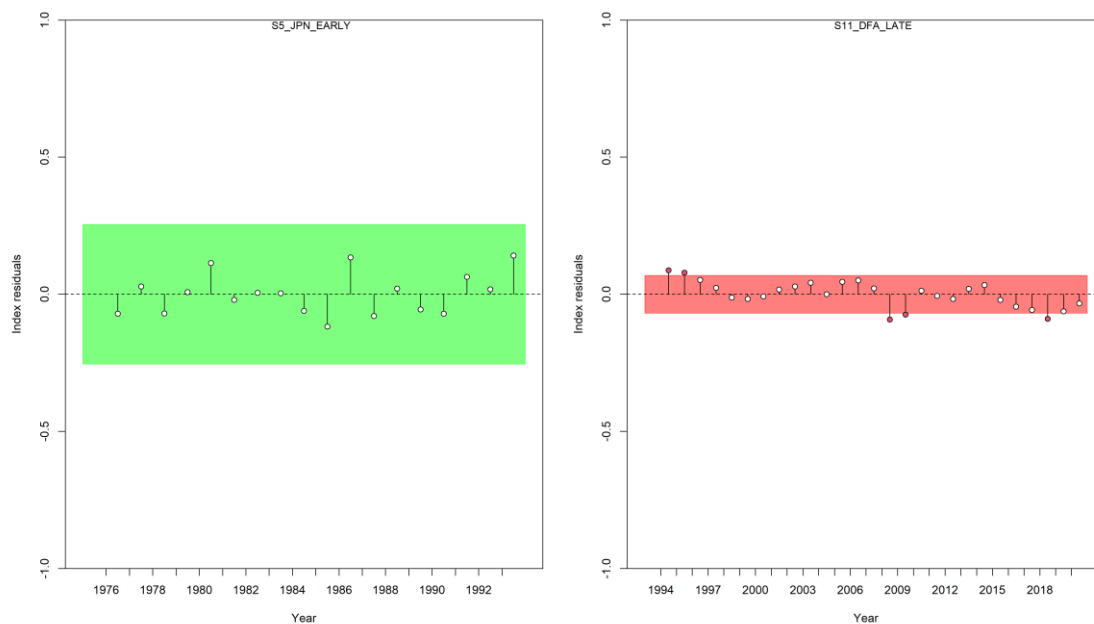


**Figure 27.** Runs tests results for the two survey indices in the *S11\_base* model. Green shading indicates no evidence ( $p \geq 0.05$ ) and red shading evidence ( $p < 0.05$ ) to reject the hypothesis of a randomly distributed time-series of residuals, respectively. The shaded (green/red) area spans three residual standard deviations to either side from zero, and the red points outside of the shading violate the ‘three-sigma limit’ for that series.

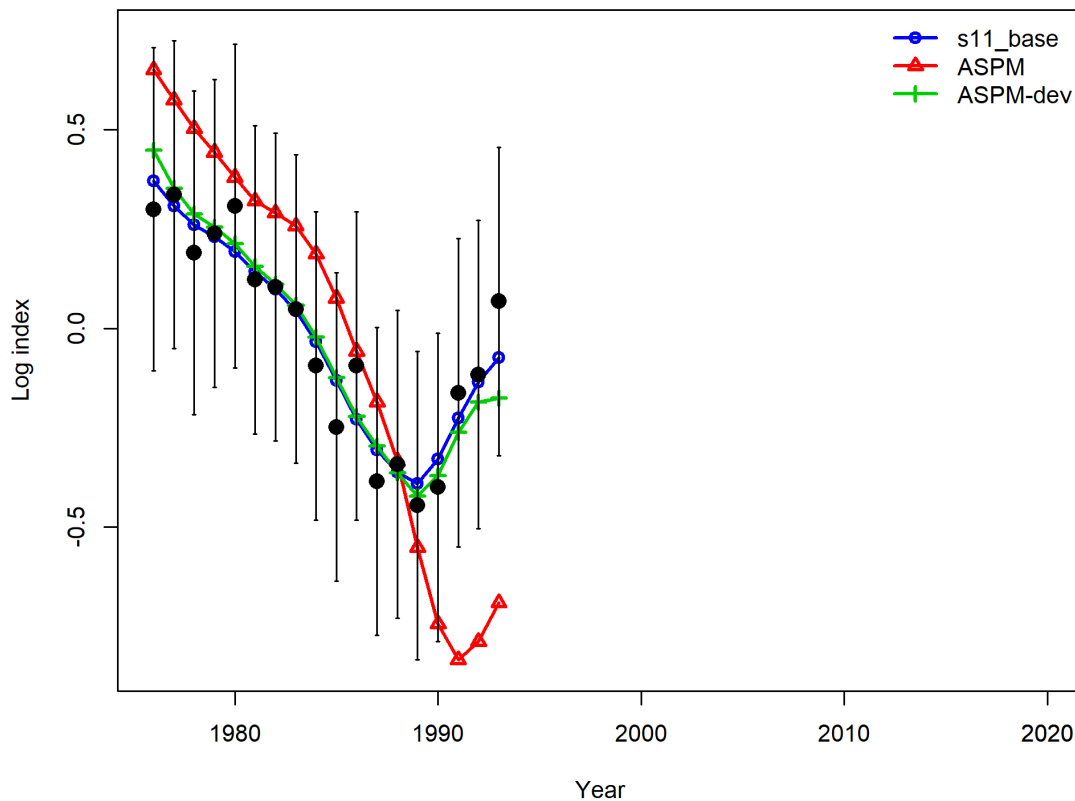


**Figure 28.** Model fits to the S5: JPN\_EARLY standardized catch-per-unit-effort (CPUE) (in log scale) data set for each of the *S11\_base* model and two versions of age-structured production models (ASPM and ASPM-dev). The solid colored line is the model predicted value and the solid black circles are observed data values. Vertical black lines represent the estimated confidence intervals ( $\pm 1.96$  standard deviations) around the CPUE values.

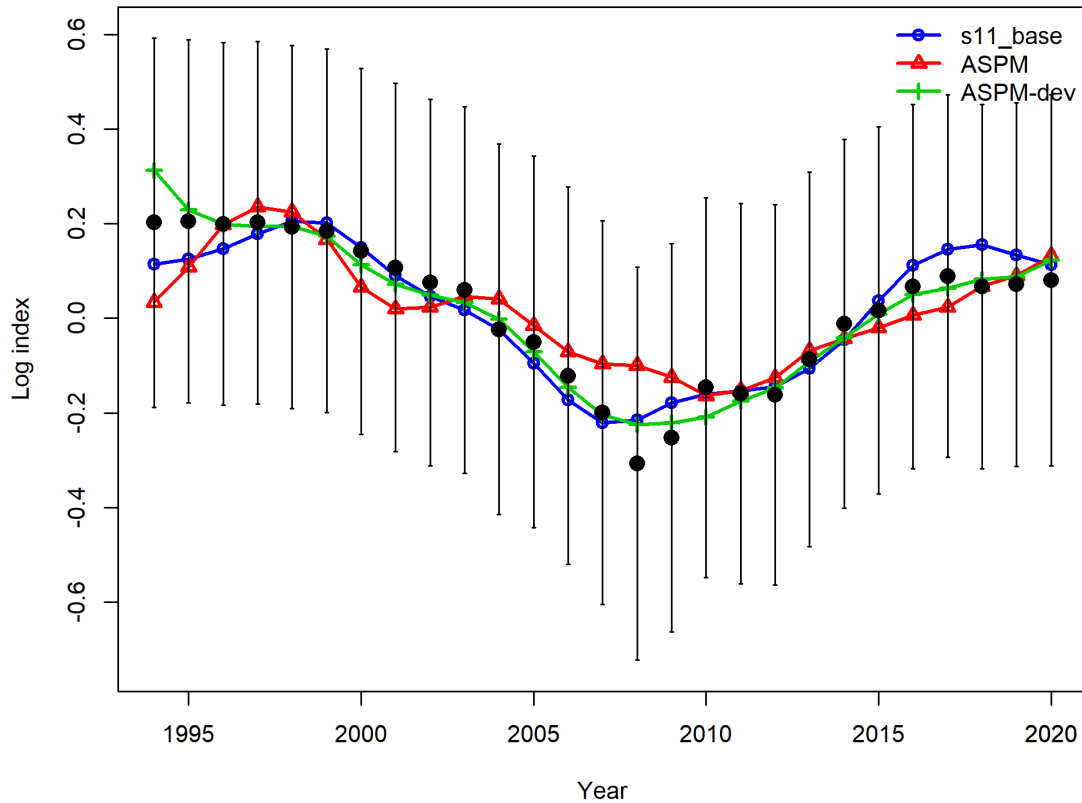


**Figure 29.** Model fits to the S11 DFA composite late standardized catch-per-unit-effort (CPUE) (in log scale) data set for each of the *S11\_base* model and two versions of age-structured production models (ASPM and ASPM-dev). The solid colored line is the model predicted value and the solid black circles are observed data values. Vertical black lines represent the estimated confidence intervals ( $\pm 1.96$  standard deviations) around the CPUE values.

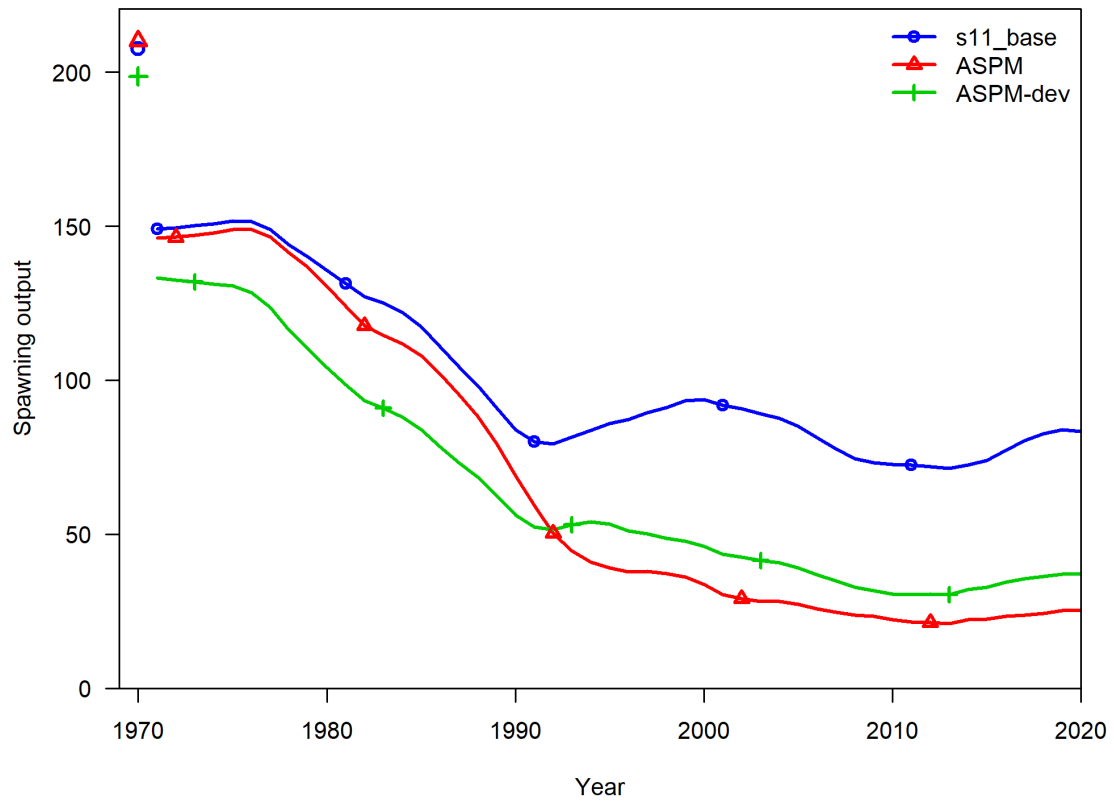


**Figure 30.** Annual spawning biomass estimates for the *S11\_base* model and two versions of the age-structured production models (ASPM and ASPM-dev).

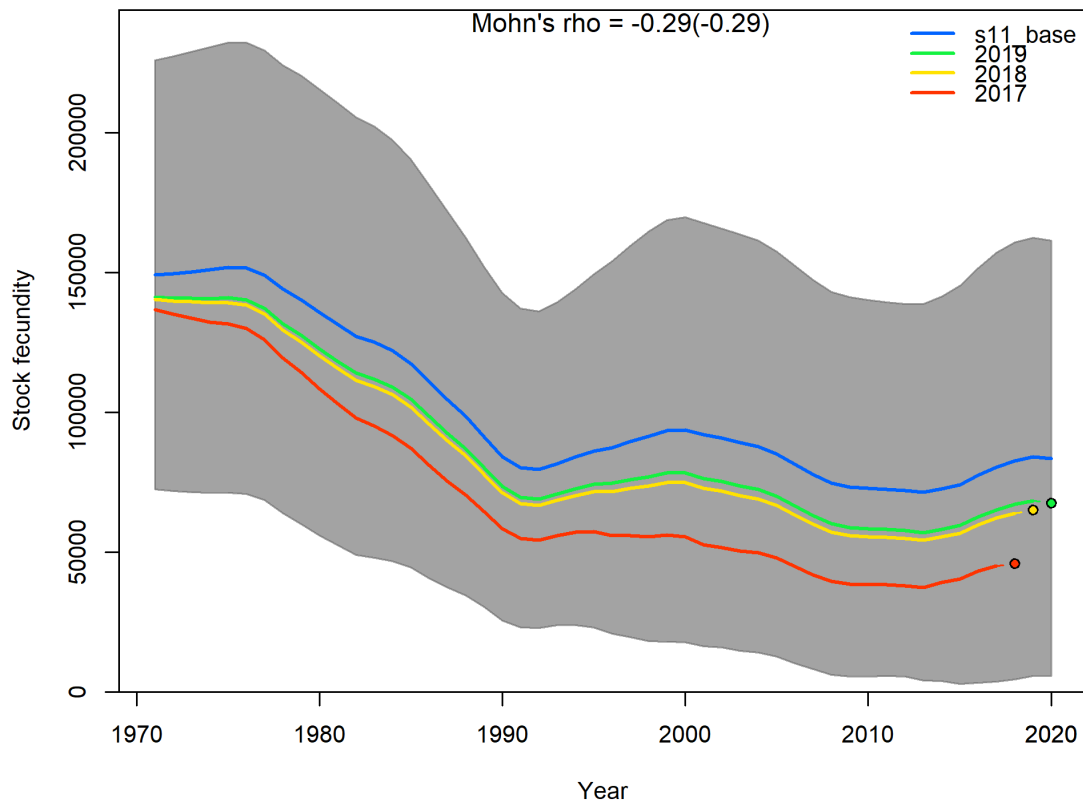


**Figure 31.** Retrospective analysis of spawning stock biomass (metric tons) for the *S11\_base* model conducted by sequentially removing the last three years of data from the model. Mohn's rho statistic and the corresponding 'hindcast rho' values (in brackets) are printed at the top of the figure. Grey shaded areas are the 95 % confidence intervals from the reference model.

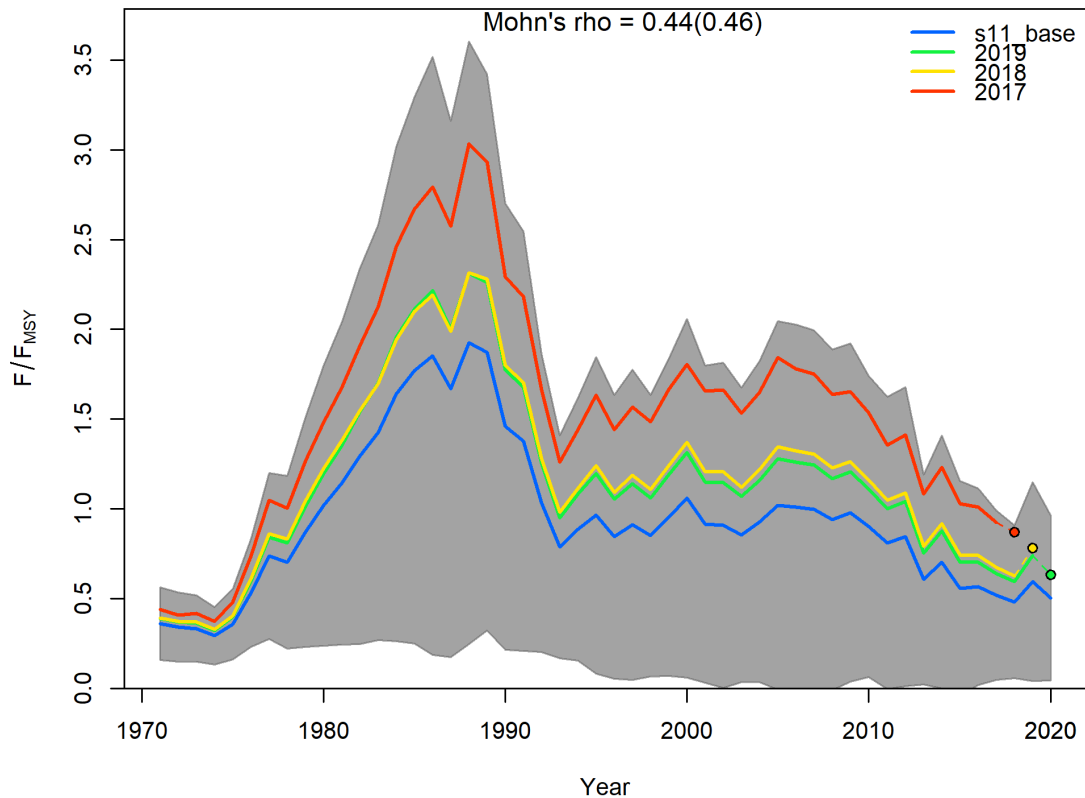


**Figure 32.** Retrospective analysis of fishing mortality rate relative to maximum sustainable yield (MSY) level for the *S11\_base* model conducted by sequentially removing the last three years of data from the model. Mohn's rho statistic and the corresponding 'hindcast rho' values (in brackets) are printed at the top of the figure. Grey shaded areas are the 95 % confidence intervals from the reference model.

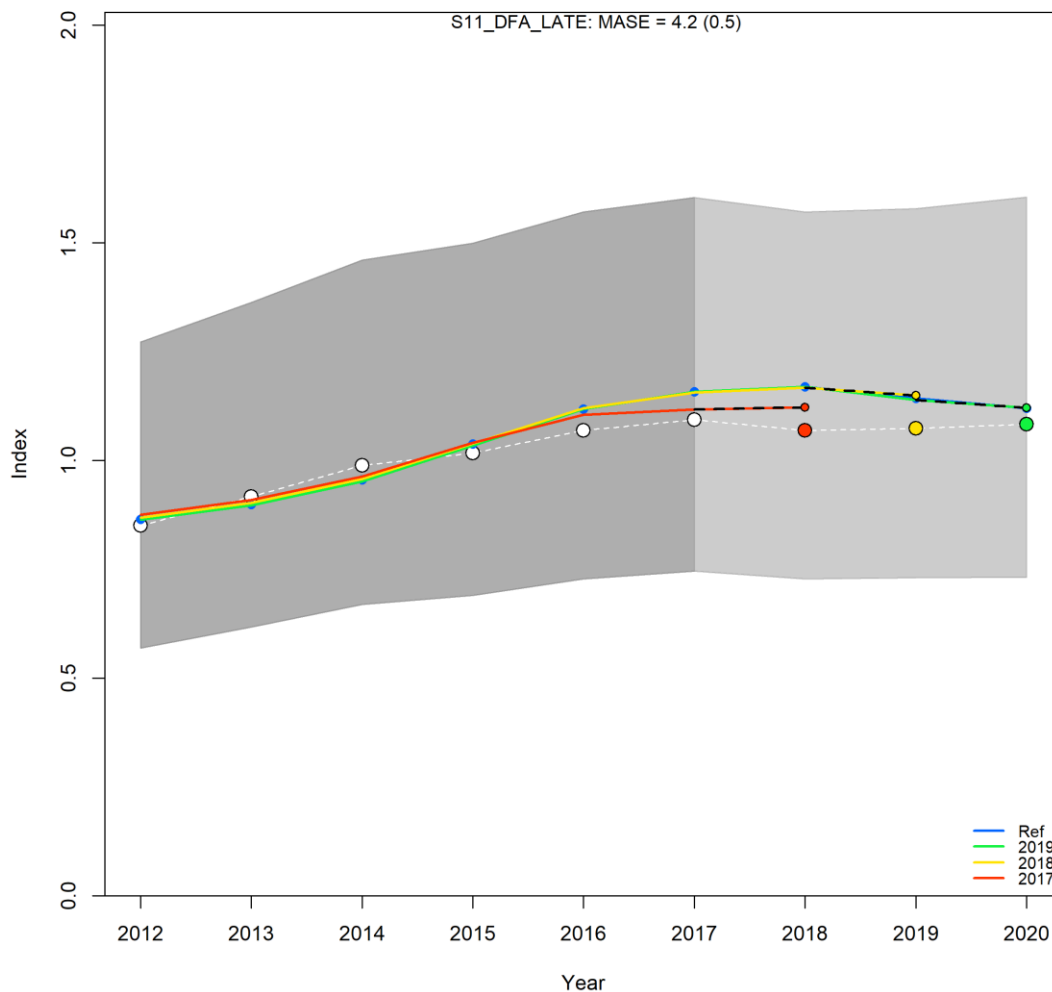


**Figure 33.** Hindcasting cross-validation (HCxval) results for the fit to the S11 DFA composite late standardized catch-per-unit-effort (CPUE) data set for each of the *S11\_base* model, showing observed (large points connected with dashed line), fitted (solid lines) and one-year-ahead forecast values (small terminal points). HCxval was performed using one reference model (S6-base) and three hindcast model runs (solid lines) relative to the expected CPUE. The observations used for cross-validation are highlighted as color-coded solid circles with associated 95 % confidence intervals (light-gray shading). The model reference year refers to the endpoints of each one-year-ahead forecast and the corresponding observation (i.e., year of peel + 1). The mean absolute scaled error (MASE) score and adjusted MASE (in parentheses) is shown at the top of the figure.

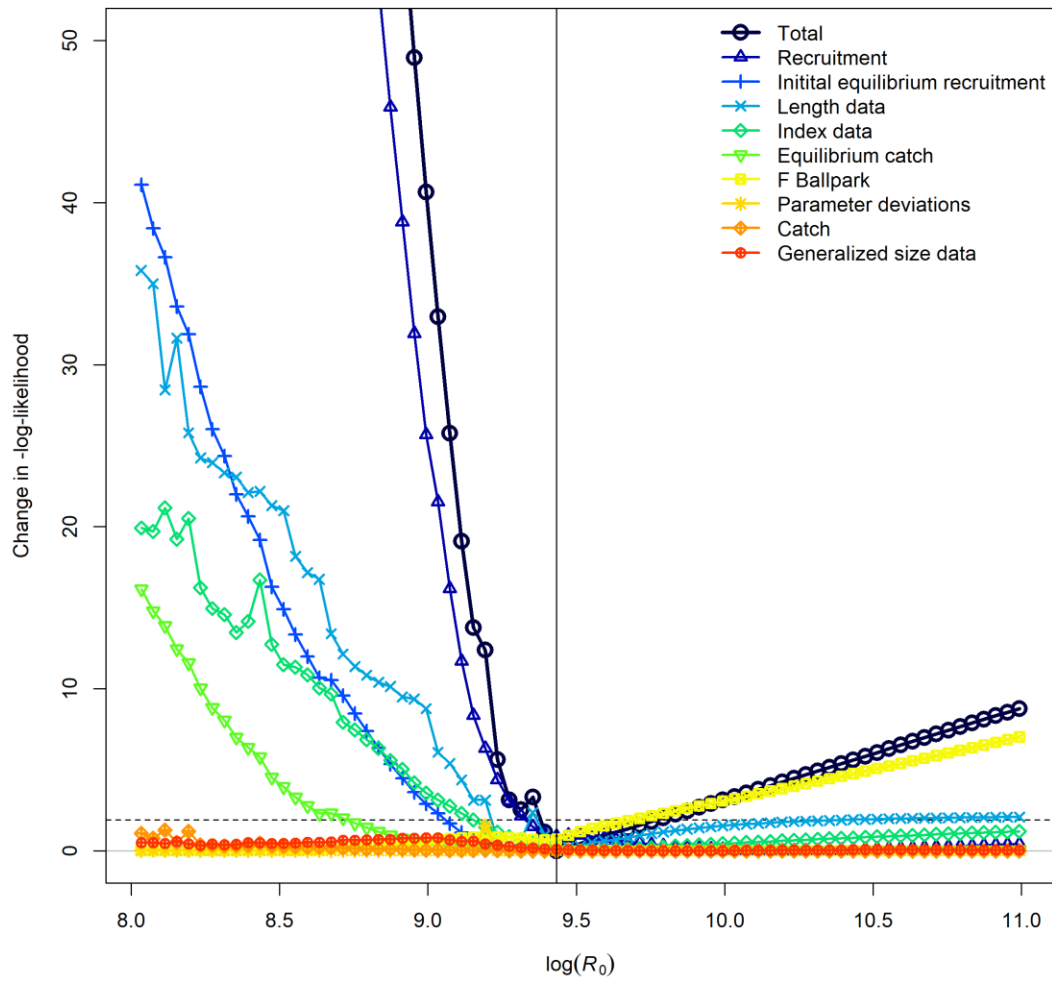


**Figure 34.** Profiles of the relative-negative log likelihoods by different data components for the virgin recruitment in log-scale ( $\log(R_0)$ ) for the *SII\_ess* model. The vertical line denotes the maximum likelihood estimate (MLE).

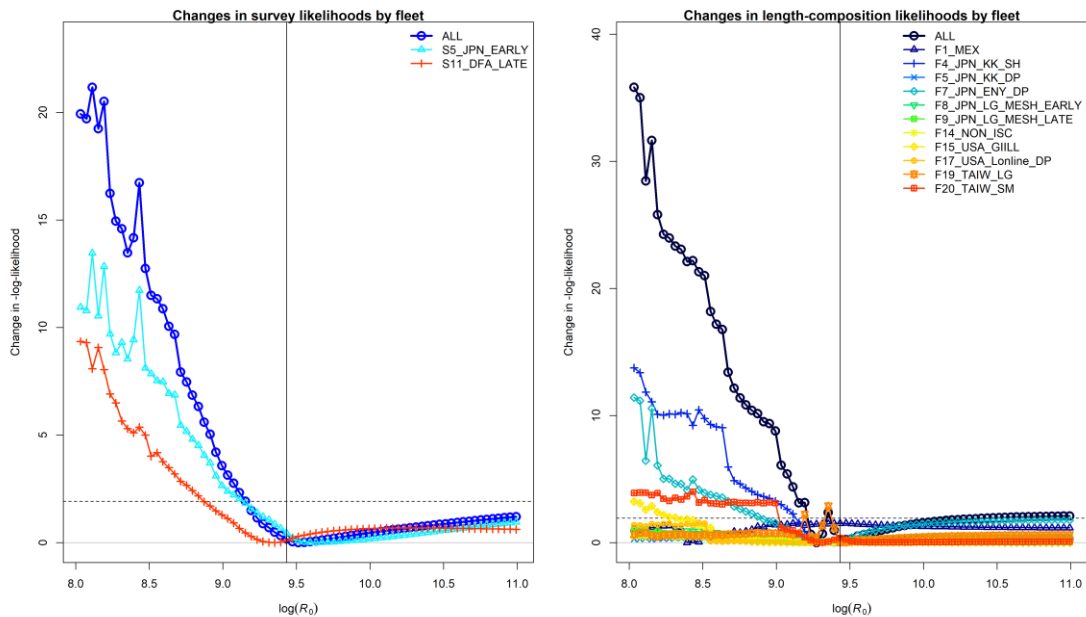


**Figure 35.** Profiles of the relative-negative log likelihoods by survey index (left panel) and fishery length composition (right panel) for the virgin recruitment in log-scale ( $\log(R_0)$ ) for the *S11\_ess* model. The vertical line denotes the maximum likelihood estimate (MLE).

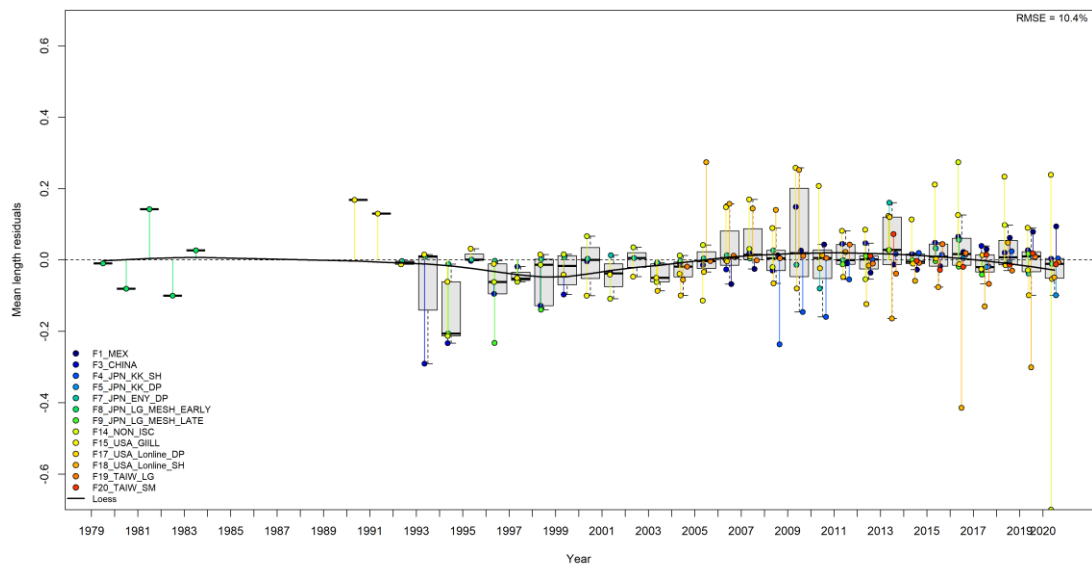


**Figure 36.** Joint residual plot for annual mean length estimates for multiple fishing fleets from the *SII\_ess* model. Vertical lines with points show the residuals (in colors by fishery), and solid black lines show loess smoother through all residuals. Boxplots indicate the median and quantiles in cases where residuals from the multiple indices are available for any given year. The overall root-mean squared error (RMSE) is included in the upper right-hand corner.

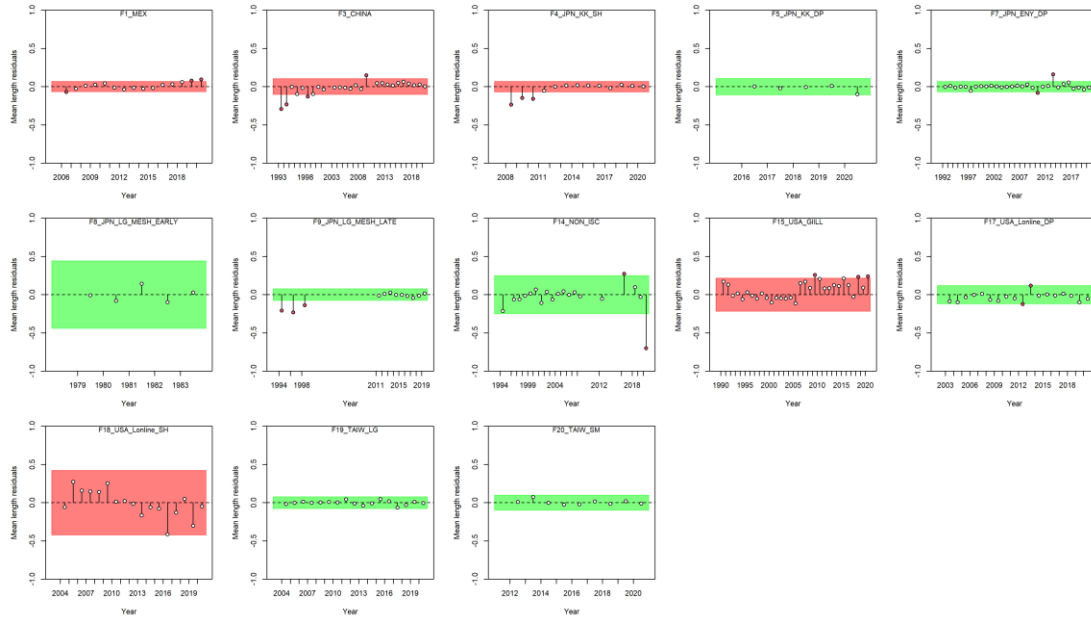


**Figure 37.** Runs tests results from the mean length residuals illustrated for all fisheries in the *SII\_ess* model. Green shading indicates no evidence ( $p \geq 0.05$ ) and red shading evidence ( $p < 0.05$ ) to reject the hypothesis of a randomly distributed time-series of residuals, respectively. The shaded (green/red) area spans three residual standard deviations to either side from zero, and the red points outside of the shading violate the ‘three-sigma limit’ for that series.

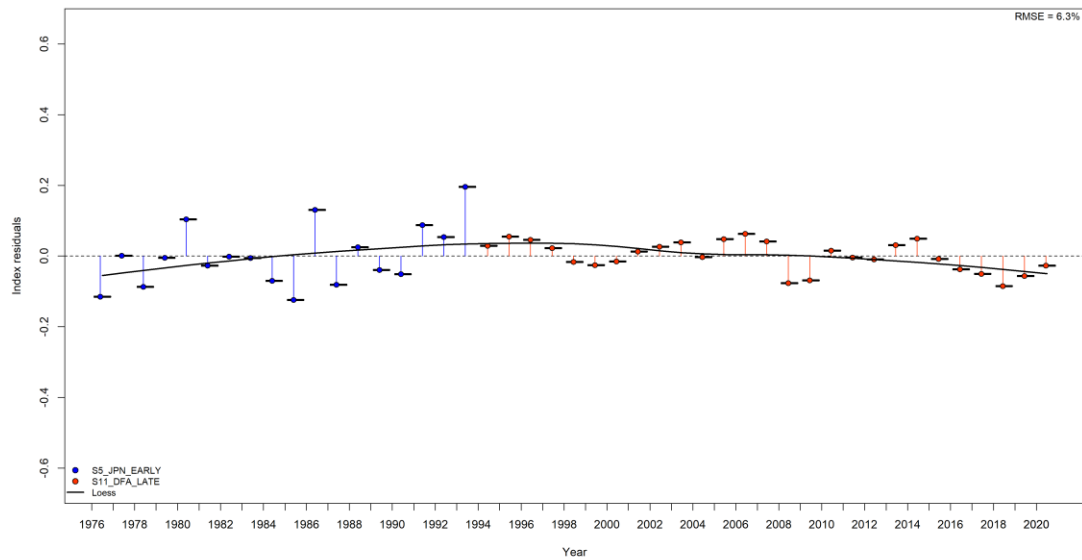


**Figure 38.** Joint residual plot for the two survey indices in the *SII\_ess* model. Vertical lines with points show the residuals (in colors by fishery), and solid black lines show loess smoother through all residuals. Boxplots indicate the median and quantiles in cases where residuals from the multiple indices are available for any given year. The overall root-mean squared error (RMSE) is included in the upper right-hand corner.

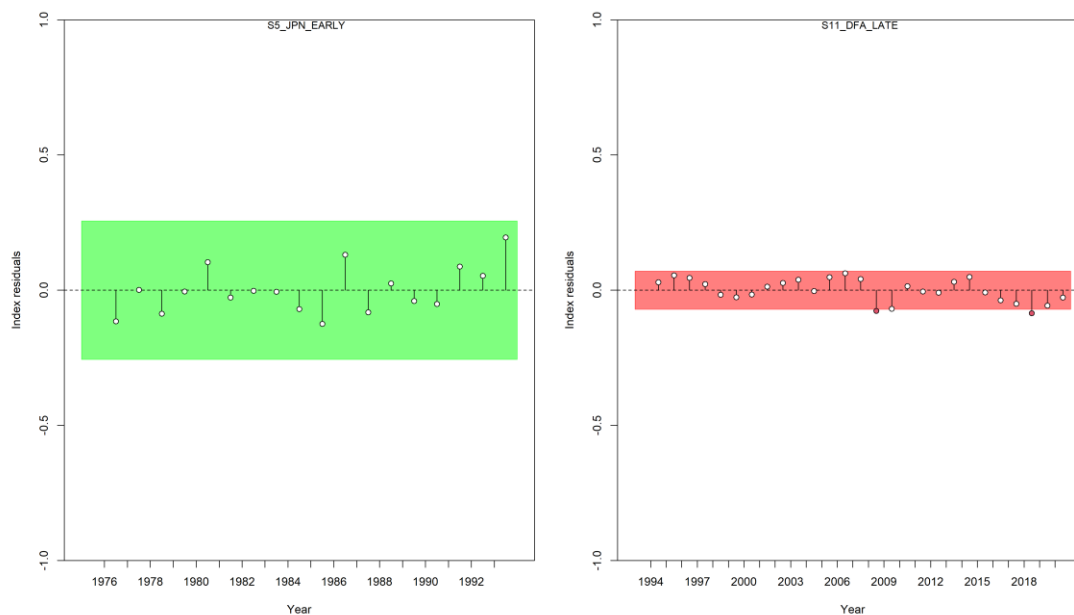


**Figure 39.** Runs tests results for the two survey indices in the *SII\_ess* model. Green shading indicates no evidence ( $p \geq 0.05$ ) and red shading evidence ( $p < 0.05$ ) to reject the hypothesis of a randomly distributed time-series of residuals, respectively. The shaded (green/red) area spans three residual standard deviations to either side from zero, and the red points outside of the shading violate the ‘three-sigma limit’ for that series.

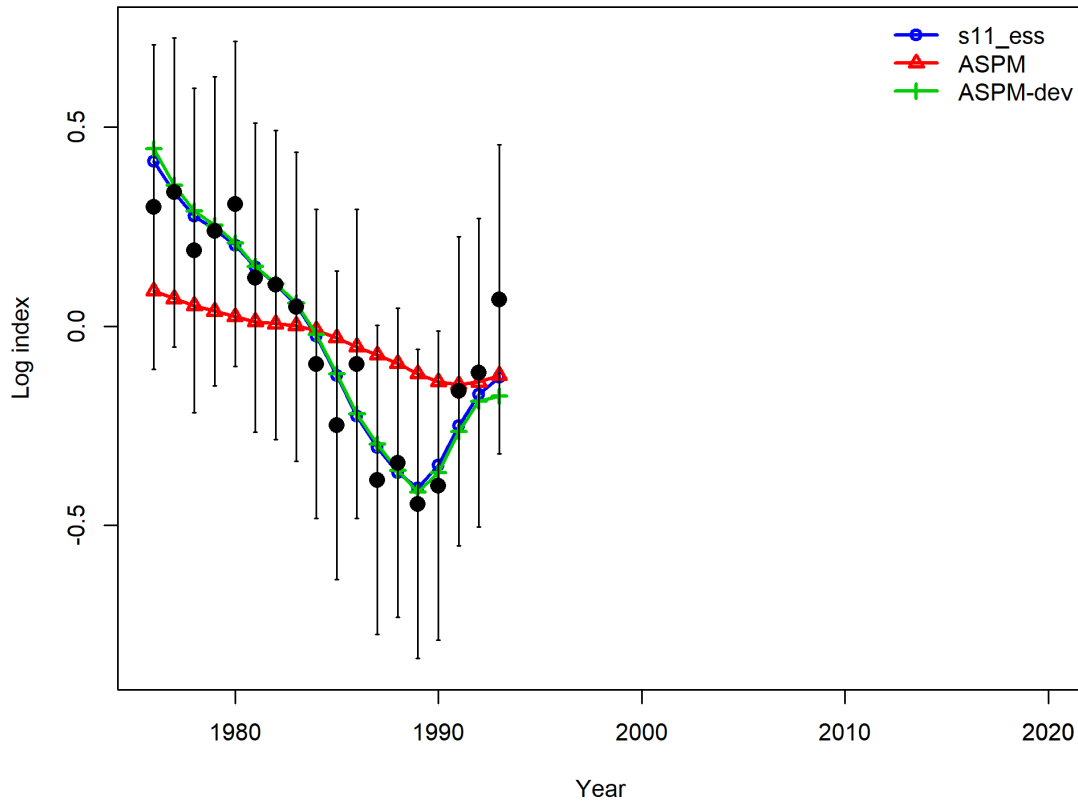


**Figure 40.** Model fits to the S5 Japanese Kinkai shallow early standardized catch-per-unit-effort (CPUE) (in log scale) data set for each of the *S11\_ess* model and two ASPM models. The solid colored line is the model predicted value and the solid black circles are observed data values. Vertical black lines represent the estimated confidence intervals ( $\pm 1.96$  standard deviations) around the CPUE values.

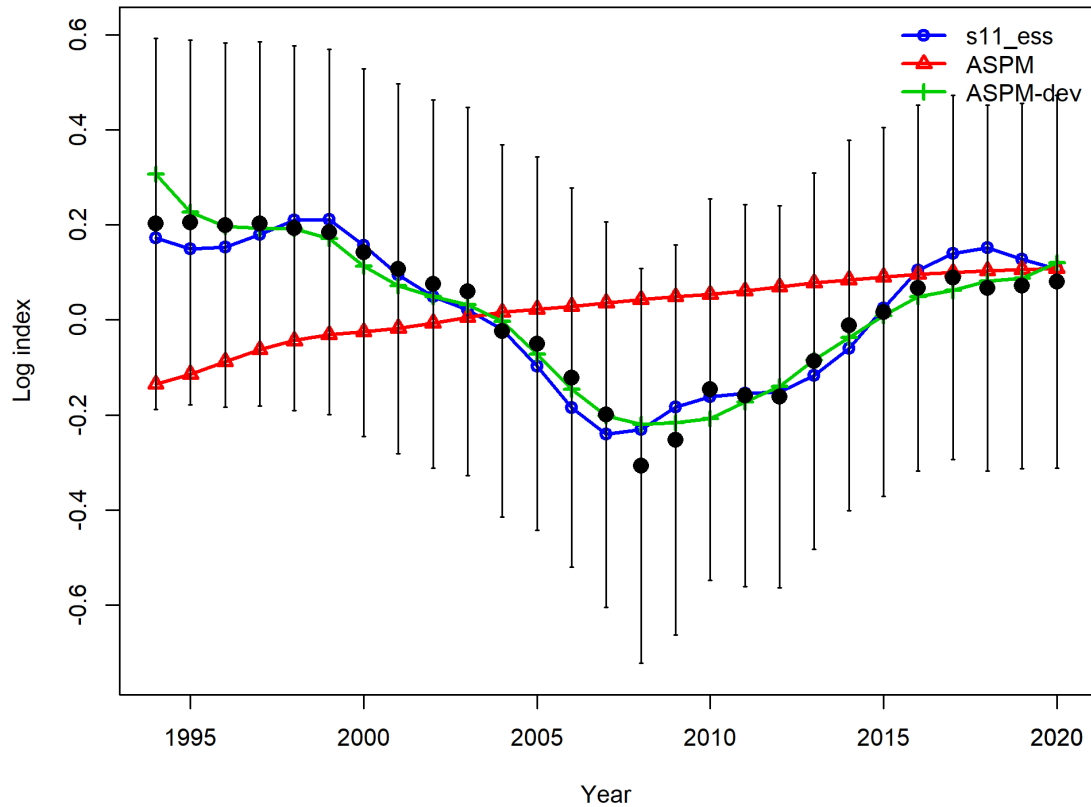


**Figure 41.** Model fits to the S11 DFA composite late standardized catch-per-unit-effort (CPUE) (in log scale) data set for each of the *S11\_ess* model and two ASPM models. The solid colored line is the model predicted value and the solid black circles are observed data values. Vertical black lines represent the estimated confidence intervals ( $\pm 1.96$  standard deviations) around the CPUE values.

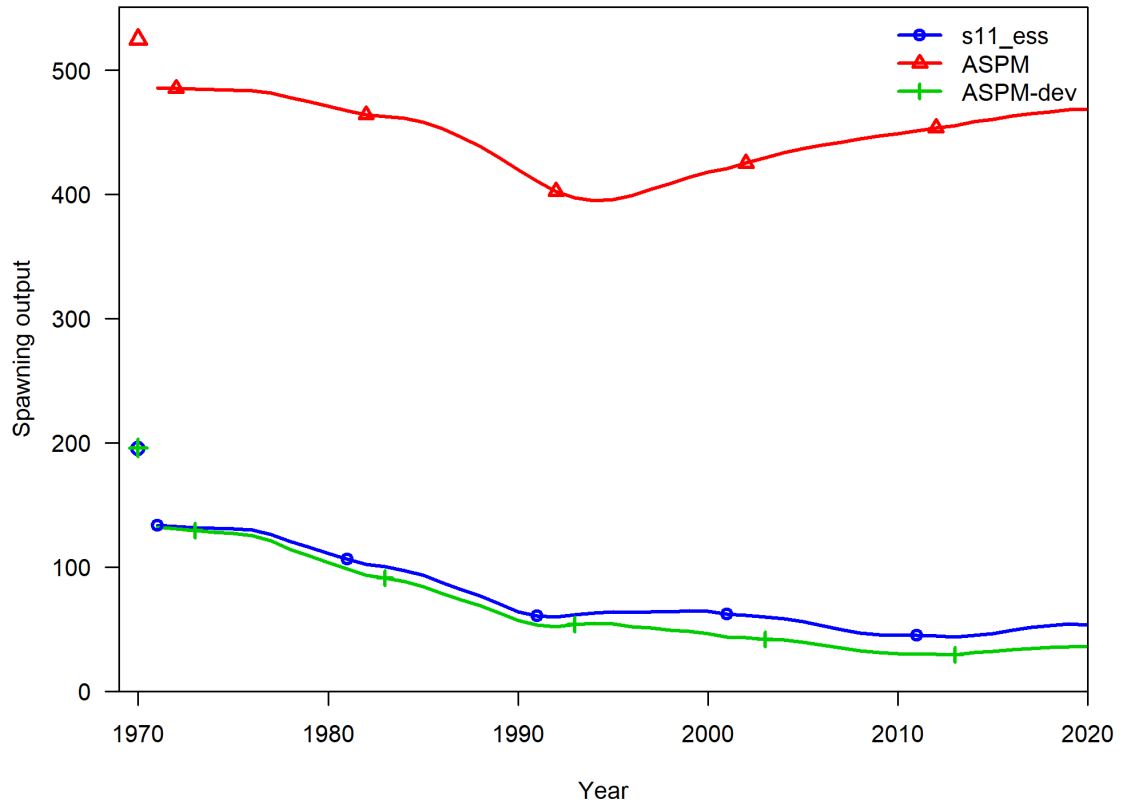


**Figure 42.** Annual spawning biomass estimates for the *S11\_ess* model and two versions of the ASPM.

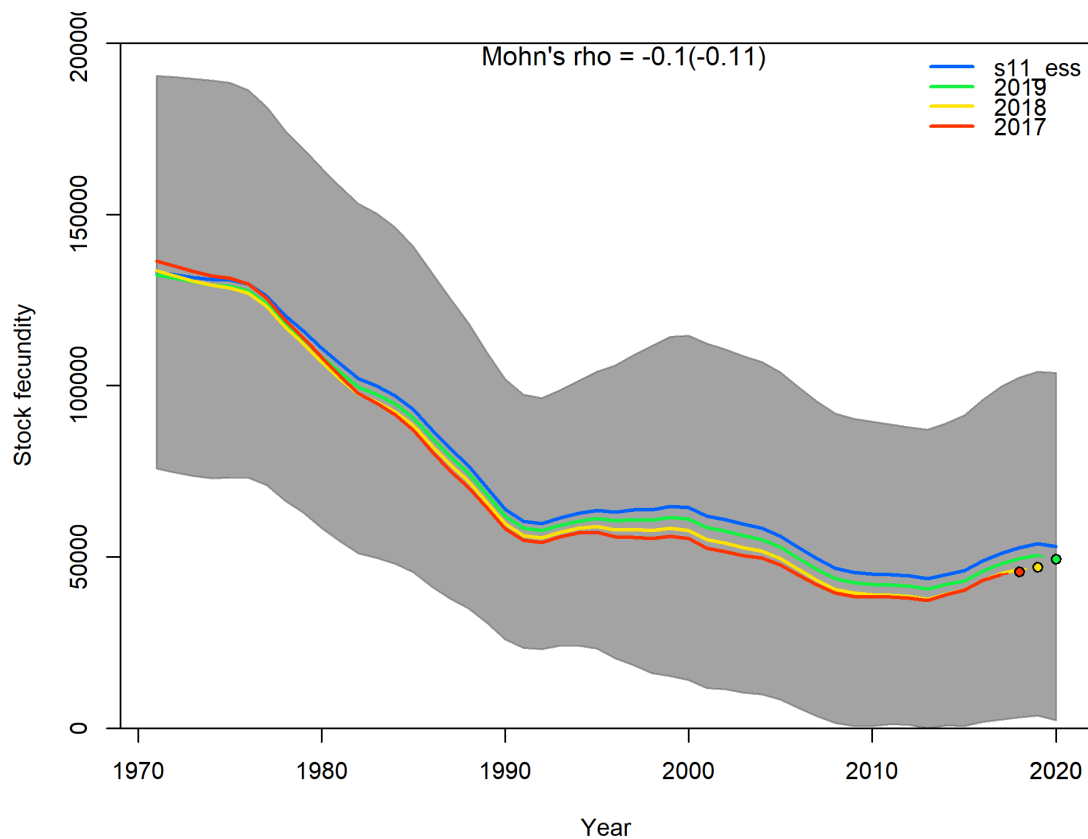


**Figure 43.** Retrospective analysis of spawning stock biomass (metric tons) for the *S11\_ess* model conducted by sequentially removing the last three years of data from the model. Mohn's rho statistic and the corresponding 'hindcast rho' values (in brackets) are printed at the top of the figure. Grey shaded areas are the 95 % confidence intervals from the reference model.

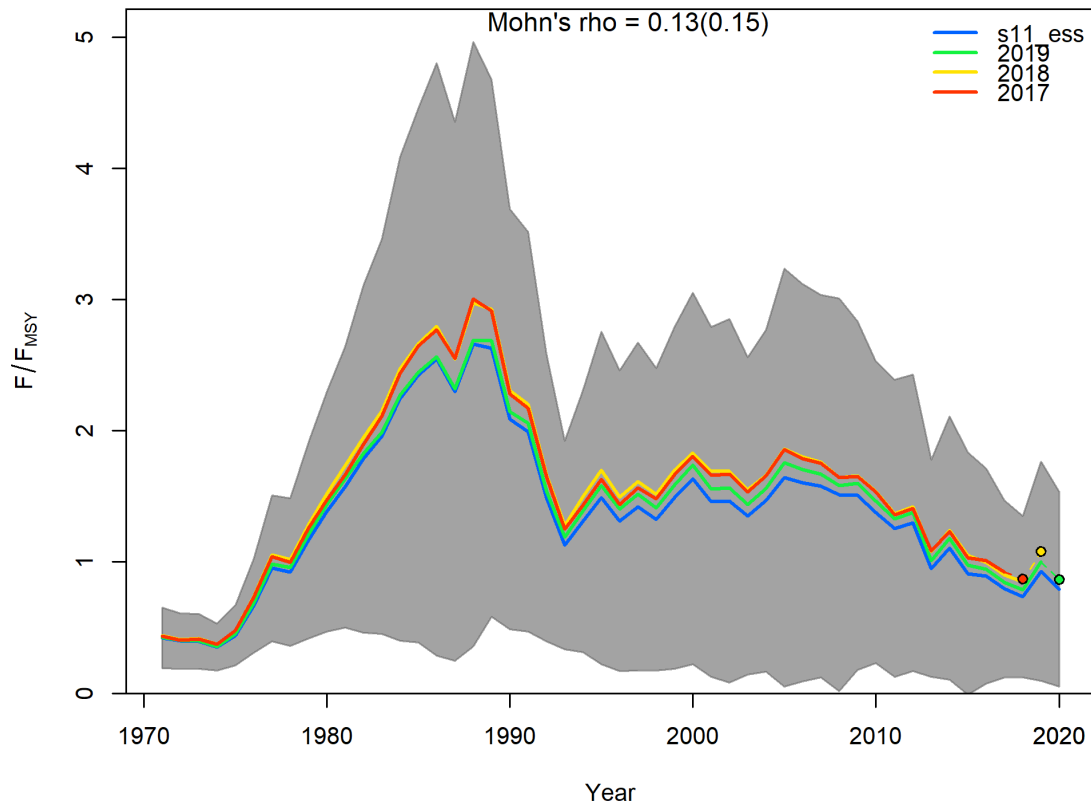


**Figure 44.** Retrospective analysis of fishing mortality rate relative to maximum sustainable yield (MSY) level for the *S11\_ess* model conducted by sequentially removing the last three years of data from the model. Mohn's rho statistic and the corresponding 'hindcast rho' values (in brackets) are printed at the top of the figure. Grey shaded areas are the 95 % confidence intervals from the reference model.

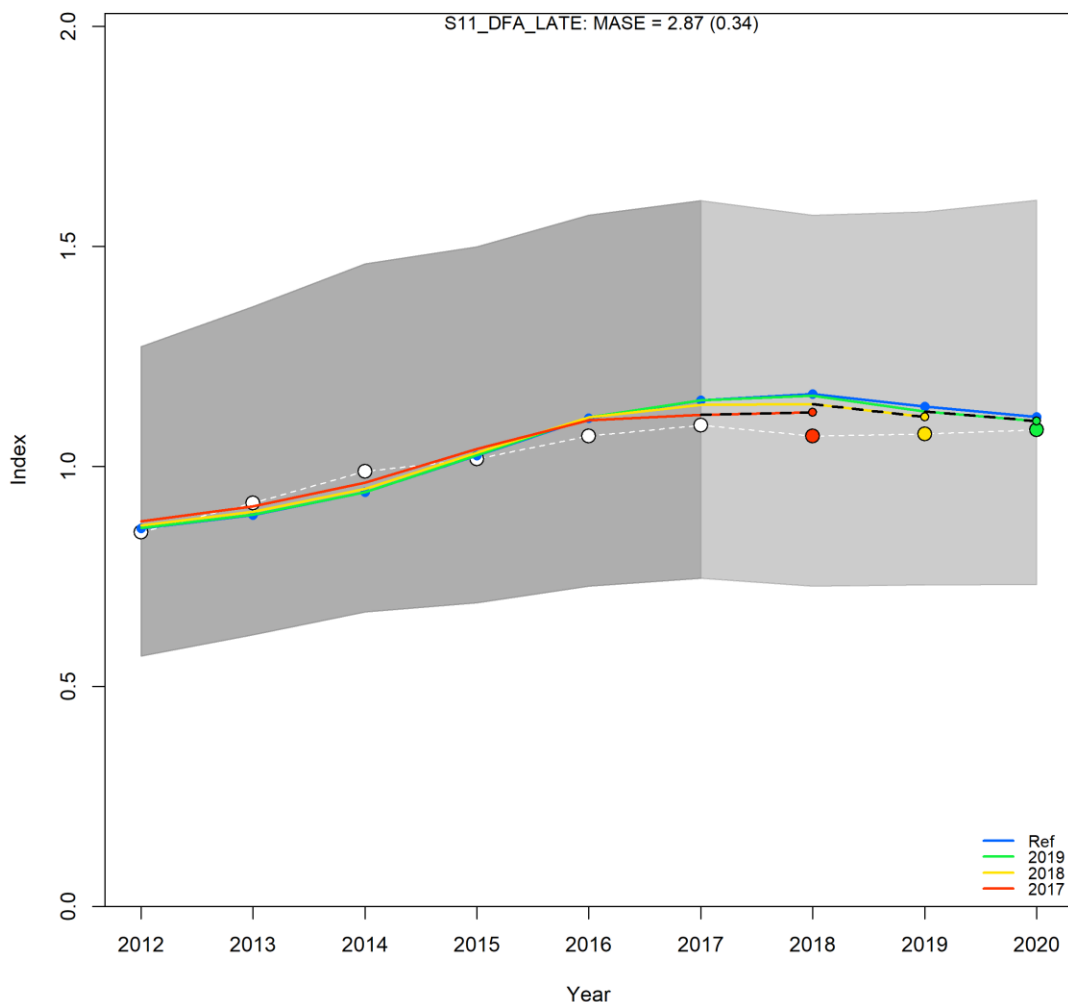


**Figure 45.** Hindcasting cross-validation (HCxval) results for the fit to the S11 DFA composite late standardized catch-per-unit-effort (CPUE) data set for each of the *S11\_ess* model, showing observed (large points connected with dashed line), fitted (solid lines) and one-year-ahead forecast values (small terminal points). HCxval was performed using one reference model (S6-base) and three hindcast model runs (solid lines) relative to the expected CPUE. The observations used for cross-validation are highlighted as color-coded solid circles with associated 95 % confidence intervals (light-gray shading). The model reference year refers to the endpoints of each one-year-ahead forecast and the corresponding observation (i.e., year of peel + 1). The mean absolute scaled error (MASE) score and adjusted MASE (in parentheses) is shown at the top of the figure.

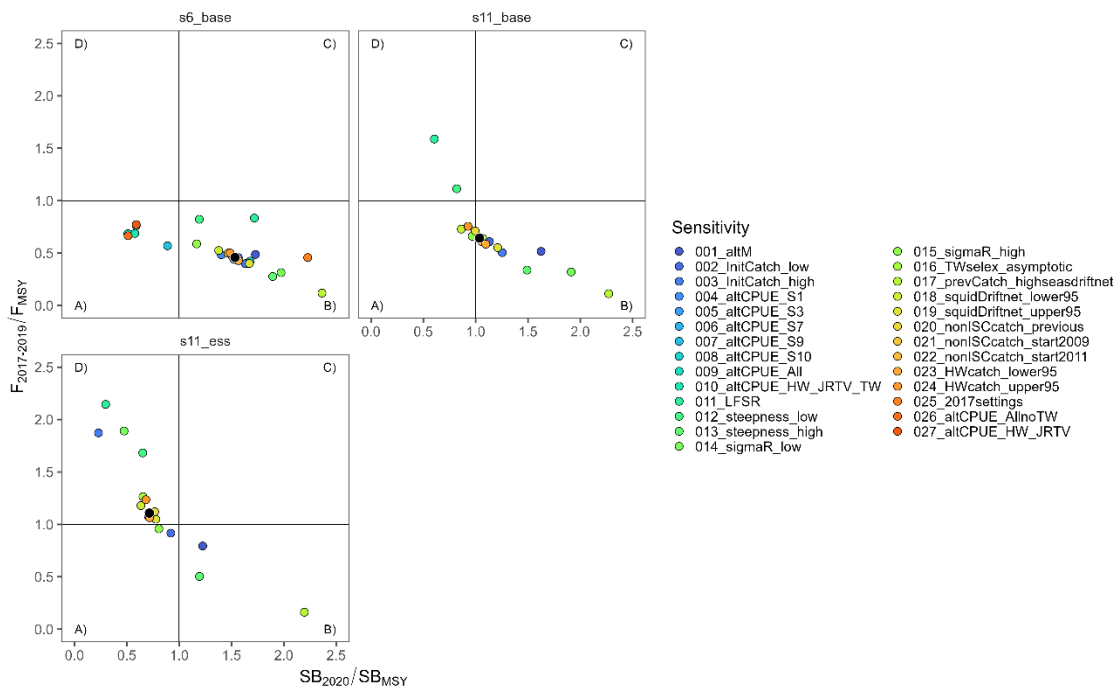


**Figure 56.** Kobe plot of the latest stock status on spawning stock biomass (SSB) and fishing mortality rates (F) relative to maximum sustainable yield (MSY) level for North Pacific blue shark derived from 27 scenarios of sensitivity analysis for three base models (*s6\_base* model, *S11\_base* model, and *S11\_ess* model). See **Table 11** for the details in the sensitivity analysis.

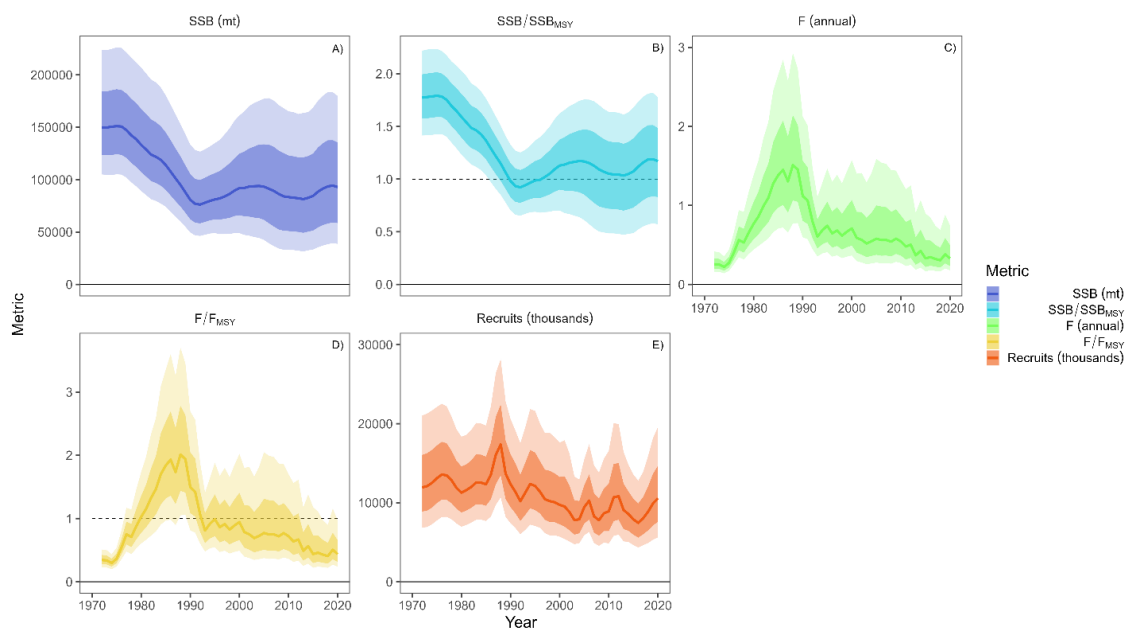


**Figure 57.** Model ensemble results for spawning stock biomass (SSB) (A), SSB/SSB<sub>MSY</sub> (B), fishing mortality rate (F) (C), F/F<sub>MSY</sub> (D), and recruitment (E). The solid line indicates the median across the ensemble. The lighter shaded region gives the 80<sup>th</sup> percentile and the darker shaded region gives the 50<sup>th</sup> percentile around the median estimate.

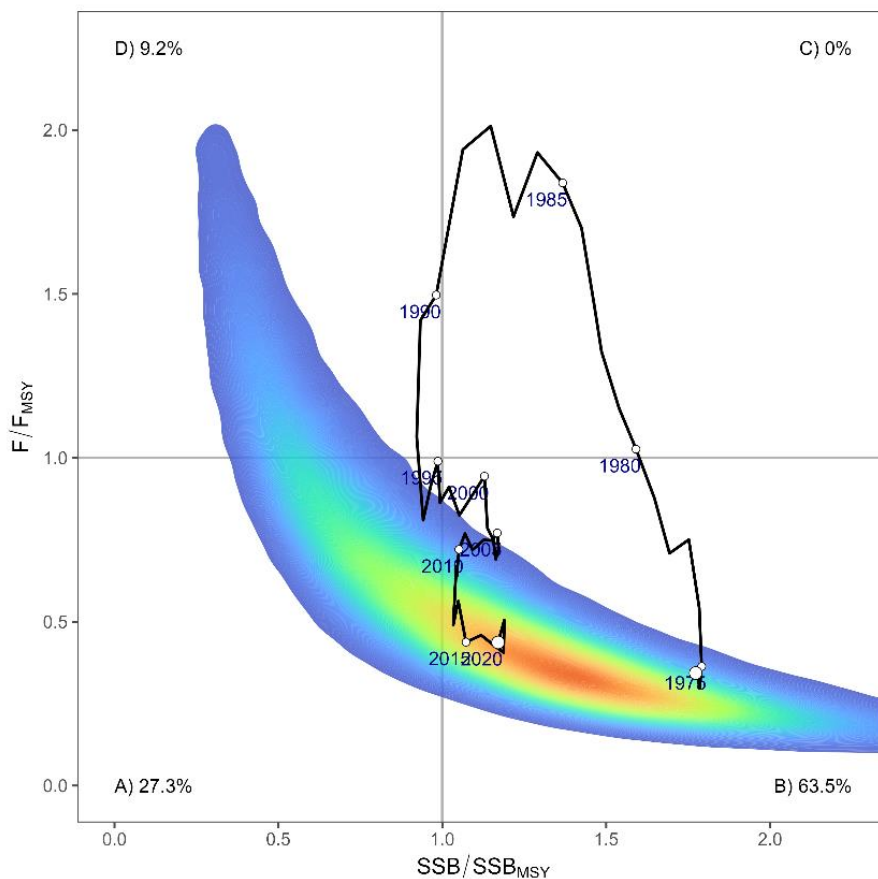


**Figure 46.** Uncertainty in terminal stock status given by the Kobe plot, based on the 100,000 bootstrap samples characterizing the model and estimation uncertainty from the model ensemble. Warmer colors indicate a greater density of samples, while cooler colors show the fringe of the distribution. The black line gives the median historical trajectory in stock status. The proportion of bootstrap samples falling within each quadrant is listed.

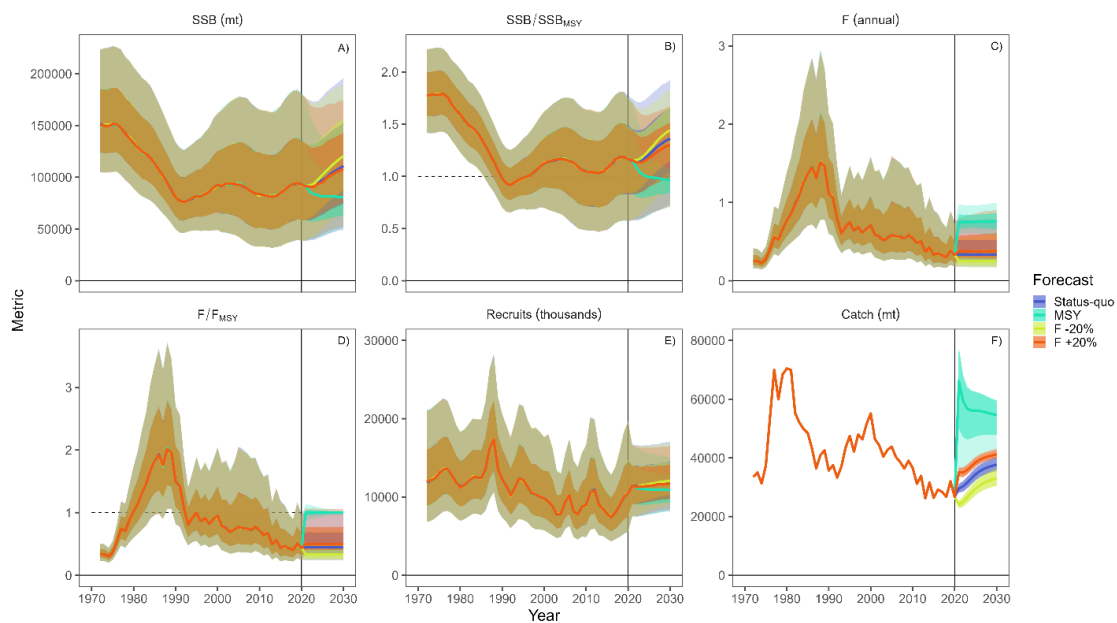


**Figure 59.** Ten-year forecasting results for the four projection scenarios across the model ensemble for spawning stock biomass (A),  $SSB/SSB_{MSY}$  (B), fishing mortality rate ;  $F$  (C),  $F/F_{MSY}$  (D), recruitment (E), and catch (F). The solid line indicates the median across the ensemble for each scenario. The lighter shaded region gives the 80<sup>th</sup> percentile and the darker shaded region gives the 50<sup>th</sup> percentile around the median estimate. Color indicates the forecast scenario.

### 13. APPENDIX

The following is the code of control file used in the stock assessment of North Pacific blue shark. If you want to use the other SS3-files used in the stock assessment, please contact to members of the ISC SHARKWG modeling team: Mikihiro Kai (Chair, [kaim@affrc.go.jp](mailto:kaim@affrc.go.jp)) or Nicholas Ducharme-Barth ([nicholas.ducharme-barth@noaa.gov](mailto:nicholas.ducharme-barth@noaa.gov)).

SS Control File (*S6\_base* model)

#V3.30

#C file created using the SS\_writectl function in the R package r4ss

#C file write time: 2022-04-01 19:48:10

#

0 # 0 means do not read wtatage.ss; 1 means read and use wtatage.ss and also read and use growth parameters

1 # N\_Growth\_Patterns

1 # N\_platoons\_Within\_GrowthPattern

4 # recr\_dist\_method for parameters

1 # not yet implemented; Future usage: Spawner-Recruitment; 1=global; 2=by area

1 # number of recruitment settlement assignments

0 # unused option

# for each settlement assignment:

#\_GPattern month area age

1 7 1 0 #\_recr\_dist\_pattern1

#

#\_Cond 0 # N\_movement\_definitions goes here if N\_areas > 1

#\_Cond 1.0 # first age that moves (real age at begin of season, not integer) also cond on do\_migration>0

#\_Cond 1 1 1 2 4 10 # example move definition for seas=1, morph=1, source=1 dest=2, age1=4, age2=10

#

2 # Nblock\_Patterns

1 2 #\_blocks\_per\_pattern

#\_begin and end years of blocks

1970 1970

1973 1981 1982 1992

#

# controls for all timevary parameters

1 #\_env/block/dev\_adjust\_method for all time-vary parms (1=warn relative to base parm bounds; 3=no bound check)

#

# AUTOGEN

1 1 1 1 1 # autogen: 1st element for biology, 2nd for SR, 3rd for Q, 4th reserved, 5th for selex

# where: 0 = autogen all time-varying parms; 1 = read each time-varying parm line; 2 = read then autogen if parm min== -12345

#

# setup for M, growth, maturity, fecundity, recruitment distribution, movement

#

3 #\_natM\_type: \_0=1Parm;

```

1=N_breakpoints; 2=Lorenzen; 3=agespecific; 4=agespec_withseasinterpolate
# #_Age_natmort_by sex x growthpattern
#_Age_0      Age_1 Age_2 Age_3 Age_4 Age_5 Age_6 Age_7 Age_8 Age_9
      Age_10 Age_11 Age_12 Age_13 Age_14 Age_15 Age_16 Age_17 Age_18 Age_19
      Age_20 Age_21 Age_22 Age_23 Age_24
0.787  0.489  0.371  0.307  0.267  0.240  0.221  0.207  0.196  0.187  0.180
      0.175  0.170  0.167  0.164  0.161  0.159  0.157  0.156  0.154  0.153
      0.152  0.151  0.151  0.150  #_natM1
0.726  0.491  0.382  0.320  0.279  0.251  0.230  0.214  0.202  0.192  0.184
      0.178  0.172  0.168  0.164  0.160  0.158  0.155  0.153  0.151  0.150
      0.148  0.147  0.146  0.145  #_natM2
2 # GrowthModel: 1=vonBert with L1&L2; 2=Richards with L1&L2; 3=age_specific_K_incr;
4=age_specific_K_decr;5=age_specific_K_each; 6=NA; 7=NA; 8=growth cessation
1 #_Age(post-settlement)_for_L1;linear growth below this
20 #_Growth_Age_for_L2 (999 to use as Linf)
-999 #_exponential decay for growth above maxage (value should approx initial Z; -999
replicates 3.24; -998 to not allow growth above maxage)
0 #_placeholder for future growth feature
#
0 #_SD_add_to_LAA (set to 0.1 for SS2 V1.x compatibility)
0 #_CV_Growth_Pattern: 0 CV=f(LAA); 1 CV=F(A); 2 SD=F(LAA); 3 SD=F(A); 4
logSD=F(A)
1 #_maturity_option: 1=length logistic; 2=age logistic; 3=read age-maturity matrix by
growth_pattern; 4=read age-fecundity; 5=disabled; 6=read length-maturity
4 #_First_Mature_Age
2 #_fecundity option:(1)eggs=Wt*(a+b*Wt);(2)eggs=a*L^b;(3)eggs=a*Wt^b; (4)eggs=a+b*L;
(5)eggs=a+b*W
0 #_hermaphroditism option: 0=none; 1=female-to-male age-specific fxn; -1=male-to-female
age-specific fxn
1 #_parameter_offset_approach (1=none, 2= M, G, CV_G as offset from female-GP1, 3=like
SS2 V1.x)
#
#_growth_parms
#_LO  HI  INIT  PRIOR  PR_SD  PR_typePHASE  env_var&link  dev_link
      dev_minyr  dev_maxyr  dev_PH Block  Block_Fxn
1e+01 120.000000 6.430e+01 6.50000e+01 10.0 0 -4 0 0
      0 0 0.5 0 0 #_L_at_Amin_Fem_GP_1
4e+01 410.000000 2.452e+02 4.00000e+02 10.0 0 -2 0 0
      0 0 0.5 0 0 #_L_at_Amax_Fem_GP_1
1e-01 0.250000 1.460e-01 1.50000e-01 0.8 0 -4 0 0
      0 0 0.5 0 0 #_VonBert_K_Fem_GP_1
-1e+01 10.000000 1.000e+00 1.00000e+00 0.8 0 -4 0 0
      0 0 0.5 0 0 #_Richards_Fem_GP_1
1e-02 1.000000 2.500e-01 8.34877e-02 0.8 0 -3 0 0
      0 0 0.5 0 0 #_CV_young_Fem_GP_1
-3e+00 3.000000 1.000e-01 0.00000e+00 0.8 0 -3 0 0

```



3.0	20	9.66115	9.000	10.00	0	1	0	0	0	0	0
	0	0	#_SR_LN(R0)								
0.2	1	0.61300	0.613	0.05	0	-4	0	0	0	0	0
	0	0	#_SR_BH_steep								
0.0	2	0.40000	0.600	0.80	0	-3	0	0	0	0	0
	0	0	#_SR_sigmaR								
-5.0	5	0.00000	0.000	1.00	0	-1	0	0	0	0	0
	1	1	#_SR_regime								
0.0	0	0.00000	0.000	99.00	0	-1	0	0	0	0	0
	0	0	#_SR_autocorr								

# timevary SR parameters

#\_LO HI INIT PRIOR PR\_SD PR\_type PHASE

-5 5 0.00492594 0 2.5 0 4

#\_SR\_regime\_BLK1add\_1970

2 #do\_recdev: 0=none; 1=devvector (R=F(SSB)+dev); 2=deviations (R=F(SSB)+dev);

3=deviations (R=R0\*dev; dev2=R-f(SSB)); 4=like 3 with sum(dev2) adding penalty

1971 # first year of main recr\_devs; early devs can precede this era

2020 # last year of main recr\_devs; forecast devs start in following year

1 #\_recdev phase

1 # (0/1) to read 13 advanced options

-10 #\_recdev\_early\_start (0=none; neg value makes relative to recdev\_start)

2 #\_recdev\_early\_phase

-1 #\_forecast\_recruitment phase (incl. late recr) (0 value resets to maxphase+1)

1 #\_lambda for Fcast\_recr\_like occurring before endyr+1

1969.3 #\_last\_yr\_nobias\_adj\_in\_MPD; begin of ramp

2014 #\_first\_yr\_fullbias\_adj\_in\_MPD; begin of plateau

2019.5 #\_last\_yr\_fullbias\_adj\_in\_MPD

2020 #\_end\_yr\_for\_ramp\_in\_MPD (can be in forecast to shape ramp, but SS sets bias\_adj to 0.0 for fcast yrs)

0.5 #\_max\_bias\_adj\_in\_MPD (-1 to override ramp and set biasadj=1.0 for all estimated recdevs)

0 #\_period of cycles in recruitment (N parms read below)

-10 #min rec\_dev

10 #max rec\_dev

0 #\_read\_recdevs

#\_end of advanced SR options

#

#\_placeholder for full parameter lines for recruitment cycles

# read specified recr devs

#\_Yr Input\_value

#

#Fishing Mortality info

0.2 # F ballpark

2013 # F ballpark year (neg value to disable)

3 # F\_Method: 1=Pope; 2=instan. F; 3=hybrid (hybrid is recommended)

5 # max F or harvest rate, depends on F\_Method

4 # N iterations for tuning F in hybrid method (recommend 3 to 7)

```

#
#_initial_F_parms
#_LO  HI      INIT  PRIOR PR_SD PR_type PHASE
0.001 5       0.249539  0.01  99    0      1
      #_InitF_seas_1flt_4F4_JPN_KK_SH
#
#_Q_setup for fleets with cpue or survey data
#_fleet link   link_info      extra_se biasadj float # fleetname
  21  1       0      0      0      1    #_S1_HW_DP
  23  1       0      0      0      1    #_S3_TAIW_LG
  25  1       0      0      0      1    #_S5_JPN_EARLY
  26  1       0      0      0      1    #_S6_JPN_LATE
  27  1       0      0      0      1    #_S7_JPN_RTV
  29  1       0      0      0      1    #_S9_SPC_OBS_TROPIC
  30  1       0      0      0      1    #_S10_MEX
  31  1       0      0      0      1    #_S11_DFA_LATE
-9999 0       0      0      0      0    #_terminator
#_Q_parms(if_any);Qunits_are_ln(q)
#_LO  HI      INIT  PRIOR PR_SD PR_type PHASE env-var use_dev dev_mnyr
      dev_mxyr      dev_PH Block  Blk_Fxn #  parm_name
-25  25      -8.15168  0      1      0      -1    0      0      0
      #_LnQ_base_S1_HW_DP(21)
-25  25      -7.51272  0      1      0      -1    0      0      0
      #_LnQ_base_S3_TAIW_LG(23)
-25  25      -8.05065  0      1      0      -1    0      0      0
      #_LnQ_base_S5_JPN_EARLY(25)
-25  25      -8.15599  0      1      0      -1    0      0      0
      #_LnQ_base_S6_JPN_LATE(26)
-25  25      -7.60901  0      1      0      -1    0      0      0
      #_LnQ_base_S7_JPN_RTV(27)
-25  25      -8.29024  0      1      0      -1    0      0      0
      #_LnQ_base_S9_SPC_OBS_TROPIC(29)
-25  25      -8.21581  0      1      0      -1    0      0      0
      #_LnQ_base_S10_MEX(30)
-25  25      -7.58984  0      1      0      -1    0      0      0
      #_LnQ_base_S11_DFA_LATE(31)
#_no timevary Q parameters
#
#_size_selex_patterns
#_Pattern      Discard Male  Special
24      0      4      0    #_1 F1_MEX
  5      0      0      1    #_2 F2_CAN
24      0      4      0    #_3 F3_CHINA
24      0      4      0    #_4 F4_JPN_KK_SH
24      0      4      0    #_5 F5_JPN_KK_DP
  5      0      0      4    #_6 F6_JPN_ENY_SHL

```

24	0	4	0	#_7 F7_JPN_ENY_DP
24	0	4	0	#_8 F8_JPN_LG_MESH_EARLY
24	0	4	0	#_9 F9_JPN_LG_MESH_LATE
5	0	0	9	#_10 F10_JPN_CST_Oth
24	0	0	0	#_11 F11_JPN_SM_MESH
5	0	0	1	#_12 F12_IATTC
5	0	0	3	#_13 F13_KOREA
24	0	4	0	#_14 F14_NON_ISC
24	0	4	0	#_15 F15_USA_GIILL
5	0	0	15	#_16 F16_USA_SPORT
24	0	4	0	#_17 F17_USA_Lonline_DP
27	0	2	5	#_18 F18_USA_Lonline_SH
24	0	4	0	#_19 F19_TAIW_LG
24	0	4	0	#_20 F20_TAIW_SM
5	0	0	17	#_21 S1_HW_DP
5	0	0	18	#_22 S2_HW_SH
5	0	0	19	#_23 S3_TAIW_LG
5	0	0	20	#_24 S4_TAIW_SM
5	0	0	4	#_25 S5_JPN_EARLY
5	0	0	4	#_26 S6_JPN_LATE
5	0	0	7	#_27 S7_JPN_RTV
5	0	0	14	#_28 S8_SPC_OBS
5	0	0	14	#_29 S9_SPC_OBS_TROPIC
5	0	0	1	#_30 S10_MEX
5	0	0	7	#_31 S11_DFA_LATE

#

#\_age\_selex\_patterns

#_Pattern	Discard	Male	Special
0	0	0	#_1 F1_MEX
0	0	0	#_2 F2_CAN
0	0	0	#_3 F3_CHINA
0	0	0	#_4 F4_JPN_KK_SH
0	0	0	#_5 F5_JPN_KK_DP
0	0	0	#_6 F6_JPN_ENY_SHL
0	0	0	#_7 F7_JPN_ENY_DP
0	0	0	#_8 F8_JPN_LG_MESH_EARLY
0	0	0	#_9 F9_JPN_LG_MESH_LATE
0	0	0	#_10 F10_JPN_CST_Oth
0	0	0	#_11 F11_JPN_SM_MESH
0	0	0	#_12 F12_IATTC
0	0	0	#_13 F13_KOREA
0	0	0	#_14 F14_NON_ISC
0	0	0	#_15 F15_USA_GIILL
0	0	0	#_16 F16_USA_SPORT
0	0	0	#_17 F17_USA_Lonline_DP
0	0	0	#_18 F18_USA_Lonline_SH

```

0      0      0      0      #_19 F19_TAIW_LG
0      0      0      0      #_20 F20_TAIW_SM
0      0      0      0      #_21 S1_HW_DP
0      0      0      0      #_22 S2_HW_SH
0      0      0      0      #_23 S3_TAIW_LG
0      0      0      0      #_24 S4_TAIW_SM
0      0      0      0      #_25 S5_JPN_EARLY
0      0      0      0      #_26 S6_JPN_LATE
0      0      0      0      #_27 S7_JPN_RTV
0      0      0      0      #_28 S8_SPC_OBS
0      0      0      0      #_29 S9_SPC_OBS_TROPIC
0      0      0      0      #_30 S10_MEX
0      0      0      0      #_31 S11_DFA_LATE

```

#

#\_SizeSelex

#_LO	HI	INIT	PRIOR	PR_SD	PR_type	PHASE	env-var	use_dev	dev_mnyr
dev_mxyr	dev_mxyr	dev_PH	Block	Blk_Fxn	#	parm_name			
35.000		250.000		1.57527e+02	50	0.000	0	2	0
	0	0	0.5	0	0	#_SizeSel_P_1_F1_MEX(1)			
-15.000		15.000		-6.00000e+00	0	0.000	0	-4	0
	0	0	0.5	0	0	#_SizeSel_P_2_F1_MEX(1)			
-15.000		15.000		7.36579e+00	0	0.000	0	4	0
	0	0	0.5	0	0	#_SizeSel_P_3_F1_MEX(1)			
-15.000		15.000		6.80182e+00	0	0.000	0	4	0
	0	0	0.5	0	0	#_SizeSel_P_4_F1_MEX(1)			
-999.000		-999.000		-9.99000e+02	0	0.000	0	-2	0
	0	0	0.5	0	0	#_SizeSel_P_5_F1_MEX(1)			
-999.000		-999.000		-9.99000e+02	0	5.000	0	-2	0
	0	0	0.5	0	0	#_SizeSel_P_6_F1_MEX(1)			
-20.000		200.000		-6.68529e+00	125	50.000	0	4	0
	0	0	0.0	0	0	#_SizeSel_PFemOff_1_F1_MEX(1)			
-15.000		15.000		1.23966e-01	4	50.000	0	4	0
	0	0	0.0	0	0	#_SizeSel_PFemOff_2_F1_MEX(1)			
-15.000		15.000		2.20324e-02	4	50.000	0	4	0
	0	0	0.0	0	0	#_SizeSel_PFemOff_3_F1_MEX(1)			
-15.000		15.000		0.00000e+00	4	50.000	0	-4	0
	0	0	0.0	0	0	#_SizeSel_PFemOff_4_F1_MEX(1)			
0.000		5.000		3.36280e-01	4	50.000	0	5	0
	0	0	0.0	0	0	#_SizeSel_PFemOff_5_F1_MEX(1)			
-1.000		200.000		1.00000e+00	50	99.000	0	-99	0
	0	0	0.5	0	0	#_SizeSel_P_1_F2_CAN(2)			
-1.000		239.000		6.00000e+01	50	99.000	0	-99	0
	0	0	0.5	0	0	#_SizeSel_P_2_F2_CAN(2)			
35.000		250.000		1.71126e+02	50	0.000	0	2	0
	0	0	0.5	0	0	#_SizeSel_P_1_F3_CHINA(3)			
-15.000		15.000		-6.00000e+00	0	0.000	0	-4	0

0	0	0.5	0	0	#_SizeSel_P_2_F3_CHINA(3)				
-15.000	15.000		7.28940e+00	0	0.000	0	4	0	0
0	0	0.5	0	0	#_SizeSel_P_3_F3_CHINA(3)				
-15.000	15.000		7.81161e+00	0	0.000	0	4	0	0
0	0	0.5	0	0	#_SizeSel_P_4_F3_CHINA(3)				
-999.000	-999.000		-9.99000e+02	0	0.000	0	-2	0	0
0	0	0.5	0	0	#_SizeSel_P_5_F3_CHINA(3)				
-999.000	-999.000		-9.99000e+02	0	5.000	0	-2	0	0
0	0	0.5	0	0	#_SizeSel_P_6_F3_CHINA(3)				
-20.000	200.000		-9.03685e+00	125	50.000	0	4	0	0
0	0	0.0	0	0	#_SizeSel_PFemOff_1_F3_CHINA(3)				
-15.000	15.000		1.94023e-02	4	50.000	0	4	0	0
0	0	0.0	0	0	#_SizeSel_PFemOff_2_F3_CHINA(3)				
-15.000	15.000		-8.67034e-01	4	50.000	0	4	0	0
0	0	0.0	0	0	#_SizeSel_PFemOff_3_F3_CHINA(3)				
-15.000	15.000		0.00000e+00	4	50.000	0	-4	0	0
0	0	0.0	0	0	#_SizeSel_PFemOff_4_F3_CHINA(3)				
0.000	5.000		5.81209e-01	4	50.000	0	5	0	0
0	0	0.0	0	0	#_SizeSel_PFemOff_5_F3_CHINA(3)				
35.000	250.000		1.51059e+02	50	0.000	0	2	0	0
0	0	0.5	0	0	#_SizeSel_P_1_F4_JPN_KK_SH(4)				
-15.000	15.000		-6.00000e+00	0	0.000	0	-3	0	0
0	0	0.5	0	0	#_SizeSel_P_2_F4_JPN_KK_SH(4)				
-15.000	15.000		6.86811e+00	0	0.000	0	3	0	0
0	0	0.5	0	0	#_SizeSel_P_3_F4_JPN_KK_SH(4)				
-15.000	15.000		7.84481e+00	0	0.000	0	3	0	0
0	0	0.5	0	0	#_SizeSel_P_4_F4_JPN_KK_SH(4)				
-999.000	-999.000		-9.99000e+02	0	0.000	0	-3	0	0
0	0	0.5	0	0	#_SizeSel_P_5_F4_JPN_KK_SH(4)				
-999.000	-999.000		-9.99000e+02	0	5.000	0	-3	0	0
0	0	0.5	0	0	#_SizeSel_P_6_F4_JPN_KK_SH(4)				
-20.000	200.000		-1.63523e+00	0	50.000	0	4	0	0
0	0	0.0	0	0	#_SizeSel_PFemOff_1_F4_JPN_KK_SH(4)				
-15.000	15.000		2.60705e-01	4	50.000	0	4	0	0
0	0	0.0	0	0	#_SizeSel_PFemOff_2_F4_JPN_KK_SH(4)				
-15.000	15.000		-1.85740e-01	4	50.000	0	4	0	0
0	0	0.0	0	0	#_SizeSel_PFemOff_3_F4_JPN_KK_SH(4)				
-15.000	15.000		0.00000e+00	4	50.000	0	-4	0	0
0	0	0.0	0	0	#_SizeSel_PFemOff_4_F4_JPN_KK_SH(4)				
0.000	5.000		2.73030e-01	4	50.000	0	5	0	0
0	0	0.0	0	0	#_SizeSel_PFemOff_5_F4_JPN_KK_SH(4)				
35.000	250.000		1.72299e+02	50	0.000	0	2	0	0
0	0	0.5	0	0	#_SizeSel_P_1_F5_JPN_KK_DP(5)				
-15.000	15.000		-6.00000e+00	0	0.000	0	-3	0	0
0	0	0.5	0	0	#_SizeSel_P_2_F5_JPN_KK_DP(5)				
-15.000	15.000		6.31504e+00	0	0.000	0	4	0	0

0	0	0.5	0	0	#_SizeSel_P_3_F5_JPN_KK_DP(5)				
-15.000	15.000		6.18229e+00	0	0.000	0	4	0	0
0	0	0.5	0	0	#_SizeSel_P_4_F5_JPN_KK_DP(5)				
-999.000	-999.000		-9.99000e+02	0	0.000	0	-2	0	0
0	0	0.5	0	0	#_SizeSel_P_5_F5_JPN_KK_DP(5)				
-999.000	-999.000		-9.99000e+02	0	5.000	0	-2	0	0
0	0	0.5	0	0	#_SizeSel_P_6_F5_JPN_KK_DP(5)				
-80.000	200.000		-1.53097e+01	0	50.000	0	4	0	0
0	0	0.0	0	0	#_SizeSel_PFemOff_1_F5_JPN_KK_DP(5)				
-15.000	15.000		-6.92640e-01	4	50.000	0	4	0	0
0	0	0.0	0	0	#_SizeSel_PFemOff_2_F5_JPN_KK_DP(5)				
-15.000	15.000		2.26300e-02	4	50.000	0	4	0	0
0	0	0.0	0	0	#_SizeSel_PFemOff_3_F5_JPN_KK_DP(5)				
-15.000	15.000		0.00000e+00	4	50.000	0	-4	0	0
0	0	0.0	0	0	#_SizeSel_PFemOff_4_F5_JPN_KK_DP(5)				
0.000	5.000		1.47135e-01	4	50.000	0	5	0	0
0	0	0.0	0	0	#_SizeSel_PFemOff_5_F5_JPN_KK_DP(5)				
-1.000	200.000		1.00000e+00	50	99.000	0	-99	0	0
0	0	0.5	0	0	#_SizeSel_P_1_F6_JPN_ENY_SHL(6)				
-1.000	239.000		6.00000e+01	50	99.000	0	-99	0	0
0	0	0.5	0	0	#_SizeSel_P_2_F6_JPN_ENY_SHL(6)				
35.000	250.000		1.73991e+02	50	0.000	0	2	0	0
0	0	0.5	0	0	#_SizeSel_P_1_F7_JPN_ENY_DP(7)				
-15.000	15.000		-6.00000e+00	0	0.000	0	-4	0	0
0	0	0.5	0	0	#_SizeSel_P_2_F7_JPN_ENY_DP(7)				
-15.000	15.000		6.40144e+00	0	0.000	0	4	0	0
0	0	0.5	0	0	#_SizeSel_P_3_F7_JPN_ENY_DP(7)				
-15.000	15.000		6.73893e+00	0	0.000	0	4	0	0
0	0	0.5	0	0	#_SizeSel_P_4_F7_JPN_ENY_DP(7)				
-999.000	-999.000		-9.99000e+02	0	0.000	0	-2	0	0
0	0	0.5	0	0	#_SizeSel_P_5_F7_JPN_ENY_DP(7)				
-999.000	-999.000		-9.99000e+02	0	5.000	0	-2	0	0
0	0	0.5	0	0	#_SizeSel_P_6_F7_JPN_ENY_DP(7)				
-80.000	200.000		-1.54564e+01	125	50.000	0	4	0	0
0	0	0.0	0	0	#_SizeSel_PFemOff_1_F7_JPN_ENY_DP(7)				
-15.000	15.000		-8.54843e-01	4	50.000	0	4	0	0
0	0	0.0	0	0	#_SizeSel_PFemOff_2_F7_JPN_ENY_DP(7)				
-15.000	15.000		-5.83817e-01	4	50.000	0	4	0	0
0	0	0.0	0	0	#_SizeSel_PFemOff_3_F7_JPN_ENY_DP(7)				
-15.000	15.000		0.00000e+00	4	50.000	0	-4	0	0
0	0	0.0	0	0	#_SizeSel_PFemOff_4_F7_JPN_ENY_DP(7)				
0.000	5.000		5.03734e-01	4	50.000	0	5	0	0

0	0	0.0	0	0					
#_SizeSel_PFemOff_5_F7_JPN_ENY_DP(7)									
35.000	250.000		1.10416e+02	120	0.000	0	-2	0	0
0	0	0.5	2	2					
#_SizeSel_P_1_F8_JPN_LG_MESH_EARLY(8)									
-15.000	15.000		-1.99692e+00	0	0.000	0	3	0	0
0	0	0.5	0	0					
#_SizeSel_P_2_F8_JPN_LG_MESH_EARLY(8)									
-15.000	15.000		8.38994e+00	5	0.000	0	4	0	0
0	0	0.5	0	0					
#_SizeSel_P_3_F8_JPN_LG_MESH_EARLY(8)									
-15.000	15.000		6.21242e+00	5	0.000	0	4	0	0
0	0	0.5	0	0					
#_SizeSel_P_4_F8_JPN_LG_MESH_EARLY(8)									
-999.000	-999.000		-9.99000e+02	0	0.000	0	-3	0	0
0	0	0.5	0	0					
#_SizeSel_P_5_F8_JPN_LG_MESH_EARLY(8)									
-999.000	-999.000		-9.99000e+02	0	5.000	0	-3	0	0
0	0	0.5	0	0					
#_SizeSel_P_6_F8_JPN_LG_MESH_EARLY(8)									
-80.000	200.000		-4.83700e+00	125	50.000	0	-4	0	0
0	0	0.0	2	2					
#_SizeSel_PFemOff_1_F8_JPN_LG_MESH_EARLY(8)									
-15.000	15.000		-1.48476e+00	4	50.000	0	4	0	0
0	0	0.0	0	0					
#_SizeSel_PFemOff_2_F8_JPN_LG_MESH_EARLY(8)									
-15.000	15.000		6.34020e-01	4	50.000	0	4	0	0
0	0	0.0	0	0					
#_SizeSel_PFemOff_3_F8_JPN_LG_MESH_EARLY(8)									
-15.000	15.000		0.00000e+00	4	50.000	0	-4	0	0
0	0	0.0	0	0					
#_SizeSel_PFemOff_4_F8_JPN_LG_MESH_EARLY(8)									
0.000	5.000		5.45660e-01	4	50.000	0	5	0	0
0	0	0.0	0	0					
#_SizeSel_PFemOff_5_F8_JPN_LG_MESH_EARLY(8)									
35.000	250.000		1.32092e+02	120	0.000	0	2	0	0
0	0	0.5	0	0					
#_SizeSel_P_1_F9_JPN_LG_MESH_LATE(9)									
-15.000	15.000		-6.00000e+00	0	0.000	0	-3	0	0
0	0	0.5	0	0					
#_SizeSel_P_2_F9_JPN_LG_MESH_LATE(9)									
-15.000	15.000		6.14067e+00	5	0.000	0	4	0	0
0	0	0.5	0	0					
#_SizeSel_P_3_F9_JPN_LG_MESH_LATE(9)									
-15.000	15.000		6.85760e+00	5	0.000	0	4	0	0
0	0	0.5	0	0					

```

#_SizeSel_P_4_F9_JPN_LG_MESH_LATE(9)
-999.000      -999.000      -9.99000e+02    0    0.000 0    -3    0    0
    0    0 0.5    0    0
#_SizeSel_P_5_F9_JPN_LG_MESH_LATE(9)
-999.000      -999.000      -9.99000e+02    0    5.000 0    -3    0    0
    0    0 0.5    0    0
#_SizeSel_P_6_F9_JPN_LG_MESH_LATE(9)
-80.000       200.000      -4.83700e+00   125   50.000 0    -4    0    0
    0    0 0.0    0    0
#_SizeSel_PFemOff_1_F9_JPN_LG_MESH_LATE(9)
-15.000       15.000      -5.49376e-02    4    50.000 0    4    0    0
    0    0 0.0    0    0
#_SizeSel_PFemOff_2_F9_JPN_LG_MESH_LATE(9)
-15.000       15.000      -5.34531e-01    4    50.000 0    4    0    0
    0    0 0.0    0    0
#_SizeSel_PFemOff_3_F9_JPN_LG_MESH_LATE(9)
-15.000       15.000      0.00000e+00    4    50.000 0    -4    0    0
    0    0 0.0    0    0
#_SizeSel_PFemOff_4_F9_JPN_LG_MESH_LATE(9)
0.000         5.000       5.95938e-01    4    50.000 0    5    0    0
    0    0 0.0    0    0
#_SizeSel_PFemOff_5_F9_JPN_LG_MESH_LATE(9)
-1.000       200.000      1.00000e+00   50   99.000 0    -99    0    0
    0    0 0.5    0    0 #_SizeSel_P_1_F10_JPN_CST_Oth(10)
-1.000       239.000      6.00000e+01   50   99.000 0    -99    0    0
    0    0 0.5    0    0 #_SizeSel_P_2_F10_JPN_CST_Oth(10)
25.000       250.000      2.78590e+01   120   0.000 0    2    0    0
    0    0 0.5    0    0 #_SizeSel_P_1_F11_JPN_SM_MESH(11)
-15.000       15.000      -6.00000e+00    0    0.000 0    -3    0    0
    0    0 0.5    0    0 #_SizeSel_P_2_F11_JPN_SM_MESH(11)
-15.000       15.000      -3.93768e+00    5    0.000 0    4    0    0
    0    0 0.5    0    0 #_SizeSel_P_3_F11_JPN_SM_MESH(11)
-15.000       15.000      7.77230e+00    5    0.000 0    4    0    0
    0    0 0.5    0    0 #_SizeSel_P_4_F11_JPN_SM_MESH(11)
-1003.000    -1003.000    -1.00300e+03    0    0.000 0    -3    0    0
    0    0 0.5    0    0 #_SizeSel_P_5_F11_JPN_SM_MESH(11)
-999.000      -999.000      -9.99000e+02    0    5.000 0    -3    0    0
    0    0 0.5    0    0 #_SizeSel_P_6_F11_JPN_SM_MESH(11)
-1.000       200.000      1.00000e+00   50   99.000 0    -99    0    0
    0    0 0.5    0    0 #_SizeSel_P_1_F12_IATTC(12)
-1.000       239.000      6.00000e+01   50   99.000 0    -99    0    0
    0    0 0.5    0    0 #_SizeSel_P_2_F12_IATTC(12)
-1.000       200.000      1.00000e+00   50   99.000 0    -99    0    0
    0    0 0.5    0    0 #_SizeSel_P_1_F13_KOREA(13)
-1.000       239.000      6.00000e+01   50   99.000 0    -99    0    0
    0    0 0.5    0    0 #_SizeSel_P_2_F13_KOREA(13)

```

35.000	250.000	1.67342e+02	50	0.000	0	2	0	0
0	0	0.5	0	0				
-15.000	15.000	-6.00000e+00	#_SizeSel_P_1_F14_NON_ISC(14)	0	0.000	0	-4	0
0	0	0.5	0	0				
-15.000	15.000	7.12531e+00	#_SizeSel_P_2_F14_NON_ISC(14)	0	0.000	0	4	0
0	0	0.5	0	0				
-15.000	15.000	6.36943e+00	#_SizeSel_P_3_F14_NON_ISC(14)	0	0.000	0	4	0
0	0	0.5	0	0				
-999.000	-999.000	-9.99000e+02	#_SizeSel_P_4_F14_NON_ISC(14)	0	0.000	0	-2	0
0	0	0.5	0	0				
-999.000	-999.000	-9.99000e+02	#_SizeSel_P_5_F14_NON_ISC(14)	0	5.000	0	-2	0
0	0	0.5	0	0				
-20.000	200.000	-6.53552e+00	#_SizeSel_P_6_F14_NON_ISC(14)	125	50.000	0	4	0
0	0	0.0	0	0				
-15.000	15.000	-9.10712e-02	#_SizeSel_PFemOff_1_F14_NON_ISC(14)	4	50.000	0	4	0
0	0	0.0	0	0				
-15.000	15.000	-3.35981e-02	#_SizeSel_PFemOff_2_F14_NON_ISC(14)	4	50.000	0	4	0
0	0	0.0	0	0				
-15.000	15.000	0.00000e+00	#_SizeSel_PFemOff_3_F14_NON_ISC(14)	4	50.000	0	-4	0
0	0	0.0	0	0				
0.000	5.000	7.99889e-01	#_SizeSel_PFemOff_4_F14_NON_ISC(14)	4	50.000	0	5	0
0	0	0.0	0	0				
28.000	250.000	1.05621e+02	#_SizeSel_PFemOff_5_F14_NON_ISC(14)	50	0.000	0	3	0
0	0	0.5	0	0				
-15.000	15.000	-6.00000e+00	#_SizeSel_P_1_F15_USA_GIILL(15)	0	0.000	0	-3	0
0	0	0.5	0	0				
-15.000	15.000	6.86387e+00	#_SizeSel_P_2_F15_USA_GIILL(15)	0	0.000	0	3	0
0	0	0.5	0	0				
-15.000	15.000	8.24143e+00	#_SizeSel_P_3_F15_USA_GIILL(15)	0	0.000	0	3	0
0	0	0.5	0	0				
-999.000	-999.000	-9.99000e+02	#_SizeSel_P_4_F15_USA_GIILL(15)	0	0.000	0	-3	0
0	0	0.5	0	0				
-999.000	-999.000	-9.99000e+02	#_SizeSel_P_5_F15_USA_GIILL(15)	0	0.000	0	-3	0
0	0	0.5	0	0				
-20.000	200.000	1.42848e+00	#_SizeSel_P_6_F15_USA_GIILL(15)	0	50.000	0	4	0
0	0	0.0	0	0				
			#_SizeSel_PFemOff_1_F15_USA_GIILL(15)					
-15.000	15.000	3.72869e-01		4	50.000	0	4	0
0	0	0.0	0	0				
			#_SizeSel_PFemOff_2_F15_USA_GIILL(15)					
-15.000	15.000	-1.22617e+00		4	50.000	0	4	0
0	0	0.0	0	0				
			#_SizeSel_PFemOff_3_F15_USA_GIILL(15)					
-15.000	15.000	0.00000e+00		4	50.000	0	-4	0
0	0	0.0	0	0				
			#_SizeSel_PFemOff_4_F15_USA_GIILL(15)					

0.000	5.000	6.56839e-01	4	50.000	0	5	0	0
0	0 0.0	0 0						
#_SizeSel_PFemOff_5_F15_USA_GIILL(15)								
-1.000	200.000	1.00000e+00	50	99.000	0	-99	0	0
0	0 0.5	0 0						
#_SizeSel_P_1_F16_USA_SPORT(16)								
-1.000	239.000	6.00000e+01	50	99.000	0	-99	0	0
0	0 0.5	0 0						
#_SizeSel_P_2_F16_USA_SPORT(16)								
35.000	250.000	1.73288e+02	50	0.000	0	3	0	0
0	0 0.5	0 0						
#_SizeSel_P_1_F17_USA_Lonline_DP(17)								
-15.000	15.000	-6.00000e+00	0	0.000	0	-3	0	0
0	0 0.5	0 0						
#_SizeSel_P_2_F17_USA_Lonline_DP(17)								
-15.000	15.000	6.51678e+00	0	0.000	0	3	0	0
0	0 0.5	0 0						
#_SizeSel_P_3_F17_USA_Lonline_DP(17)								
-15.000	15.000	8.92744e+00	0	0.000	0	3	0	0
0	0 0.5	0 0						
#_SizeSel_P_4_F17_USA_Lonline_DP(17)								
-999.000	-999.000	-9.99000e+02	0	0.000	0	-3	0	0
0	0 0.5	0 0						
#_SizeSel_P_5_F17_USA_Lonline_DP(17)								
-999.000	-999.000	-9.99000e+02	0	0.000	0	-3	0	0
0	0 0.5	0 0						
#_SizeSel_P_6_F17_USA_Lonline_DP(17)								
-80.000	200.000	-1.86922e+01	0	50.000	0	4	0	0
0	0 0.0	0 0						
#_SizeSel_PFemOff_1_F17_USA_Lonline_DP(17)								
-15.000	15.000	-9.13869e-01	4	50.000	0	4	0	0
0	0 0.0	0 0						
#_SizeSel_PFemOff_2_F17_USA_Lonline_DP(17)								
-15.000	15.000	-2.03209e+00	4	50.000	0	4	0	0
0	0 0.0	0 0						
#_SizeSel_PFemOff_3_F17_USA_Lonline_DP(17)								
-15.000	15.000	0.00000e+00	4	50.000	0	-4	0	0
0	0 0.0	0 0						
#_SizeSel_PFemOff_4_F17_USA_Lonline_DP(17)								
0.000	5.000	8.01517e-01	4	50.000	0	5	0	0
0	0 0.0	0 0						
#_SizeSel_PFemOff_5_F17_USA_Lonline_DP(17)								
0.000	2.000	2.00000e+00	0	1.000	0	-99	0	0
0	0 0.0	0 0						
#_SizeSel_Spline_Code_F18_USA_Lonline_SH(18)								
-0.001	1.000	2.35778e-01	0	0.001	1	3	0	0
0	0 0.0	0 0						
#_SizeSel_Spline_GradLo_F18_USA_Lonline_SH(18)								
-1.000	0.001	-7.95877e-02	0	0.001	1	3	0	0
0	0 0.0	0 0						
#_SizeSel_Spline_GradHi_F18_USA_Lonline_SH(18)								
5.000	300.000	5.07096e+01	152	1.000	0	-99	0	0
0	0 0.0	0 0						
#_SizeSel_Spline_Knot_1_F18_USA_Lonline_SH(18)								

5.000	300.000	7.44584e+01	152	1.000	0	-99	0	0
0	0	0.0	0	0				
#_SizeSel_Spline_Knot_2_F18_USA_Lonline_SH(18)								
5.000	300.000	1.09805e+02	152	1.000	0	-99	0	0
0	0	0.0	0	0				
#_SizeSel_Spline_Knot_3_F18_USA_Lonline_SH(18)								
5.000	300.000	1.44765e+02	152	1.000	0	-99	0	0
0	0	0.0	0	0				
#_SizeSel_Spline_Knot_4_F18_USA_Lonline_SH(18)								
5.000	300.000	1.92065e+02	152	1.000	0	-99	0	0
0	0	0.0	0	0				
#_SizeSel_Spline_Knot_5_F18_USA_Lonline_SH(18)								
-9.000	7.000	-1.82180e+00	0	0.001	1	2	0	0
0	0	0.0	0	0				
#_SizeSel_Spine_Val_1_F18_USA_Lonline_SH(18)								
-9.000	7.000	-1.21986e+00	0	0.001	1	2	0	0
0	0	0.0	0	0				
#_SizeSel_Spine_Val_2_F18_USA_Lonline_SH(18)								
-9.000	7.000	-1.00000e+00	0	1.000	0	-99	0	0
0	0	0.0	0	0				
#_SizeSel_Spine_Val_3_F18_USA_Lonline_SH(18)								
-9.000	7.000	-6.03609e-01	0	0.001	1	2	0	0
0	0	0.0	0	0				
#_SizeSel_Spine_Val_4_F18_USA_Lonline_SH(18)								
-9.000	7.000	-1.46308e+00	0	0.001	1	2	0	0
0	0	0.0	0	0				
#_SizeSel_Spine_Val_5_F18_USA_Lonline_SH(18)								
180.000	190.000	1.85000e+02	0	0.000	0	-1	0	0
0	0	0.0	0	0				
#_SizeSel_PFemOff_1_F18_USA_Lonline_SH(18)								
-1.000	1.000	0.00000e+00	0	0.000	0	-1	0	0
0	0	0.0	0	0				
#_SizeSel_PFemOff_2_F18_USA_Lonline_SH(18)								
-9.000	9.000	1.14940e-01	0	0.000	0	3	0	0
0	0	0.0	0	0				
#_SizeSel_PFemOff_3_F18_USA_Lonline_SH(18)								
-9.000	9.000	-5.43291e+00	0	0.000	0	3	0	0
0	0	0.0	0	0				
#_SizeSel_PFemOff_4_F18_USA_Lonline_SH(18)								
35.000	297.000	2.13088e+02	50	0.000	0	2	0	1
2004	2020	0.5	0	0				
#_SizeSel_P_1_F19_TAIW_LG(19)								
-15.000	15.000	-6.00000e+00	0	0.000	0	-3	0	0
0	0	0.5	0	0				
#_SizeSel_P_2_F19_TAIW_LG(19)								
-15.000	15.000	7.55274e+00	0	0.000	0	3	0	0
0	0	0.5	0	0				
#_SizeSel_P_3_F19_TAIW_LG(19)								
-15.000	15.000	6.83243e+00	0	0.000	0	3	0	0

0	0	0.5	0	0	#_SizeSel_P_4_F19_TAIW_LG(19)			
-999.000	-999.000		-9.99000e+02	0	0.000	0	-3	0
0	0	0.5	0	0	#_SizeSel_P_5_F19_TAIW_LG(19)			
-999.000	-999.000		-9.99000e+02	0	5.000	0	-3	0
0	0	0.5	0	0	#_SizeSel_P_6_F19_TAIW_LG(19)			
-199.000	200.000		-3.27503e+01	9	50.000	0	4	0
2004	2020	0.0	0	0	#_SizeSel_PFemOff_1_F19_TAIW_LG(19)			1
-15.000	15.000		-7.13663e-01	4	50.000	0	4	0
0	0	0.0	0	0	#_SizeSel_PFemOff_2_F19_TAIW_LG(19)			
-15.000	15.000		5.44714e-01	4	50.000	0	4	0
0	0	0.0	0	0	#_SizeSel_PFemOff_3_F19_TAIW_LG(19)			
-15.000	15.000		0.00000e+00	4	50.000	0	-4	0
0	0	0.0	0	0	#_SizeSel_PFemOff_4_F19_TAIW_LG(19)			
0.000	5.000		3.21303e-01	4	50.000	0	5	0
0	0	0.0	0	0	#_SizeSel_PFemOff_5_F19_TAIW_LG(19)			
35.000	250.000		1.75816e+02	50	0.000	0	2	0
0	0	0.5	0	0	#_SizeSel_P_1_F20_TAIW_SM(20)			
-15.000	15.000		-6.00000e+00	0	0.000	0	-3	0
0	0	0.5	0	0	#_SizeSel_P_2_F20_TAIW_SM(20)			
-15.000	15.000		6.81310e+00	0	0.000	0	3	0
0	0	0.5	0	0	#_SizeSel_P_3_F20_TAIW_SM(20)			
-15.000	15.000		6.58646e+00	0	0.000	0	3	0
0	0	0.5	0	0	#_SizeSel_P_4_F20_TAIW_SM(20)			
-999.000	-999.000		-9.99000e+02	0	0.000	0	-3	0
0	0	0.5	0	0	#_SizeSel_P_5_F20_TAIW_SM(20)			
-999.000	-999.000		-9.99000e+02	0	5.000	0	-3	0
0	0	0.5	0	0	#_SizeSel_P_6_F20_TAIW_SM(20)			
-80.000	200.000		-9.41270e+00	9	50.000	0	4	0
0	0	0.0	0	0	#_SizeSel_PFemOff_1_F20_TAIW_SM(20)			
-15.000	15.000		-3.38038e-01	4	50.000	0	4	0
0	0	0.0	0	0	#_SizeSel_PFemOff_2_F20_TAIW_SM(20)			
-15.000	15.000		1.02736e-01	4	50.000	0	4	0
0	0	0.0	0	0	#_SizeSel_PFemOff_3_F20_TAIW_SM(20)			
-15.000	15.000		0.00000e+00	4	50.000	0	-4	0
0	0	0.0	0	0	#_SizeSel_PFemOff_4_F20_TAIW_SM(20)			
0.000	5.000		3.36895e-01	4	50.000	0	5	0
0	0	0.0	0	0	#_SizeSel_PFemOff_5_F20_TAIW_SM(20)			
-1.000	200.000		1.00000e+00	50	99.000	0	-99	0
0	0	0.5	0	0	#_SizeSel_P_1_S1_HW_DP(21)			
-1.000	239.000		6.00000e+01	50	99.000	0	-99	0
0	0	0.5	0	0	#_SizeSel_P_2_S1_HW_DP(21)			
-1.000	200.000		1.00000e+00	50	99.000	0	-99	0
0	0	0.5	0	0	#_SizeSel_P_1_S2_HW_SH(22)			
-1.000	239.000		6.00000e+01	50	99.000	0	-99	0
0	0	0.5	0	0	#_SizeSel_P_2_S2_HW_SH(22)			
-1.000	200.000		1.00000e+00	50	99.000	0	-99	0

```

0      0  0.5    0      0      #_SizeSel_P_1_S3_TAIW_LG(23)
-1.000 239.000 6.00000e+01 50 99.000 0 -99 0 0
0      0  0.5    0      0      #_SizeSel_P_2_S3_TAIW_LG(23)
-1.000 200.000 1.00000e+00 50 99.000 0 -99 0 0
0      0  0.5    0      0      #_SizeSel_P_1_S4_TAIW_SM(24)
-1.000 239.000 6.00000e+01 50 99.000 0 -99 0 0
0      0  0.5    0      0      #_SizeSel_P_2_S4_TAIW_SM(24)
-1.000 200.000 1.00000e+00 50 99.000 0 -99 0 0
0      0  0.5    0      0      #_SizeSel_P_1_S5_JPN_EARLY(25)
-1.000 239.000 6.00000e+01 50 99.000 0 -99 0 0
0      0  0.5    0      0      #_SizeSel_P_2_S5_JPN_EARLY(25)
-1.000 200.000 1.00000e+00 50 99.000 0 -99 0 0
0      0  0.5    0      0      #_SizeSel_P_1_S6_JPN_LATE(26)
-1.000 239.000 6.00000e+01 50 99.000 0 -99 0 0
0      0  0.5    0      0      #_SizeSel_P_2_S6_JPN_LATE(26)
-1.000 200.000 1.00000e+00 50 99.000 0 -99 0 0
0      0  0.5    0      0      #_SizeSel_P_1_S7_JPN_RTV(27)
-1.000 239.000 6.00000e+01 50 99.000 0 -99 0 0
0      0  0.5    0      0      #_SizeSel_P_2_S7_JPN_RTV(27)
-1.000 200.000 1.00000e+00 50 99.000 0 -99 0 0
0      0  0.5    0      0      #_SizeSel_P_1_S8_SPC_OBS(28)
-1.000 239.000 6.00000e+01 50 99.000 0 -99 0 0
0      0  0.5    0      0      #_SizeSel_P_2_S8_SPC_OBS(28)
-1.000 200.000 1.00000e+00 50 99.000 0 -99 0 0
0      0  0.5    0      0
#_SizeSel_P_1_S9_SPC_OBS_TROPIC(29)
-1.000 239.000 6.00000e+01 50 99.000 0 -99 0 0
0      0  0.5    0      0
#_SizeSel_P_2_S9_SPC_OBS_TROPIC(29)
-1.000 200.000 1.00000e+00 50 99.000 0 -99 0 0
0      0  0.5    0      0      #_SizeSel_P_1_S10_MEX(30)
-1.000 239.000 6.00000e+01 50 99.000 0 -99 0 0
0      0  0.5    0      0      #_SizeSel_P_2_S10_MEX(30)
-1.000 200.000 1.00000e+00 50 99.000 0 -99 0 0
0      0  0.5    0      0      #_SizeSel_P_1_S11_DFA_LATE(31)
-1.000 239.000 6.00000e+01 50 99.000 0 -99 0 0
0      0  0.5    0      0      #_SizeSel_P_2_S11_DFA_LATE(31)

#_AgeSelex
#_No age_selex_parm
# timevary selex parameters
#_LO HI INIT PRIOR PR_SD PR_type PHASE
35.0000 250.00 161.0590 120.0 0.0 0 4
#_SizeSel_P_1_F8_JPN_LG_MESH_EARLY(8)_BLK2repl_1973
35.0000 250.00 185.1140 120.0 0.0 0 4
#_SizeSel_P_1_F8_JPN_LG_MESH_EARLY(8)_BLK2repl_1982
-80.0000 200.00 -59.0849 125.0 50.0 0 4

```

```

#_SizeSel_PFemOff_1_F8_JPN_LG_MESH_EARLY(8)_BLK2repl_1973
-80.0000    200.00    11.6317    125.0    50.0    0    4
#_SizeSel_PFemOff_1_F8_JPN_LG_MESH_EARLY(8)_BLK2repl_1982
0.0001     2.00     0.6000     0.6     0.5     0    -5
#_SizeSel_P_1_F19_TAIW_LG(19)_dev_se
-0.9900    0.99     0.0000     0.0     0.5     0    -6
#_SizeSel_P_1_F19_TAIW_LG(19)_dev_autocorr
0.0001     2.00     0.6000     0.6     0.5     0    -5
#_SizeSel_PFemOff_1_F19_TAIW_LG(19)_dev_se
-0.9900    0.99     0.0000     0.0     0.5     0    -6
#_SizeSel_PFemOff_1_F19_TAIW_LG(19)_dev_autocorr
# info on dev vectors created for selex parms are reported with other devs after tag parameter
section
#
0# use 2D_AR1 selectivity(0/1):  experimental feature
#_no 2D_AR1 selex offset used
# Tag loss and Tag reporting parameters go next
0# TG_custom:  0=no read; 1=read if tags exist
#_Cond -6 6 1 1 2 0.01 -4 0 0 0 0 0 0 #_placeholder if no parameters
#
# Input variance adjustments factors:
#_Factor      Fleet      Value
1 21          0.000000    #_Variance_adjustment_list1
1 23          0.136000    #_Variance_adjustment_list2
1 25          0.188000    #_Variance_adjustment_list3
1 26          0.000000    #_Variance_adjustment_list4
1 27          0.000000    #_Variance_adjustment_list5
1 29          0.056000    #_Variance_adjustment_list6
1 30          0.134000    #_Variance_adjustment_list7
1 31          0.161100    #_Variance_adjustment_list8
4 1           0.002161    #_Variance_adjustment_list9
4 3           0.002161    #_Variance_adjustment_list10
4 4           0.000652    #_Variance_adjustment_list11
4 5           0.002161    #_Variance_adjustment_list12
4 7           0.002161    #_Variance_adjustment_list13
4 8           0.002161    #_Variance_adjustment_list14
4 9           0.002161    #_Variance_adjustment_list15
4 14          0.002161    #_Variance_adjustment_list16
4 15          0.002161    #_Variance_adjustment_list17
4 17          0.002161    #_Variance_adjustment_list18
4 18          0.002161    #_Variance_adjustment_list19
4 19          0.002161    #_Variance_adjustment_list20
4 20          0.002161    #_Variance_adjustment_list21
7 11          0.002161    #_Variance_adjustment_list22
-9999    0          0.000000    #_terminator
#

```

```

1 #_maxlambdaphase
1 #_sd_offset; must be 1 if any growthCV, sigmaR, or survey extraSD is an estimated parameter
# read 67 changes to default Lambdas (default value is 1.0)
#_like_comp  fleet  phase  value  sizefreq_method
1 1 1 0 1 #_Surv_F1_MEX_Phz1
1 2 1 0 1 #_Surv_F2_CAN_Phz1
1 3 1 0 1 #_Surv_F3_CHINA_Phz1
1 4 1 0 1 #_Surv_F4_JPN_KK_SH_Phz1
1 5 1 0 1 #_Surv_F5_JPN_KK_DP_Phz1
1 6 1 0 1 #_Surv_F6_JPN_ENY_SHL_Phz1
1 7 1 0 1 #_Surv_F7_JPN_ENY_DP_Phz1
1 8 1 0 1 #_Surv_F8_JPN_LG_MESH_EARLY_Phz1
1 9 1 0 1 #_Surv_F9_JPN_LG_MESH_LATE_Phz1
1 10 1 0 1 #_Surv_F10_JPN_CST_Oth_Phz1
1 11 1 0 1 #_Surv_F11_JPN_SM_MESH_Phz1
1 12 1 0 1 #_Surv_F12_IATTC_Phz1
1 13 1 0 1 #_Surv_F13_KOREA_Phz1
1 14 1 0 1 #_Surv_F14_NON_ISC_Phz1
1 15 1 0 1 #_Surv_F15_USA_GIILL_Phz1
1 16 1 0 1 #_Surv_F16_USA_SPORT_Phz1
1 17 1 0 1 #_Surv_F17_USA_Lonline_DP_Phz1
1 18 1 0 1 #_Surv_F18_USA_Lonline_SH_Phz1
1 19 1 0 1 #_Surv_F19_TAIW_LG_Phz1
1 20 1 0 1 #_Surv_F20_TAIW_SM_Phz1
1 21 1 0 1 #_Surv_S1_HW_DP_Phz1
1 22 1 0 1 #_Surv_S2_HW_SH_Phz1
1 23 1 0 1 #_Surv_S3_TAIW_LG_Phz1
1 24 1 0 1 #_Surv_S4_TAIW_SM_Phz1
1 25 1 1 1 #_Surv_S5_JPN_EARLY_Phz1
1 26 1 1 1 #_Surv_S6_JPN_LATE_Phz1
1 27 1 0 1 #_Surv_S7_JPN_RTV_Phz1
1 28 1 0 1 #_Surv_S8_SPC_OBS_Phz1
1 29 1 0 1 #_Surv_S9_SPC_OBS_TROPIC_Phz1
1 30 1 0 1 #_Surv_S10_MEX_Phz1
1 31 1 0 1 #_Surv_S11_DFA_LATE_Phz1
4 1 1 1 0 #_length_F1_MEX_sizefreq_method_0_Phz1
4 2 1 0 0 #_length_F2_CAN_sizefreq_method_0_Phz1
4 3 1 1 0 #_length_F3_CHINA_sizefreq_method_0_Phz1
4 4 1 1 0
#_length_F4_JPN_KK_SH_sizefreq_method_0_Phz1
4 5 1 1 0
#_length_F5_JPN_KK_DP_sizefreq_method_0_Phz1
4 6 1 0 0
#_length_F6_JPN_ENY_SHL_sizefreq_method_0_Phz1
4 7 1 1 0
#_length_F7_JPN_ENY_DP_sizefreq_method_0_Phz1

```

```

4  8  1  1  0
#_length_F8_JPN_LG_MESH_EARLY_sizefreq_method_0_Phz1
4  9  1  1  0
#_length_F9_JPN_LG_MESH_LATE_sizefreq_method_0_Phz1
4 10  1  0  0
#_length_F10_JPN_CST_Oth_sizefreq_method_0_Phz1
4 11  1  0  0
#_length_F11_JPN_SM_MESH_sizefreq_method_0_Phz1
4 12  1  0  0 #_length_F12_IATTC_sizefreq_method_0_Phz1
4 13  1  0  0 #_length_F13_KOREA_sizefreq_method_0_Phz1
4 14  1  1  0 #_length_F14_NON_ISC_sizefreq_method_0_Phz1
4 15  1  1  0
#_length_F15_USA_GIILL_sizefreq_method_0_Phz1
4 16  1  0  0
#_length_F16_USA_SPORT_sizefreq_method_0_Phz1
4 17  1  1  0
#_length_F17_USA_Lonline_DP_sizefreq_method_0_Phz1
4 18  1  1  0
#_length_F18_USA_Lonline_SH_sizefreq_method_0_Phz1
4 19  1  1  0 #_length_F19_TAIW_LG_sizefreq_method_0_Phz1
4 20  1  1  0 #_length_F20_TAIW_SM_sizefreq_method_0_Phz1
4 21  1  0  0 #_length_S1_HW_DP_sizefreq_method_0_Phz1
4 22  1  0  0 #_length_S2_HW_SH_sizefreq_method_0_Phz1
4 23  1  0  0 #_length_S3_TAIW_LG_sizefreq_method_0_Phz1
4 24  1  0  0 #_length_S4_TAIW_SM_sizefreq_method_0_Phz1
4 25  1  0  0
#_length_S5_JPN_EARLY_sizefreq_method_0_Phz1
4 26  1  0  0 #_length_S6_JPN_LATE_sizefreq_method_0_Phz1
4 27  1  0  0 #_length_S7_JPN_RTV_sizefreq_method_0_Phz1
4 28  1  0  0 #_length_S8_SPC_OBS_sizefreq_method_0_Phz1
4 29  1  0  0
#_length_S9_SPC_OBS_TROPIC_sizefreq_method_0_Phz1
4 30  1  0  0 #_length_S10_MEX_sizefreq_method_0_Phz1
4 31  1  0  0
#_length_S11_DFA_LATE_sizefreq_method_0_Phz1
6 11  1  1  1
#_SizeFreq_F11_JPN_SM_MESH_sizefreq_method_1_Phz1
9  1  1  1  0 #_init_equ_catch_F1_MEX_Phz1
10 1  1  1  0 #_recrdev_Phz1
11 1  1  0  0 #_parm_prior_F1_MEX_Phz1
12 1  1  1  0 #_parm_dev_Phz1
-9999 0  0  0  0 #_terminator
#
0 # 0/1 read specs for more stddev reporting
#
999

```